J Pharmacokinet Pharmacodyn (2014) 41:S7–S101
DOI 10.1007/s10928-014-9379-8

ABSTRACTS

Abstracts Accepted for American Conference on Pharmacometrics 2014 (ACoP5)

M-001

Time-to-Event (TTE) Pharmacokinetic/Pharmacodynamic Analysis for Tafenoquine (TQ; SB252263) in Subjects with Malaria

David Tenero[1,*], Ann Miller[1], Justin Green[2], Navin Goyal[1]

[1] GlaxoSmithKline, Clinical Pharmacology Modeling & Simulation, King of Prussia, PA, USA; [2] GlaxoSmithKline, Clinical Development, Stockley Park, UK

Objectives: Investigate the TQ PK/PD relationship.
Methods: Tafenoquine possesses activity against all stages of the Plasmodium vivax lifecycle. In a Phase IIb study, subjects received single TQ doses of 50–600 mg. A population PK model determined TQ exposure. Parametric TTE modeling (NONMEM v7.2) evaluated the time-to-relapse; classification and regression tree (CART; R v2.15.3) analysis estimated the probability of being relapse-free at 6 months.
Results: CART identified a clinically-derived breakpoint as a predictor of relapse status (success rate 89 % for AUC $\geq$ 56.4 μg h/mL, 48 % for <56.4 μg h/mL). The TTE model included a Weibull distribution hazard function, a delay function for an initial period of low relapse, AUC, and country. The final model adequately described the survival probability (relapse-free status) over time and was used to simulate the survival probability for subjects with an AUC above and below 56.4 μg h/mL. The probability of being relapse-free at 6 months was 52 % (95 % CI 44–61 %) for subjects with an AUC < 56.4 μg h/mL and 85 % (95 % CI 80–90 %) for an AUC $\geq$ 56.4 μg h/mL. Clinical trial simulations (CTS) indicated that the 300 mg dose provides an AUC $\geq$ 56.4 μg h/mL in >90 % of subjects.
Conclusions: Parametric time-to-event and logistic regression PK/PD models were successfully developed for tafenoquine after administration to subjects with Plasmodium vivax malaria in a Phase IIb dose-range study. The probability of being relapse free at 6 months increases with increasing TQ exposure. CTS demonstrated that the TQ dose of 300 mg would provide an AUC greater than the clinically-derived breakpoint (56.4 μg h/mL) in over 90 % of subjects and consequently result in high probability of being relapse-free at 6 months. This model based approach was critical in selecting an appropriate Phase III dose.

M-002

Does It Have to be a 12-Week Proof of Concept (POC) Study? Prediction of Week 12 Efficacy from Short-Term HbA1c Treatment Effect Using Model-based Meta-analysis of Literature Data

Jing Liu[1,*], Rebecca Boyd[1], Jaap Mandema[2]

[1] Clinical Pharmacology, Pfizer, Groton, CT, USA; [2] Quantitative Solutions, Menlo Park, CA, USA

Objectives: Model-based meta-analysis (MBMA) has been applied in the assessments of comparative efficacy [1,2] and time-course of glucose effect [3] with anti-diabetic drugs in Type 2 diabetes mellitus (T2DM). However, there has been no publication of a systematic quantitative analysis of how early efficacy in glycemic endpoints translates to longer term efficacy. The objective of this analysis was to evaluate the predictability of HbA1c treatment effect at Week 12 from Week 4 HbA1c response using summary-level data from the literature and a MBMA, to aid in the interpretation of short-term study results and to potentially provide justification for shorter POC studies in drug development for T2DM.
Methods: A database of study-level aggregate data from published clinical trials in T2DM was constructed by Quantitative Solutions (Version: April 20, 2014). From this database, a total of 119 trials with 29 drugs in 12 drug classes containing both Week 4 and Week 12 HbA1c data were selected for modeling. HbA1c(%) difference from control at Week 12 (DFC12) was described by a mixed-effect linear function of HbA1c(%) difference from control at Week 4 (DFC4): $DFC12,ij = E0 + (SLP + ETAi)*DFC4,ij$, in which E0 is the intercept, SLP is the typical slope, ETA is the additive inter-trial random effect. The variance was fixed to the inverse standard error squared of each trial (i) and study arm (j). The final model was evaluated using a predictive check of selected sitagliptin trials. R2.15.2 and S-PLUS 8.0 were used for data processing and modeling, respectively.
Results: Across all 29 anti-diabetic drugs, except for thiazolidinediones, with known slow onset, HbA1c(%) DFC12 was described by a single linear function of DFC4, with SLP of 2.00[1.88–2.12], E0 of 0.033[0.008–0.058], and inter-trial variability on the SLP of 23 %[19–28 %], (mean[90 % CI]). The predictive check suggested that the model adequately predicted the observed HbA1c treatment effects of sitagliptin at Week 12 in similar populations across multiple trials (Fig. 1).

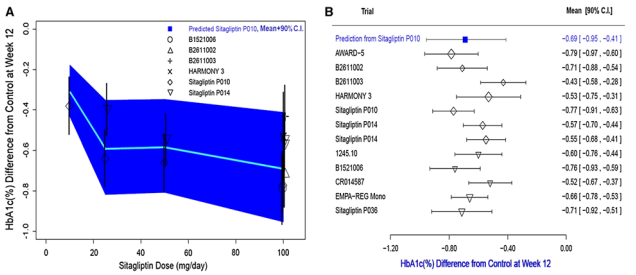

Fig. 1 **a** Within model validation at different doses of sitagliptin using trials included in the model (*open symbols*), and **b** external validation at 100 mg/day of sitagliptin using trials excluded in the model (*inverted open triangle*) in addition to those included in the model (*open diamond*), in similar diabetic populations. The observed mean values of HbAlc(%) Difference from Control at Week 12 in these trials are all within the 90 % confidence interval (CI) of the model prediction using Week 4 HbA1c(%) Difference from Control in trial Sitagliptin PO10. One thousand trial simulations were performed using randomly sampled fixed effect parameters from a multivariate normal distribution and the random effect parameter from a normal distribution and using the observed mean HbA1c difference from control at Week 4 in trial Sitagliptin P010

Conclusions: The HbA1c treatment effect at Week 12 is predicted to be 2-fold greater than the effect at Week 4 in a similar population, with 23 % inter-trial variability using the direct linear MBMA model. Additional characterization of inter-trial variability and potential prediction across populations and at different time-points is being further evaluated using MBMA of longitudinal data.

References:

1. Mandema J, et al. Diabetes. 61(suppl. 1): A1015, 2012
2. Gross, JL, et al. BMJ Open. 3(3): e001844, 2013
3. Denney, WS, et al. JPKPD. 40: S141, 2013

M-003

Pharmacokinetic/Pharmacodynamic Modeling to Support A Lack of Effect of Tafenoquine (TQ) on the QT Interval in a Thorough QT (TQT) Study

Bela Patel[1,*], Ann Miller[1], David Tenero[1], Justin Green[2]

[1] GlaxoSmithKline, Clinical Pharmacology Modeling & Simulation, PA, USA; [2] GlaxoSmithKline, Clinical Development, Diseases of the Developing World, Stevenage, UK

Objectives: TQ, is an 8-aminoquinoline primaquine analogue currently being developed for the radical cure of *P. vivax* malaria. This analysis characterized the exposure-relationship between TQ and moxifloxacin (M) concentration versus duration of QTcF interval.
Methods: In this parallel group TQT study, subjects (18–65 years) received placebo, TQ (300, 600 mg), M 400 mg (Day 3) or 1200 mg (given over 3 days) with food (n = 52/group). Triplicate electrocardiographs were acquired 24 h prior to dose administration (Day -1), at pre-dose (Days 1–3), and post final dose up to 72 h (Day 3) with matching PK samples. A PK/PD model was developed with final model evaluation using bootstrap analysis and a visual predictive check.
Results: The PK/PD model included sex and race (black and all others), 8 and 24 h circadian rhythms and linear slope terms for TQ and M. For all TQ doses, the median predicted ΔΔQTcF and 90 % confidence interval [CI] were <10 ms threshold at the geometric mean observed Cmax. Administration of 400 mg M in the fed state decreased both Cmax and AUC values (47 and 30 %) compared to the fasted state [1]. PK/PD modeling confirmed the expected QTcF prolongation with M (slope = 3.11 ms/mg ml^{-1}). Simulated ΔΔQTcF data (N = 1,000 datasets) based on doubling of M Cp resulted in a lower bound of the 90 % CI for the of ΔΔQTcF interval of ≥5.0 ms at two timepoints demonstrating that M would have the expected effect on QTcF interval, had M Cp been in the range of those typically observed confirming assay sensitivity.
Conclusions: PK/PD modeling confirmed a lack of effect by TQ on the QT interval.

Sponsored by GlaxoSmithKline and Medicines for Malaria Venture.

References:

1. Florian JA, Tornoe CW, Brundage R, Parekh A, Garnett CE. Population pharmacokinetic and concentration-QTc models for moxifloxacin: pooled analysis of 20 thorough QT studies. J Clin Pharmacol 2011;51(8):1152–62

M-004

Clinical Trial Simulations Based on a Meta-analysis of Studies with Advanced Hepatocellular Carcinoma Patients Receiving Antiangiogenic Therapy

Matthew L. Zierhut[1], Ying Chen[2], Yazdi K. Pithavala[2], Dana J. Nickens[1], Olga Valota[3], Michael A. Amantea[1,*]

[1] Pharmacometrics, [2] Clinical Pharmacology, [3] Oncology Clinical Development, Pfizer, La Jolla, CA, USA

Objectives: The primary aim was to develop a model to: (1) describe median overall survival (mOS) in trials with advanced hepatocellular carcinoma (aHCC) patients (pts) treated with antiangiogenic therapy (AAT) and (2) simulate clinical trial designs to gain a better understanding of expected mOS after AAT and quantify the impact of covariates on response.
Methods: Modeling and simulations were performed using R or NONMEM software. Studies of AAT (with or without a placebo (PBO) arm) were considered for inclusion. A linear mixed-effects model was fit to log-transformed mOS data, with a between-trial random effect ($\eta_{BT} \sim N(0,\omega^2)$) and residual term ($\varepsilon_{res} \sim N(0,SEi^2)$), where SEi is the reported standard error of the ith arm). Potential confounding or prognostic factors were tested as covariates. Various PBO-controlled trial designs were simulated and true# response and probability of superiority to PBO were calculated.
Results: Final analysis data consisted of 68 arms from 59 studies (4813 pts). The final model is shown below Table 1, where therapy (AAT, PBO, sorafenib (SOR), locoregional (LOC) and chemo (CTx)) and prior therapy (PTx) are indicators (0 or 1) and %HepB (% pts with hepatitis B) is continuous and median-centered. Estimated parameter values (θ_x and ω) are shown in Table 1.
Simulations show that AAT leads to an increased mOS versus PBO, with an expected true# AAT:PBO ratio (95 % prediction interval) of 1.45 (1.35–1.56) and 1.20 (1.12–1.29) for SOR or other AAT, respectively. Simulations also suggest that AAT superiority to PBO may be demonstrated in 80 % of trials with as few as 125 patients per arm.
Conclusions: A model has been developed to describe mOS in AAT clinical trials with aHCC pts, while identifying important prognostic covariates. As new data become available, this model can be refined to improve simulation-based predictions.

Not dependent on number of patients in trial

Table 1 Parameter for Final Model

θ_{AAT}[a]	θ_{PBO}[a]	θ_{SOR}	θ_{LOC}	θ_{HepB}	θ_{PTx}	θ_{CTx}	ω(CV)
8.49 mo	7.06 mo	↑21 %	↑42 %	↓∼0.4 %	↓7 %	↓4 %	24 %

Final Model: $\ln(mOS) = AAT \cdot \ln(\theta_{AAT}) + PBO \cdot \ln(\theta_{PBO}) + SOR \cdot \ln\theta_{SOR} + LOC \cdot \ln(\theta_{LOC}) + \%HepB \cdot \theta_{HepB} + PTx \cdot \ln(\theta_{PTx}) + CT_x \cdot \ln(\theta_{CTx}) + \eta_{BT} + \varepsilon_{res}$

[a] θ_{AAT} and θ_{PBO} are mutually exclusive parameters. All other θ_x are additional effects

M-005

Similar Exposure and Pharmacokinetics of Bevacizumab in Pediatric and Adult Cancer Patients: Analysis of Individual Data from 152 Pediatric Patients

Kelong Han[1,*], Thomas Peyret[2], Nathalie H. Gosselin[2], Angelica Quartino[1], Sridharan Gururangan[3], Clinton F. Stewart[4], Fariba Navid[4], Mohamad-Samer Mouksassi[2], David E. Allison[1], Jin Jin[1]

[1] Clinical Pharmacology, Genentech Inc., South San Francisco, CA, USA; [2] Pharsight Consulting Services, Montreal, QC, Canada; [3] Pediatric Clinical Services, Duke University Medical Center, Durham, NC, USA; [4] St. Jude Children's Research Hospital, Memphis, TN, USA

Objectives: Bevacizumab pharmacokinetics is well established by a population pharmacokinetic (PPK) model in adults, but has not been comprehensively evaluated in children. Four pediatric studies were conducted to assess bevacizumab pharmacokinetics in children and compare bevacizumab exposure and pharmacokinetics between children and adults.

Methods: Bevacizumab was administered at 5, 7.5, 10 or 15 mg/kg (Q2W or Q3W) with chemotherapy to children with primary CNS tumor (n = 76), metastatic soft tissue sarcoma (n = 39), osteosarcoma (n = 27), or other refractory solid tumors (n = 10). A nonlinear mixed-effects model was fitted to bevacizumab serum concentrations (Cs). Pediatric bevacizumab exposure (trough Cs) were simulated by the pediatric PPK model under equivalent BSA-based, Tier-based or WT-based dose, and compared to adult exposure simulated by the adult PPK model.

Results: Totally 1,464 bevacizumab Cs from 152 patients between 6 months and 21 years old (median 10.8) were analyzed, with 9 patients under the age of 3 years. Body weight (WT) ranged from 5.9 to 125 kg (median 43.8 kg). Typical bevacizumab clearance (CL), central volume of distribution (V1) and half-life for a 75 kg individual are 9.47 mL/h, 2.98 L and 18 days in children (vs. 9.31 mL/h, 2.91 L and 20 days in adults). In pediatric patients, CL and V1 increase with WT and are lower in females and primary CNS tumor, and CL decreases with albumin. Age is not correlated with WT-normalized CL or V1. Bevacizumab exposure in children decreases with decreasing WT given the same mg/kg dose. Bevacizumab exposure under BSA-based (mg/m2), Tier-based and WT-based dose generally falls within the 90 % predictive interval of adult exposure across pediatric age and WT range.

Conclusions: A robust bevacizumab PPK model for children that can be used to perform simulations was developed based on this large pediatric population with a wide range of age (0.5–21 years) and WT (5.9–125 kg). Bevacizumab pharmacokinetics is similar across pediatric age range when corrected for WT. Bevacizumab pharmacokinetics and factors correlated with bevacizumab pharmacokinetics are similar in children and adults. Pediatric bevacizumab exposure is similar to adult exposure across pediatric WT range. BSA-based or Tier-based dose offers no substantial advantage over WT-based dose.

M-006

A Novel Interdisciplinary Pharmacometric Approach: Linking Oseltamivir PK/PD to Dynamic Transmission and Health Economic Models to Inform Antiviral Use in Pandemic Scenarios

M. A. Kamal[1,*], P. F. Smith[2,3], N. Chaiyakunapruk[4], D. B. C. Wu[4], C. Kirkpatrick[4], C. Pratoomsoot[4], K. K. C. Lee[4], H. Y. Chong[4], R. E. Nelson[5], K. Nieforth[3], G. Dall[3], S. Toovey[3], D. C. M. Kong[4], A. Kamauu[6], C. R. Rayner[3,4]

[1] Roche; [2] University at Buffalo, Buffalo, NY, USA; [3] D3 Medicine; [4] Monash University, Clayton VIC, Australia; [5] University of Utah, Salt Lake City, UT, USA; [6] Anolinx

Objectives: Recent PK/PD evaluations found that higher oseltamivir exposures reduce duration of viral shedding and symptoms. This study investigated the potential epidemiological and economic impact of oseltamivir dose optimization for pandemic planning purposes.

Methods: Oseltamivir active metabolite (OC) AUC distributions were simulated for 75 and 150 mg po BID via a published population PK model. Distributions of influenza viral shedding duration (Tshed) around published OC AUC breakpoints were determined. Treatment effect with OC on Tshed was linked to a SEIR (sensitive, exposed, infected, recovered) compartmental model via the relationship: Basic Reproductive Number (Ro) = β*Tshed, where β is the transmission coefficient. Using Monte Carlo simulation (including sampling relevant OC AUC and Tshed distributions), populations of n = 100,000 were created. The number infected was simulated for scenarios including high (150 mg BID) vs. standard dose (75 mg BID), varying Ro/transmissibility [low vs. high attack rates (37 vs. 67.5 % respectively)], and drug uptake (25, 50, and 80 %). The number of infected patients for each scenario was entered into a decision analytic model populated with the probability, disease utility and cost of patients hospitalized, developing complications, and case-fatality rates using published databases. The analysis was conducted from the US societal perspective, incorporating direct and indirect costs. Drug effectiveness was measured using Quality Adjusted Life Years (QALY) gained.

Results: Increase in both oseltamivir dose and drug uptake decreased the number infected. Oseltamivir was cost saving under most pandemic scenarios and cost effective [incremental cost-effectiveness ratios (ICER) < $100,000/QALY] in some. High dose oseltamivir had economic value particularly in high transmissibility scenarios.

Conclusions: This analysis demonstrated proof of concept that PK/PD endpoints (AUC and viral shedding) can be linked to epidemiological endpoints of transmissibility (Ro) and economic endpoints (ICER) to optimize use of antivirals under various pandemic scenarios.

M-007

A Population Pharmacokinetic Model for D-β-Hydroxybutyrate Following Administration of Ketone Monoester

Vittal Shivva[1,*], Pete Cox[2], Kieran Clarke[2], Richard L. Veech[3], Ian G. Tucker[1], Stephen B. Duffull[1]

[1] School of Pharmacy, University of Otago, Dunedin, New Zealand; [2] Department of Physiology, Anatomy and Genetics, University of Oxford, Oxford, UK; [3] Laboratory of Metabolic Control, NIAAA/NIH, Rockville, MD, USA

Objectives: Ketone bodies, the evolutionary response to starvation in humans, are produced in the liver from fatty acids in response to low blood glucose and insulin concentrations, and used by the body as

fuels. Ketogenic diets have long been used to treat intractable pediatric epilepsy, with therapeutic evidence for ketosis in other neurodegenerative disorders such as Alzheimer's and Parkinson's disease [1]. A novel means of achieving ketosis by nutritional consumption of a ketone monoester has recently been established [2].
The aim of this project is to understand the pharmacokinetics (PK) of D-β-hydroxybutyrate (BHB), and to determine sources of variability following nutritional ketone monoester ingestion.
Methods: Serial blood BHB concentration data (n = 37) were obtained in healthy volunteers following administration of a single oral dose of ketone monoester ((*R*)-3-hydroxybutyl (*R*)-3-hydroxybutyrate). Two different formulations were administered at five dose levels. A nonlinear mixed effect modelling approach was used to develop a population PK model using NONMEM (v7.2).
Results: A one compartment disposition model with negative feedback effect on endogenous production of BHB provided the best description of the data. Absorption was best described by two consecutive first-order inputs and elimination by dual processes involving first-order and capacity limited elimination. Important covariates describing variability in absorption parameters were formulation and dose. Lean body weight (on first-order clearance) and sex (on apparent volume of distribution) were also significant covariates.
Conclusions: The PK of BHB is complicated by a complex absorption process, endogenous production and nonlinear elimination. Formulation appears to strongly influence the kinetic profile following ketone monoester ingestion. Multiple peak concentrations were predominant at higher doses requiring further exploration.

References:

1. Veech R.L. (2004). Prostaglandins Leukotrienes and Essential Fatty Acids. 70(3):309–319
2. Clarke K. et al. (2012). Regul Toxicol Pharmacol. 63(3):401–408

M-008

Population Pharmacokinetics Analysis for Fedratinib

Yaming Su*, Christine Xu, Vanaja Kanamaluru

Pharmacokinetics Projects/Pharmacometrics, Disposition, Safety & Animal Research, Sanofi US, Bridgewater, NJ, USA

Objectives: The main objective was to develop and qualify a population pharmacokinetic (PopPK) model for fedratinib in healthy volunteers and patients with myelofibrosis (MF) and to investigate the influence of key demographic characteristics or selected laboratory tests covariates. The second objective was to estimate the exposure parameters in MF patients from the final model for potential exposure-response analysis.
Methods: Data from 3 Phase 1 studies in healthy volunteers, 3 studies (Phase 1, Phase 2 study, and phase 3) in MF patients were combined for this analysis. Fedratinib was administered as a single oral dose in healthy subjects (N = 42) or as once-daily repeated oral doses in MF patients (N = 272). Current analysis consists of total 2,483 fedratinib concentrations associated with doses ranging from 100 to 800 mg.
Results and Conclusions: The PK of fedratinib was best described by a two compartment model with first order absorption from the depot to the central compartment and first order elimination from the central compartment, with inter individual variability on all parameters except Ka and a proportional residual error.

Age, weight and albumin were identified as significant covariates influencing fedratinib PK. The corresponding impacts on steady state exposure over the range of 25th–75th percentile values of covariates in MF patients in the current dataset are below:

- From age of 58–71 years, CL/F decreased by 15.4 %, corresponding to 1.2- and 1.1-fold increase of AUC0-24 and Cmax, respectively.
- From weight of 62–80 kg, CL/F increased by 1.1-fold, and Q/F increased by 1.2-fold, corresponding to 12.5 and 9.7 % decrease of AUC0-24 and Cmax, respectively.
- From albumin of 44–38 g/L, V2/F decreased by 29.2 % corresponding to minimal increase (1.05-fold) of steady state Cmax and no effect on AUC0-24.

The final PK model appeared to adequately describe fedratinib concentration data and allowed to derive individual PK parameters that can be used in exposure-response analyses.

M-009

Physiologically Based Pharmacokinetic (PBPK) Approach to Discern Potential Population Differences in Patients with Refractory Solid Tumors and Healthy Subjects: The Effects of Fedratinib on CYP3A4 Substrate Midazolam

Christine Xu[1,*], Nassim Djebli[2], Vanaja Kanamaluru[1]

[1] DSAR Sanofi, Bridgewater, NJ, USA; [2] Sanofi, Montpellier, France

Background: Fedratinib is a substrate of CYP3A4 with dose- and time-dependent nonlinear pharmacokinetics (PK). In vitro studies, fedratinib demonstrated the time-dependent inhibition, with a concentration-dependent increase in CYP3A gene expression (induction) of CYP3A4.
Methods and Results: A PBPK model was developed in SimCYP using physic-chemical parameters, in vitro, and in vivo PK data. Despite that the PBPK model predicted the fedratinib PK profiles of a single dose and repeated dosing, and was verified by an vivo drug-interaction study of ketoconazole effects on fedratinib, the interaction between fedratinib and the midazolam in aged and sex matched healthy subjects was estimated to be higher than the observed in patients with refractory solid tumors. Furthermore, the observed fedratinib effects on midazolam in solid tumors patients (N = 13–16) were lower than the prediction using the basic and static mechanistic models. Comparing with healthy subjects, the unexpected high midazolam exposure (2-fold) when midazolam was administrated alone and high fedratinib exposure (1.6-fold) at steady state suggested lower clearance of CYP3A4 substrates in solid tumor patients. We hypothesized that the population differences in CYP3A4 enzyme activity in solid tumor patients and healthy subjects was responsible for the unexpected observations. Modifying the PBPK model by reducing the CYP3A4 enzyme abundances (down to 50 % for healthy subjects) in liver and gastric-intestinal or adjusting CLintCYP3A4 for midazolam and fedratinib, we successfully predicted the fedratinib effects on the midazolam (3.76-fold predicted vs 3.84-fold observed) as well as the observed PK profiles of midazolam and fedratinib in the solid tumors patients. The hypothesis was confirmed by the literature which suggests reduced CYP3A4 activity in solid tumor patients with concurrent elevations in liver transaminases and alkaline phosphatase or elevated total bilirubin.
Conclusion: The PBPK modeling and simulation is a useful tool for evaluating the potential for drug interaction in the context of various clinical factors present in patients.

M-010

Population Pharmacokinetics of Mycophenolic Acid and Its Main Glucuronide Metabolite: Comparison Between Chinese and Caucasian Healthy Subjects Receiving a Single Oral Dose of Mycophenolate Mofetil

Jing Ling[1], Zheng Jiao[1,*], Qiudi Jiang[2], Jun Shi[2]

[1] Department of Pharmacy, Huashan Hospital, Fudan University, Shanghai, China; [2] Roche R&D Center (China), Ltd. Shanghai, China

Objectives: Mycophenolate mofetil (MMF), a prodrug of the immunosuppressive agent mycophenolic acid (MPA), is widely used for prophylaxis of solid organ transplant rejection. MPA is mainly metabolized to 7-*O*-mycophenolic acid glucuronide (MPAG), which undergoes enterohepatic recirculation (EHC). In clinical practice, the dose of MMF in Chinese renal transplant patients is lower than that in Caucasians. The aim of this study was to assess the ethnic difference of MPA and MPAG pharmacokinetics (PK) among Chinese and Caucasian healthy subjects by population PK analysis.
Methods: Data were pooled from 132 subjects (80 Chinese, 52 Caucasians) in 8 clinical trials, in which MMF was administered as a single oral dose. Population PK analysis was performed using NONMEM. Covariates including ethnicity and other demographics were screened by a forward inclusion ($p < 0.01$) and backward elimination ($p < 0.001$) approach. Final model was internally evaluated using visual predictive check (VPC), normalized prediction distribution errors and cross-validation. Twenty-five previously published studies were integrated for external evaluation.
Results: The PK of MPA and MPAG were best described with a 5-chain compartment model including a gallbladder compartment for EHC, along with transit absorption model in which body weight was a significant covariate on MPA and MPAG apparent clearance (CL/F). Ethnicity showed significant correlations with CL/F and volume of distribution of MPAG, but not of MPA. MPA CL/F was 11.5 L/h for a 70 kg healthy subject, and MPAG CL/F was 1.36 and 1.90 L/h for a 70 kg Chinese and Caucasian, respectively. Both internal and external evaluation indicated the validity of the model. Shown below was VPC result for model outputs (Fig. 1).
Conclusions: This study demonstrated there is no difference in the PK of MPA between Chinese and Caucasian healthy subjects. The faster elimination of the inactive metabolite MPAG in Caucasians may have no clinical relevance.

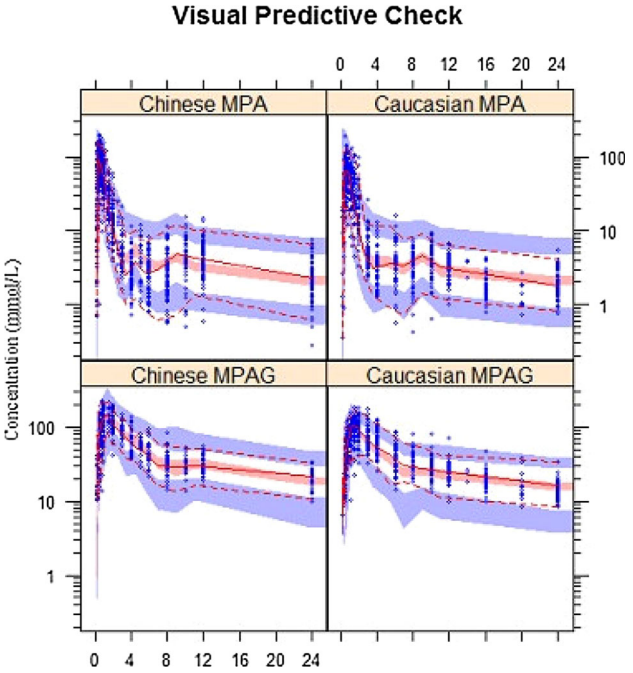

Fig. 1 A visual predictive check of the final model showing the observations (*open circles*), the fifth (*dashed line*). 50th (*solid line*) and 95th percentile (*dashed line*) of the observations and the simulated 90 % confidence intervals for the fifth, 50th and 95th percentiles (*shaded areas*). Dose normalized to 1,000 mg

M-011

Application of Modeling and Simulation to Dose Selection in Pediatric Subjects with Sickle Cell Disease

Brinda Tammara*, Lutz Harnisch

Global Innovative Pharma Business, Pfizer Inc, New York, NY, USA

Objective: Provide dose recommendation for the PF-06460031 Phase 3 program in children 6–11 years of age with sickle cell disease (SCD).
Methods: PK data (109 subjects receiving doses of 2–40 mg/kg) from 4 previously completed studies (three phase 1 and one phase 2) were integrated to build a 3 compartment model, which was used to perform simulations to aid pediatric dose selection. Since PF-06460031 is almost completely renally eliminated, the simulations of clearance across the proposed age range took the development of renal function as well as a postulated hyper-filtration in SCD patients into account [1]. The resulting simulated exposure distributions from three dosing regimens were compared against the efficacious average concentrations at steady state (Cavg,ss) observed in the Phase 2 study [2].
Results: For each dosing regimen tested, the simulated demographic target distribution in pediatric SCD patients was used to derive concentration-time profiles. A summarization of the Cavg,ss distribution across different ages is shown in Fig. 1. Since this drug is exclusively renally eliminated creatinine clearance was used as a surrogate for renal function. It is assumed, that the scaling of creatinine clearance is the main determinant for PF-06460031 clearance and together with a body scale measure like weight this will be sufficient to predict future exposures. Creatinine clearance in kids ages 6–11 was estimated using the standard Schwartz formula, which takes into account the height and weight of the kids. The height and weights were obtained from the CDC growth charts for the simulations. Also allometric scaling usually scales total clearance to given body size, but in the model we are reflecting both on renal clearance and also taking hyper filtration into account. From the population PK in Phase 2 study, age and weight were not found to be significant covariates. Since this is

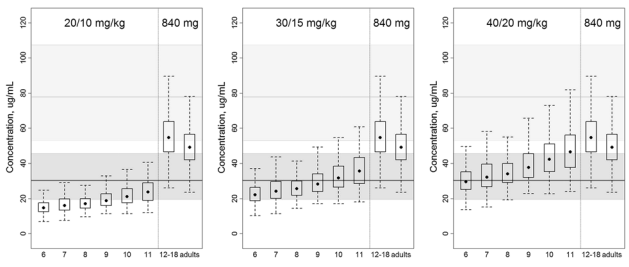

Fig. 1 Cavg,ss distributions at different dosing regimen across the age range to be studied. Each *panel* corresponds to a dosing regimen. *Left* 20/10 mg/kg, *middle* 30/15 mg/kg, and *right* 40/20 mg/kg. Distribution of Cavg,ss after the the low dose (*pink*) and high dose (*green*) as observed in t he Phase 2 study is shown in the back ground, with the *line* indicating the median, and *shaded area* the 95 % prediction interval

only a prediction exercise, additional covariates will be studied later in the modeling.

Conclusions: Based on this evaluation, a dose regimen of 40 mg/kg loading dose, followed by a 20 mg/kg maintenance dose q12 hrs was chosen as it will likely provide a concentration range shown to be efficacious in the Phase 2 study. To confirm the validity of the exposure predictions, PK assessments will be performed in the Phase 3 program.

References:

1. Russel E Ware and Babu Hug investigators: Renal Function in Infants with Sickle Cell Anemia: Baseline Data from the BABY HUG Trial. J Pediatrics 156:66–70
2. MJ Telen, Ted Wun et al.: Reduction In Time To Resolution Of VOC and Decreased Opioid Use In a Prospective, Randomized, Multi-Center Double Blind, Adaptive Phase 2 Study In SCD. Blood 2013 122:776

M-012

Selection of First-in-Patient Dose for a Novel Antibacterial That is Robust to Translational Assumptions

S. Aksenov*, K. Vishwanathan, J. Newman, M. Huband, H. Gardner, J. Mueller

AstraZeneca Pharmaceuticals LP, Waltham, MA, USA

Objectives: AZD0914 is a novel spiropyrimidinetrione DNA gyrase inhibitor that is being developed to treat Neisseria gonorrhoeae (NG) infections. Our goal was to select a dose with high probability of cure in patients that is not sensitive to deviations from model assumptions.

Methods: We assumed that cure will be achieved at a drug exposure corresponding to bacteriostasis in a *S. aureus* murine infection model. A target efficacy index expressed as a ratio of drug concentration area under the curve (AUC) to the minimum inhibitory concentration (MIC) was determined in a dose-response experiment in mice. Probability of target attainment (PTA), or cure was calculated as proportion of patients whose AUC was greater than the target index multiplied by the highest MIC = 0.25 μg/mL observed in a collection of 250 NG isolates. Distribution of AUC in patients was predicted by simulation of a population pharmacokinetic model of AZD0914 from an oral Phase I dose escalation study.

Results: The target AUC/MIC was 63 (90 % CI 44–82) for bacteriostasis and 115 (90 % CI 82–148) for a one-log10 reduction in colony forming units (CFU). A two-compartment model described the PK adequately (visual predictive check and precision of parameter estimates were acceptable). It was qualified for simulation using a posterior predictive check. An oral dose of 3,000 mg achieved a PTA = 1. The PTA remained ≥0.8 if cure corresponds to a more stringent one-log10 reduction in CFU, or if the target is at the upper bound (the 95th percentile) of its plausible range. The cumulative fraction of response remained >95 % even if a NG strain is encountered such that the 90th percentile of the new MIC distribution equals twice the current maximum MIC.

Conclusions: A single dose of 3,000 mg is predicted to achieve a high clinical response rate in patients with NG. This choice of dose is robust enough to support an MIC twice as high as the current maximum and may help suppress the development of resistance Fig. 1.

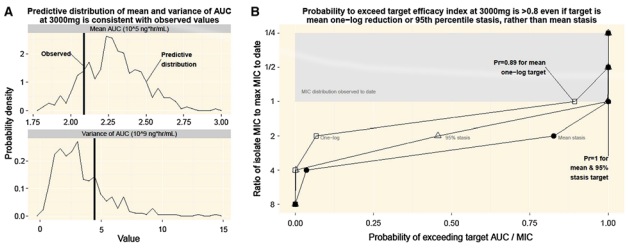

Fig. 1 The population PK mode was qualified for simulation using a posterior predictive check (**a**). An oral dose of 3,000 mg achieved a PTA = 1 and was robust to deviations from model assumptions (**b**)

M-013

Population Pharmacokinetics of Insulin-Like Growth Factor-I (IGF-I) in Pre-term Infants

Jyoti Sharma[1,*], Allison Gaudy[2], Martin Graham[1], Gerald Fetterly[2], Patricia Meholick[2], Ingrid Pupp[3], Boubou Hallberg[4], Chatarina Lofqvist[5], Ann Hellstrom[5], Mary Ann Mascelli[6], Thomas McCauley[6], Jouku Chung[6], Nerissa Kreher[6], Lois Smith[7], David Ley[3]

[1] PKPD Incorporated, Exton, PA 19341, USA; [2] Roswell Park Cancer Institute, Buffalo, NY 14263, USA; [3] Skane University Hospital and Lund University, Lund 22185, Sweden; [4] Karolinska Institute, Stockholm, 14186, Sweden; [5] Sahlgrenska Academy, Gothenburg, 41685, Sweden; [6] Shire, Lexington, MA 02421, USA; [7] Boston Children's Hospital/Harvard Medical School, Boston, MA 02115, USA

Objectives: (1) To establish the normal intrauterine fetal serum IGF-I concentration levels and (2) To establish an optimal dosing regimen of rhIGF-I/rhIGFBP-3 in very preterm infants to maintain serum IGF-I levels within the intrauterine physiologic range utilizing population pharmacokinetic (PK) modeling, as low levels of IGF-1 are associated with retinopathy of prematurity in preterm infants.

Methods: A meta-analysis of published literature [1, 2], was performed to establish the normal in utero physiological levels of IGF-I. A population PK model was developed to estimate IGF-I PK parameters using data from Phase 1 and Phase 2 studies of investigational IV rhIGF-I/rhIGFBP-3 replacement and data from a non-treated control population of very preterm infants. The final PopPK model was then used to simulate IGF-I concentration-time profiles to identify the optimal dosing regimen that would result in IGF-I concentrations within the physiological range.

Results: The mean (95 % prediction intervals) predicted normal in utero IGF-I level between 23–28 weeks GA was 54 (28–109) μg/L. Population PK simulations under different rhIGF-I/rhIGFBP-3 dosing regimen indicated that a dose of ≥250 μg/kg administered as a continuous 24 h infusion up to approximately 30 weeks post-menstrual age (PMA) was needed to achieve IGF-I levels within the target range of normal intrauterine levels.

Conclusions: Preterm infants have significantly lower levels of circulating IGF-I than fetuses with a corresponding GA in utero. Physiological replacement of IGF-I aiming to achieve normal intrauterine levels requires at least 250 μg/kg/day of rhIGF-I/rhIGFBP-3 administration for a substantial time.

References:

1. Lassarre C., et al., Pediatr Res, 1991 Mar; 29(3):219–25
2. Bang P., et al., Pediatr Res, 1994 Oct; 36(4):528–36

Table 1 Parameter estimates and standard errors for Base and Final Model

	Base parameter estimates	Model	Interindividual variability (%)		Final parameter estimates	Model	Interindividual variability (%)	
	Base	%SEM	Base	%SEM	Final	%SEM	Final	%SEM
CSS (μg/L)	7.77	3.64	38.3	25.6	7.85	3.77	38.2	25.5
ALAG (h)	72	0.01	–	–	72	0.01	–	–
K (1/h)	0.000744	10.2	–	–	0.000737	10.6	–	–
CL (L/h)	1.66	33.3	160	41.8	0.793	35.9	–	–
V (L)	2.25	18.6	–	–	2.39	36.8	–	–
Residual variability (%)	40.1	10.3			39.7	10.2		
MVOF	4281.116				4298.648			

CSS baseline IGF-1, *ALAG* lag time to production of endogenous IGF-1, *K* first-order production rate constant of endogenous IGF-1

The results in this abstract have been previously presented in part at [PAS/ASPR, Vancouver, May 6, 2014] and published in the conference proceedings as abstract [752154] Table 1.

M-014

Using Simulations to Support Design of Preclinical and Clinical Trials of Prophylactic Vaccines

Jeffrey R. Sachs[1,*], Kapil Mayawala[1], Jonathan Hartzel[2]

[1] PPDM/QP2, [2] BARDS/LDS, Merck/MRL

Objectives: Design clinical/preclinical trials with reduced complexity and sufficient power. Prophylactic vaccine development depends on the use of biomarkers of immune response. This requires understanding how to interpret results and how to design experiments ensuring reliability of those results. Here "design" includes choices of doses, formulations, and the number of animals or subjects in each arm. Because vaccines are often multivalent (containing one immunogen for each of several pathogens/variants), factorial design for an n-valent vaccine with one formulation factor (such as adjuvant concentration) is impractical, requiring $2^{(n+1)}$ arms.
Clinical trial design addressed dose-ranging across multiple antigens and adjuvant, enabling the team to drop other formulation variables. Preclinical design was needed to power a study with the minimum number of animals.
Methods: Both clinical and preclinical design benefited from a 4-step strategy to quantify interplay between design parameters, assumptions about response amplitudes, sensitivity, and specificity:

(1) Development team was engaged to quantify the key questions and assumptions.
(2) Specific statistical analyses were planned to answer those questions.
(3) Different designs were simulated based on the assumptions and prior data.
(4) Simulated data were analyzed as though they were final experimental results, allowing comparison of the utility of different designs.

Clinical trial simulations used comparator modeling, dose–response models accounting for titer covariance between antigens, and classical design of experiments. Figure 1 shows the workflow for simulation and comparison of different designs via a reduced design space, simulated responses for a full-factorial study, and summary representation of the size-power-sensitivity tradeoffs.

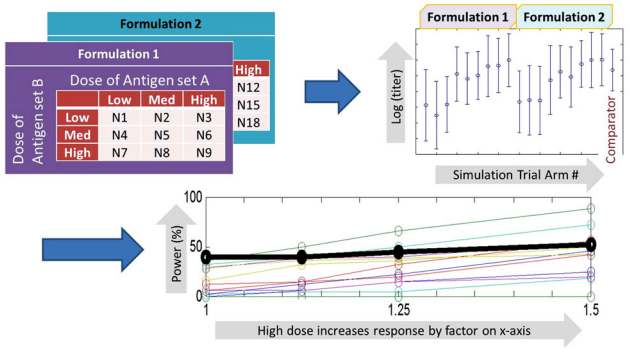

Fig. 1 Workflow for simulating ability to detect effects across different designs and assumptions of dose-response characteristics. *Step 1 (top left)* Dimensionally-reduce design space to nine dose-pairs for each of two formulations. Dimensional reduction achieved by grouping antigens into two sets based on prior data. N1 through N18 are the numbers of subjects in respective arms. *Step 2 (top right)* Simulate titer response for one antigen and for one assumed value of fold-increase associated with "High" dose, using the same N for Nl…N18. *Step 3 (bottom):* Summarize many simulations across a range of fold-increase values. Under the given assumptions only the strongest effects are likely to be detectable for some antigens (*colored lines*), and formulation change effects are only about 50 % likely to be detectable (*black line*)

Preclinical design required preprocessing prior data: compensating for between-individual variability of titer dynamics allowed better estimation of the variability.
Results: Clinical work informed team choice of doses and formulations and the strategy for planned follow-on studies. Preclinical results demonstrated that a planned experiment would lack the power to detect some of the anticipated response differences, thus justifying the resources for an appropriately sized study.
Conclusions: The 4-steps enabled quantitative approaches to impact experimental strategy.

M-015

Population Pharmacokinetics of Intravenous Acetaminophen in Preterm and Term Neonates

Sarah F. Cook[1,*], Catherine M. T. Sherwin[2], Elaine F. Williams[3], Jessica K. Roberts[2], Amber D. King[1], Nina Deutsch[3], Samira Samiee-Zafarghandy[3], Syamala Mankala[3], Diana G. Wilkins[1,4], John N. van den Anker[3]

[1] Center for Human Toxicology, Department of Pharmacology and Toxicology, University of Utah, Salt Lake City, UT, USA; [2] Division of Clinical Pharmacology, Department of Pediatrics, University of Utah, Salt Lake City, UT, USA; [3] Division of Pediatric Clinical Pharmacology, Children's National Medical Center, Washington, DC, USA; [4] Department of Pathology, University of Utah, Salt Lake City, UT, USA

Objectives: The aims of this study were to evaluate the pharmacokinetics of intravenous acetaminophen in preterm and term neonates and to identify covariates that influence acetaminophen disposition.
Methods: Neonates with a clinical indication for intravenous analgesia received acetaminophen by 30-min infusion at 15 mg/kg/dose. Patients <28 weeks gestation received five doses at 12-h intervals; patients ≥28 weeks gestation received seven doses at 8-h intervals.

Plasma samples were collected throughout the 72-h study period, and acetaminophen concentrations were quantified by liquid chromatography-mass spectrometry. Nonlinear mixed effects models of acetaminophen concentration-time data were constructed in Monolix 4.3.2. Parameter estimation was performed using the stochastic approximation expectation maximization algorithm. Potential covariates included weight, gestational age, postnatal age, postmenstrual age, gender, and serum creatinine concentration.

Results: This preliminary analysis included 89 concentrations from the first 10 enrolled patients. Mean (SD) gestational age was 35.5 (5.5) weeks, mean postnatal age was 8.3 (6.5) days, and mean weight was 2.6 (1.1) kg. The preliminary data were well described by a one-compartment model with first-order elimination. In the final covariate model, clearance and volume of distribution were estimated as 0.151 L/h/kg (95 % CI 0.110–0.192; 21 % between-subject variability) and 1.21 L/kg (95 % CI 0.86–1.56; 12 % between-subject variability), respectively. After accounting for the influence of weight on pharmacokinetic parameters ($P < 0.001$), no other potential covariates were significant.

Conclusions: The reported one-compartment model successfully characterized intravenous acetaminophen pharmacokinetics in preterm and term neonates. Clearance and volume of distribution increased with weight. Future analyses will incorporate acetaminophen metabolite concentrations and data from additional patients.

M-016

Population Pharmacokinetics (PPK) and Optimal Dosing of Oseltamivir Administered IV and Orally to Healthy Subjects and Subjects with Renal Impairment

Leonid Gibiansky[1,*], Mylene Giraudon[2], Craig R. Rayner[3,4], Barbara Brennan[5], Vishak Subramoney[5], Richard Robson[6], Mohamed A. Kamal[5]

[1] QuantPharm LLC, North Potomac, MD, USA; [2] Roche, Basel, Switzerland; [3] D3 Medicine LLC, NJ, USA; [4] Monash University, Melbourne, VIC, Australia; [5] Roche, New York, NY, USA; [6] Christchurch Clinical Studies Trust, Christchurch, New Zealand

Objectives: To characterize the pharmacokinetics of oseltamivir phosphate (OP) and its active metabolite oseltamivir carboxylate (OC) and propose oseltamivir IV dosing regimens for treatment of influenza in patients with normal renal function and with various degrees of renal impairment.

Methods: Initially, data of 149 subjects with normal renal function and mild to severe renal impairment administered 40–200 mg oseltamivir IV were described by a 4-compartment model. Two compartments described OP, one compartment described OC, and one compartment described OP to OC metabolism (Fig. 1). Then, data of 128 subjects administered 20–1,000 mg oseltamivir orally were added. The absorption model consisted of absorption and recirculation compartments with the direct (via first-pass) and indirect (via oseltamivir) input in the OC compartment. Simulations and PK bridging were used to recommend the IV dosing regimens.

Results: Renal function had a major effect on OC clearance (CLM) and exposure. CLM for subjects with mild, moderate, and severe renal impatient was, respectively, 18, 51, and 84 % lower than for subjects with normal renal function. Simulations indicated that 75 mg IV BID dose administered to subjects with normal renal function or subjects with mild renal impairment, 30 mg IV BID dose administered to subjects with moderate renal impairment, and 30 mg IV QD dose administered to subjects with severe renal impairment provides OC Cmin coverage and exposures that are comparable to that of 75 mg BID oral dose administered to subjects with normal renal function.

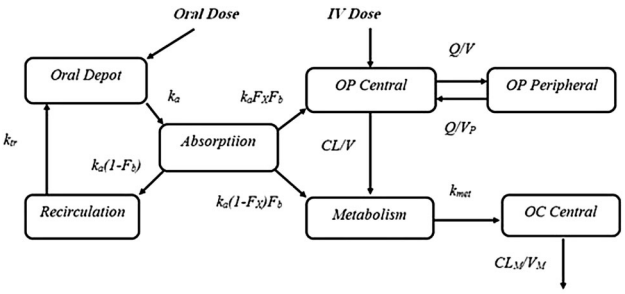

Parameter	Estimate	95%CI	Variability	Shrinkage
CL (L/hr)	184	173 - 195	CV=24.2%	6.1%
Γ	0.236	0.16 - 0.313	$CL_{OP}=CL\cdot(CL_{CR}/100)^{\gamma}$	
V (L)	25.0	20.4 - 29.5		
Q (L/hr)	92.5	85.6 - 99.3		
V_P (L)	122	115 - 129		
V_M (L)	8.91	8.55 - 9.27		
k_{met}	0.0998	0.0954 - 0.104	CV=27.5%	6.3%
$CL_{M\text{-}Emax}$ (L/hr)	33.5	28.3 - 38.8	CV=35.0%	1.2%
β	1.73	1.43 - 2.03	$CL_{OC}= CL_{M\text{-}Emax}(CL_{CR}/100)^{\beta}/[(CL_{M\text{-}EC50}/100)^{\beta}+(CL_{CR}/100)^{\beta}]$	
$CL_{M\text{-}EC50}$	70.4	54.7 - 86		
$CL_{M\text{-}AGE>80}$	0.506	0.302 - 0.71		
$k_{met\text{-}CRCL}$	0.107	0.0349 - 0.18		
k_a (1/hr)	1.63	1.47 - 1.78	CV=44.2%	35.9%
F_X	0.282	0.264 - 0.301		
k_{tr2}	0.0399	0.0359 - 0.0439		
F_b	0.874	0.868 - 0.879		

Fig. 1 Diagram and parameters of the Population PK Model for oseltamivir

Conclusions: Similar to oral dosing, IV dosing regimens of 75 mg BID, 75 mg BID, 30 mg BID, and 30 mg QD can be recommended for treatment of influenza in subjects with normal renal function, mild, moderate, and severe renal impairment, respectively.

M-017

Population Pharmacokinetics (PPK) and Optimal Dosing of Oseltamivir in Patients with End Stage Renal Disease (ESRD) on Hemodialysis (HD)

Leonid Gibiansky[1,*], Richard Robson[2], Vishak Subramoney[3], Mohamed A. Kamal[3]

[1] QuantPharm LLC, North Potomac, MD, USA; [2] Christchurch Clinical Studies Trust, Christchurch, New Zealand; [3] Roche, New York, NY, USA

Objectives: ESRD patients are at increased risk of influenza and its complications. There is no consensus on dosing of oseltamivir for treatment and prophylaxis of influenza in ESRD patients on HD. Different regimens are recommended in US and EU. We aimed to characterize the pharmacokinetics oseltamivir phosphate (OP) and its active metabolite oseltamivir carboxylate (OC) and propose optimal oseltamivir dosing regimens in this patient population.

Methods: Rich PK data of 24 subjects with ESRD on hemodialysis administered oral oseltamivir 30 or 75 mg doses were described by a 5-compartment PPK model. Two compartments with first-order absorption described OP, two compartments described OC, and one compartment described OP to OC metabolism. HD clearance was described by an additional term that was turned on during HD sessions. Simulations of several dosing regimens (30 mg after every or every other session) and PK bridging (comparison of exposures to that for subjects with normal renal function at recommended doses) were used to select the dosing regimen.

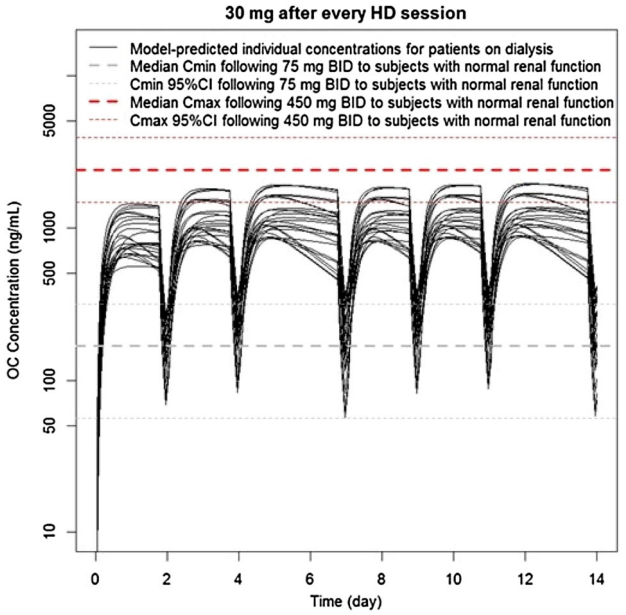

Fig. 1 Conditional predictions of OC concentrations following administration of 30 mg oseltamivir after every HD session

Results: OC clearance in ESRD subjects was very low. For a typical subject, OC apparent clearance was estimated at CLM/F = 0.189 L/h (95 % CI 0.0383–0.484 L/h), while apparent HD clearance was CLHD/F = 7.43 L/h (95 % CI 5.74–9.34 L/h). Simulated concentration-time profiles (Fig. 1) and bridging indicated the adequate OC exposure following 30 mg dose administered after every HD session. HD had no clinically relevant influence on OP exposure.

Conclusions: Results of the analysis support a regimen of 30 mg oseltamivir administered after each dialysis session for treatment of influenza in subjects with ESRD on hemodialysis. The previously recommended dose of 30 mg after alternate sessions would provide sub-therapeutic Cmin coverage. If the treatment is initiated between the dialysis sessions, the post-HD session dose should also be administered independently of the treatment initiation time. A 30 mg dose administered after alternate hemodialysis sessions, as currently recommended, is sufficient for prophylaxis.

M-018

Population Pharmacokinetics of Obinutuzumab (GA101) in Patients with Chronic Lymphocytic Leukemia (CLL) and Non-Hodgkin's Lymphoma (NHL)

Ekaterina Gibiansky[1,*], Leonid Gibiansky[1], David Carlile[2], Candice Jamois[3], Vincent Buchheit[3], Nicolas Frey[3]

[1] QuantPharm LLC, North Potomac, MD, USA; [2] Roche Innovation Center Welwyn, UK; [3] Roche Innovation Center, Basel, Switzerland

Objectives: Obinutuzumab is a novel, humanized type II anti-CD20 monoclonal antibody (mAb) with a glycoengineered Fc region. The analysis aimed to establish a predictive population model that describes PK of GA101 following IV administration and to identify covariate factors that influence its disposition.

Methods: Serum concentrations (12,634) of 678 patients (50.4 % with CLL) from 4 Phase I–III studies were analyzed in NONMEM. The full model approach was used for covariate model development.

Results: Consistent with other mAbs targeting B-cells, the two-compartment population PK model with time-dependent clearance ($CL = CL_{inf} + CL_T \times \exp(-k_{des} \times t)$) described GA101 concentrations. Parameters were estimated precisely (Table 1), and predictive check procedures indicated good predictive abilities of the model. CL_T was 2.8-fold higher than CLinf. Both values depended on diagnosis. They were 17 % lower for B-cell lymphomas and diffuse large B-cell lymphomas, and 75 % higher for Mantle cell lymphomas compared to CLL. For patients with CLL and baseline tumor size (BSIZ) >1,750 mm^2, decline of time-dependent clearance ($t_{1/2}$ = 19 days) led to steady-state after approximately 4 months for 1,000 mg q4w dosing (with 2 additional doses at weeks 1 and 2 of cycle 1). Clearance declined faster (higher k_{des}) for patients with NHL (by 108 %) and patients with BSIZ <1,750 mm^2 (by 165 %). The results are consistent with target-mediated CL (with higher CL for higher tumor burden and higher CD20 expression) that decreases with elimination of target cells.

The parameters at steady-state were typical for mAbs. CL_{inf}, CL_T, and V_c were higher in males and increased with body weight, but differences in steady-state exposure based on weight and gender were <30 %.

GA101 PK was independent of age, renal function or anti-drug antibodies (detected in 17 subjects).

Conclusions: In CLL patients, the expected differences in steady-state exposure based on weight and gender do not warrant a dose modification for the proposed 1,000 mg IV q4w dosing regimen.

Table 1 Parameter estimates of the Final Model

Parameter	Estimate	% RSE	Parameter	Estimate	% RSE
k_{des} (1/day)	0.0359	10.8	$CL_{T,DIS23} = CL_{inf,DIS23}$	0.834	3.54
CL_T (L/day)	0.231	8.43	$CL_{T,DIS4} = CL_{inf,DIS4}$	1.75	17
CL_{inf} (L/day)	0.0828	3.37	$k_{des,BSIZ<1,750}$	2.65	11.9
Vc (L)	2.76	1.38	ω^2_{kdes}	CV = 127 %	7.95[b]
Vp[a] (L)	1.01	4.47	ω^2_{CLT}	CV = 95.3 %	11.1[b]
Q (L/day)	1.29	11.5	ω^2_{CLinf}	CV = 39.9 %	7.12[b]
$CL_{inf,WT} = CL_{T,WT}$	0.615	14.8	ω^2_{Vc}	CV = 18.5 %	9.03[b]
$V_{C,WT}$	0.383	12.1	ω^2_{Vp}	CV = 60.1 %	10.6[b]
$CL_{T,SEX}$	1.49	9.7	ω^2_{Q}	CV = 94.3 %	17.5[b]
$CL_{inf,SEX}$	1.22	3.6	ω^2_{EPS}	CV = 52.3 %	10[b]
$V_{C,SEX}$	1.18	1.83	$\sigma^2_{proportional}$	CV = 17.8 %	4.52[b]
$k_{des,NHL}$	2.08	12.3	$\sigma^2_{additive}$ $(\mu g/mL)^2$	SD = 0.165	69.1[b]

CL_{inf}, non-specific time-independent clearance; CL_T, initial value of time-dependent clearance; kdes, decay coefficient of time-dependent clearance; ω^2_{EPS}, variance of inter-individual error on proportional residual error. P_{COV}, effect of covariate COV on parameter P, where DIS23 is B-cell lymphoma and diffuse large B-cell lymphoma; DIS4 is mantle cell lymphoma; WT is weight; SEX is sex; BSIZ is the baseline tumor size (mm^2)

[a] Parameters Q and Vp were scaled as (BW/75)3/4 and (BW/75), respectively

[b] Relative Standard Error (%RSE) for the estimate of variance

M-019

Modeling Population Heterogeneity in Viral Dynamics for Chronic Hepatitis C Infection: Insights from Phase 3 Telaprevir Clinical Studies

Eric Haseltine[1,*], Haobin Luo[2], John Tolsma[2], Holly Kimko[3], Doug Bartels[1], Tara Kieffer[1], Varun Garg[1]

[1] Vertex Pharmaceuticals Incorporated, Boston, MA, USA; [2] RES Group, Cambridge, MA, USA; [3] Janssen Research & Development, Raritan, NJ, USA

Objectives: We constructed a viral dynamic model to predict non-inferiority of b.i.d. (twice daily) versus q8h (every 8 h) telaprevir dosing for patients infected with the hepatitis C virus (HCV). We hypothesized that accurately estimating the viral dynamics below the limit of detection (LOD) would require incorporation of sequence data, prior interferon response, and the typical measurements of viral dynamics.
Methods: We used data from Phase 3 clinical studies of the direct-acting antiviral telaprevir combined with pegylated-interferon alfa and ribavirin (T/PR). Due to LOD, heterogeneity in some model parameters could only be estimated in specific patient subpopulations, such as patients who experienced viral breakthrough (vBT) on telaprevir or patients treated only with PR. We modified the iterative-two stage method to estimate parameter variability from these subpopulations. To verify the model, data from the treatment-naive population were withheld for (1) a T/PR regimen where telaprevir was dosed q8h for 8 weeks (T8(q8h)/PR) and (2) a T/PR regimen where telaprevir was dosed b.i.d. for 12 weeks (T12(b.i.d.)/PR).
Results: The model accurately predicted (1) sustained virologic response rates for the withheld data and (2) vBT characteristics of the T8(q8h)/PR regimen. Since the viral variants observed in vBT depend on telaprevir exposure, the second verification suggests that the model is correctly sensitive to the telaprevir dose even though the model was developed using data from a single telaprevir dosing regimen (T12(q8h)/PR). Clinical data confirmed the model prediction of non-inferiority of b.i.d. versus q8h telaprevir dosing in the treatment-naive population, and the model predicted a similar result in the PR-experienced population.
Conclusions: The developed method was useful for inferring the viral load dynamics below the LOD. Additionally, the model predicted that for T/PR regimens, b.i.d. telaprevir dosing was non-inferior to q8h telaprevir dosing in the HCV genotype 1 PR-experienced population.

M-020

Leveraging Biomarker-Outcome Relationship to Aid Early Decision Making in Multiple Sclerosis Clinical Development

Mukul Minocha, Jogarao Gobburu, Mathangi Gopalakrishnan*

Center for Translational Medicine, University of Maryland, Baltimore, Baltimore, MD, USA

Objective: Currently, go/no-go decision making in early phase multiple sclerosis trials for promising drug/dose selection is qualitative in nature. Early phase trials employ (difference in) magnetic resonance imaging lesion counts (MRI T2 counts) as endpoint, whereas, registration trials employ annualized relapse rate at 24 months (ARR-24) as the efficacy endpoint. The objective of the current investigation is to predict the probability of registration trial technical success given the early phase MRI results using the MRI T2 at 12 months and ARR-24 data digitized from Food and Drug Administration (FDA)'s 2012 Science Day presentation [1].
Methods: The ARR-24 and MRI T2 at 12 months relationship was developed assuming a negative binomial (NB) distribution for the number of relapses. This relationship was validated by clinical trial simulations. MRI T2 lesion counts at 12 months for placebo and test treatment arm were simulated assuming a NB distribution with mean and the overdispersion information available from published trials [2–4]. ARR-24 was predicted based on the relationship, given the published phase-2 results and relative bias was computed. Further, simulations were conducted assuming varying treatment effect differences in the MRI-lesion counts at 12 months to predict ARR-24. The null hypothesis of no difference in the predicted ARR-24 between test and the placebo groups was tested to project the probability of technical success of the registration trial. All simulations and statistical analysis were performed in R software (version 3.0.3).
Results: Out of the six published trials, the developed ARR-24 – MRI T2 at 12 months relationship predicted the outcomes for four of the trials correctly ($p < 0.05$), with individual trial predicted ARR-24 values within ±60 % bias. Trial simulations indicated that at least 60 % reduction in MRI T2 counts from placebo is needed to achieve a minimum of 80 % probability of technical success in the registration trial.
Conclusion: This decision toolkit will aid in selection of promising candidates early in drug development and comparing the probability of registration trial success rate to the already approved drugs. A potential regulatory application could be to employ MRI as a surrogate for ARR for approval of extensions (other populations [5, 6], dosing regimen or formulation change) of already approved new drug applications.

References:

1. Owen RP, Jain L, Zhang L, Zineh I, Office of clinical pharmacology science day: a forum to stimulate innovation in clinical pharmacology. Clin Pharmacol Ther. 2013 Jun;93(6):471–3
2. Rudick RA, Stuart WH, Calabresi PA et.al, Natalizumab plus interferon beta-1a for relapsing multiple sclerosis. N Engl J Med. 2006 Mar 2;354(9):911–23
3. Cohen JA, Barkhof F, Comi G et.al, Oral fingolimod or intramuscular interferon for relapsing multiple sclerosis. N Engl J Med. 2010 Feb 4;362(5):402–15
4. Comi G, Pulizzi A, Rovaris M et.al, Effect of laquinimod on MRI-monitored disease activity in patients with relapsing-remitting multiple sclerosis: a multicentre, randomised, double-blind, placebo-controlled phase IIb study. Lancet. 2008 Jun 21;371(9630):2085–92
5. http://www.ema.europa.eu/docs/en_GB/document_library/Scientific_guideline/2012/10/WC500133438.pdf
6. Leonard HV, Alessio S et.al, Clinical and MRI activity as determinants of sample size for pediatric multiple sclerosis trials. Neurology. 2013 Oct 1;81(14):1215–21

M-021

Cellular Network Model of Bortezomib and Vorinostat Interactions in Multiple Myeloma

Charvi Nanavati, Donald E. Mager*

Department of Pharmaceutical Sciences, University at Buffalo, SUNY, Buffalo, NY, USA

Objectives: To provide a systems-pharmacology based approach using logic-based Boolean network modeling and biomarker dynamics to identify intracellular factors regulating bortezomib and vorinostat interactions in U266 multiple myeloma cells.
Methods: A Boolean network model was developed that incorporates intracellular transduction pathways in U266 cells and mechanisms of action of bortezomib [1] and vorinostat. Network visualization, structural analysis and calculation of centrality measures were performed in yEd (yWorks GmbH, Germany). Network model simulations were conducted in Odefy, a MATLAB compatible toolbox. A reduction algorithm [2] was applied to the Boolean model to identify critical protein biomarkers for the combinatorial effects. Relative expressions of the critical proteins were measured in U266 cells with immunoblotting and compared against model simulations.
Results: The developed Boolean network model consisted of 77 nodes (intracellular proteins) and 213 edges (connections). Structural

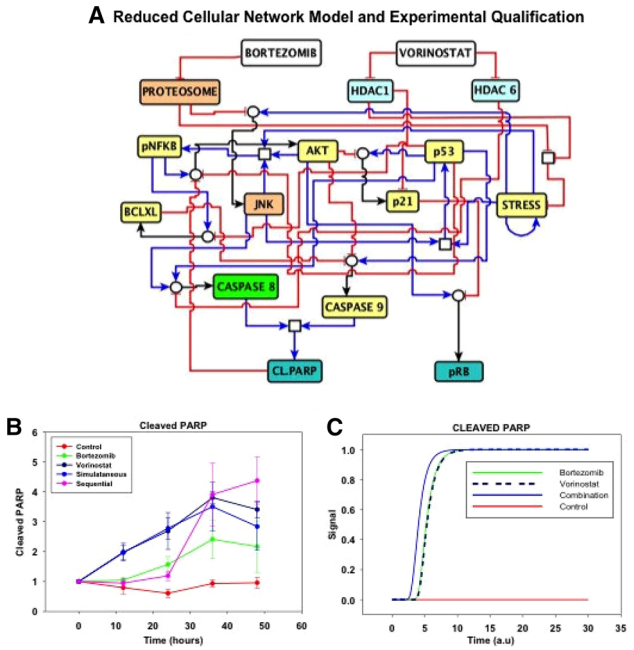

Fig. 1 Reduced network model (**a**), measured (**b**) and simulated (**c**) PARP dynamics of bortezomib and vorinostat effects (48 h exposure as single agents, in combination and 24 h preincubation with bortezomib sequence) in U266 cells. *Square*, *circle*, *blue arrow*, *left tack* and *black arrow* represent 'OR, 'AND', stimulatory, inhibitory and stimulatory plus inhibitory relationships respectively

analysis revealed pNFKB, p53, AKT, STRESS, MYC and p21 as central proteins or nodes within the combination network. A smaller network model with 16 nodes and 31 edges resulted from the application of the reduction algorithm. Model simulations qualitatively agreed with the measured time-courses of pNFKB, p21, caspase 8 and cleaved PARP. The model predicted an enhanced apoptotic effect for the bortezomib and vorinostat combination, which agreed with cleaved PARP expression from in vitro immunoblotting (Fig. 1).
Conclusions: A logic-based network model was successfully developed to evaluate the bortezomib and vorinostat combination a priori of experimentation. Model predictions agreed with temporal profiles of important proteins; however, further experiments are needed to confirm the predictions for additional proteins. This model can be used to guide the development of an enhanced pharmacodynamic model that can serve as a platform for optimizing this combination with a mechanistic rationale.

References:

1. Chudasama V and Mager DE. Poster presentation. AAPS, Washington, DC (2011)
2. Veliz-Cuba A. J Theor Biol. 289:167 (2011)

M-022

Simultaneous Modeling of SA237 Pharmacokinetics and Its Circulating Target in human Using Two-Target Quasi-Steady-State (QSS) Model

Yoshimasa Ishida*, Ryoko Takubo, Akinori Yamada, Kimio Terao, Satofumi Iida, Takehiko Kawanishi, Takahiro Kake[1]

Chugai Pharmaceutical CO., LTD, Tokyo, Japan

Objectives: SA237 is a humanized IgG2 monoclonal antibody against anti-IL-6 receptor (IL-6R). The purpose of this study is to develop a mechanism-based model to simultaneous describe the kinetics of both the unbound drug (SA237) and total circulating target (sIL-6R) in human. We attempted to determinate dose level in late stage clinical study based on mechanism-based model.
Methods: SA237 was dosed in healthy volunteer at 30, 60, 120, 240 mg (SC administration), 60 or 120 (IV administration). Blood samples for SA237 and sIL-6R were collected at pre-dose and various time points up to Day 71 post dose following SC or IV single administration. The population PK/PD model was developed using 1154 serum SA237 concentrations and 1259 serum sIL-6R concentrations from 72 subjects. Pop PK estimation was undertaken using NONMEM (version 7.1.2) by FOCE-I. The two-target quasi-steady-state (QSS) model [1] was applied to describe sIL-6R (by QSS approximation) and membrane target (by Michaelis–Menten elimination). Model performance was tested with diagnostic methods and bootstrap.
Results: The concentration-time profiles of both SA237 and sIL-6R after single administration were described by the two-target QSS model. Parameters for SA237, membrane-bound target, and sIL-6R were reasonable estimated. The model characterized the concentration time profiles for SA237 and sIL-6R with no major bias. The fixed effect parameters were: CL 0.174 [L/day], Vc 3.27 [L], CLint 0.507 [L/day], Vp 1.26 [L], F 0.831, Ka 0.228 [/day], Vmax 1.24 [nM/day], Km 2.85 [nM], Kss 0.265 [nM], Kint 0.0972 [/day], Kdeg 1.98 [/day].
Conclusions: The two-target QSS model provides mechanistic understanding of the nonlinear kinetics of SA237 and sIL-6R. PK/PD Modeling & Simulation are useful and helpful to guide late stage clinical dose selection.

References:

[1] Gibiansky L, Gibiansky E. Target-mediated drug disposition model for drugs that bind to more than one target. J Pharmacokinet Pharmacodyn. 2010 Aug;37(4):323–46

M-023

Establishing A Priori Identifiability of Target Mediated Drug Disposition Models

Rena Eudy*, Marc R. Gastonguay

Metrum Research Group, Tariffville, CT, USA; University of Connecticut, Storrs, CT, USA

Objectives: Identifiability analyses are important first steps in model design; non-identifiability can necessitate model simplification and/or areas for more informative experimental design. To date, causes of estimation difficulties of full parameter sets with target mediated drug disposition models (TMDD) [1] have not been fully investigated. This work established a priori identifiability of the TMDD model and the quasi-equilibrium/rapid-binding (QE/RB), quasi-steady state (QSS), and Michaelis-Menton (MM) approximations to this model using two systematic approaches. Identifiability of the 2-target TMDD model [2] was also established.
Methods: The differential identifiability of systems (DAISY) and exact arithmetic rank (EAR) approaches were used to analyze global and local parameter identifiability within each model with different output scenarios. Profile likelihood (PL) approach was also used with a Monte Carlo simulated dataset to mimic a "real-world" experimental system. This analysis highlighted the differences between a priori and a posteriori identifiability.

Results: The full TMDD model was a priori identifiable with any system output, as were QE/RB and QSS approximations. MM was only a priori identifiable if both free drug and total target were measured. TMDD models with two targets were identifiable if either free drug and targets or free drug and complexes were measured. The PL approach confirmed a priori identifiability of all parameters in the single-target TMDD; several of the parameters, however, were a posteriori unidentifiable with the simulated sampling scheme and model structure.
Conclusions: A priori, a posteriori, and PL diagnostic results indicated that the inability to sample on the timescale of receptor binding is the most likely culprit limiting a posteriori identifiability of the TMDD system. The number of system outputs does not affect its identifiability. Recent advances of computational algorithms allow for easy and fast determination of a priori identifiability of systems models.

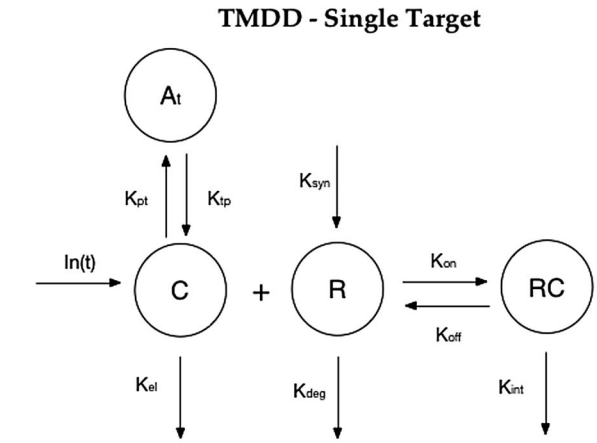

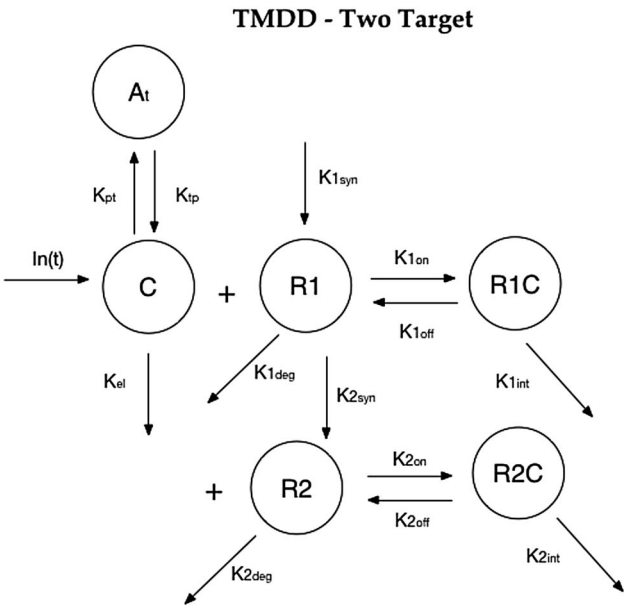

References:

1. D. E. Mager and W. J. Jusko. J Pharmacokinet Pharmacodyn, 28(6):507–532, 2001.
2. L. Gibiansky and E. Gibiansky. J Pharmacokinet Pharmacodyn, 37(4):323–346, 2010.

M-024

Pharmacokinetic–Pharmacodynamic (PK–PD) Modeling and Trial Simulation for Selection of Optimal Dose of Fedratinib (SAR302503)

Li Liu*, Christine Xu, Yaming Su, Lei Ma, Hui Quan, Vanaja Kanamaluru, Zhenming Shun, Paul Deutsch, Tal Zaks

Biostatistics, DSAR, CEP, IPP, Oncology, SANOFI, Bridgewater, NJ, USA

Objectives: Fedratinib was a JAK2-selective inhibitor for the treatment of myelofibrosis. In the pivotal Phase 3 study, two fedratinib treated groups (400 and 500 mg) showed significant and similar treatment effects compared with placebo (N = 96–97/arm). The primary objective of PK-PD modeling and simulation for fedratinib was to better understand the relationship between dose and treatment effect of Fedratinib to support selection of the optimal dose following Phase 2 and 3.
Methods: Exposure-response analyses were performed to evaluate the relationships between PK exposure and efficacy and safety endpoints of interest. Dose response relationships were constructed based on the established exposure-response relationship together with the established dose-exposure relationship from the population PK model. These analyses were utilized to predict the treatment effects of doses not studied in Phase 3 (e.g. 300 mg), and support the selection of the optimal dose. Clinical trial simulations were also conducted to investigate the treatment effect of 300 mg that was not evaluated in Phase 3.
Results: The PK-PD model predicted mean percent change in spleen volume was greater than the clinically targeted meaningful benefit of 35 % reduction for 400 mg (36.60 %) and 500 mg (40.23 %), but was less than the targeted 35 % reduction with 300 mg (30.56 %). Clinical trial simulations clearly demonstrated that 300 mg had a lower probability of achieving 35 % spleen volume reduction. The model predicted spleen response rates for 500 and 400 mg were similar (49.7 and 48.3 % respectively), but higher than 300 mg (34.0 %). The PK-PD model of anemia and exposure suggested that the patients treated with 400 mg had a lower risk for anemia than those treated with 500 mg. There was no clear exposure-response relationship with thrombocytopenia, diarrhea, nausea, and vomiting.
Conclusions: The PK-PD modeling and simulation supported the selection of 400 mg as the optimal dose, as 300 mg was suboptimal for efficacy while 500 mg had higher risk for some safety endpoints compared with 400 mg.

M-025

Quantification of the Effect of AZD5213 on Sleep in Subjects with Alzheimer's Disease or Mild Cognitive Impairment Using a Two State Markov Model

Oliver Ackaert[1,*], Tamara van Steeg[1], Kristin Hannesdotir[2], Robert Alexander[2], Karen Raudibaugh[2], Alan Kugler[2], Peter Vis[1]

[1] LAP&P Consultants BV; [2] AstraZeneca, R&D, Neuroscience iMed

Objectives: H3 antagonists have been investigated for the (symptomatic) treatment of cognitive disorders, such as Alzheimer's disease (AD) or mild cognitive impairment (MCI). H3 antagonists are effective across multiple cognitive domains (attention, memory) in preclinical studies at high receptor occupancy. However, administration of H3 antagonists in man is often accompanied by alterations in sleep patterns. This may be the result of enhanced histamine release during prolonged H3 receptor occupancy. In a Phase IIa study in

patients with mild AD and MCI the effect of AZD5213, a novel and highly selective histamine H3 antagonist, on sleep was quantified.
Methods: 81 subjects with mild AD or MCI were randomized in this double-blind, parallel group, placebo-controlled study of 4 weeks of treatment of three different doses of AZD5213. Repeated, nightly polysomnography (PSG) assessments were conducted at baseline, Week 2 and Week 4. During the PSG the sleep state per 30 s epoch was reported. This highly correlated longitudinal data was analyzed using a Markov modeling approach, in which two states were considered, WAKE and SLEEP [1].
Results: Both intensity of acquisition (u) and clearance of sleep (v) changed over time with a change in the ratio between the two intensities over time. No placebo effect was identified, while the drug concentration decreased u and v. AZD5213 plasma concentrations inhibited transitions to sleep more markedly than transitions to wakefulness. Simulations for various doses at steady state demonstrated that overall time awake increased with increasing dose with a maximum effect at doses above medium strength.
Conclusion: Simulations showed a dose-related increase in the total time awake and increased wakefulness appeared to be associated with receptor occupancies above 70 % during the entire night.

Reference:

1. Diack C. et al. A hidden Markov model to assess drug-induced sleep fragmentation in the telemetered rat. Journal of Pharmacokinetics and Pharmacodynamics, 38(6):697–711, 2011

M-026

Can We Predict Free Soluble Target Levels from Total Drug and Total Target Data alone?

Songmao Zheng, Weirong Wang*

Biologics Clinical Pharmacology, Janssen R&D, 1400 McKean Road, Spring House, PA 19438, USA

Objectives: For therapeutic monoclonal antibodies against soluble targets with rapid turnover, the parameter identifiability of a "quasi-equilibrium" target-mediated drug disposition model from total antibody and total ligand data alone was evaluated using siltuximab and interleukin-6 (IL-6) as model compounds.
Methods: The previously described model fitting was performed in NONMEM V7.2.0 with or without free target (IL-6) data after intravenous doses of siltuximab in cynomolgus monkey (Wang et al. AAPS J 2013). The parameter identifiability was examined by constructing likelihood profiles, where equilibrium dissociation constant (KD), elimination rate constant of IL-6 ($k_{el\_IL\text{-}6}$), synthesis rate of IL-6 ($k_{syn\_IL\text{-}6}$) and elimination rate constant of the IL-6-siltuximab complex (k_{el_cplx}) were fixed over a wide range of values, and the same model was re-fitted to observed total siltuximab and total IL-6 data.
Results: When all fixed-effects parameters were left to float, the model fitted observed total drug and total target data well, while the estimated KD, $k_{el\_IL\text{-}6}$ and k_{el_cplx} were significantly different from estimates when free IL-6 were included in fitting. KD, $k_{el\_IL\text{-}6}$, $k_{syn\_IL\text{-}6}$ and k_{el_cplx} can vary over 50-fold while maintaining the good fittings of total drug and total target profiles, but the predicted free IL-6 differed more than 3-fold from the observed except when KD or $k_{el\_IL\text{-}6}$ was fixed around its estimated value when free IL-6 were included in fitting. When $k_{syn\_IL\text{-}6}$ or k_{el_cplx} was fixed to estimates when free IL-6 was included in fitting, $k_{el\_IL\text{-}6}$ and K_D cannot be estimated accurately. Furthermore, $k_{el\_IL\text{-}6}$ and K_D are highly correlated.
Conclusions: K_D and $k_{el\_IL\text{-}6}$ may not be uniquely identifiable when only total drug and total target data are available. Knowledge about $k_{syn\_IL\text{-}6}$ or k_{el_cplx} does not appear to warrant accurate prediction of the free target profiles. The knowledge of k_{el_target} (e.g. via administration and measurement of radiolabeled exogenous target) should in theory allow for better prediction of the free target suppression from total drug and total target data only.

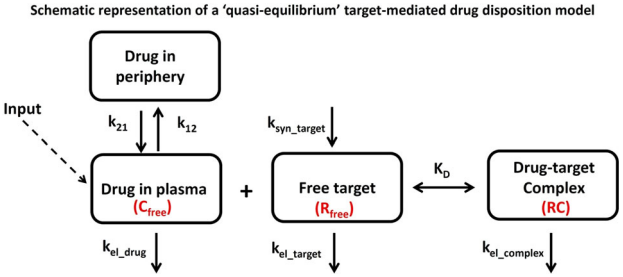

M-027

Apixaban Exposure and Anti-Xa Activity in Nonvalvular Atrial Fibrillation Patients: An Application of Population PK/PD Analysis

Ken Kowalsk[1], Jace Nielsen[1], Amit Roy[2], Neelima Thanneer[2], Wonkyung Byon[3], Rebecca Boyd[3], Xiaoli Wang[2,*], Tarek Leil[2], Frank LaCreta[2], Charles Frost[2]

[1] Ann Arbor Pharmacometrics Group, Ann Arbor, MI, USA; [2] Clinical Pharmacology and Pharmacometrics, Bristol Myers Squibb, Hopewell, NJ, USA; [3] Clinical Pharmacology, Pfizer, CT

Objectives: Apixaban is a direct, reversible Factor Xa inhibitor used in the management of thromboembolic disorders. A population pharmacokinetic (PPK) analysis was performed to describe apixaban PK and evaluate the apixaban concentration-anti Factor Xa activity (AXA) relationship in nonvalvular atrial fibrillation (NVAF) patients treated with apixaban 2.5 mg or 5 mg BID from the ARISTOTLE trial.
Methods: The PPK analysis was based on a total of 4,385 subjects, from 12 healthy volunteer and 4 patient trials, and included 2,932 ARISTOTLE patients. PPK model development occurred in 2 stages. First, phase 1 and 2 trial data were used to develop base, full and final models and evaluate the influence of covariates; then, the final Stage 1 model was adapted to incorporate ARISTOTLE data and final covariate model development. Covariate model development was performed using the WAM procedure to select a final parsimonious model based on Schwartz–Bayesian Criterion. The Stage 2 final PPK model was used to develop the PK-AXA model.
Results: A 2-compartment PPK model with first-order absorption and elimination and a linear PK-AXA model adequately described the observed data. The estimated apixaban total apparent oral CL was 3.09 L/h in a reference subject: 65 year, 70 kg, non-Asian, male NVAF patient with CrCL = 80 mL/min. Predictive covariates of apixaban PK included age, gender, Asian race, renal function, and patient status. However, individual covariate effects generally resulted in <25 % change versus the reference subject. The Table 1 provides the predicted apixaban steady-state exposure and AXA in NVAF patients.
Conclusions: PPK and PK-PD models were successfully developed and applied to predict apixaban steady state exposure and AXA in NVAF patients. Individual intrinsic and extrinsic factors had a modest effect on apixaban exposure, thus supporting twice daily administration of apixaban without dose adjustment due to effects of individual factors.

Table 1 Predicated apixaban steady-state exposure and AXA in NVAF patients

Steady state parameters[a] (Units)	5 mg BID			2.5 mg BID[b]		
	Median (90 % CI)	5th percentile	95th percentile	Median (90 % CI)	5th percentile	95th percentile
AUC (ng h/mL)	3280 (3170–3390)	1600	6590	2410 (2320–2510)	1250	4560
Cmax (ng mL)	171 (167–177)	91	321	123 (119–128)	68.5	221
Cmin (ng/mL)	103 (98.7–107)	40.9	230	79.2 (75.2–83.2)	34.4	162
Maximum anti-Xa activity (IU/mL)	2.55 (2.47–2.64)	1.36	4.79	1.84 (1.78–1.91)	1.02	3.29
Minimum anti-Xa activity (IU/mL)	1.54 (1.47–1.6)	0.068	3.43	1.18 (1.12–1.24)	0.513	242

[a] Represents daily steady state parameters

[b] Patients; received apixaban 2.5 mg BID if they met at least 2 of the following criteria: weight $\leq$ 60 kg, age $\geq$ 80 years or serum creatinine $\geq$1.5 mg/dL

M-028

Designing Optimal Basal Insulin Analogs Using a Quantitative Systems Pharmacology Model

Rukmini Kumar[1,*], Jeanne Geiser[2], Jennifer Leohr[2], Derek Leishman[2], Brian Topp[2]

[1] Vantage Research, Chennai, India; [2] Eli Lilly and Company, Indianapolis, IN, USA

Objectives: To identify optimal PK/PD characteristics for a next generation basal insulin analog that maximize efficacy and minimize hypoglycemic risk. Here we focus on quantifying the relationship between the rate of insulin absorption from the subcutaneous space into plasma (Ka) and clinical outcomes (HbA1c, Fasting Plasma Glucose and rates of hypoglycemia).
Methods: A systems pharmacology model of plasma glucose regulation was developed (Lilly Metabolism Model) and calibrated to clinical data on existing insulin therapies. Virtual patients (250) were developed and calibrated to baseline characteristics and response to basal insulin treatment (Glargine) from Zinman et al. [1]. Five theoretical insulin analogs were created with a wide range of Ka values, but identical values for clearance, bioavailability, and volume of distribution. Chronic dosing for 26 weeks was simulated for each analog in each virtual patient
Results: Ka was increased to achieve a Tmax of 6, 9, 12, 24 and 48 hr resulting in a peak to trough ratio of 5.3, 2.2, 1.6, 1.1, and 1.0 and reduced hypoglycemia (23, 13, 10, 9, 9 events <70 mg/dL per patient year) in a moderately severe Type 2 diabetic population (Initial HbA1c = 8.1 %) when predicted efficacy was similar for all insulin analogs. Similar results were obtained when titrating to various Plasma Glucose targets.
Conclusions: Simulation results presented here suggest that slowing absorption is a promising strategy for decreasing hypoglycemic risk with insulin treatment, however, this relationship appears to saturate at a Tmax of about 24 h. Since insulin analogs presently in development are approaching optimal Ka values, other characteristics, such as tissue distribution will need to be manipulated to see further reductions in hypoglycemic risk. Quantitative Systems Pharmacology models of relevant physiology can be used to visualize clinical outcomes of novel therapies and provide direction to drug development.

References:

1. Zinman B, Philis-Tsimikas A, Cariou B, Handelsman Y, Rodbard HW, Johansen T, Endahl L, Mathieu C, on behalf of the NN1250-3579 (BEGIN Once Long) Trial Investigators. Insulin Degludec Versus Insulin Glargine in Insulin-naive Patients with Type 2 Diabetes: A 1-year, Randomized, Treat-to-Target Trial (BEGINTM Once Long). Diabetes Care December 2012; 35 (12): 2464–2471

M-030

Using Innovative Tools for Personalizing Antiplatelet Therapy

Snehal Samant[1], Xi-Ling Jiang[1], Richard B. Horenstein[2], Alan R. Shuldiner[2], Laura M. Yerges-Armstrong[2], Lambertus A. Peletier[3], Xiaoyan Zhang[1], Mirjam N. Trame[1], Lawrence J. Lesko[1], Stephan Schmidt[1,*]

[1] Center for Pharmacometrics & Systems Pharmacology, University of Florida, Orlando, FL, USA; [2] Division of Endocrinology, Diabetes and Nutrition, University of Maryland School of Medicine, Baltimore, MD, USA; [3] Mathematical Institute, Leiden University, Leiden, The Netherlands

Objective: Clopidogrel (CLOP), a widely used antiplatelet agent, is associated with high between-subject variability in response to antiplatelet therapy. The objective of this study was to identify the clinically important drivers of variability in treatment response to clopidogrel by expanding a previously developed CYP2C19 genotype-directed population pharmacokinetic/pharmacodynamic (PK/PD) model by Jiang et al. (CPT 93, S1 (2013) 68) and incorporating information on all additional cytochrome P450 (CYP) and carboxyl esterase 1 (CES1) enzymes that convert CLOP to its active (CLOP-AM) and inactive metabolites.
Methods: In vitro enzyme kinetic data on CYP2C19, CYP3A4, CYP2B6, CYP2C9 and CYP1A2 enzymes (Kazui et al. DMD 38 (2010) 92–99) and clinical and genetic information from PGXB2B study (NCT01341600) was used to develop a physiology-based and genotype-directed population PK/PD model. Sobol sensitivity analysis was performed using MOEA Framework-2.0 to identify the relative contribution of each parameter to the variability in clopidogrel's PK.
Results: A model integrating information on CLOP metabolism and CYP2C19 polymorphisms was successfully established. CES1, with a 25-fold higher intrinsic clearance compared to CYP enzymes, was identified as the main driver of the system with the largest total-order sensitivity index (Fig. 1). Based on these findings, the model was mathematically reduced to make it applicable for fitting to clinical data. The reduced model improved parameter identifiability and described PGXB2B study PK data as well as the associated variability reasonably well.
Conclusion: This analysis provides an example for how information from clinical, in vitro and in silico experiments can be successfully integrated into a single unifying model and for how this model can be used to identify the clinically important drivers of the system as well as their relative contributions to interindividual variability in treatment response.

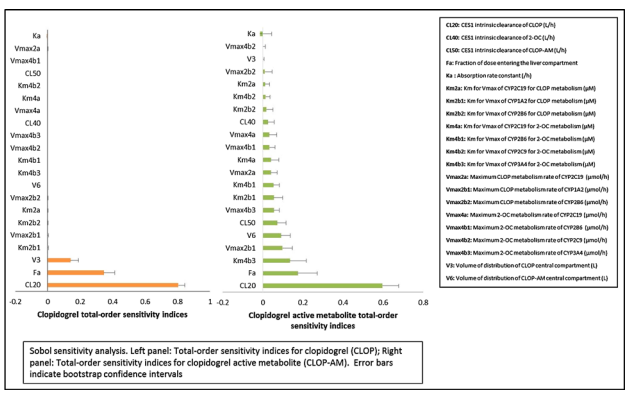

Fig. 1 Sobol sensitivity analysis

M-031

Assessment of the Therapeutic Potential of GLP-1 + GIP Using an Integrated Model of human Metabolism

Theodore Rieger[1,*], David Tess[2], Juli Jones[3]

[1] Cardiovascular and Metabolic Disease Research Unit, [2] Pharmacokinetics, Dynamics, and Metabolism, Pfizer Inc., Cambridge, MA, USA; [3] Novartis, Cambridge, MA, USA

Objectives: To predict, using a systems pharmacology model, the combined glucose-lowering potential of co-administered glucagon-like peptide 1 (GLP-1) and gastric inhibitory peptide (GIP) for the treatment of type 2 diabetes.
Methods: We constructed a mathematical model for the incretin action of GLP-1 and GIP using several published and in-house data sources, including: co-administration of the peptides on dispersed human islets, joint infusions in healthy volunteers [1], sitagliptin [2] and GLP-1 analogues [3, 4]. We then coupled the calibrated incretin sub-model into a larger, previously validated, model of human metabolism [5] to predict the effect of co-administration of these peptides on hemoglobin A1c (HbA1c). We used the integrated model to simulate a 12-week trial in patients with type 2 diabetes. Additionally, we performed a sensitivity analysis on the model to guide further experimentation, to constrain predictions of efficacy, and to understand if GIP's effect on adipocytes affects its glucose lowering potential.
Results: The integrated model successfully captured the monotherapy and joint infusion calibration data. In simulations of a 12-week clinical trial, the model predicted that additional lowering of HbA1c is possible through the addition of GIP to high-dose GLP-1, but the combination likely would not meet pre-set criteria that would justify development of a combination therapy. Our sensitivity analysis showed that uncertainty around GIP's effects on adipocytes may impact efficacy predictions.
Conclusions: Based on our current understanding of incretin biology, a dual-agonist is unlikely to yield the clinical benefit desired for a new injectable product. However, as our understanding of the non-pancreatic effects of GIP continues to evolve, this target remains of interest for further study.

References:

1. Nauck et al. JCEM. 1993.
2. Zhan et al. JEBM. 2012.
3. DeFronzo et al. Curr. Med. Res. 2008.
4. Vilsboll et al. Diabetic Medicine. 2008.
5. Entelos, Inc. http://www.entelos.com/type-ii-diabetes/

M-032

Markov Mixed Effects Modeling of Adherence using MEMS® Dosing Records from Partner's PrEP Ancillary Adherence Substudy

Kumpal Madrasi[1], Ayyappa Chaturvedula[1,*], Jessica Haberer[2], Mark Sale[4], Michael Fossler[5], David Bangsberg[2], Jared Baeten[6], Connie Celum[6], Craig Hendrix[3]

[1] Mercer University, Macon, GA, USA; [2] Massachusetts General Hospital/Harvard Medical School, Boston, MA, USA; [3] Johns Hopkins University, Baltimore, MD, USA; [4] Next Level Solutions LLC; [5] GlaxoSmithKline; [6] University of Washington, Seattle, WA, USA

Objectives: Adherence is a major factor in the effectiveness of pre-exposure prophylaxis (PrEP). Modeling adherence can help identify covariates influencing adherence which may be useful for adherence interventions. Here, we develop a Markov mixed effects model to discern covariates influencing adherence.
Methods: Medication Event Monitoring Systems (MEMS®) data from 1,147 individuals from Partners PrEP ancillary adherence substudy was used for model building [1]. Multiple openings on the same day were considered as only one dose taking event. One coin and, first, second and third order Markov models were fit to the data using NONMEM 7.2 and the Laplacian estimation method. Model selection criteria included NONMEM objective function value (OFV), Akaike information criterion (AIC), visual predictive checks and posterior predictive checks using longest drug holiday (LDH) [2] or non-therapeutic time (NTT) [2]. Covariates were included based on forward addition ($\alpha = 0.05$) and backward elimination ($\alpha = 0.001$) tests.
Results: Markov models satisfied model diagnostics better than the one coin model. A third order Markov model gave the lowest OFV and AIC but the simpler first order model was used for covariate model building as no additional benefit on LDH and NTT prediction was observed for higher order models. Final parameters were listed in Table 1. Women had better adherence while younger age, weekend dosing and no sex as well as sex with an outside partner had negative impact on adherence. Arms of trial, heavy alcohol use and polygamy were also tested, but were not significant.
Conclusions: A first order Markov model was developed to describe the adherence using MEMS®. Our findings suggest adherence interventions should consider the role of gender, age and nature of sexual relationship.

Table 1 Final parameter estimates with relative standard errors (RSE)

Parameter	Estimate	RSE (%)
P_{01} (Positively correlated with adherence)	0.7	1.8
P_{10} (Negatively correlated with adherence)	0.067	5.5
Effect of no sex on P_{01}	−0.14	20.8
Effect of sex with partner other than study partner on P_{10}	0.4	14.14
Effect of sex with partner other than study partner on P_{01}	−0.13	36.9
Effect of no sex on P_{10}	0.18	19.94
Effect of female gender on P_{10}	−0.6	12.18
Effect of youth (age: 19–28) on P_{10}	0.51	18.73
Effect of sex with other partner and study partner on P_{01}	0.056	43.61
Effect of weekend on P_{01}	−0.036	24.45
Effect of weekend on P_{10}	0.063	28.75

References:

1. Haberer, J.E., et al., PLoS Med, 2013. 10(9): p. e1001511
2. Girard, P. et al., Stat Med, 1998. 17(20): p. 2313–33g

M-033

A Model-Based Meta-analysis of Monoclonal Antibody Pharmacokinetics

Jasmine P. Davda*, Michael G. Dodds, Megan A. Gibbs, Wendy Wisdom, John P. Gibbs

Amgen Inc., Pharmacokinetics and Drug Metabolism, Seattle, WA, South San Francisco, CA, and Thousand Oaks, CA, USA

Objectives: The objectives of this retrospective analysis were (1) to characterize the population pharmacokinetics (popPK) of 4 different monoclonal antibodies (mAbs) in a combined analysis of individual data collected during first-in-human (FIH) studies and (2) to provide a scientific rationale for prospective design of FIH studies with mAbs.
Methods: The data set was comprised of 171 subjects contributing a total of 2716 mAb serum concentrations, following intravenous (IV) and subcutaneous (SC) doses. mAb PK was described by an open 2-compartment model with first-order elimination from the central compartment and a depot compartment with first-order absorption. Parameter values obtained from the popPK model were further used to generate optimal sampling times for a single dose study.
Results: A robust fit to the combined data from 4 mAbs was obtained using the 2-compartment model. Population parameter estimates for systemic clearance and central volume of distribution were 0.20 L/day and 3.6 L with intersubject variability of 31 and 34 %, respectively. The random residual error was 14 %. Differences (<2-fold) in PK parameters were not apparent across mAbs. Rich designs (22 samples/subject), minimal designs for popPK (5 samples/subject), and optimal designs for non-compartmental analysis (NCA) and popPK (10 samples/subject) were examined by stochastic simulation and estimation. Single-dose PK studies for linear mAbs executed using the optimal design are expected to yield high quality model estimates, and accurate capture of NCA estimations.
Conclusions: This model-based meta-analysis has determined typical popPK values for 4 mAbs with linear elimination and enabled prospective optimization of FIH study designs, potentially improving the efficiency of FIH studies for this class of therapeutics.

M-034

Disease Progression Model for Clinical Dementia Rating Sum of Boxes in Mild Cognitive Impairment and Alzheimer's Subjects from Alzheimer's Disease Neuroimaging Initiative

Mahesh N. Samtani*, Nandini Raghavan, Gerald Novak, Partha Nandy, Vaibhav A. Narayan, for the Alzheimer's Disease Neuroimaging Initiative

Janssen Research & Development, LLC, Raritan, NJ, USA

Objectives: The objective of this analysis was to develop a non-linear disease progression model using an expanded set of covariates that captures the longitudinal clinical dementia rating scale-sum of boxes (CDRSB) scores from the ADNI-1 study that consisted of 301 Alzheimer's disease (AD) and mild cognitive impairment (MCI) patients who were followed for 2 3 years.
Methods: The model describes progression rate and baseline disease score as a function of covariates. The covariates that were tested fell into 5 groups: (a) hippocampal volume; (b) serum and CSF biomarkers; (c) demographics and ApoE4 status; (d) baseline cognitive tests; (e) disease state and co-medications.
Results: Covariates associated with baseline disease severity were disease state, hippocampal volume and co-medication use. Disease progression rate was influenced by baseline CSF biomarkers, trail making test part A score, delayed logical memory test score, and current level of impairment as measured by CDRSB. Rate of disease progression was dependent on disease severity, with intermediate scores around the inflection point score of 10 exhibiting high disease progression rate. The CDRSB disease progression rate in a typical patient with late MCI and mild AD was estimated to be approximately 0.5 and 1.4 points/year.
Conclusions: In conclusion, this model describes disease progression in terms of CDRSB changes in patients and its dependency on novel covariates. The CSF biomarkers included in the model discriminate MCI subjects into progressors and non-progressors. Therefore, the model may be utilized for optimizing study designs through patient population enrichment and clinical trial simulations.

M-035

A Quantitative Systems Pharmacology (QSP) Approach to Understand the Pathogenesis of Acne and to Evaluate New Acne Therapies

Loveleena Bansal[1,*], Tom Wilde[3], Akanksha Gupta[2], Grace Kang[2], Steve Frey[2], Betty Hussey[2], Valeriu Damian-Iordache[3]

[1] Stiefel, Discovery & Preclinical Development, Upper Merion, PA, USA; [2] Stiefel, Discovery & Preclinical Development, RTP, NC, USA; [3] GlaxoSmithKline, Modeling and Translational Biology, Upper Merion, PA, USA

Objectives: Acne is a multifactorial disease with limited understanding of its pathogenesis in part due to a lack of animal models. Thus, a QSP based approach was used to understand the complex interplay between the processes involved in acne and their role in disease progression.
Methods: The QSP model for Acne was developed previously [1] with a detailed description of processes like sebum production, *P. acnes* growth, comedogenesis and inflammation, their modulation by currently available treatments and resulting effects on clinical outcomes. The parameters describing the rate of different processes were perturbed to study the effect on disease progression and its severity. Also, novel acne treatments were simulated by inhibiting potential targets in the model and the results were compared with currently available acne treatments.
Results: Our analysis demonstrates that changes in sebum composition due to an increase in oxidized inflammatory lipids can be a major precursor for Acne. Moreover, excessive *P. acnes* colonization in the hair follicles was observed to occur much later than altered sebum composition and comedogenesis. Also, in contrast to the current therapies that work primarily by killing *P. acnes*, our results show that potential therapies that inhibit the formation of oxidized lipid leukotriene B4 (LTB4) and inflammatory cytokines (e.g. IL17) should be quite significant in reducing the acne severity (Figure 1).

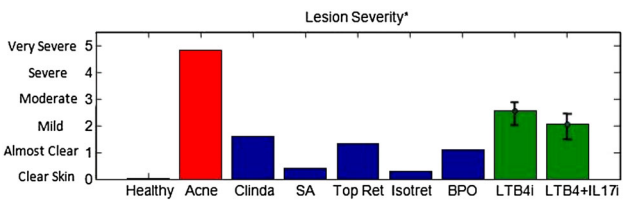

Fig. 1 Comparison of the effect of current and novel acne treatments in reducing lesion severity for an acne patient. *Healthy* healthy person with clear skin, *Acne* patient with very severe acne; Effect of different treatments: *Clinda* Clindamycin, *SA* salicylic acid, *Top Ret* topical retinoids, *Isotret* isotretinoin, *BPO* benzoyl peroxide, *LTB4i* LTB4 inhibition (70–95 %), *LTB4+1L17i* LTEA and IL17 inhibition (70–95 % each); *Equivalent to Investigator's Global Assessment (IGA) Scale by FDA

Conclusions: These findings support the new paradigm for acne pathogenesis in which the presence of oxidized inflammatory lipids rather than *P. acnes* proliferation is the major factor in causing the disease. Moreover, this highlights the importance of a new class of acne treatments that target the oxidized lipids and inflammatory mediators in the skin.

References:

1. Kang, E. G. et al. Annual Meeting of the Society for Investigative Dermatology, May 2014, Alburquerque, NM (Poster).

M-036

Population Pharmacokinetics (PK) of Sorafenib: A Meta-analysis of Patients with Hepatocellular Carcinoma (HCC), Renal Cell Carcinoma (RCC), and Differentiated Thyroid Carcinoma (DTC)

N.H. Prins[1,*], J. Grevel[2], D. Mitchell[3], J. Lettieri[4], B. Ploeger[5], C. Peña[4]

[1] qPharmetra, Netherlands; [2] BAST Inc., UK; [3] Mitchell Pharmaceutical Consulting, Lafayette, CO, USA; [4] Bayer HealthCare Pharmaceuticals, Montville, NJ, USA; [5] Bayer Pharma AG, Berlin, Germany

Objectives: A meta-analysis was conducted to develop a population PK model with important covariate influences for the multikinase inhibitor sorafenib.

Methods: Plasma was collected from healthy volunteers (dense sampling) and oncology patients (dense or sparse sampling) enrolled in 10 Phase I, II, and III clinical trials. Healthy volunteers received a single dose of sorafenib and oncology patients were treated with sorafenib 400 mg orally twice daily. Population PK were analyzed using NONMEM v7.2.

Results: 3,141 sorafenib concentrations from 859 subjects (211 women), including 39 healthy volunteers, 332 patients with RCC, 332 with HCC, and 156 with DTC were included in the analysis. The data supported a 1-compartment model with 3 sequential transit absorption compartments that resulted in a flat steady-state profile over the 12-h dosing interval. The impact of covariates on sorafenib apparent clearance (CL/F) was assessed using forward inclusion ($p < 0.01$) and backward elimination ($p < 0.001$). Body weight, body mass index, race (Asian/non-Asian), age, liver transaminases, albumin, bilirubin, alkaline phosphatase, lactate dehydrogenase, prothrombin time, creatinine clearance, co-medication with CYP3A4 or UGT1A9 inducers or inhibitors, or thyroxine did not significantly influence CL/F. The only significant covariate was gender, with females having on average a 27 % higher exposure. An average 103 % increase in sorafenib exposure was observed in DTC patients (DECISION Study 14295), which was unexplained by covariates and therefore modeled as a study effect on CL/F. The analysis suggested steady-state sorafenib concentrations do not change over time. The apparent volume of distribution was estimated as 554 L with inter-individual variability of 75 % CV for proportional error. The inter-individual variability of CL/F was 52 % CV.

Conclusions: The proposed model describes sparse data from late-phase clinical studies and densely sampled profiles from healthy volunteers. Gender and a study effect for DTC patients were the only significant covariates affecting sorafenib exposure.

Sorafenib clearance and exposure estimated from a population PK meta-analysis

Gender	CL/F(L h^{-1})		Study 14295 effect (%)	$AUC(0\text{-}12)_{ss}$ (mg h L^{-1})		Study 14295 effect
	Non-DTC[a]	DTC		Non-DTC[a]	DTC	
Male	9.44	4.66	−50.6	42.4	85.8	103 %
Female	7.45	3.68		53.7	109	
Gender effect	−21.1 %			26.7 %		

AUC area under the curve

[a] Non-DTC: excludes 156 patients with DTC

M-037

Model-Based Comparison of Monoclonal Antibody Dosing Strategies for Application in Children

Songmao Zheng[1], Puneet Gaitonde[1], Marilee A Andrew[2], Megan A Gibbs[2], Lawrence J Lesko[1], Stephan Schmidt[1,*]

[1] Center for Pharmacometrics and Systems Pharmacology, University of Florida, Gainesville, FL, USA; [2] Department of Pharmacokinetics and Drug Metabolism, Amgen, Seattle, WA, USA

Objectives: Body weight (BW)-based and/or tiered fixed dosing is widely utilized to scale adult clinical doses to children for monoclonal antibodies (mAbs) that exhibit linear clearance. However, whether these scaling strategies are also applicable to mAbs that exhibit target-mediated drug disposition (TMDD) is unclear and warrants further investigation.

Methods: A published TMDD model for an anti-ALK1 receptor mAb was adopted (Luu et al., JPET 2012) and its linear clearance component and volume of distribution were scaled from adults to children using a BW-based allometric function with fixed exponents of 0.75 and 1, respectively. A set of hierarchical simulations was performed to compare BW-based versus fixed dosing and Full TMDD versus Michaelis–Menten approximation for the same target concentration versus same target amount in adults and children, respectively. Sensitivity analysis was performed for target concentrations and amounts to determine their relative impact on free drug concentrations and target occupancy.

Results: For the same target concentrations, drug exposure becomes increasingly similar between adults and children with increasing target concentrations and decreasing doses following BW-based dosing, whereas the opposite holds true if the target amount is the same. In comparison, fixed dosing results in increased mAb exposure in children of young age, at low doses and high amounts of target. Despite different systemic mAb concentrations, target occupancy is quite similar between adults and children. Michaelis–Menten approximation yielded similar profiles compared to the full TMDD model and may be used to guide the selection of pediatric dosing regimen.

Conclusions: The pharmacokinetics of mAbs exhibiting TMDD has to be interpreted in a pharmacokinetic/pharmacodynamic context

because similar drug exposure does not have to result in similar target occupancy in adults and children. Our simulations suggest that BW-based dosing is superior to fixed dosing for the same target concentration, whereas the opposite is observed for the same target amount in adults and children.

M-038

A Population Pharmacokinetic Analysis of Once-Daily Intravenous Bsulfan in Pediatric Patients Undergoing Hematopoietic Stem Cell Transplantation

Su-Jin Rhee, Kyung-Sang Yu, Kyoung Soo Lim, Howard Lee*

Department of Clinical Pharmacology and Therapeutics, Seoul National University College of Medicine and Hospital, Seoul, Korea

Objectives: Busulfan is a bifunctional alkylating agent, which is indicated for use in combination with cyclophosphamide as a conditioning regimen prior to hematopoietic stem cell transplantation (HSCT). The aims of this study were (1) to characterize the population pharmacokinetics of once-daily intravenous (IV) busulfan in pediatric patients undergoing HSCT, and (2) to identify significant covariates that might affect the pharmacokinetic parameters of busulfan in this population.
Methods: A population pharmacokinetic analysis was performed using 1894 busulfan concentrations in 119 pediatric patients, who received an IV busulfan and cyclophosphamide regimen for 4 days before undergoing HSCT. The first-order conditional estimation with interaction estimation method implemented in NONMEM (version 7.2) was used, which was followed by model qualification using bootstrapping and visual predictive checks (VPCs).
Results: A one-compartment open linear model with proportional residual error, which also included inter-individual (IIV) and inter-occasion variability (IOV) for clearance (CL) and volume of distribution (V), and their covariance, adequately described the concentration-time profiles of busulfan. Body surface area (BSA) was a significant covariate for CL and V, while age was significant only for CL. The typical population estimates of CL and V for an adult with BSA of 1.73 m^2 were 10.4 L/h and 45.1 L, respectively. Busulfan CL matured as age was increased with 99.2 % of the adult value being achieved at 2.6 years. The IIV of CL and V was 24.7 and 22.4 %, respectively, while the IOV of CL and V was 12.7 and 10.1 %, respectively. Model evaluation by bootstrapping and VPCs suggested that the proposed model was adequate, robust, and stable, and the parameters were estimated with good precision.
Conclusions: Population pharmacokinetic parameters for IV busulfan were successfully estimated in pediatric patients. This robust model can be utilized for further population pharmacokinetic–pharmacodynamic investigation, which is currently ongoing.

M-039

Early Clinical Development of a Potent Immunomodulator for Dermal Application: Use of Probabilistic Risk Analysis Approaches to Address Uncertainty

Cathrine Leonowens[1,*], James Lee[5], Jean-Philippe Therrien[5], Claire Ambery[2], Diana Quint[3], Mark Price[4], Ginny Schmith[1]

GlaxoSmithKline, Research Triangle Park, NC, USA[1]; Stockley Park, London, UK[2] ; Stevenage, UK[3]; Ware, UK[4] ; Stiefel, a GSK Company, Research Triangle Park, NC, USA[5]

Objectives: GSK2245035B is a potent, selective TLR7 agonist undergoing development for dermal and intranasal application. Historically, criteria used to guide dose selection and study design in early clinical development of dermal products were qualitative and characterized by high uncertainty and variability in preclinical models. The objective of this work was to use probabilistic risk analysis (PRA) approaches that allow for comprehensive use of all available data (formulation, skin penetration and exposure, and in vitro response), accounting for variability and uncertainty, to quantitatively optimize dose selection and study design in early clinical development while maximizing PoS and minimizing risks to patients and development timelines.
Methods: Preclinical in vitro and in vivo data, clinical study results, published data, and questions raised by team members were used to inform and simulate ($n = 10{,}000$) several scenarios (ModelRisk, Vose Software, Belgium) to predict pharmacokinetics and pharmacodynamics of GSK2245035B in humans including efficacy, tolerability, skin penetration, accumulation, and amount reaching target cells.
Results: Simulations suggest that the safe and clinically effective dermal dose is most likely ($Pr \geq 80$ %) between 0.001 and 0.05 % GSK2245035B. Clinical response data simulated for a 16- and 160-subject clinical study revealed that there is a low probability of differentiating from comparator based on efficacy ($Pr \leq 20$–40 %) and a high probability ($Pr > 80$ %) of differentiating based on tolerability.
Conclusions: Results from PRA analysis lead to the design of a more efficient FTIH, adaptive design, dose-escalation clinical study and allowed the project team to set realistic goals and expectations around how GSK2245035B can achieve its asset profile.

References:

1. Quint, D. Preclinical evaluation of GSK2245035, a potent and selective toll-like receptor 7 (TLR7) agonist. European Respiratory Society 2014 International Congress, #850362
2. Quint, D. Single and repeat dose safety and pharmacodynamics studies with the selective intranasal TLR7 agonist GSK2245035. European Respiratory Society 2014 International Congress, #851395.

M-040

Population Pharmacokinetic Analysis of Pregabalin Controlled-Release Formulation in Patients with Partial Seizures and Fibromyalgia

Guangli Ma[1], Rujia Xie[1], Scott Marshall[1], Verne Pitman[2], Holly Posner[2], Jeffrey Patrick[2], Joseph Scavone[2], Marci L. Chew[1]

[1] Clinical Pharmacology, Lund, Sweden; [2] Clinical Sciences, Pfizer, Inc., Groton, CT, USA

Objectives: A population pharmacokinetic (PK) model was developed to characterize the PK of pregabalin controlled-release formulation (PGB-CR) in patients.
Methods: Two Phase 3 studies were included in the analysis with a total of 612 patients receiving once daily PGB-CR (165–495 mg) following the evening meal. Up to 3 trough PK samples were collected on separate occasions for each patient. A previously developed model based on 14 Phase 1 (including 9 PGB-CR) studies was used to initiate current analysis. Due to the sparse data, structural parameters and covariates for absorption and volume of distribution (V/F) were fixed to Phase 1 estimates. The relationship between baseline creatinine clearance (CLcr) and PGB-CR clearance (CL/F) (linear with a breakpoint), interindividual variability (IIV) on CL/F, and residual error were estimated. This analysis was conducted in two steps (1) individual study and (2) joint analysis.

Table 1 Parameter estimates for final model

Parameter	Patients with partial seizures Estimate [95 % CI][a]	Patients with fibromyalgia Estimate [95 % CI][a]	Both patient groups Estimate [95 % CI][a]	Units
CL/F[b]	4.96 [4.73, 5.19]	4.67 [4.33, 5.01]	4.77 [4.56, 4.98]	L/h
Breakpoint[c]	127 [118.9, 135.1]]	129 [114.4, 143.6]	129 [116.1, 141.9]	ml/min
IIV on CL/F	0.207 [0.161, 0.244]	0.313 [0.132, 0.422]	0.285 [0.227, 0.333]	
Residual	0.437 [0.390, 0.484]	0.518 [0.407, 0.629]	0.480 [0.445, 0.515]	
V/F[d]	45.1 [fixed]	45.1 [fixed]	45.1 [fixed]	L

$CLcr_{ref}$: median CLcr from Phase 1 data (112.7 ml/min), FLAG = 0 when CLcr > breakpoint (θ_{BP}) and FLAG = 1 when CLcr ≤ breakpoint

CI confidence interval, *CL/F* PGB-CR clearance,*IIV* interindividual variability, *V/F* volume of distribution

[a] 95 % CI was calculated using the standard error reported in the NONMEM output

[b] $CL/F = \theta 1 * (CLcr_i/CLcr_{ref}) * FLAG + \theta 1 * (\theta_{BP}/CLcr_{ref}) * (1\text{-}FLAG)$

[c] A creatinine clearance breakpoint was introduced to account for overestimation of clearance by Cockcroft–Gault equation for overweight patients

[d] Fixed based on phase 1 estimate

Results: PGB-CR PK was adequately characterized using a one compartment model with first order elimination and Weibull function for absorption fixed to prior estimates. CL/F was directly related to CLcr when CLcr below the breakpoint and CL/F was independent of CLcr when CLcr greater than breakpoint. The typical CL/F for patients with CLcr of 112.7 ml/min was 4.77 L/h from joint analysis (Table 1), while for patients with CLcr greater than breakpoint 129 ml/min, CL/F was calculated to be 5.46 L/h. Only IIV on CL/F was kept and estimated in the model because of lack of information in current data to support IIV on other parameters. In general, the diagnostic plots and visual predictive check demonstrated that the final model described PGB-CR phase 3 data well.
Conclusions: The final model adequately characterized Phase 3 data. The relationship between CLcr and CL/F and the observed increase in variability with the Phase 3 data are consistent with the analyses of PGB-CR Phase 1 data as well as PGB immediate release patient data.

M-041

The Modelling and Simulation Workbench: Enabling Model-Based Decisions in Drug Development

Richard Pugh[1,*] for the Core Team: Chris James[1], Jonathan Chard[1], Angela Stringer[1], Vicky Paul[1], Kam Chana[2], Carolyn Cho[2], Anna Kondic[2], Eric Keaton[2], Mark Kruger[2], Extended team: Malidi Ahamadi[2], Mark Atkinson[2], John Burke[2], Navin Das[2], Jeroen Elassaiss-Schaap[2], Peter Forster[2], Vern Henry[2], Janet Kutner[2], Junghoon Lee[2], John Panek[2], Teun Post[2], Matt Rizk[2], Carol Rohl[2], Murali Samala[2], Ad Thiers[2], Pavan Vaddady[2], Ryan Vargo[2], Sandra Allerheiligen[2], Jason Johnson[2], Jerry Schindler[2], Greg Winchell[2], Thomas Kerbusch[2], Henrik Nyberg[1], Richard Corfield[1], Mike Creed[1], Dylan Turner[1]

[1] Mango Solutions, Chippenham, UK; [2] Merck Sharp & Dohme, Whitehouse Station, NJ, USA

Objectives: The aims of this work are to develop a software platform that would:

- Provide a regulated environment for modeling work supporting health regulatory drug development activities
- Provide a secure, auditable model management system
- Allow for the storage, management and searching of modelling knowledge
- Provide a sophisticated model development platform
- Apply rigour to the modelling process without adding overhead to the modeller
- Provide a basis for standardisation and best practices across a modelling team

Methods: The MSWB team collaborated to design an integrated knowledge management and model development platform, meeting the requirements of a health regulated system. The platform has been deployed at Merck, and is required for all PKPD modelling activities at Merck. The MSWB team developed requirements, architecture and software to create a platform that integrates several elements.

- Security and controlled access, allowing for blinded and due diligence modeling projects
- Searchable and annotated model repository
- Supports model development workflow around NONMEM, including R and Matlab scripting
- Execution of jobs on a high performance computing systems
- Invisiblë rigour (audit trail, versioning, meta data discovery)

Notably, the system supports a range of technical use, encompassing everything from "command line" access to visual "model review" tools.
Results: Key system features will be demonstrated via screenshots, highlighted by the factors driving the design (such as model review, knowledge integration, remote execution).
Conclusions: Navigator Workbench provides a knowledge driven modelling platform that effectively supports the use of modelling for decision-making on drug development programs at Merck.

M-042

Model-Based-Meta-analysis to Characterize Unified Parkinson's Disease Rating Scale Part 3 Motor Score (UPDRS-Motor) in Parkinson's Disease (PD) Patients: Longitudinal Time Course and Short-Term Relationship with respect to Levodopa Concentrations

Jae Eun Ahn[1,*], Timothy Nicholas[2], Danny Chen[1]

[1] PTx Neuroscience Clinical Pharmacology, Pfizer, Cambridge, MA, USA; [2] Pharmacometrics, Pfizer, Groton, CT, USA

Objectives: UPDRS has been primarily used to evaluate PD. As PD patients develop motor fluctuations over time, it is important to understand the short-term variation in UPDRS-motor as well as the longitudinal disease progression when designing clinical studies. The objectives of these analyses were to: (1) develop a longitudinal model for UPDRS-motor in PD patients with levodopa background therapy, and (2) characterize a short-term pharmacokinetic–pharmacodynamic relationship using metadata from the literature.
Methods: (I). Literature search with the keywords of PD, anti-Parkinson medications, and randomized clinical trials returned 151 papers published between 1978 and 2013, and 73 papers reported UPDRS-motor for ≥4 weeks were included in the analysis. Exponential decrease plus linear disease progression model was applied for placebo data that were on levodopa or other background therapy. Treatment effects in addition to the background therapy were also characterized for each drug class. (II). Eight studies evaluated UPDRS-motor hourly for up to 6 h following levodopa administration were included for short-term pharmacokinetic/pharmacodynamic

analysis. Inhibitory E_{max} model with an effect compartment characterized was fitted to such data.
Results: In long-term analysis, maximum placebo response (P_{max}) was estimated to be 2.73 points (RSE 12.6 %) with the half-life to reach Pmax of 4.35 weeks (4.85 %). The estimated rate for disease progression was 2.5 points worsening per year. In the short-term analysis, a maximum response in UPDRS-motor was 19.6 (RSE 94.9 %). In both analyses, residual variability was estimated to be $\sim$3 points (in SD).
Conclusions: The amplitude of hourly changes in UPDRS-motor was greater than the ones captured in longitudinal studies for PD patients. In addition to understanding the duration of study needed for the placebo response to stabilize, assessing when to measure UPDRS-motor in relation to dosing is an important consideration in designing PD clinical studies.

M-043

Pharmacokinetic–Pharmacodynamic Modeling and Simulation to Guide Dose Selection for a Compound in Early Clinical Development

Kai Wu*, Peiming Ma

GlaxoSmithKline, Clinical Pharmacology Modeling & Simulation, Shanghai, China

Objectives: To characterize the dose–exposure–response relationship for compound X, and conduct simulation to support dose selection for the further clinical development
Methods: The plasma pharmacokinetic (PK) and pharmacodynamic (PD) data from the first-time-in-human (FTIH) study of compound X was used for the modeling. The FTIH study was a single-dose, dose-escalating, crossover study in healthy subjects. The evaluated doses ranged from 0.5 to 750 mg and were administered in the fasted or the fed condition. Plasma samples were taken to measure drug concentration and PD response from pre-dose up to 96 h post dose. Population PK and PK-PD models were developed using NONMEM-VII. Simulation was then conducted to evaluate PD response after repeat dosing of different doses.
Results: A two compartment model with 1st order absorption described the plasma concentration time course well. It was observed that the exposure (C_{max} and AUC) increased less than dose proportionally in both fasted condition from 0.5 to 250 mg and fed condition from 8 to 750 mg. To account for such nonlinearity, relative bioavailability parameter (F1) was introduced into the model and described as functions of dose:

$$0.5\,\text{mg} \leqslant \text{dose} \leqslant 8\,\text{mg},\ \text{fasted},\ F1 = 1.24 \times \text{dose}^{(-0.28)};$$
$$\text{dose} > 8\,\text{mg},\ \text{fasted},\ F1 = F1 \text{ of } 8\,\text{mg};$$
$$8\,\text{mg} \leqslant \text{dose} \leqslant 750\,\text{mg},\ \text{fed},\ F1 = 0.0639 + (1 - 0.0639) \times 1{,}120/(1{,}120 + \text{dose}).$$

The functions of dose for F1 require a necessary condition in the specified dose range, which was verified for all functions used. In the range of 8–250 mg, dosing compound X with food increased its F1, and the food effect was higher at lower dose.

Graphical analysis showed that there was no apparent time lag between the PK exposure and PD response. The direct inhibitory effect of PK on PD was well described by an E_{max} model: $E = E_0 \times (1 - Cp/(Cp + IC50))$. IC50 was estimated as 11.6 ng/mL.

Simulation showed that lower daily dose is required for a twice-daily regimen than a once-daily regimen to reach the same level of PD response (Figure 1).
Conclusions: Population PK-PD model was established to characterize the dose–exposure–response relationship of compound X.

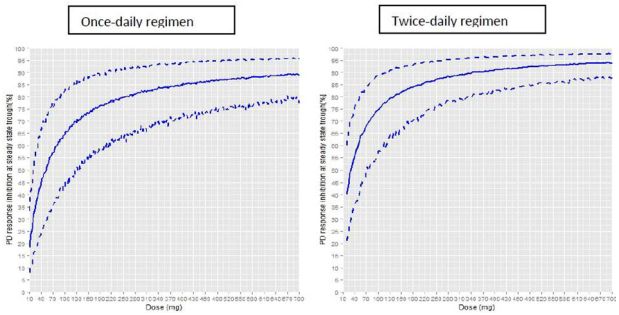

Fig. 1 Predicted dose–response for trough PO inhibition at steady state after once-daily or twice-daily repeat dosing of compound X. *Solid lines* represent medium response of 1,000 simulated subjects; *dashed lines* represent 5th and 95th percentile response of 1,000 simulated subjects

Simulation showed that a twice-daily regimen would be favored over a once-daily regimen. Simulation also provided guidance on dose selection for the future study.

M-044

Development of a Population PK Model of Unfractionated Heparin in Paediatric Patients

Hesham S Al-Sallami[1,*], Fiona Newall[2], Paul Monagle[2], Vera Ignjatovic[3], Noel Cranswick[4], Stephen Duffull[1]

[1] School of Pharmacy, University of Otago, Dunedin, New Zealand; [2] Department of Paediatrics/Royal Children's Hospital, University of Melbourne, Melbourne, VIC, Australia; [3] Murdoch Childrens Research Institute, Melbourne, VIC, Australia; [4] Department of Pharmacology, University of Melbourne, Melbourne, VIC, Australia

Introduction: Unfractionated heparin (UFH) is the anticoagulant of choice in paediatric patients undergoing a variety of cardiac procedures. The ability to predict the dose–response relationship of UFH is essential in order to optimise its dosage. Total body weight is often used as a size descriptor, however it may not correlate well with drug clearance and the use of this parameter in dose calculation may result in over- or under-dosing particularly at the extrema of size. Recently a fat-free mass (FFM) model has been developed for children and may be a suitable descriptor of size in relation to drug disposition.
Objectives: To develop and evaluate a model to predict the dose–response relationship of UFH in paediatrics using various size descriptors as covariates.
Methods: Data from 64 infants and children who received 75–100 IU/kg of UFH during cardiac angiography were analysed. Four plasma samples were collected at 15, 30, 45, and 120 min post-dose. UFH concentration was measured using a protamine titration assay. One and two compartment pharmacokinetic models with linear and non-linear elimination were fitted to the data using the non-linear mixed effects modelling software NONMEM v7.2. Various patient covariates such as age, sex, weight, and FFM were tested. The final model was evaluated using the likelihood ratio test and visual predictive checks (VPCs).
Results: A one compartment pharmacokinetic model with linear elimination provided the best fit. Between-subject variance for clearance and volume of distribution were estimated and were allowed to co-vary. Size (weight and FFM) had substantial influence on model performance. FFM was preferred statistically.
Conclusion: A model to describe the time-course of heparin concentration was developed in a paediatric population. FFM was shown

to describe drug disposition well and can potentially be used in dose calculation after appropriate evaluation.

M-045

Recommendations for Dose Adjustments of Infliximab in Crohn's Disease Patients with Higher Clearance

Helena Andersson[1,2,*], Akexander Eser[3], Wilhelm Huisinga[4], Walter Reinisch[3], Charlotte Kloft[1]

[1] Department of Clinical Pharmacy and Biochemistry, Institute of Pharmacy, Freie Universitaet Berlin, Berlin, Germany; [2] Graduate Research Training Program PharMetrX, Berlin, Germany; [3] Department for Gastroenterology and Hepatology, Medical University of Vienna, Vienna, Austria; [4] Institute of Mathematics, Universitaet Potsdam, Potsdam, Germany

Objectives: A substantial proportion of Crohn's disease patients lose response to the monoclonal antibody infliximab [1]. Loss of response, possibly a result of sub-therapeutic concentrations, is commonly handled by dose intensification [2]. However, no guidelines for how to adjust dosing regimens exist. A simulation study was designed, based on a published pharmacokinetic (PK) model [3], to systematically evaluate different dose-intensified regimens.
Methods: Concentration-time profiles were simulated in NONMEM 7.2 using the PK model and Crohn's disease representative demographics. Dose-intensified regimens were simulated for a subpopulation with higher CL to optimize the profiles with respect to a reference group. Regimens with increase of dose or decrease of dosing interval were investigated and compared based on: area under the curve (AUC), maximum concentration (C_{max}), and minimal concentration (C_{min}).
Results: Two subpopulations were generated: low (<35 g/L) and physiological (35–55 g/L, reference) serum albumin concentration at baseline. Evaluating the PK parameters separately resulted in several options for dose adjustments. AUC and C_{max} were highly influenced by an increase of IFX dose; even a small dose increase resulted in a large increase. Decreasing the dosing interval modestly, yet sufficiently, changed the AUC and Cmin without affecting C_{min}. When all parameters were considered together the optimal regimen was 5 mg/kg every fifth week.
Conclusions: Considering all PK parameters and the potential risk of adverse events with too high exposure, shortening the dosing interval should be preferred to increasing the dose when a higher CL is the cause of sub-therapeutic concentrations. Further studies are needed to evaluate the PK/pharmacodynamic relationship for infliximab in Crohn's disease.

References:

1. Gisbert et al. Lancet (2002)
2. Regueiro et al. Inflamm Bowel Dis (2007)
3. Fasanmade et al. Clin Ther (2011)

M-046

Utility of Physiologically based Pharmacokinetics (PBPK) in Pediatric Drug Development

Yan Xu[1,*], Georgy Hartmann[1], Christopher Gibson[1], Tina Frobel[1], Thomas Kerbusch[1], Rebecca Wrishko[1], Filippos Kesisoglou[2], Martijn Rooseboom[1], Venkatesh Pilla Reddy[1], Amitava Mitra[2], Karen Thompson[2]

[1] Pharmacokinetics, Pharmacodynamics, and Drug Metabolism, West Point, PA, USA; [2] Pharmaceutical Science and Clinical Supply, Merck Research Laboratory, West Point, PA, USA

Objectives: Pediatric drug development integrating modeling and simulation (M&S) is highly advocated by the scientific community and regulatory agencies. It provides the ability to optimize dose, sample size, sampling scheme; potentially reducing patient burden and streamlining development. Applications of Physiologically-Based Pharmacokinetics (PBPK) in pediatrics have been expanding, driven by major technological advances and increasing confidence in this approach. As with the traditional scaling approaches based on adult data, PBPK provides a computational framework for predicting dose–exposure relationships in children but with a more physiologically based model that incorporates physicochemical properties and known maturation trajectories.
Methods and Results: The results presented highlight a retrospective analysis of PBPK (simCYP) in montelukast and raltegavir, compounds eliminated primarily by CYP and UGT metabolism respectively. Also presented are applications of PBPK to two active pediatric programs whereby M&S has facilitated decision-making. PBPK predictions provided valuable information and were helpful in supporting choice of dose/formulation development in the first pediatric study.
Conclusion: Applicability of PBPK in pediatric depends on the clinical development question, targeted pediatric age range, expected age-dependent changes in pharmacokinetics and the availability of preclinical and clinical data. Early planning is the key to maximize the potential for PBPK to improve decision making in pediatric drug development.

M-047

Simplification of a Pharmacokinetic Model for Red Blood Cell Methotrexate Disposition

Shan Pan[1,*], Julia Korell[2], Lisa Stamp[3], Stephen Duffull[1]

[1] School of Pharmacy, University of Otago, Dunedin, New Zealand; [2] Model Answers Pty Ltd., Brisbane, Australia; [3] Department of Medicine, University of Otago, Christchurch, New Zealand

Objectives: A 9-compartment pharmacokinetic (PK) model was previously developed for describing the time course of the concentrations of red blood cell (RBC) methotrexate (MTX, MTXGlu1) and the active polyglutamated metabolites (MTXGlu2-5) in patients with rheumatoid arthritis [1]. From previous work the sum of MTXGlu3-5 was predicted to provide the best link with clinical response as measured by disease activity score (DAS28). The overall aim of this study is to simplify the existing population MTX PK model for use as a driver to predict DAS28. The specific objectives of current work are:

(1) To simplify the MTX PK model to predict the sum of RBC MTXGlu3-5 concentrations.
(2) To assess the structural identifiability of the simplified model.
(3) To optimise the sampling schedule for future designs of RBC MTXGlu3-5.

Methods: A formal lumping technique [2] was applied to simplify the existing MTX PK model. Structural identifiability of the simplified model was assessed using an informal approach [3]. An optimal design was constructed in POPT [4] for the simplified model.

Results: The existing MTX PK model was simplified into a 3-compartment model with 6.3 % relative difference in RBC MTXGlu3-5 concentrations over time. Three fixed effect parameters were fixed to obtain a structurally identifiable model. The optimal design from the structurally identifiable model suggested 4 samples of RBC MTX-Glu3-5 on the first visit and 1 sample on each of 5 clinic visits thereafter.
Conclusions: The existing 9-compartment MTX PK model could be simplified to a 3-compartment model. Ultimately, the simplified PK model is intended to be applied in a full population pharmacokinetic–pharmacodynamic modelling analysis of DAS28.

References:

1. Korell et al. Clin Pharmacokinet. 2013;52(6):475–485
2. Gulati et al. CPT Pharmacometrics Syst Pharmacol. 2014;3:e90
3. Shivva et al. CPT Pharmacometrics Syst Pharmacol. 2013;2:e49
4. Duffull et al. Population OPTimal design. http://www.winpopt.com

M-048

Systems Pharmacology Based Biomarker Potentially Predicts Clinical Anti-cancer Activity of MM-398, Nanoliposomal irinotecan, nal-IRI

Kim, Jaeyeon[1,*]; Korn, Ron[2]; Fetterly, Gerald[3]; Sachdev, Jasgit[4]; Raghunand, Natarajan[5]; Prey, Joshua[3]; Clark, Kimberley[3]; Kalra, Ashish[1]; Klinz, Stephan[1]; Bayever, Eliel[1]; Ramanathan, Ramesh[4]; Fitzgerald, Jonathan[1]

[1] Merrimack Pharmaceuticals, Inc., Cambridge, MA, USA; [2] Imaging Endpoints, Scottsdale, AZ, USA; [3] Roswell Park Cancer Institute, Buffalo, NY, USA; [4] Virginia G Piper Cancer Center, Scottsdale Healthcare, Scottsdale, AZ, USA; [5] Translational Cancer Imaging, Arizona Cancer Center, Tucson, AZ, USA

Objectives: With a systems pharmacology approach we have identified tumor permeability to nal-IRI and ability of tumor carboxylesterase to activate irinotecan as critical factors for in vivo activity. In order to test the importance of these parameters for anti-cancer activity of nal-IRI in patients we have conducted a clinical study to measure and quantify them by using tissue- and imaging-based methods as well as mechanistic PK model.
Methods: Eligible patients ($n = 12$) with refractory solid tumors were treated with nal-IRI (80 mg/m^2 q^{2}w). Plasma PK was measured at multiple time points, and tissue biopsies were collected 72 h post-treatment, with drug metabolite levels measured by mass spectrometry. Prior to nal-IRI treatment patients underwent ferumoxytol-MRI to test the feasibility to non-invasively measure nanoparticle permeability in tumors. A mechanistic tumor PK model for ferumoxytol was developed to estimate the permeability of ferumoxytol in tumor.
Results: Patient-derived data showed that SN-38 concentrations in tumor were 5-fold higher than in plasma 72 h post-treatment in agreement with our simulations incorporating the enhanced permeability and retention effect for tumor deposition of liposomes. The ferumoxytol tumor PK model was able to describe both plasma and tumor ferumoxytol-MRI data ($R^2 > 0.9$, $n = 9$). Analyses indicated that tumor permeability to ferumoxytol contributed to MRI signals at 24 h, while tissue retention capacity of ferumoxytol via binding contributed at 72 h. Ferumoxytol levels above the median were significantly associated with better lesion responses as measured by change in lesion size ($p < 0.001$ at 1 h; $p < 0.003$ at 24 h) resulting in the receiver operating characteristics AUC >0.8 for lesion classification. However, no significant relationship was observed at 72 h.
Conclusion: Systems pharmacology approaches can be used to identify parameters of clinical relevance for biomarker development.

M-049

ApoA-I Enhancement, by CSL112 Administration, Leads to a Linear Increase in ABCA1-Dependent Cholesterol Efflux

Zhenling Yao[1,*], Marc Pfister[2], Craig Comisar[2], Andreas Gille[3], Samuel Wright[1], Chuck Shear[1], Denise D'Andrea[1]

[1] CSL Behring, King of Prussia, PA 19406, USA; [2] Quantitative Solution, Bridgewater, NJ 08807, USA; [3] CSL Limited, Parkville, VIC, Australia

Objectives: CSL112 is a novel formulation of apolipoprotein A-I (apoA-I) reconstituted to form high density lipoprotein particles suitable for infusion. It is in clinical development with the aim of reducing recurrent cardiovascular (CV) events in patients with acute coronary syndrome. We hypothesize that CSL112 will reduce plaque cholesterol by increasing cholesterol efflux from cells. The objective of the analysis is to characterize CSL112 pharmacokinetics (PK) and the relationships between apoA-I and ABCA1-dependent cholesterol efflux.
Methods: PK and cholesterol efflux data were pooled from two phase 1 studies in healthy subjects and a phase 2a study in patients with stable atherothrombotic disease. A total of 102 subjects, including 69 healthy adults and 33 patients, received single or multiple doses up to 135 mg/kg. A population two-compartment PK model was developed for apoA-I along with covariate analyses to identify and quantify clinically relevant factors affecting PK parameters. The relationship between apoA-I exposure and cholesterol efflux was evaluated.
Results: ApoA-I demonstrated linear PK with no accumulation following weekly dosing at 6.8 g. No major toxicity or safety events were observed within the dose range tested. Covariate analyses demonstrated that body weight affects clearance. After accounting for weight differences, no PK difference between healthy subjects and stable patients was observed. All evaluated doses in the phase 2a study (1.7, 3.4, 6.8 g) led to significant increases in cholesterol efflux, resulting in 37, 49 and 62 % increases over placebo. A linear model well characterized the relationship between apoA-I exposure and increase in cholesterol efflux AUEC. Model-based simulation suggested CSL112 2 and 6 g cover a wide exposure–response range.
Conclusion: PK and pharmacodynamic data support the suitability of developing CSL112 as a therapy for prevention of recurrent CV events. Weekly administration of CSL112 2 and 6 g have been selected for the phase 2b study.

M-050

Meta-analysis of Active Placebo Response on Glycosylated Haemoglobin (HbA1c) in Type II Diabetes Clinical Trials

Tina Marie Checchio[*], Melissa O'Gorman, Kevin Sweeney, Tom Tensfeldt

Pfizer Inc., Groton, CT, USA

Objectives: Changes in clinical practice for the treatment of Type II Diabetes (T2DM) may be expected to have an effect on observed placebo (PBO) response. Prior to 1997, diagnosis of diabetes was based on fasting plasma glucose (FPG) levels with an upper limit of 140 mg/dL. By 2000, the American Diabetes Association recommended the use of glycosylated hemoglobin (HBA1c) rather than FPG. Subsequently, study designs transitioned from PBO-controlled

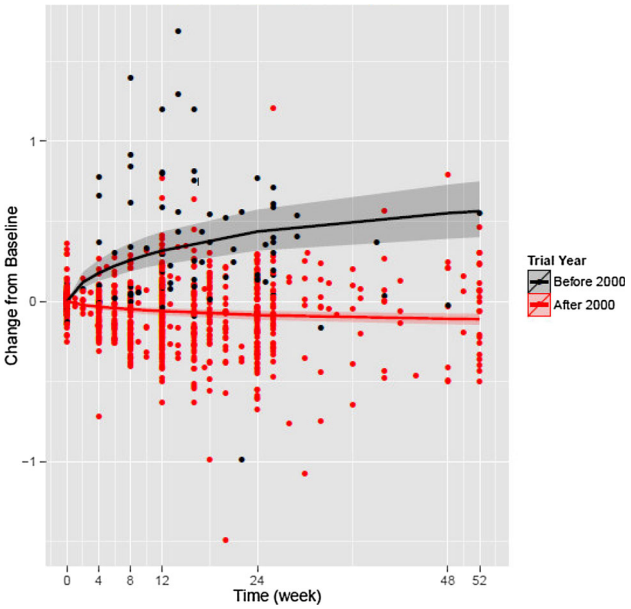

Fig. 1 Model-predicted HbA1c change from baseline in trials before and after 2000

trials toward superiority designs involving maintenance of stable background therapy. Therefore, the primary objective of this investigation was to create a longitudinal model to describe reported means of HbA1c in patients allocated to PBO and explore covariates that may explain PBO response variability.

Methods: Longitudinal meta-analyes of reported HbA1c in placebo subjects from 274 randomized-controlled clinical trials between 1994 and 2013 were conducted using NONMEM version 7.2 to quantify week 12 change from baseline (CFB) and determine factors that may affect the magnitude of the PBO response. A nonlinear mixed effect base model incorporating a durability term was shown to provide an adequate fit to the data. Covariates explored included baseline HbA1c, disease duration, background therapy and trial year.

Results: Large variability in reported HbA1c -time profiles across studies was reflected in wide uncertainly around predicted week 12 CFB. After accounting for both disease duration and background therapy, the predicted week 12 CFB was −0.014 [90 % CI −0.058, 0.034]. Incorporation of covariates did not sufficiently account for the variance related to trial year. In an independent model, trial year was shown to be statistically significant on the PBO response, with predicted week 12 CFB for studies conducted before or after the year 2000 were 0.32 [0.23, 0.43] and −0.061 [−0.085, −0.043], respectively, reflecting changes to clinical study designs over time.

Conclusions: These findings suggest that changes in clinical practice that may impact glycemic control for PBO subjects during 12 week studies should be accounted for during study design and conduct Figure 1.

M-051

Development and Application of an Adherence Metric Derived from Population Pharmacokinetics to Inform Clinical Trial Enrichment

Jonathan Knights[1,*], and Shashank Rohatagi[1]

[1] Otsuka Pharmaceutical Development & Commercialization, Inc., Princeton, NJ, USA

Objectives: To construct and evaluate an objective metric of relative adherence from sparse plasma sampling using a population pharmacokinetic (POPPK) approach in a clinical population, which could be used to inform selection of potentially nonadherent patients.

Methods: A single visit clinical trial was conducted in 47 patients of bipolar-1 or schizophrenic disposition, who were on stable doses of oral aripiprazole for at least two weeks to ensure the assumption of "presumed steady-state" could be made. During the visit, four plasma samples were drawn at one-hour intervals and patients filled out the Modified 8-item Morisky Adherence scale (MMAS8). Preceding study conduct, a POPPK model was built for oral aripiprazole using 24 independent studies and over 440 subjects. An objective metric for adherence (ADHMET) was defined as the ratio of observed versus "expected" exposure: ADHMET = AUCobs/AUCexpected = CLexpected/CLobs. The expected clearance (CLexpected) was defined using the expression for the typical value of clearance in the POPPK model accounting for relevant covariates, while the observed clearance (CLobs) was defined by the empirical Bayesian estimates (EBEs) for each individual after applying the model to the new clinical data. During modeling, all parameters were fixed except for the interindividual variability term on clearance, and the residual error term. Deviation from expected variability of apparent clearance was attributed in part to a deviation from the prescribed dosing regimen. Additional simulations were conducted to test the sensitivity and specificity of the approach to distinguish between adherent and nonadherent patients.

Results: The metric was adequate for comparing relative adherence levels across groups. Such a comparison using questionnaire responses as groups showed that aggregate MMAS8 scores were not correlated with relative adherence levels; however, one question was statistically correlated with relative adherence levels.

Conclusions: Population pharmacokinetic principles can be applied to reverse-engineer an objective adherence-like metric that may be used to compare relative adherence levels across groups. Applying this metric to correlate clinical questionnaire responses represents a novel "pseudo" pharmacodynamic application of population pharmacokinetics.

M-052

A Sensitivity Analysis of Sample Size and BSV in Serial Sacrifice Designs for Brain Distribution Studies: Application to Sunitinib

Rajneet Oberoi[1], William Elmquist[1], Richard Brundage[2,*]

[1] Department of Pharmaceutics, [2] Experimental & Clinical Pharmacology, University of Minnesota, Minneapolis, MN, USA

Objectives: Brain distribution studies in rodents are often limited to one sample per animal. In a serial sacrifice design, a naive-pooled approach is often used to estimate AUCs in tissue and plasma and the AUC ratio estimates tissue distribution (Kp). Such ratios ignore within-animal correlations and estimates of precision are not obtained. The goals of this study were to estimate the brain distribution Kp of sunitinib using NLME in a murine model; and evaluate the influence of sample size and assumed magnitude of BSV on bias and precision of Kp.

Methods: Sunitinib was administered as single oral doses (20 mg/kg) or steady-state infusions (30 μg/h) to 128 FVB-wild type, Mdr1(−/−), Bcrp1(−/−) and Mdr1a/b(−/−)-Bcrp1(−/−) mice. Animals were sacrificed and paired plasma (Cpl) and brain (Cbr) concentrations were obtained at eight time points (oral) or at steady state (infusion). NONMEM7 was used to simultaneously fit a one-compartment model to Cpl, which was used as forcing function to describe a one-compartment Cbr. BSV was fixed to 20 %; other parameters were

estimated. PsN (SSE) was used to simulate 1,000 Cpl,Cbr data sets for each level of sample sizes per time point (n = 2, 3, 4, 8, 12) assuming 20 % BSV. These were analyzed assuming 3 levels of BSV (10, 20, 40 %). Bias of Kp was calculated as a relative error and precision as the fraction of estimates within 10 % error.
Results: The observed Cpl and Cbr were reasonably predicted under the model; Kp estimates were comparable to the naive-pooled method and insensitive to assumptions regarding BSV. From the simulation study, bias was <1 % for all levels of sample size and BSV. Precision varied 5–95 %, improved dramatically with sample size, and was minimally sensitive to the assumed BSV.
Conclusions: Estimates of all system parameters and uncertainties were obtained from a serial sacrifice design using NLME. The magnitude of BSV had little impact on bias or precision of Kp; sample size had little influence on bias but highly influenced precision.

M-053

Combing Model Coarse Graining, Optimal Design and Quantitative Risk Assessment for Simulating Adaptive Clinical Trials

Garrit Jentsch*, Rupert Austin, Aaron Hayman, Joachim Grevel

BAST Inc. Ltd., Loughborough, UK

Objectives: Recent years have witnessed the emergence of various model informed drug development (MIDD) strategies all of which centre around a continuum of mathematical statistical models that capture the developing project from the patho-physiology of the disease and the pharmacology of the drug to the conduct of clinical studies. The model continuum is maintained to simulate experiments and clinical studies in order to optimise their design and to quantitatively assess their chance of success.
Methods: We designed an agent-based computational framework for the simulation of adaptive clinical trials. The design is capable of easily combining models operating on different scales and focusing of different aspects of a clinical trial. Responses of individual patients are used to infer the parameters of a coarse grained dose response model which is used in an adaptive design to evaluate futility and allocate patients to different dose levels or treatments. Simulating multiple replicates enables us to evaluate the operating characteristics and compare different trial designs.
Results: A case study is presented in which an adaptive clinical trial is optimised and simulated in order to evaluate whether the new drug is suitable for further clinical development. A GO decision is issued if the dose response curve exhibits a certain slope at half the maximally tolerated dose. The operating characteristics of multiple adaptive trial designs differing in the number of interim analyses are determined in order to select the design which yields the highest probability of a correct decision.
Conclusions: The case study demonstrates the utility of our simulator to evaluate the operating characteristics and success chances of adaptive clinical trials. The case study further demonstrates how the computational prototype can be used to guide study design optimisation while accounting for complex models underlying the responses of individual patients.

M-054

Understanding the Interaction Between Hepatic Bile Acid Accumulation and Mitochondrial Toxicity Using Mechanistic Modeling

Jeffrey Woodhead*, Kyunghee Yang, Yuching Yang, Brett Howell, Scott Siler

The Hamner-UNC Institute for Drug Safety Sciences, Research Triangle Park, NC, USA

Objectives: Both mitochondrial dysfunction and accumulation of bile acids are thought to be important mechanisms that lead to drug-induced liver injury (DILI). Recent research has shown that certain bile acids can reduce the mitochondria proton gradient [1]. Previously we have constructed a model of bile acid homeostasis within DILIsym, a mechanistic mathematical model of DILI [2]. In this research we tie DILIsym's mitochondrial and bile acid mechanisms together. We use this new model to explore the interaction between the two mechanisms using simulations of bosentan and CP-724714.
Methods: We have modified DILIsym to include bile acids as an uncoupler as shown in Fig. 1. We have calibrated this effect to the decline in ATP previously measured in hepatocytes treated with bile acids [3]. We predicted incidence of toxicity for bosentan and CP-724714 using PBPK models for those compounds and simulated populations (SimPopsTM) included in DILIsym v3B.
Results: DILIsym, with the novel bile acid-mitochondrial model, predicted ALT elevations in 7 % of the simulated population, which is close to the range of 8–18 % observed in clinical trials [4], a significant improvement over previous predictions using a direct bile acid ATP effect model [5]. Furthermore, our results with CP-724714, which inhibits both bile acid transport and the mitochondrial electron transport chain, demonstrate the clear potential for a synergistic interaction between bile acid accumulation and mitochondrial toxicity; only the combination of the two mechanisms fully explains the clinically observed toxicity.
Conclusions: Our simulations demonstrate the value of considering multiple mechanisms simultaneously when attempting to predict the incidence of DILI.

References:

1. Schulz, S. et al. Biochimica Biophysica Acta 1828, 2121–33 (2013)
2. Woodhead, J.L., et al. Clinical Pharmacology and Therapeutics: Pharmacometrics and Systems Pharmacology, in press (2014)
3. Yang, K., et al. The Toxicologist, 132 (Abstract ID #1059), 2013
4. Fattinger, K., et al. Clinical Pharmacology and Therapeutics 69, 223–231 (2001)
5. Woodhead, J.L., et al. Frontiers in Pharmacology, submitted (2014).

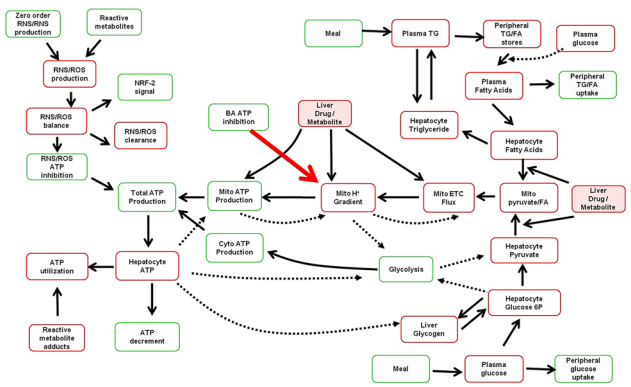

Fig. 1 Diagram of the current mitochondrial model in DILIsym® showing the inclusion of the effect of bile acid accumulation on the mitochondrial proton gradient

M-055

Prospective Prediction of the Influence of OATP1B1 Genotype on the Pharmacokinetics of Pravastatin and Rosuvastatin in Caucasian and Japanese Populations

Rui Li*, Hugh A. Barton, Tristan S. Maurer

Department of Pharmacokinetics Dynamics and Metabolism, Pfizer Worldwide R&D, Cambridge, MA, USA and Groton, CT, USA

Objectives: The organic anion-transporting polypeptide 1B1 (OATP1B1), a hepatic uptake transporter encoded by the gene SLCO1B1, has a broad substrate specificity and is a key player in the pharmacokinetics of many drugs. Although previous in vitro and in vivo studies have shown that OATP1B1 polymorphisms can influence its activity, no translational work has been done mechanistically and quantitatively to establish a link between the two. This study aims to design a physiologically based pharmacokinetic (PBPK) model capable of translating the differences among OATP1B1 genetic variants observed in vitro activity into in vivo pharmacokinetic predictions.
Methods: We incorporated in vitro information for three major OATP1B1 genetic variants into a previously reported PBPK model to predict the impact of OATP1B1 polymorphisms on plasma pharmacokinetics. The fraction of total hepatic active uptake mediated by OATB1B1 estimated in vitro, together with the ratios of in vitro uptake activities among variants, were combined with average hepatic clearance and absorption estimated from un-genotyped human plasma data to predict plasma concentration time profiles for genotyped groups.
Results: Using pravastatin and rosuvastatin as examples, we showed that the predicted plasma concentration time profiles in groups carrying different OATP1B1 genetic variants reasonably matched the clinical observations from multiple studies in Caucasian and Japanese populations.
Conclusions: This study presents a method to improve the prediction of pharmacokinetics, and potentially drug-drug interactions in groups carrying genetic variants of transporters. It can be useful in the design and selection of novel drug candidates, the design of clinical trials and ultimately for dose adjustments in clinical practice. The framework provided here to predict the impact of OATP1B1 polymorphisms on human plasma pharmacokinetics can be extended with additional compounds, additional transporters and metabolic enzymes.

M-056

Population Pharmacokinetic Model with Sparse Sampling for Mycophenolic Acid in Liver Transplant Patients

Xiaoxing Wang[1,*], Bing Chen[2], David Smith[1], Meihua Rose Feng[1]

[1] College of Pharmacy, University of Michigan, Ann Arbor, MI, USA; [2] Shanghai Jiaotong University School of medicine, Shanghai, China

Objectives: Mycophenolic acid (MPA) is the major active metabolite of the prodrug mycophenolate mofetil (MMF) widely used as an immunosuppressant for the prophylaxis of acute rejection in solid organ transplantation. The objective of this work is to develop a population pharmacokinetic (PK) model and a sparse-sampling strategy (SSS) in therapeutic monitoring for MPA in adult liver transplant recipients.
Methods: 64 adult liver transplant patients following repeated 12-h oral dose of MMF were enrolled in this study. MPA plasma concentrations (C0-12 h) were determined by HPLC-UV analysis. Population PK models were developed using nonlinear mixed effects modeling (NONMEM). SSS with 2, 3, or 4 time points were explored using multi-linear regression and NONMEM. The models were evaluated using goodness-of-fit plots, Bland and Altman analysis, and visual predictive check.
Results: MPA plasma concentration-time data were best described by a two-compartment disposition model followed by a first-order absorption process with lag time. SSS was assessed based the correlation between the predicted (AUCpred) versus the observed MPA area under the concentration-time curve (AUCobs). MPA AUCpred using 4 data points (C1 h, C2 h, C4 h and C10 h) showed the best correlation to AUCobs ($r^2 = 0.9885$) with excellent accuracy (MRPE = 2.13 %) and precision (rRMSE = 1.83 %). The correlation between AUCobs and AUCpred using 3 time points (C2 h, C4 h and C10 h) was also high ($r^2 = 0.9776$), while the correlations between AUCobs and AUCpred using 2 data points were poor. Considering the PK parameters, the sparse sampling PK model using 3 data points, C2 h, C4 h and C10 h, (CL/F = 22.1 L/h, V2/F = 21.4 L, V3/F = 214 L) was closer to the model based on full data set (CL/F = 23.4 L/h, V2/F = 31.4 L, V3/F = 221 L).
Conclusions: The POPPK models and LSS developed in this study could be used to optimize MPA dose in individual liver transplant recipient, and to project MPA concentration-time profile in future MPA therapy.

M-057

Good Practices in Model Informed Drug Discovery and Development (MID3): Practice, Application, Documentation and Reporting

EFPIA MID3 Workgroup: Peter Milligan[5,*], Rolf Burghaus[1], Valerie Cosson[2], S.Y. Amy Cheung[3], Marylore Chenel[11], Oscar DellaPasqua[4], Nicolas Frey[2], Bengt Hamren[3], Lutz Harnisch[5], Frederic Ivanow[6], Thomas Kerbusch[7], Joerg Lippert[1], Scott Marshall[5], Solange Rohou[3], Alexander Staab[8], Jean Louis Steimer[9], Christoffer Tornoe[10], Sandra Visser[7]

[1] Bayer, Leverkusen, Germany; [2] F. Hoffmann-La Roche, Basel, Switzerland; [3] AstraZeneca, London, UK; [4] GlaxoSmithKline, London, UK; [5] Pfizer, New York , NY, USA; [6] Johnson & Johnson, Antwerp, Belgium; [7] Merck/MSD, Whitehouse Station, NJ, USA; [8] Boehringer Ingelheim Pharma GmbH & Co. KG, Ingelheim, Germany; [9] Novartis, Basel, Switzerland; [10] Novo Nordisk, Bagsværd, Denmark; [11] Servier, Neuilly-sur-Seine, France

Objectives: The workgroup evolved from the original 2011 EFPIA / EMA M&S workshop committee. The aim was to continue a dialogue with EMA MSWG colleagues [1], realise EFPIA's commitments and enable an era of Model Informed Drug Discovery and Development (MID3) and Model Informed Regulatory Assessment [2–6].
Methods: A focus for the working group was the development of a "Good Practice and Standards" guidance document. Its aim was to promote a wider understanding of how MID3 could be applied across R&D (Part 1) and enhance both the clarity and efficiency in the reporting of MID3 analyses for regulatory interactions (Part 2). Detailed technical content was considered out of scope.
Results: Part 1 provides the rationale behind the MID3 paradigm, from utility in knowledge integration to provision of a framework to aid extrapolation (high regulatory impact situations). This section also provides a "good practice" grid to aid identification of pertinent questions across different themes (including Risk/Benefit and commercial viability) and activity levels (related to compound, mechanism and disease) to facilitate strategic planning of MID3 activities. A high level comparison of potential modelling approaches

(from Empirical to systems pharmacology) is additionally outlined. Finally, examples illustrating this framework in practice, highlighting the internal impact across different application sub-types (from Selection and Validation of Drug Targets to Commercial Strategies) are described.

Part 2 outlines good practices in the documentation for analyses, covering some guiding principles, documentation in regulatory submissions and QA\QC. Consideration is given to the key components of the analysis plan, simulation plan and report, with suggestions for an appropriate and acceptable level of documentation ("fit for purpose"). An important recommendation is for an explicit statement of the underlying Stat/Math, Physiological, Pharmacological and Disease related assumptions and their evaluation, both in the planning and reporting of analyses. Members of EMA MSWG were involved in the review of the document and are aligned with the covered principles.

Conclusions: Through increasing the consistency, quality and transparency of conduct and reporting of MID3 activities, we believe this document will be an important step in achieving a greater harmonisation of these approaches across the Pharmaceutical Industry and in its interactions with Regulatory Agencies.

References:

1. Shepard T, Brogren J, Manolis E and Hemmings R. How European Regulators are Facilitating the Use of Modelling and Simulation: MSWG History, Activity and Future PAGE 2014
2. Manolis E, Rohou S, Hemmings R, Salmonson T, Karlsson M, Milligan PA. The Role of Modeling and Simulation in Development and Registration of Medicinal Products: Output From the EFPIA/EMA Modeling and Simulation Workshop. CPT Pharmacometrics Syst Pharmacol. 2013 Feb 27;2:e31
3. Visser SA, Manolis E, Danhof M, Kerbusch T. Modeling and simulation at the interface of nonclinical and early clinical drug development. CPT Pharmacometrics Syst Pharmacol. 2013 Feb 27;2:e30
4. Marshall SF, Hemmings R, Josephson F, Karlsson MO, Posch M, Steimer JL. Modeling and simulation to optimize the design and analysis of confirmatory trials, characterize risk-benefit, and support label claims. CPT Pharmacometrics Syst Pharmacol. 2013 Feb 27;2:e27.
5. Harnisch L, Shepard T, Pons G, Della Pasqua O. Modeling and simulation as a tool to bridge efficacy and safety data in special populations. CPT Pharmacometrics Syst Pharmacol. 2013 Feb 27;2:e28
6. Staab A, Rook E, Maliepaard M, Aarons L, Benson C. Modeling and simulation in clinical pharmacology and dose finding. CPT Pharmacometrics Syst Pharmacol. 2013 Feb 27;2:e29

M-058

Best Practices for Preparation of Pharmacometric Analysis Data Sets

Neelima Thanneer*, Amit Roy, Prema Sukumar, Jyothi Bandaru, Eric Carleen

Clinical Pharmacology and Pharmacometrics, Bristol Myers Squibb, Princeton, NJ, USA

Objectives: Timely availability of high quality data sets is essential for accurate and impactful pharmacometric (Pm) analyses. Improvements in timeliness and quality are achieved by standardizing data set preparation, particularly when the data set requires derivations and imputations of variables and data not available in the source data. We describe Best Practices that have enabled high quality data sets to be prepared efficiently.

Methods: The three main elements of Best Practices of Pm analysis data set preparation are data cleaning, programming, and reporting. The quality of an analysis data set is only as good as the quality of the source data. Standardized edit checks of pharmacokinetic data enable effective cleaning of data during the course of a study.

Key attributes of high quality pharmacometric analysis data sets are reproducibility and logical consistency. Best Practices include Pm data set specification, standardization of derivations and imputations required to prepare data sets, dry-run data set programming (using mock data), and quality control (QC) of final output.

Finally, the reporting component of Best Practices includes documentation of data set variables, identification of outliers, and informative data summaries.

Results: The value of Best Practices is illustrated by their application to the preparation of population pharmacokinetic (PPK) analysis data sets. Issues related to data imputation are particularly acute for PPK data sets, as detailed dosing history is generally not available in the source data.

Cleaning of PK data during study conduct enables recovery of data that may not have otherwise been useable. Dry runs of data set programming enable identification of issues and improved data set specifications. Standardization of imputations enables consistency of practice among programmers and pharmacometricians.

Examples of Pm analysis data set specifications that enable transparency of imputed variable derivation, self-documentation of variables, and exclusion of data from analysis are provided.

Conclusions: The implementation of Best Practices improves the efficiency of Pm analysis data set preparation, and consistency and documentation of data sets.

M-059

Population PK-PD and Exposure–Response Modeling and Simulation to Support Dose Recommendation of Xolair in Chronic Idiopathic Urticaria/Chronic Spontaneous Urticaria

Yanan Zheng[1,*], Kha Le[1], Russ Wada[2], Jin Jin[1], Wendy Putnam[1], Karin Rosen[1], Hubert Chen[1], Hsin-Ju Hsieh[1], Philip J Lowe[3], Jennifer Visich[1]

[1] Genentech, San Francisco, CA, USA; [2] Quantitative Solutions, New York, NY, USA; [3] Novartis, Basel, Switzerland

Objectives: Omalizumab (Xolair) is a humanized anti-IgE monoclonal antibody first approved in patients (12–75 years-old) with moderate to severe persistent allergic asthma. Recently, it was approved to treat patients with Chronic Idiopathic Urticaria (CIU). Population PK-PD and exposure–response modeling and simulation were performed to evaluate the dosing strategy and support the dose recommendation of omalizumab in CIU patients.

Methods: The PK and PD of omalizumab in CIU patients were characterized using a target-mediated population PK-PD model incorporating omalizumab-IgE binding and turnover. Exposure–response (E–R) modeling was conducted to evaluate the relationship between efficacy and observed trough omalizumab concentrations in the Phase III efficacy studies. Key covariates, including patient demographics and baseline IgE level, were evaluated in the population PK-PD and exposure–response models. The final models were simulated to evaluate flat versus body weight/IgE-adjusted dosing regimens.

Results: The PK and PD characteristics of omalizumab in CIU were adequately described by the population PK-PD model. Body weight

and body mass index (BMI) had modest effects on omalizumab trough values, while baseline IgE had a negligible effect. There was a positive relationship between efficacy and exposure across the tested dose range (75–300 mg q^4w), which was described by an E_{max} model. The majority (~70 %) of patients receiving 300 mg q^4w had exposures above the EC50 of the E–R curve compared with <20 % with 150 mg q^4w. No clear effect of body weight, BMI or baseline IgE level on efficacy was observed. Simulations using the PK-PD and exposure–response models demonstrated that dose adjustments based on weight or both weight and baseline IgE level were not expected to result in additional clinically meaningful benefit compared with flat dosing.

Conclusions: Population PK-PD and E–R modeling and simulation supported flat dosing for omalizumab in CIU patients. In addition, the results supported 300 mg as a more efficacious dose than 150 mg q^4w.

M-060

A Population Pharmacokinetic–Pharmacodynamic Model for Allopurinol in Patients with Gout

Daniel F.B. Wright[1,*], Stephen B. Duffull[1], Tony R. Merriman[2], Murray L. Barclay[3], Lisa K. Stamp[2]

[1] School of Pharmacy, Dunedin, New Zealand; [2] Department of Biochemistry, Dunedin, New Zealand, [3] Department of Medicine, University of Otago, Dunedin, New Zealand; [1,2], and [3] Christchurch, New Zealand

Objectives: To determine the factors that predict allopurinol response using a population pharmacokinetic–pharmacodynamic (PKPD) analysis.

Methods: Data were sourced from five studies in patients with gout. A population analysis was conducted using NONMEM® v.7.2. A population PKPD model was developed linking the active metabolite, oxypurinol to plasma urate. The Individual PK Parameters (IPP) sequential method was used. The influence of patient characteristics, concomitant drugs, and genetic variability in renal transporters were tested in the model. Model discrimination and evaluation was based on a likelihood ratio test, parameter estimate precision, visual predictive checks and diagnostic plots.

Results: A total of 1,133 oxypurinol and 1,176 urate plasma concentrations from 133 patients were available for analysis. A one compartment PK model with first order absorption and elimination for oxypurinol was the best fit to the data. Renal function, diuretic use, and body mass were significant covariates on oxypurinol clearance. Body mass was also found to predict oxypurinol volume. Renal transporter genotype did not significantly influence oxypurinol clearance. Attempts to fit a biologically appropriate turnover model to the plasma urate data produced unrealistic estimates of the urate elimination rate constant (k-urate). The average k-urate value derived from published reports was 0.02 h^{-1}. This is the same as the elimination rate constant for oxypurinol (k-oxy) observed in this analysis (0.02 h^{-1}) suggesting that k-urate may not be identifiable in some patients. A simple, but incorrect, direct effects (E_{max}) model provided an adequate description of plasma urate data.

Conclusions: A satisfactory population model for the effect of allopurinol on plasma urate was not possible in this dataset. It is proposed that a "flip-flop"-type scenario may exist in the turnover model where k-urate > k-oxy in some patients and, in these cases, the time course of plasma urate change will reflect the oxypurinol elimination. Further work on designs to accommodate this identifiability issue is underway.

M-061

A Systems Pharmacology Model of Renal Glucose Physiology to Evaluate the Effects of SGLT1 and SGLT2 Inhibition in T1DM Subjects

Yasong Lu*, Steven C. Griffen, David W. Boulton, Frank P. LaCreta, Tarek Leil

Bristol-Myers Squibb, Princeton, NJ 08550, USA

Objectives: Sodium–glucose cotransporters (SGLT) 1 and 2 in the kidney are responsible for renal glucose reabsorption. SGLT2 is believed to account for 80–90 % of renal glucose reabsorption, with SGLT1 accounting for the remaining 10–20 %. Selective SGLT2 inhibitors (e.g., dapagliflozin) have been approved for treatment of type 2 diabetes mellitus (T2DM), and are being evaluated in T1DM. Despite tremendous advances in the biology and pharmacology of SGLT1/2, a quantitative, mechanism based approach is needed to enhance deep understanding of the dynamics of these transporters in renal glucose reabsorption. Here, we report the development of a systems pharmacology model for renal glucose physiology to evaluate SGLT1/2-mediated renal glucose reabsorption in humans with or without SGLT2 inhibition. We also demonstrate the utility of the model to predict the effect of dapagliflozin in T1DM subjects.

Methods: The structure of the systems pharmacology model is shown in Fig. 1. The proximal tubules are divided into 6 convoluted tubules (PCT) subcompartments and 3 straight tubules (PST) subcompartments to allow for detailed description of glucose transfer along the tubular lumen and reabsorption by SGLT1/2. The parameters related to glucose-SGLT1/2 and dapagliflozin-SGLT1/2 interactions were calibrated using data from DeFronzo et al. [1], and other parameters were taken from the literature. The performance of the renal glucose reabsorption model was evaluated using three separate datasets [2–4]. To predict the effect of dapagliflozin in T1DM, a dapagliflozin PK model and a glucose–insulin model were integrated with the renal

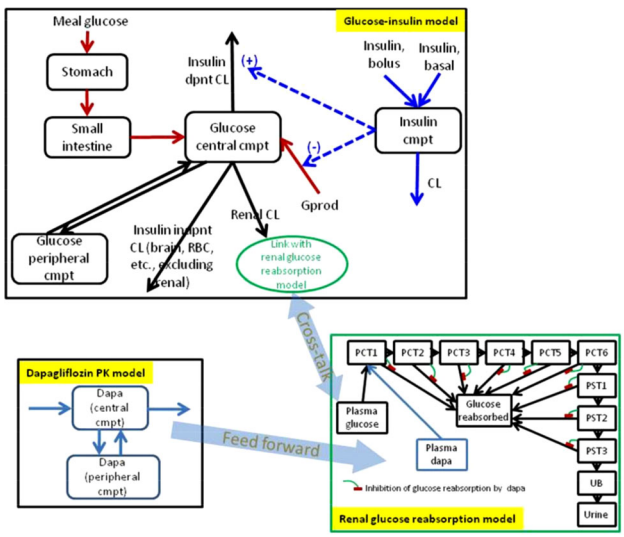

Fig. 1 The structure of the systems pharmacology model elucidating the operating characteristics of SGLT l/2 in renal glucose reabsorption and for predicting the effect of dapagliflozin on glycemic control and insulin requirement in TlDM patients

glucose reabsorption model. The model development was executed in Berkeley Madonna (v8.3.18).

Results: The renal glucose reabsorption model adequately described all four separate datasets. The model provided insights into the operating characteristics of SGLT1/2. It solidified the current concept of the relative contributions of SGLT1/2 to renal glucose reabsorption under physiological conditions; moreover, it estimated that under such conditions SGLT1 and SGLT2 operate at 20 and 40 % of their maximum capacities, respectively. With SGLT2 inhibition, SGLT1 becomes the more important pathway for glucose reabsorption, and it operates at over 90 % of its capacity. In a healthy, normoglycemic subject, a complete loss of SGLT2 function will result in 50 % inhibition of renal glucose reabsorption. The modeling and simulations in T1DM subjects predict that dapagliflozin treatment would permit lowering of basal and bolus insulin doses while improving control of blood glucose levels.

Conclusions: A systems pharmacology model was developed to quantitatively characterize the roles of SGLT1/2 in renal glucose reabsorption. The model suggests that the apparent moderate (30–50 %) inhibition of renal glucose reabsorption observed in healthy and T2DM subjects with SGLT2 inhibitors is likely a combined result of SGLT1 compensation and residual SGLT2 activity. The model will benefit the evaluation of SGLT2 inhibitors in subjects with T1DM.

References:

1. DeFronzo RA, et al. (2013) Diabetes Care 36(10): 3169–76
2. Mogensen CE (1971) Scand J Clin Lab Invest 28(1): 101–109
3. Polidori D, et al. (2013) J Clin Endocrinol Metab 98(5): E867–871
4. Wolf S et al. (2009) Horm Metab Res 41(8): 600–604

M-062

Population Pharmacokinetic Modeling of Omecamtiv Mecarbil and its Metabolites After Administration of Three Modified Release Tablets

Ramesh Palaparthy[1,*], Sam Liao[2], Juan Jose Perez Ruixo[3], John David Clements[1]

[1] Quantitative Pharmacology, PKDM, Amgen, Thousand Oaks, CA, USA; [2] Pharmax Research, Irvine, CA, USA

Objectives: Omecamtiv mecarbil (OM) is a novel small molecule being developed for the treatment of heart failure that would benefit by using modified release (MR) formulation (tablets) to minimize the peak to trough fluctuations (PTF). We aimed to select an optimal MR tablet based on a joint population PK model of OM and its metabolites (M3 and M4).

Methods: OM and M3/M4 concentration-time data were obtained in a Phase 1, randomized, single 25 mg dose, open-label, 4-way, crossover incomplete block design study in healthy adults (N = 61) with at least a 7 day washout between treatment periods. In this study, 3 MR tablets (MR-F1, MR-F2 and SCT-F2) having 3 different release rates were compared with the immediate release (IR) tablet. A Nonlinear mixed effects modeling approach was performed using NONMEM (v7.2) to jointly analyze the OM and M3/M4 PK using a pharmacostatistical model. Subsequently, OM and M3/M4 concentrations following 25 mg OM BID dosing were simulated to help select optimal formulation(s) on the basis of lower PTF.

Table 1 Summary of predicted steady-state (SS) OM and metabolites PK parameters following oral IR and MR tablets administration of 25 mg OM every 12 h in healthy subjects under fasted conditions

Predicted PK parameter	IR	MR-F1	MR-F2	SCT-F2
OMC_{max} (ng/mL)	313 (292–323)	196 (183–202)	211 (197–218)	196 (183–203)
OMC_{min} (ng/mL)	152 (137–159)	155 (142–162)	157 (143–163)	163 (149–169)
OM AUC_{ss} (ng/hr/mL)	2401 (2,216–2,488)	2,071 (1,907–2,140)	2,230 (2,059–2,510)	2,167 (1,997–2,240)
OM PTF (%)	9508 (88.2–103.5)	20.6 (19.0–22.2)	32.2 (29.7–34.7)	20.1 (18.6–21.5)
M3 PTF (%)	24.2 (21.1–28.2)	8.90 (7.80–10.0)	13.6 (12.2–15.0)	8.80 (7.70–9.80)
M4 PTF (%)	22.7 (20.3–25.6)	8.40 (7.40–9.50)	13.2 (11.9–14.7)	8.70 (7.80–9.70)

Data presented as median (90 % CI); simulation after 1,000 trials of 50 subjects each

Results: The PK of OM was best described using a two-compartment disposition model with a parallel first-order and zero-order input. M3 apparent formation was a result of OM elimination, and M4 apparent formation was a result of M3 apparent elimination. Inter-subject variability on PK parameters and residual variability were best described using an exponential and proportional error model, respectively. Steady-state (SS) simulations showed that all 3 MR formulations blunted OM C_{max}, yet provided similar total OM exposures to IR tablet, however MR-F1 and SCT-F2 tablets appeared to provide the optimal PK profiles with lower PTF relative to MR-F2 tablet (Table 1).

Conclusions: A joint population PK model was developed in describing the PK of OM, M3/M4 following single dose administration of 3 MR tablets having different release rates. Simulations suggested that MR-F1 and SCT-F2 tablets would provide comparable and optimal SS PK profiles Table 1.

M-063

Modeling Effects of Chemotherapeutics on Metastases in the Lymphatic Vessels

R.E. Griswold[1,*], S. Das[1], S. Cho[1], B.E. Griffith[2,3], S. Podgrabinska[1], J. Gallo[1,a], C.S. Peskin[3,a], M. Skobe[1,a]

[1] Icahn School of Medicine at Mount Sinai, New York, NY, USA; [2] New York University School of Medicine, New York, NY, USA; [3] New York University, New York, NY, USA; [a] Equal Contribution

Objectives: Lymphatic vasculature is an important pathway for metastasis and also a niche in which metastatic lesions grow. Most cancers metastasize via lymphatics, but it is not understood how effective chemotherapy is in targeting cancer cells which reside within the lymphatic vasculature [1]. Our objective is to computationally model survival of tumor cells in the lymphatics following chemotherapy, and to validate predictions in a mouse model. We hypothesize that the lymphatic microenvironment facilitates

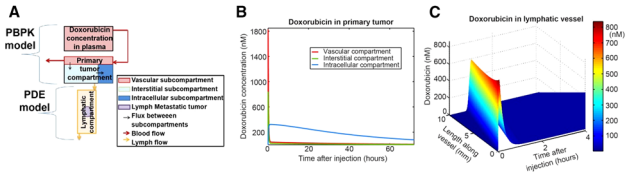

Fig. 1 Predicted exposure of tumor and intralymphatic metastases to doxorubicin

resistance to therapy and metastatic recurrence by limiting drug access and facilitating drug removal.

Methods: We created a physiologically-based pharmacokinetic (PBPK) model consisting of a model of doxorubicin distribution in tumor connected to a spatiotemporal PDE model of its disposition in lymphatics (Fig. 1a). We have measured drug concentration in mouse plasma, tumors, and lymph which will improve parameter fitting and test model predictions.

Results: PBPK model predicts that over 72 h, area under the doxorubicin concentration time curve in primary tumor is 7,647 nM-h. C_{max} of interstitial fluid, which drains into the lymphatic compartment, is predicted to be 842 nM (Fig. 1b). Doxorubicin distributes along a 10 mm lymphatic vessel within 1 h of drug administration and will reach a transient peak of 839–540 nM (Fig. 1c).

Conclusions: Computational model of doxorubicin distribution thus far predicts that 10 mm into a lymphatic vessel, C_{max} is high (540 nM), suggesting the chemotherapeutic is likely to affect intralymphatic metastases. We will next refine the PDE model to include metastatic cells and to calculate lymph flow in a 3D vessel using the Immersed Boundary Method [2], which will more accurately predict drug efficacy in the lymphatic compartment.

References:

1. Mumprecht, V. and M. Detmar, Lymphangiogenesis and cancer metastasis. J Cell Mol Med, 2009. 13(8A): p.1405–16
2. Peskin, C.S., The immersed boundary method. Acta Numerica, 2002: p.1–39

M-064

Three Case Studies of Pharmacokinetic Model Selection Using Genetic Algorithms

Eric A. Sherer[1,2,*], Mark Sale[2,3], Robert R. Bies[2]

[1] Louisiana Tech University, Ruston, LA, USA; [2] Indiana University School of Medicine, Indianapolis, IN, USA; [3] Nuventra Pharma Science, Research Triangle Park, NC, USA

Objectives: In an effort to thoroughly search the global solution space when building population pharmacokinetic models, a single-objective, hybrid genetic algorithm (SOHGA) [1] and a multi-objective genetic algorithm (MOGA) were developed. The objective of this work is to compare the fits of pharmacokinetic models identified using manual, SOHGA, and MOGA methods.

Table 1 Comparison of final models selected using forward addition *I* backward elimination, single-objective hybrid genetic algorithm (SOHGA), and multi-objective genetic algorithm (MOGA)

	ADVAN/TRAN	NONMEM OFV	Number of parameters	Inter-individual variability	Residual error structure	Covariate effe-cts
Citalopram						
Forward/backward	A3, T4	5,695.5	16	Vl, Q, V2	Combined	CL-WT, VI-SEX, Q-FAT, V2-WT
vs. MOGA	A3, T4	5,353.1		Vl, Q, V2	Proportional	CL-BMI, CL-SEX, V1-SEX, V2-FFM, V2-WT
SOHGA	A3, T4	5,335.6	17	VI, Q, V2	Proportional	VI-BMI, VI-SEX, Q-FAT, Q-FFM, V2-FFM, V2-FAT
vs. MOGA	A3, T4	5,339.7		VI, Q, V2	Proportional	CL-BMI, CL-SEX, VI-BMI, VI-SEX, V2-FFM, V2-SEX
Perphenazine						
Forward/backward	A2, T2	540.7	9	CL, V, Ka	Combined	CL-SMK, CL-RACE
vs.MOGA	A2, T2	539.6		CL	Proportional	CL-SMK, CL-CIG, CL-FLUX, V-SMK
SOHGA	A2, T2	531.9	12	CL	Proportional	CL-SMK, CL-CIG, CL-RACE, CL-FLUX, V-SMK, V-AGE, V-SEX
vs. MOGA	A2, T2	529.0		CL	Proportional	CL-SMK, CL-CIG, CL-PARX, V-SMK, V-AGE, V-CIG, V-RACE
Ziprasidone						
Forward/backward	A2 T2	4,751.2	6	GL and V	Proportional	
vs. MOGA	A2 T2	4,746.7		GL and V	Proportional	
SOHGA	A2 T2	4,746.7	6	GL and V	Proportional	
vs. MOGA	A2 T2	4,746.7		GL and V	Proportional	

Methods: Pharmacokinetic models were developed independently using traditional forward addition/backward elimination, SOHGA, and MOGA methods for each of three compounds: intravenous citalopram [2], oral perphenazine [3], and oral ziprasidone [4]. All search methods were given identical options which included ADVAN/TRANS structure, inclusion of inter-occasion variability and block structure, covariate inclusion and associated function form, and form of the residual variability. Final models with the same number of parameters were compared.

Results: The MOGA model for citalopram had a NONMEM OFV value that was more than 10 points lower than the manual models. The OFV of the final SOHGA and MOGA models were within 10 points for all compounds. (see Table 1).

Conclusions: For three test cases, a MOGA identified models with equal or lower OFV versus the forward addition/backward elimination approach. The MOGA approach identified models with equal OFV versus the SOHGA approach but with the intrinsic advantage of incorporating subjective criteria for model selection.

References:

1. Bies RR, et al. A Genetic Algorithm-Based, Hybrid Machine Learning Approach to Model Selection. Journal of Pharmacokinetics and Pharmacodynamics, 33: 195–221, 2006
2. Muldoon MF, et al. The metabolic syndrome is associated with reduced central serotonergic responsivity in healthy volunteers. The Journal of Clinical Endocrinology & Metabolism 91: 718–721, 2006

3. Jin Y, et al. Population pharmacokinetics of perphenazine in schizophrenian patients from CATIE: Impact of race and smoking. The Journal of Clinical Pharmacology 50: 73–80, 2010
4. Wessels AM, et al. Population pharmacokinetic modeling of ziprasidone in patients from the CATIE Study. The Journal of Clinical Pharmacology, 11: 1587–1591, 2011

M-065

Dose- and Formulation-Dependent Non-linear Pharmacokinetic Model of ABT-450, a Protease Inhibitor for the Treatment of HCV: Combined Analyses from 12 Phase 1 Studies

Akshanth Polepally*, Sven Mensing, Amit Khatri, Wei Liu, Walid Awni, Rajeev Menon, Sandeep Dutta

AbbVie, North Chicago, IL, USA and Ludwigshafen, Germany

Objectives: To develop a population pharmacokinetic model of ABT-450 when coadministered with pharmacokinetic enhancer, ritonavir (r). ABT-450 is an HCV NS3/4A protease inhibitor identified by AbbVie and Enanta as a lead compound for clinical development. ABT-450 pharmacokinetics are dependent on dose and formulation and are characterized by a high degree of non-linearity where dose-normalized C_{max} and AUC increase by approximately 60- and 50-fold, respectively, over a 25–400 mg dose range with no change in half-life.

Methods: Pharmacokinetic data from 12 Phase 1 studies in healthy volunteers (N = 369) were used to build a nonlinear mixed-effects model in NONMEM 7.3. Volunteers received ABT-450 hard-gelatin capsules (HGCs) or spray-dried dispersion (SDD) tablets at doses ranging from 50–300 mg ABT-450/r alone or combined with other direct acting antivirals (DAAs), ombitasvir and/or dasabuvir. Effect of dose, formulation and other DAAs on ABT-450 bioavailability and accumulation were estimated. Subject-specific covariates were tested on apparent clearance and volume of distribution parameters. Model development was guided by diagnostic plots, likelihood ratio tests, and prior knowledge of ABT-450 pharmacokinetics.

Results: A two-compartment model with first order absorption and elimination optimally described ABT-450 pharmacokinetic data (Table 1). The nonlinear increase in bioavailability was described by:

$$F = \theta_{bio}^{\left(\theta_{capsule} \times \frac{Dose}{50} - 1\right)}$$

Estimated ABT-450 exposures from SDD tablets for the final 150 mg Phase 3 dose were 7.1- and 2.3-fold of exposures from 50 and 100 mg doses, respectively, and approximately 51 and 75 % lower than the exposures from 200 mg and 250 mg doses, respectively. Multiplicative models best described the estimation of accumulation and effect of dasabuvir on ABT-450 bioavailability. None of the covariates had a significant effect on clearance or volume.

Conclusions: Dose- and formulation-dependent nonlinear ABT-450 bioavailability was characterized using a population based approach. Estimated ABT-450 accumulation and the effect of dasabuvir on ABT-450 were consistent with the results from other studies.

Table 1 ABT-450 population pharmacokinetic parameter estimates

Parameter	Population Estimate (SEE[a])	%RSE[b]	95 % CI[c]
CL/F (L/day)	4360 (849)	19.47	2,696–6,024
Vc/F (L)	965 (187)	19.38	598–1331
Q/F (L day)	185 (66.8)	36.11	54–316
Vp/F (L)	146 (37.2)	25.48	73–219
ka (L/day)	10.5 (0.43)	4.13	9.65–11.35
Relative bioavailability (θ_{bio})	1.54 (0.11)	7.34	1.32–1.76
Formulation effect ($\theta_{capsule}$)	1.27 (0.09)	7.26	1.09–1.45
Accumulation factor	1.57 (0.14)	8.85	1.30–1.84
Effect of dasabuvir on ABT-450 bioavailability	1.59 (0.19)	11.82	1.22–1.96
IIV of CL/F	0.791		
(CV = 110 %)	7.46		0.68–0.91
IIV of Vc/F and Vp/F	1.24		
(CV = 157 %)	7.65		1.05–1.43
Covarianee of IIV parameters	0.959 (r^d = 0.968)	7.61	0.82–1.10
RUV (proportional)	0.441 (66 % CV)	2.97	0.42–0.47
RUV (additive)	1.00 E-07 (fixed)	NA	NA
η CL/F-shrinkage	1.11 %		
$\eta_{Vc/F}$ or $\eta_{Vp/F}$-shrinkage	1.75 %		
ε_{prop}-shrinkage	3.43 %		

NA not applicable

[a] SEE = standard error of estimate

[b] %RSE was estimated as the SEE divided by the population estimate multiplied by 100; c. 95 % CI was approximated as the point estimate ± 1.96* SEE; d. r (correlation of ITV parameters) was calculated from block OMEGA matrix as OMEGA[1,2]/sqrt(OMEGA[1,1])/sqrt(OMEGA[2,2])

[c] 95 % CI was approximated as the point estimate ± 1.96* SEE; d. r (correlation of ITV parameters) was calculated from block OMEGA matrix as OMEGA[1,2]/sqrt(OMEGA[1,1])/sqrt(OMEGA[2,2])

[d] r (correlation of ITV parameters) was calculated from block OMEGA matrix as OMEGA[1,2]/sqrt(OMEGA[1,1])/sqrt(OMEGA[2,2])

M-066

Exposure–Response Analysis for Bapineuzumab Using Imaging and Cerebrospinal Fluid Biomarkers

Alberto Russu[1,a,*], Mahesh N. Samtani[1,b], Steven Xu[1,b], Omoniyi J. Adedokun[1,c], Ming Lu[1,c], Kaori Ito[2,d], Brian Corrigan[2,d], Sangeeta Raje[2,e], Enchi Liu[3], H. Robert Brashear[3], Scot Styren[2,d], Chuanpu Hu[1,c]

[1] Janssen Research & Development, [a] Beerse, Belgium, [b] Raritan, NJ, USA; [c] Spring House, PA, USA; [2] Pfizer, [d] Groton, CT, USA, [e] Collegeville, PA, USA; [3] Janssen Alzheimer Immunotherapy Research & Development, South San Francisco, CA, USA

Objectives: To model the impact of bapineuzumab exposure on Week 71 change from baseline in brain fibrillar amyloid burden as measured by 11C-labeled Pittsburgh compound B positron emission

tomography, global cortical average of Standardized Uptake Value ratio (PiB PET GCA SUVr), cerebrospinal fluid phosphorylated tau (CSF p-tau) concentration, and brain volume as measured by brain boundary shift integral (BBSI), using combined data from two bapineuzumab Phase 3 studies in mild-to-moderate Alzheimer's disease (AD) subjects [1].

Methods: The exposure–response relationship was modeled for each biomarker separately. Baseline disease status (baseline Mini Mental State Examination score 21–26 "mild" AD or 16–20 "moderate" AD), apolipoprotein E E4 allele (APOE*E4) carriers/noncarriers, and baseline biomarker levels were investigated as exposure–response covariates.

Results: A linear relationship between steady-state bapineuzumab serum area-under-curve and PiB PET GCA SUVr response was identified, with larger baseline SUVr associated to larger effect, increased SUVr from baseline for placebo APOE*E4 carriers, but no change for placebo noncarriers. Bapineuzumab steady-state trough serum concentration correlated with CSF p-tau reduction in APOE*E4 carriers. In noncarriers, a weak but not significant trend was observed. Higher baseline p-tau concentration and moderate AD baseline status were associated with larger p-tau reduction. BBSI analysis evidenced no effect on brain shrinkage.

Conclusions: Bapineuzumab was confirmed to induce modifications in selected AD biomarkers [1]. Positive intercepts in PiB PET GCA SUVr exposure–response for APOE*E4 carriers and in CSF p-tau exposure–response for APOE*E4 carriers with mild baseline AD suggest biomarker increases consistent with disease progression in placebo groups. Bapineuzumab effect on p-tau reduction was stronger in APOE*E4 carriers. An exposure–response relationship on brain volume was not confirmed.

References:

1. Salloway S et al. NEJM 2014;370:322–33.

M-067

Population Pharmacokinetic Evaluation and Missed Dose Simulations for Eslicarbazepine Acetate Monotherapy

Soujanya Sunkaraneni[2,*], Luann Phillips[1], Vaishali Chudasama[1], Elizabeth Ludwig[1], David Blum[2], Jill Fiedler-Kelly[1]

[1] Cognigen Corporation, Buffalo, NY, USA; [2] Sunovion Pharmaceuticals Inc., Marlborough, MA, USA

Objectives: Eslicarbazepine acetate (ESL) is approved as an adjunctive therapy for partial-onset seizures in adults. ESL is not approved for use as monotherapy. The effect of missing a dose of ESLwhen used as monotherapy on plasma and cerebrospinal fluid (CSF) eslicarbazepine (primary active metabolite of ESL) concentrations is not known.

Methods: Plasma eslicarbazepine pharmacokinetics (PK) was determined from Phases 1/3 trials, including 2 monotherapy studies. CSF concentrations were available from 6 healthy subjects. A peripheral (CSF) compartment was added to the previously developed plasma PK model for eslicarbazepine, with plasma parameters and covariate effects fixed to estimates from the Phases 1/3 studies used for model development. Stochastic simulations of 1,200 virtual monotherapy patients were performed using the final PK model for eleven ESL missed dose scenarios.

Results: The exploratory PK model that adequately predicted CSF concentrations was a 2-compartment model with first-order absorption/elimination. Typical parameter values (%SEM) were 0.018 1/h (91.4) and 0.145 1/h (15.2) for drug transfer in and out of CSF from plasma, respectively; apparent CSF distribution volume was 16.9 L (81.2). Based on the simulations of missed doses, when doses were delayed 12–16 or 36–42 h, the immediate administration of a 1,600 mg dose followed by an additional dose at the regular scheduled time (6–12 later) maintained plasma concentrations within a selected target range. When the dose was delayed by 20, 24 or 48 h, administration of 1.5 times the proposed maximum monotherapy dose of 1,600 mg was required to achieve plasma concentrations similar to levels achieved after all doses were administered on time. When doses were delayed 12–44 h, following the dosing pattern for plasma, CSF concentrations remained above CSF concentrations without delayed dosing for the majority of the dosing interval.

Conclusions: Eslicarbazepine CSF concentration time profiles were adequately predicted with an exploratory 2-compartment model, thus allowing for simulation of missed dose scenarios to understand the impact on plasma and CSF concentrations.

M-068

Virtual Systems Pharmacology (ViSP) Flexible Web-Based Environment for Running Large Multi-scale Models

Sergey Ermakov[1], Peter Forster[2], Jyotsna Pagidala[1], Marko Miladinov[1], Al Wang[1], Derek Bartlett[3], Rebecca Baillie[3], Mike Reed[3], Tarek Leil[1]

[1] Bristol-Myers Squibb, Princeton, NJ, USA; [2] Forster Solutions, Wilmington, DE, USA; [3] Rosa & Co LLC, San Francisco, CA, USA

Objectives: Software packages used for Mechanistic Systems Level Modeling are judged by their model development capabilities, user interface, available solvers, convenience of handling large number of parameters and simulations, export-import capabilities, cost of software and support, etc. Lack of a single software ranking favorably against all criteria forced us to look for a way of using several software packages while having a common tool that can be employed by any of them for running large scale simulation tasks. Thus the goal is to develop a simple and user-friendly platform designed to easily set up, handle and run multiple simulation tasks in a flexible hardware/software environment.

Methods: The key feature of ViSP is that it separates the instance of performing a simulation from the software that sets up the simulation. The simulation instance is a self-contained executable file produced by compiling the model code and converting it to a binary file. The executable file is then initialized with a number of numeric parameters, some are model specific, for instance, disease characteristics, properties of a particular patient, drug properties, while other parameters define simulation time, output frequency etc. Multiple executable files with different initial conditions can be initiated and run in parallel on separate processors, or in a cloud environment (see Fig. 1). This process is quite general and it was implemented in ViSP to handle executable files originating from different modeling software packages provided with appropriate initial data.

ViSP relies on web-based UI designed to be configurable by a user to accommodate the specifics of a particular model. It is capable of handling multiple models and large number of parameters presenting them in tree-like structure.

Results: ViSP was used for simulation using a mechanistic metabolic diseases model to simulate the effects of metformin and a GPR40 agonist (TAK-875) on glycemic biomarkers in type 2 diabetes patients. ViSP permitted easy set up of the clinical study design and simulations for a high dimensional model (>100 ODEs) with multiple virtual patients each containing more than 800 parameters.

Conclusions: Web-based user-friendly software (ViSP) was developed to quickly set up, handle and run multiple simulation tasks in a

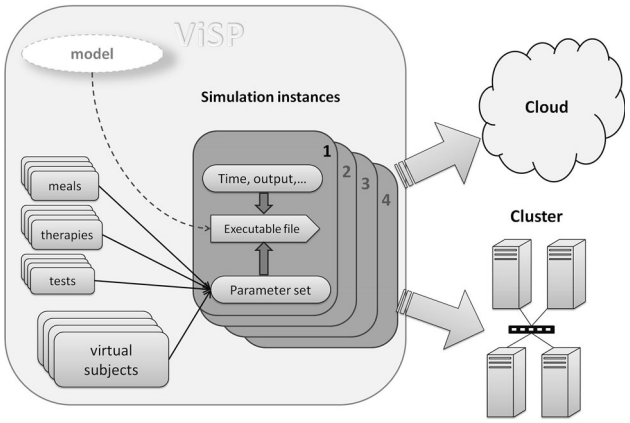

Fig. 1 .

flexible hardware/software environment. It is not model or software specific and can utilize existing cluster or cloud computing environments for conducting large scale clinical trial simulations.

M-069

Riociguat Dosing Recommendations in Pulmonary Arterial Hypertension (Pah)/Chronic Thromboembolic Pulmonary Hypertension (Cteph), Based on Pharmacometric Analyses

Dhananjay Marathe*, Divya Menon-Andersen, Rajanikanth Madabushi, Preston Dunnmon, Yaning Wang

U.S. FDA, Philadelphia, PA, USA

Objectives: Riociguat was approved in 2013 for treatment of PAH and CTEPH. The objective of this work was to evaluate exposure–response (E–R) relationships for safety/efficacy of riociguat and to quantify the impact of covariates on plasma riociguat exposure in patients to support the dosing recommendations for the starting dose and highest capped dose in overall population and specific sub-populations (esp. smokers) [1].
Methods: In placebo-controlled pivotal phase 3 studies in PAH and CTEPH populations, the starting dose was 1 mg TID and there was up-titration till 2.5 mg TID maximum dose. PAH trial had an additional arm with 1.5 mg TID maximum dose. E–R relationship for efficacy (change in 6-minute walk distance) was evaluated using responses binned by quantiles of riociguat exposure. Since $\sim$45 % of all on treatment patients had hypotension, an important safety signal (SBP <90 mmHg) occurring within 1–2 days of therapy initiation with 1 mg TID dose, the E–R relationship for this safety signal was evaluated by logistic regression analysis using observed first day Ctrough. The impact of smoking on drug exposure/clearance was evaluated using empirical Bayes estimates from Population-PK model.
Results: In the PAH phase 3 trial, both 1.5 mg and 2.5 mg capped dose arms of riociguat had clinically significant benefit over placebo. The E–R relationship for efficacy endpoint was flat indicating no additional benefit with higher dose/exposure at population level. There was statistically significant correlation ($p < 0.05$) of higher incidences of early hypotension for patients with higher Ctrough. Smoking induces CYP1A1, the main enzyme responsible for metabolism of riociguat. Consistent with this, the sponsor's observation of smokers having nearly half the plasma exposure of riociguat compared to nonsmokers was confirmed by us.
Conclusions: Based on these analyses, the dosing recommendation in the label included consideration of 0.5 mg instead of 1 mg TID as the starting dose for patients who may not tolerate the hypotensive effect of drug. For smokers, consideration of doses higher than 2.5 mg TID was recommended to match the exposures seen in nonsmokers.

References:

1. Riociguat Clinical Pharmacology Review: http://www.accessdata.fda.gov/drugsatfda_docs/nda/2013/204819Orig1s000ClinPharmR.pdf

M-070

Exposure-Efficacy Analysis for Daclatasvir and Asunaprevir in DUAL Combination in Subjects with Genotype 1b Hepatitis C Virus Infection

Li Zhu[1], Phyllis Chan[1], Timothy Eley[1], Marc Bifano[1], Mayu Osawa[2], Takayo Ueno[2], Eric Hughes[1], Malaz AbuTarif[1], Richard Bertz[1], Tushar Garimella[1,*]

[1] Bristol-Myers Squibb Research and Development, Lawrenceville, NJ, USA; [2] Bristol-Myers K. K., Tokyo, Japan

Objectives: Daclatasvir (DCV) is a potent pangenotypic once-daily NS5A inhibitor and asunaprevir (ASV) is a potent, twice-daily NS3 inhibitor under regulatory review for treatment of chronic HCV infection as DUAL combination. The current analysis characterized the relationship between exposures of DCV and ASV and sustained virological response (SVR12) in HCV genotype 1b subjects.
Methods: The relationship between the probability of achieving SVR12 and model predicted Cavgss for ASV and DCV was described using a logistic regression (LR) model with data from 4 studies in HCV-infected genotype 1b subjects (N = 947). Model development steps included characterization of functional form for relationship between exposure and response and covariate identification (demographic, laboratory, prognostic and treatment covariates). Non-parametric bootstrap and visual predictive checks (VPC) stratified by significant covariates were used for model evaluations.
Results: The base ER model was a linear LR model with intercept, slopes for DCV and ASV Cavgss, and interaction between DCV and ASV. Presence of NS5A baseline resistance mutations (BRMs) Y93H and L31 M/V, interaction between ASV and presence of BRMs, age greater than or equal to 65 years and baseline HCV RNA were statistically significant covariates in the full model. In the final model only BRMs were statistically significant predictors of SVR12. Unlike the slope for DCV Cavgss, slope for ASV Cavgss and interaction between DCV and ASV were not statistically significant suggesting no or very flat relationship with ASV. Race, cirrhosis status and patient type were not significant covariates on SVR.
Conclusions: The ER model demonstrated a shallow relationship between DCV exposure and SVR12 and flat and non-statistically significant relationship between ASV exposure and SVR12. Presence of the NS5A BRMs were significant predictors of lower SVR12. Overall the ER model supported the high SVR12 rates for the DUAL combination (DCV 60 mg QD and ASV 100 mg BID) in GT-1b HCV infected subjects.

M-071

Utility of Clinical Trial Simulation in Bioequivalence Modeling of Combination Products

Wen-I Li, Li (Lilly) Liu and Ryan Turncliff*

Alkermes, Inc., Waltham, MA, USA

Objectives: General guidance and consideration for the evaluation of bioequivalence (BE) of combination products are limited, particularly when the active components exhibit divergent pharmacokinetic characteristics. The utility of clinical trial simulation (CTS) in informing the design of definitive BE trials was explored for the combination of drugs "INV-1" and "INV-2".
Methods: Two- and one-compartmental models with 1st-order oral absorption were generated to create the PK time course of INV-1 and INV-2 plasma concentrations, respectively. Reference and test formulations were simulated using Monte Carlo simulations (Pharsight Trial Simulator v2.2.1) with inter-subject variability for INV-1 (high 30 % CV range) and INV-2 (low 20 % CV range). CTS (two-way crossover design) were conducted using sample sizes ranging from 12 to 100 per trial, with 10 replicates of each to evaluate the BE (C_{max} and AUCinf) of INV-1 and INV-2.
Results: The 90 % CIs of the ratios of INV-1 for C_{max} (0.91–1.12) and AUC (0.91–1.11) were within the BE limits for all trials when sample size was $\geq$52. For INV-2, 28 subjects were sufficient to demonstrate BE between two formulations for C_{max} (0.91–1.13) and AUC (0.93–1.16), with statistical power >90 %.
Conclusions: CTS were successfully conducted to predict the clinical outcome and provide guidance on the study design of a definitive BE trial for a combination product of INV-1 and INV-2. To achieve BE between the two formulations, a larger sample size of $\geq$ 52 subjects was recommended due to the higher inter-subject variability associated with INV-1 in comparison to INV-2. Additionally, PK sampling and study duration should be guided by INV-2 PK due to the longer elimination half-life and biphasic disposition governed by the model. The modeling and simulation approach presented provides a generalizable strategy for the evaluation of optimal BE trial design and sampling schemes for combination drug products.

Disclosures: Drs. Li, Liu and Turncliff are employees of Alkermes Inc.

M-072

Alternatives to Random Coefficients Mixed Effects Models

Kuenhi Tsai*, Zifang Guo

Biostatistics and Research Decision Sciences, Merck Research Laboratories, Merck and Co., Rahway, NJ, USA

Objectives: The random coefficients mixed effects model (RCMM) is highly prevalent in the PK and PK-PD modeling arena. However, in some settings, an alternative such as a population-averaged model (PAM), which focuses on the population (rather than individual) mean response may be more appropriate, such as in sparse data situations and when interest lies primarily in assessing the impact of covariates on population response means. Two examples of PAM are provided and examined.
Methods: The first example is from a PK/receptor occupancy study. Each subject had three measurements and there were only six subjects in the study. An E_{max} model with random (subject-specific) coefficients was intended to be built. In the second example, PK and QTc data from two clinical studies were pooled to assess the potential for a drug-induced QTc prolongation. A linear PK/QTc model was constructed to predict the effect of higher plasma concentrations of the study drug on QTc, and to quantify potential covariate effects, with special attention to race. PAM with correlated errors was utilized in both examples.
Results: RCMM cannot be used for the first example because of insufficient data to quantify the random effect involving the EC50. However, a population-averaged E_{max} model with correlated errors offers a legitimate alternative model, which takes within-subject correlation into consideration. In the second example, a linear PK-QTc PAM with double compound symmetry error correlation structure provided a simple avenue for addressing the modeling objectives.
Conclusions: Although RCMM is very useful in PK and PK-PD modeling, it may not be the most appropriate model in every setting, and how to incorporate the random effect and covariates usually becomes a challenging issue. The two examples provided illustrate that PAM with correlated errors provides a solution for this modeling problem.

M-073

Assessing Labeling Claims for Drug Interactions Using a Population PK Approach: Vedolizumab

Justin C. Earp[1], Lucy Fang[1], Lian Ma[1], Yow-Ming Wang[1], Maria Rosario[2], Nathanael L. Dirks[3], Nitin Mehrotra[1]

[1] US FDA, Office of Clinical Pharmacology, Silver Spring, MD, USA; [2] Takeda, Cambridge, MA, USA; [3] Metrum Research Group, Tariffville, CT, USA

Objectives: Assess the reliability of using population PK approach to support claim of four concomitant medications not affecting Vedolizumab PK in patients with ulcerative colitis or Crohn's disease.
Methods: Previous simulation work was examined to determine the statistical power of a population PK approach to detect no interaction based on variability and a pre-established PK model [1]. The applicant conducted population PK analysis of vedolizumab in the presence and absence of concomitant medications. The effects of these medications were characterized by a time-dependent factor on clearance. Structural characteristics of the PK model and inter-subject variability used in the simulation work [1] were assessed to determine their relevance to the Vedolizumab population PK analysis and to identify necessary data characteristics for a specific set of model assumptions. Dosing amounts, sample-size, and timing of PK samples were reviewed for patients who received azathioprine, 6-mercaptopurine, methotrexate, or various amino-salicylates and compared to the necessary requirements to achieve at least 80 % power to detect no-interaction.
Results: There were more than 30 subjects, for each comedication, receiving azathioprine, 6-mercaptopurine, methotrexate, or amino-salicylates and more than 100 subjects that did not receive comedications. The median duration of use for each concomitant medication was sufficient to establish steady-state concentrations and ensure that the timing of Vedolizumab PK samples overlapped dosing of the concomitant medications. Both applicant's model and prior simulation model developed by the POPPK TP-DDI task force were similar to apply criteria needed to determine no-interaction. For all the interactions, clearance was not significantly different in presence of the comedication.
Conclusions: Population PK analysis was utilized for concluding a lack of DDI, specifically no effect of coadmininstered azathioprine, 6-mercaptopurine, methotrexate, and amino-salicylate on Vedolizumab PK and this information was included in the label.

Reference:

1. Wang, D. et al. The Utility of a Population Approach in DDI Assessments: An Evaluation Using Simulation Approaches. 2013 ACOP Poster

M-074

Application of Pharmacometrics to Guide Regulatory Decisions for Drugs to Treat Rare Diseases

Lian Ma*, Xiaofeng Wang*, Nitin Mehrotra, Atul Bhattaram, Justin Earp, Jeffry Florian, Kevin Krudys, Jee Eun Lee, Fang Li, Hongshan Li, Jiang Liu, Anshu Marathe, Dhananjay Marathe, Jeffrey Tworzyanski, Yaning Wang, Jingyu Yu, Li Zhang, Liang Zhao, Ping Zhao, Vikram Sinha

* First Authorship with Equal Contribution; Division of Pharmacometrics, OCP/OTS/CDER/FDA, Silver Spring, MD, USA

Background: For rare diseases, pharmacometric approaches have become an increasingly important component for drug development and regulatory decisions in early development (INDs) and NDA/BLA applications to support drug approval, labelling and inform trial design. Disease progression models are being used to understand the natural history of these diseases specifically in identifying baseline factors, characterizing endpoints and duration with the aim of understanding likelihood of success.
Methods: An internal survey was conducted to evaluate the impact of pharmacometric analyses on regulatory decisions for orphan drug NDA and BLA submissions reviewed by FDA pharmacometricians between January 2008 and January 2014. Case studies are briefly summarized to illustrate the impact of pharmacometric analyses in regulatory decision making.
Results: A total of 300 NDA and BLA submissions were reviewed during these 6 years, among which 76 (25 %) were for rare disease indications. Of these, pharmacometric analysis in 26 and 84 % were pivotal for approval and labeling decisions, respectively. The pharmacometric analyses contributed to several decisions including optimization of dosing regimens, selection of doses for further clinical testing, and providing evidence of effectiveness. For example, exposure–response analysis was pivotal for dose selection for infliximab for the treatment of ulcerative colitis in pediatrics and was also utilized to support the approval of a lower starting dose of pasireotide for Cushing's disease that did not meet the pre-specified primary endpoint. For accelerated approval of everolimus for the treatment of Subependyal Giant Cell Astrocytoma, exposure–response analysis provided supportive evidence of effectiveness.
Conclusions: Pharmacometrics has potential to address several challenges in orphan drug development especially in maximizing the utilization of all available data. Application of Pharmacometrics in drug development of rare diseases offers a significant return on investment.

T-001

Population Pharmacokinetic Analysis of Asunaprevir in Subjects with Hepatitis C Virus (HCV) Infection

Li Zhu[1], Hanbin Li[2], Phyllis Chan[1], Timothy Eley[1], Marc Bifano[1], Mayu Osawa[3], Takayo Ueno[3], Eric Hughes[1], Malaz AbuTarif[1], Richard Bertz[1], Tushar Garimella[1,*]

[1] Bristol-Myers Squibb Research and Development, Lawrenceville, NJ, USA; [2] Quantitative Solutions, Menlo Park, CA, USA; [3] Bristol-Myers K.K., Tokyo

Objectives: Asunaprevir (ASV) is a potent, twice daily HCV NS3 inhibitor currently under regulatory review for the treatment of chronic HCV infection. A population pharmacokinetic (PPK) model was developed to evaluate the effects of covariates on ASV PK in subjects with chronic HCV infection and provide individual exposure data for exposure–response analyses.
Methods: The PPK model for ASV was developed using ASV plasma concentration data from five studies in HCV infected subjects (N = 1236). A non-linear mixed effects modeling approach as implemented in NONMEM 7.1.2 was used. Significant demographic, laboratory, prognostic and treatment covariates ($p < 0.05$) from univariate screening were included in the full model. The final model was reached using backward elimination ($p < 0.001$). Simulations were performed to evaluate the impact of covariates on ASV exposures.
Results: Plasma PK of ASV was described by a two-compartment model with first-order elimination and zero-order release followed by first order absorption into the central compartment. Typical value for CL/F was 50.8 L/h (8.0 % RSE) after single dose, increasing by 43 % after 48 h to 72.5 L/h at steady state. Vc/F was 47.6 L (10.9 % RSE). Modest inter-individual variability was estimated for CL/F (41 %) but was large for Vc/F (148 %). Statistically significant covariates in the final model were formulation on Ka, age, gender, race, AST and cirrhosis on CL/F and gender and cirrhosis on Vc/F. Compared to a Caucasian non-cirrhotic patient with median baseline AST, simulations that take into account covariate correlations indicate that, AUC (TAU) is expected to be 58, 84 and 45 % higher in subjects with baseline AST in the fourth quartile, in cirrhotic (Child Pugh A) and Asian subjects, respectively.
Conclusions: The model adequately described ASV PK, including auto-induction. ASV CL/F decreases with cirrhosis and increasing baseline and time-varying AST indicating an association between hepatic markers and CL/F.

T-002

Population Pharmacokinetic Analysis of Daclatasvir in Subjects with Hepatitis C Virus (HCV) Infection

Phyllis Chan[1], Hanbin Li[2], Li Zhu[1], Marc Bifano[1], Timothy Eley[1], Mayu Osawa[3], Takayo Ueno[3], Eric Hughes[1], Richard Bertz[1], Tushar Garimella[1,*], Malaz AbuTarif[1]

[1] Bristol-Myers Squibb Research and Development, Lawrenceville, NJ, USA; [2] Quantitative Solutions, Menlo Park, CA, USA; [3] Bristol-Myers K.K, Tokyo

Objectives: Daclatasvir (DCV) is a potent, pangenotypic once daily HCV NS5A inhibitor currently under regulatory review for the treatment of chronic HCV infection. A population pharmacokinetic (PPK) model was developed to evaluate effects of covariates on DCV PK in subjects with chronic HCV infection and provide individual exposure data for exposure–response analyses.
Methods: The PPK model for DCV was developed using DCV plasma concentration data from 11 studies in HCV infected subjects (N = 2149). A non-linear mixed effects modeling approach as implemented in NONMEM 7.1.2 was used. All significant of demographic, laboratory, prognostic and treatment covariates ($p < 0.05$) from univariate screening were included in the full model. The final model was reached by backward elimination ($p < 0.001$) and simulations were performed to evaluate the effects of covariates on DCV exposures.
Results: Plasma PK of DCV was described by a two-compartment model with linear elimination. Absorption was modeled as zero-order release followed by a first order absorption into the central compartment. Typical value of CL/F was 5.7 L/h (1.58 % RSE) and Vc/F was 58.6 L (2 % RSE). Modest inter-individual variability was estimated for CL/F (35.1 %) and Vc/F (29.5 %). Statistically significant covariates in the final model were sex, race, virus genotype, baseline CrCL and ALT on CL/F and sex, race and BW on Vc/F. Covariate

effects demonstrated a 30 % higher AUC in female subjects; effects of all other covariates were ≤16 %.
Conclusions: The model adequately described DCV PK and estimated relatively small covariate effects. Considering the exposure range for the therapeutic dose of 60 mg QD and the favorable safety profile the small difference in exposures due to these covariates is not considered clinically relevant and no dose adjustment is recommended.

T-003

Exposure-Safety Analysis for Asunaprevir and Daclatasvir in DUAL Combination in Subjects with Hepatitis C Virus Infection

Phyllis Chan, Li Zhu, Timothy Eley, Marc Bifano, Eric Hughes, Richard Bertz, Tushar Garimella*, Malaz AbuTarif

Bristol-Myers Squibb Research and Development, Lawrenceville, NJ, USA

Objectives: Asunaprevir (ASV) is a potent, twice daily NS3 inhibitor and daclatasvir (DCV) is a potent pangenotypic once-daily NS5A inhibitor currently under regulatory review for the treatment of chronic HCV infection. The current analysis of the DCV/ASV combination characterized relationships between ASV exposures and ALT, AST and total bilirubin (Tbili) elevations in HCV subjects and associations between both ASV and DCV exposures and other adverse events of interest (pyrexia, eosinophilia).
Methods: The relationship between the cumulative probability of achieving maximum grades 1/2 and 3/4 ALT, AST or Tbili elevation severity during treatment and model predicted Cavgss for ASV was described using ordinal logistic regression (OLR) models (one model for each endpoint) with ordered categorical data from five studies (N = 1413). Model development included characterization of functional form for relationship between exposure and transaminase elevations and covariate identification (demographic, laboratory, prognostic and treatment covariates). Visual predictive check stratified by significant covariates was used for model evaluations.
Results: The observed incidence of grade 3/4 ALT and AST was low during DCV/ASV treatment at clinical doses (DCV 60 mg QD and ASV 100 mg BID) (<4.5 %). The base ER models for all three endpoints were linear OLR models with slopes for ASV Cavgss. Baseline values of ALT, AST and Tbili were the most significant predictors of transaminase elevations during treatment. In final models for ALT and AST, ASV Cavgss was not statistically significant. For Tbili ASV Cavgss was statistically significant; however, the observed incidence of grade 3/4 events was very low (~0.6 %). There was a trend towards higher ASV exposures with pyrexia and eosinophilia but no relationship with DCV exposures.
Conclusions: At the Phase three doses, ER demonstrated no significant relationship between ASV exposure and incidence of transaminase elevations. Baseline transaminase values were significant predictors of the few events. No significant relationships were observed between DCV exposure and safety events.

T-004

Two-stage Adaptive Designs in Nonlinear Mixed-Effects Models: an Evaluation by Simulation for a Pharmacokinetic/Pharmacodynamic Model in Oncology

Giulia Lestini, Cyrielle Dumont, France Mentré*

IAME, UMR 1137, INSERM, University Paris Diderot, Paris, France

Objectives: Optimal design in population pharmacokinetic/pharmacodynamic needs prior information on models and parameters. Adaptive designs [1] are promising alternatives. We compared by simulation one-stage and two-stage designs using an oncology PKPD example [2, 3].
Methods: Two sets of population parameters were considered: wrong a priori parameters [3], psi0, and true parameters, psi*. We evaluated several designs of N = 50 patients: two one-stage designs, ksi0 and ksi*, optimized with psi0 and psi*, and various two-stage designs. Two-stage designs have N1 patients with design ksi0 in the first cohort and N2 patients with design lsi2 in the second cohort, where ksi2 is optimized using parameter estimates from data collected after first stage (see Fig. 1). Different cohort sizes at each stage (N1 + N2 = N) were evaluated. For each design we simulated 100 datasets using psi*. We estimated parameters (MONOLIX 4.3) and calculated relative bias and relative root mean square error to compare the designs. Design optimization was performed with PFIM 4.0 [4].
Results: Estimation results with two-stage designs were close to those with the optimal design ksi* and much better than with the priori design ksi0. The balanced two-stage design (N1 = N2 = 25) performed better than unbalanced two-stage designs.
Conclusions: Two-stage designs improve the design after the first cohort and are therefore useful when the correct prior information is not available.
This work is supported by the DDMoRe project (www.ddmore.eu).

The results in this abstract have been previously presented in part at PAGE 23, Spain, June 2014 and published in the conference proceedings as abstract 3168.

References:

1. Dumont C, Chenel M, Mentré F. Two-stage optimal designs in nonlinear mixed effect models: application to pharmacokinetics in children. Comm Stat Simulat Comput (2014)
2. Gueorguieva I, Ogungbenro K, Graham G, et al. A program for individual and population optimal design for univariate and multivariate response pharmacokinetic-pharmacodynamic models. Comput Methods Programs Biomed (2007)
3. Gueorguieva I, Cleverly A, Stauber A, et al. Defining a therapeutic window for the novel TGF-β inhibitor LY2157299 monohydrate based on a pharmacokinetic/pharmacodynamic model. Br J Clin Pharmacol (2014)
4. www.pfim.biostat.fr

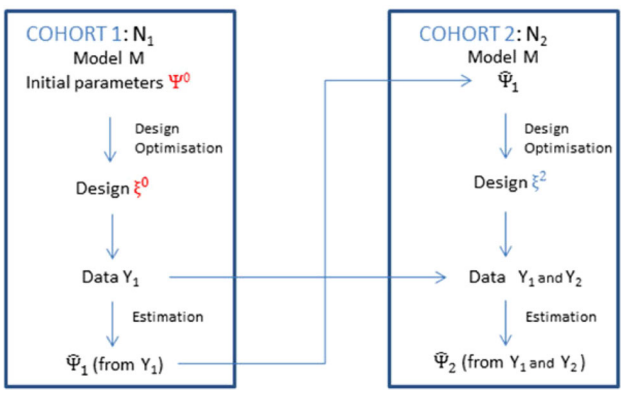

Fig. 1 Two-stage design

T-005

Working with Exposure-Limits During Phase I Dose-Escalation Studies

Ahsan Rizwan*, Walter Krauwinkel and Peter Bonate

Astellas Pharma, Tokyo, Japan

Objectives: Exposure-limits present a challenge during dose-escalation in SAD and MAD studies because they limit the permissible human exposure to a fixed AUC and/or Cmax. The limits exist when there are unexplained/severe/un-monitorable/irreversible AEs during non-clinical toxicology studies. Three cases are described here and how probability of exceeding the exposure-limit were estimated during dose-escalation.
Methods: Compound-A showed linear PK after multiple-dosing. Compound-B showed a more-than-dose-proportional increase in Cmax and AUC after single and multiple-dosing. With multiple-dosing a more than expected accumulation was observed along with ethnic differences. In all cases the general methodology used a median and standard deviation and assumed a log-normal distribution to simulate 1,000 AUC and Cmax values. Then, the percentage of subjects exceeding the exposure-limit was determined.
For Compound-A with linear PK a population model was developed and simulations were made to determine the dose where less than 5 % of subjects would likely exceed the cap.

For the Compound-B SAD study with more-than-dose-proportional PK, the dose-normalized AUC/Cmax showed a sigmoidal relationship. Therefore, an Emax model was used to predict AUC/Cmax in a future dose-cohort.

For the Compound-B MAD study the steady-state levels for the next dose cohort were estimated using non-parametric superposition from Day 1 concentrations of both the SAD and MAD study. The median exposure and the % of subjects above the predicted and 95th percentile (from the 90 % prediction interval, PI) were used to judge risk.
Results: In all three cases we were able to increase the study team's understanding about the risk of exceeding the exposure cap. In retrospect, good predictive performance was achieved while working under the constraints of short timelines and limited data. It was not always possible to develop a population model and several scenarios (best-case, worst-case) were developed to present the relative risk in the face of uncertainty.

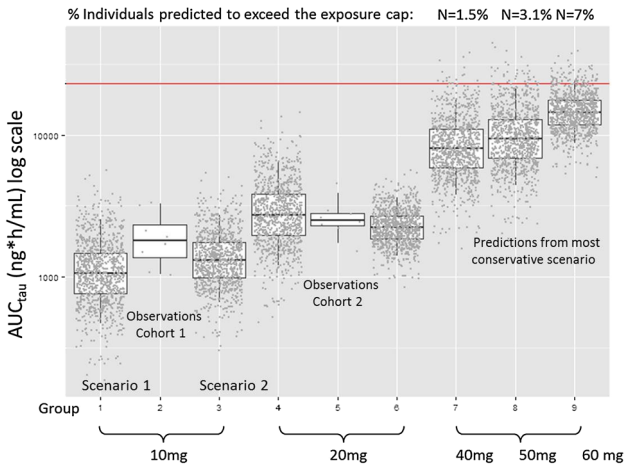

Fig. 1 Visual aid for observations and scenario (MI, M2)-based predictions (*red line* shows exposure limit)

Conclusions: As an increasing number of NCEs are being developed under exposure limits there is a need amongst pharmacometricians to discuss and share methodologies for predicting the risk to exceed exposure limits Fig. 1.

T-006

Prediction of Precision of Estimation and Shrinkage for Individual Parameters Using the Bayesian Fisher Information Matrix in Nonlinear Mixed Effect Models with PFIM 4.0

Thu Thuy Nguyen, France Mentré* and the PFIM Group

IAME-UMR 1137, INSERM and University Paris Diderot, Paris, France

Objectives: When information is sparse, individual parameters estimated by maximum a posteriori (MAP) after nonlinear mixed effect model (NLMEM) analysis can shrink to the mean. We aimed to: (1) propose an approach to predict standard errors (SE) and shrinkage of individual parameters; (2) implement this new approach in PFIM; (3) illustrate these developments in a dose-response study.
Methods: The Bayesian Fisher information matrix (MBF) is the sum of individual information (via the individual Fisher matrix MIF) and a priori information (via the random effect variance). We approximated MBF by first-order linearization and derived SE and shrinkage from MBF [1]. These developments were implemented in PFIM 4.0 released in Spring 2014, which also included several other new features (www.pfim.biostat.fr). We predicted SE and shrinkage in an Emax model with several doses per patient [2]. We studied several individual designs varying the number of doses (n), the variance of random effects (Omega) and residual errors (Sigma). We also proposed an optimal design based on the determinant of MBF.
Results: As expected, SEs predicted by MBF were lower than those predicted by MIF. SE increased when n decreased and Omega and Sigma increased; shrinkage increased when n decreased, Omega decreased and Sigma increased. Design optimisation allows sparse design while giving reasonable SE and shrinkages.
Conclusions: MBF enables prediction of shrinkage and SE of individual parameters estimated by MAP. PFIM is a relevant tool to evaluate and optimise population and Bayesian design in trials analysed by NLMEM.

References:

1. Plan EL, Maloney A, Mentré F, Karlsson MO, Bertrand J. Performance comparison of various maximum likelihood nonlinear mixed-effects estimation methods for dose-response models, AAPS J, 2012, 14:420–432
2. Combes F, Retout S, Frey N, Mentré F. Prediction of shrinkage of individual parameters using the Bayesian information matrix in nonlinear mixed-effect models with application in pharmacokinetics. Pharm Res, 2013; 30:2355–2367

T-007

Population Pharmacokinetics of ABT-450, Ombitasvir, Dasabuvir, Ritonavir and Ribavirin in Subjects with HCV Genotype 1 Infection

Sven Mensing*, Akshanth Polepally, Denise König, Amit Khatri, Wei Liu, Thomas Podsadecki, Walid Awni, Rajeev Menon, Sandeep Dutta

AbbVie, Ludwigshafen, Germany and North Chicago, IL, USA

Objectives: AbbVie currently has three direct acting antiviral agents (DAA) in clinical development for treatment of HCV genotype 1 (GT1) infection. ABT-450, an HCV NS3/4A protease inhibitor identified by AbbVie and Enanta as a lead compound for clinical development dosed with ritonavir, a pharmacokinetic enhancer. Ombitasvir is a NS5A inhibitor, and dasabuvir is a NS5B non-nucleoside polymerase inhibitor. Objective of these analyses were to characterize the population pharmacokinetics (PopPK) of ABT-450, ombitasvir, dasabuvir, ritonavir, and ribavirin and to identify the patient-specific covariates affecting their exposures.
Methods: Pharmacokinetic data were obtained from nine Phase 1b/2 studies (total N = 676) in GT1 HCV infected subjects receiving one to three DAAs or ribavirin. PopPK models were built using NONMEM 7.3. Patient-specific covariates were tested on clearance and volume. Effects of comedications were tested only on clearance. Model development was guided by diagnostic plots, likelihood ratio tests, and prior knowledge of DAA pharmacokinetics. Accumulation and formulation effect parameters of ABT-450 were fixed to values estimated from Phase 1 PopPK analysis.
Results: Model type, significant covariates and structural parameter estimates are presented in Table 1. Model estimated nonlinear bioavailability of ABT-450 predicts an approximate 2–3× increase in AUC for every 50 mg increase in dose. Prior treatment experience or HCV subtype 1a and 1b were not significant covariates on clearance or volume parameters. Presence of ribavirin was a non-significant covariate on clearance or volume parameters for the DAAs or ritonavir. Model predicted exposures based on post-hoc values indicated that exposures were comparable between healthy and HCV infected subjects.
Conclusions: The observed pharmacokinetic data for all drugs were well-described by the models. Use of ribavirin did not affect the pharmacokinetics of DAAs or ritonavir. Exposures for DAAs and ritonavir from HCV GT1 infected subjects were comparable to healthy volunteers.

Table 1 Population pharmacokinetic parameter estimates and significant covariates

Compound	Ombitasvir	Dasabuvir	ABT-450[b,c]	Ritonavir	Ribavirin
PK model	2 compartment	1 Compartment	1 Compartment	1 Compartment	3 Compartment
Ka l/day	4.97 (0.206)[a]	14.0 (0.593)	5.97 (0.32)	4.03 (0.013)	20.64 fixed[d]
CL/F (L/day)	579(11.9)	1690 (50.2)	3770 (595)	373 (1.21)	492 (10.6)
Vc/F (L)	164 (7.50)	417 (15.9)	633 (104)	46.1 (0.149)	999 (40.0)
Q/F (L/day)	224 (19.0)	–	–	–	254 (40.9)
Vp/F (L)	345 (23.6)	–	–	–	5,110 (533)
V4/F	–	–	–	–	3,090 (230)
Q2/F	–	–	–	–	2,100 (141)
IIV on CL/F	0.0360	0.323	1.32	0.542	0.0745
	CV = 30 %	CV = 62 %	CV = 166 %	CV = 85 %	CV = 23 %
IIV on	0.296	0.431	2.08	1.69	0.341
Vc/Vp	CV = 59 %	CV = 73 %	CV = 265 %	CV = 210 %	CV = 64 %
Covariates on CL/F	Age, sex, body weight	Sex	Sex, CYP 2C8 inhibitors		Sex, creatinine clearance
Covariates on volumes	Non-Hispanic/latino		Non-Hispanic/latino	Non-Hispanic/latino	Sex, body weight

Inter-individual variability (IIV) was modeled with a log normal distribution

CV coefficient of variation

[a] Standard error of estimate

[b] Dose- and formulation-dependent nonlinear AET-450 bioavailability: $F = 1.45^{\left(1.27\,(\text{fixed})\times\frac{\text{Dose}}{50}-1\right)}$

[c] Accumulation of ABT-450 (multiplicative model] fixed to 1.57

[d] The AAPS Journal 14.3(2012): 571–580

T-008

Clinically Relevant Doses for Nonclinical Oncology Applications

Mary E. Spilker[1,*], Xiaoying Chen[1], Shinji Yamazaki[1], Ravi Visswanathan[1], Michael Zager[2], Paolo Vicini[1]

[1] Pfizer Worldwide Research and Development; [2] Janssen Pharmaceutical Companies of Johnson and Johnson

Objectives: Oncology therapeutics are increasingly being evaluated in combination with standard of care (SOC) drugs. Nonclinical studies supporting these combinations are often run at a single dose of the SOC, which typically corresponds to the maximum tolerated dose. However, the concentrations at such doses may not be achieved in humans, making translation of the results difficult. We hypothesize for molecularly targeted therapies that a more informative dose, which we call the clinically relevant dose (CRD), is one that matches the area under the unbound plasma concentration–time curve (AUCu) in humans and mice.
Methods: To evaluate this hypothesis, results from Wong [1] were used to compare the simulated tumor growth inhibition (TGI) response when driven by human pharmacokinetics (PK) versus mouse PK at the CRD. If matching the AUCu is the appropriate metric for the back-translation, then similar TGI responses should be obtained. Four molecularly targeted drugs were assessed: Erlotinib, Dasatinib, Trastuzumab, and Vismodegib. The CRD in mice was determined for each drug by matching the AUCu in humans and mice. Next, the PK-TGI mathematical models developed previously using mouse TGI data [1] were implemented and TGI profiles were simulated by replacing human PK at clinical doses with mouse PK at the CRD.
Results: The results show that the simulated TGI responses driven by mouse PK at the CRDs were in good agreement with the simulated TGI responses driven by human PK (Fig. 1). They also resulted in comparable correlations to the clinical overall responses ($r^2 = 0.85$ and 0.83, respectively). These initial results are supportive of the hypothesis that for molecularly targeted agents, matching the AUCu within the dosing interval is appropriate.
Conclusions: Overall, we believe the use of CRDs is an essential element for nonclinical studies and an impactful example of back-translating information to improve the forward translation of non-clinical results.

Reference:

1. Wong H, et al., Clin Cancer Res. 2012;18(14):3846–55.

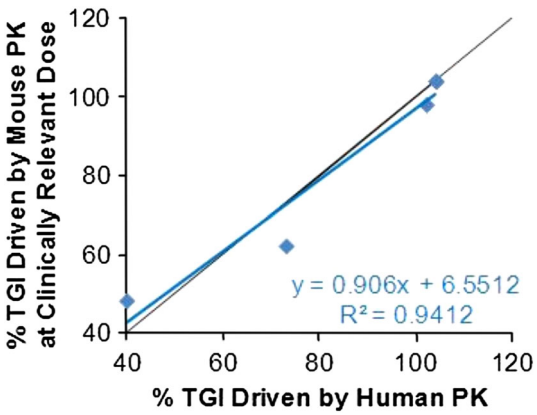

Fig. 1 Comparison of simulated TGI responses driven by human versus mouse PK

T-009

Population Pharmacokinetics of Darbepoetin alfa for the Treatment of Neonatal Hypoxic-Ischemic Encephalopathy

Jessica K. Roberts[1,*], Robert M. Ward[1,2], Joanna Beachy[2], Mariana Baserga[2], Michael G. Spigarelli[1], Catherine M. T. Sherwin[1]

[1] Division of Clinical Pharmacology, Department of Pediatrics, University of Utah, Salt Lake City, UT, USA; [2] Division of Neonatology, Department of Pediatrics, University of Utah, Salt Lake City, UT, USA

Objectives: The aim of this study was to determine the pharmacokinetics of darbepoetin alfa (darbe) used in the treatment of hypoxic-ischemic encephalopathy (HIE) among neonates undergoing hypothermia.
Methods: Neonates ≥36 weeks gestation and <12 h postpartum with moderate to severe HIE were recruited in this randomized, multicenter IRB-approved investigational new drug study. Two IV darbe treatment groups were evaluated with hypothermia: 2 and 10 μg/kg. Serum samples were collected at 4, 12, 18, 24, 36, 60, and 72 h after dose. Serum darbe concentrations were measured by ELISA. Monolix 4.3.1 (using the stochastic approximation expectation maximization algorithm) was used to estimate clearance and volume of distribution. Forward addition and backward elimination were used to identify significant covariates. Potential covariates included birthweight, gestational age, postnatal age, postmenstrual age, gender, sarnat score, and site location.
Results: This analysis included 66 concentrations from 17 patients. Mean ± SD gestational age was 38 ± 1.4 weeks, birthweight was 3.0 ± 0.4 kg, and postnatal age was 0.4 ± 0.1 days. The data were well described by a one-compartment model with first-order elimination and an exponential error model. The final covariate model included postnatal age and birthweight, both of which were centered on the mean, on clearance. There were no significant covariates on volume of distribution. Clearance and volume of distribution were estimated as 0.031 L/h (95 % CI 0.0232–0.0388; 25 % between-subject variability) and 1.63 L (95 % CI 1.10–2.16; 50 % between-subject variability), respectively.
Conclusions: This one-compartment model successfully described the pharmacokinetics of darbe among hypothermic neonates treated for HIE. Clearance increased with postnatal age and birthweight. These results will aid in the selection of an appropriate dose for the Phase II/III trial. Future analysis will compare the pharmacokinetics of darbe with and without hypothermia in this study patient population.

T-010

Clinical Dose Selection of a Topically Applied Immunomodulatory Agent Based on the Probability of Efficacy Target Attainment

April M. Barbour[1,*], Jessica Neil[2], Leandro Santos[2], Jon Lenn[2], Steven Cook[2], Alan Stokes[3], Betty Hussey[2], Carlos Peredo[2], and Javier Cote-Sierra[2]

[1] Merck, Quantitative Pharmacology and Pharmacometrics, North Wales, PA, USA; [2] GlaxoSmithKline, Stiefel Discovery & Preclinical Development, RTP, NC, USA; [3] GlaxoSmithKline, Safety Assessment, RTP, NC, USA

Objectives: The purpose of this exercise was to utilize nonclinical data to predict the probability of target attainment of a topically applied immunomodulatory agent for selection of the clinical dose range. Predicted safety and tolerability of this dose range was evaluated.

Table 1 Probability of achieving 65 % inhibition and corresponding ratio of the amount of drug in the skin following topical versus systemic delivery (exposure ratio)

Biomarker X				Biomarker Y			
Dose (μM)	PTA[Error!] reference source not found	Exposure ratio 10th and 90th percentiles		Dose (μM)	PTA[Error!] reference source not found	Exposure ratio 10th and 90th percentiles	
0.005	10.1	209.91	1547.71	0.04	33.5	26.24	193.47
0.01	25.6	110.59	773.36	0.08	38.4	13.82	96.67
0.02	42	59.43	376.47	0.16	41.9	7.43	47.06
0.04	**50.4**	**27.54**	**187.93**	0.32	46	3.44	23.49
0.08	58.6	13	94.99	0.64	48.4	1.63	11.87
0.16	64.1	6.95	46.09	**1**	**50.5**	**1.11**	**7.37**
0.32	71.3	3.45	22.93	1.28	54.3	0.86	5.73
0.64	65.6	1.86	11.68	2.56	53.8	0.46	2.92
1.28	69.1	0.86	5.09	5.12	60.3	0.21	1.27

[a] Probability of target attainment

Methods: An ex vivo target engagement study measuring inhibition of mRNA levels of relevant biomarkers (cytokines) in human skin established the dose/response relationship. As these experiments mimicked systemic delivery, the permeation of drug into the skin was measured in a separate experiment. The ratio of drug in the skin following topical delivery to systemic delivery (exposure ratio) was calculated and should be greater than 1. Simulation was used to calculate the target attainment rate (target of 65 % inhibition with a 50 % probability) and exposure ratio at various doses. Safety was evaluated locally and systemically based on data following topical delivery in two nonclinical species (rat and minipig). Allometric scaling was used to predict human systemic exposure and calculate the most conservative (lowest) safety margin based on nonclinical safety findings.
Results: Maximal effect models were fit to the biomarker data. A linear model described the dose/skin permeation relationship following systemic delivery. Simulation results are presented in the Table 1. Considering the efficacy results, skin permeation ratios, and likely differences in flux at various dose strengths, a topical dose strength range of 0.1–4 % was recommended. The predicted systemic steady state concentration of 0.037 ng/mL, based on a 50 cm^2 application area, provided a safety margin of 337. There were no local safety/tolerability signals.
Conclusion: A clinical dose strength range of 0.1–4 % is predicted to be efficacious and safe and well tolerated.

T-011

Integrated Pharmacokinetic Model for Antibody-Drug-Conjugate (ADC) in Patients with B-cell Malignancy: Implications for Optimal Sampling

Dan Lu[1,*], Leonid Gibiansky[2], Jin Yan Jin[1], Priya Agarwal[1], Chunze Li[1], Rong Zhang[1], Randell C. Dere[3], Yu-Waye Chu[1], Sandhya Girish[1]

[1] Clinical Pharmacology, Genentech Inc, San Francisco, CA, USA; [2] QuantPharm LLC, North Potomac, MD, USA; [3] Bioanalytical sciences, Genentech Inc., San Francisco, CA, USA

Objectives: Pinatuzumab vedotin, a MMAE-containing ADC targeting CD22, is in clinical development for treatment of B-cell malignancies. Dense and relatively sparse pharmacokinetic (PK) data for total antibody (tAb), conjugate (antibody-conjugated MMAE [acMMAE]), and unconjugated MMAE (MMAE) from Phase I and II studies following IV administration at doses 0.1–3.2 mg/kg were used to for mechanistic modeling to describe their PK and understand the quantitative relationships among these analytes.
Methods: The ADC model proposed in ref. [1] is simplified from a multi-compartmental model with the assumptions that deconjugation rate is linearly proportional to drug-to-antibody-ratio (DAR) and proteolytic degradation rate is independent of DARs. The model was used to describe tAb and acMMAE data. The model was further expanded to describe unconjugated MMAE PK. Phase I PK data with extensive PK sampling were used for model development (patient number = 89). Phase II PK data with relatively sparse sampling were used to assess the ability of the model to predict tAb PK based on observed acMMAE and unconjugated MMAE data (patient number = 61).
Results: PK of tAb and acMMAE was well described by two 2-compartment models with shared parameters. Unconjugated MMAE generated from deconjugation and proteolytic degradation is input to a delay compartment before appearing in the systemic circulation. Non-linear elimination from the MMAE delay compartment was included in the model. MMAE apparent systemic clearance increased with time with the steady-state value of 3.96 L/h, initial value of 1.92 L/h, and the half-life of the increase of 1.97 months. CL and V1 were 6.61 and 1.47 times higher in CLL patients compared to NHL patients; CL and V1 were 1.20 and 1.16 times higher in males. CL, Q, V1, and V2 increased with weight with the powers of 0.75, 0.75, 0.47, and 1.0, respectively. CLMMAE increased with weight and albumin concentration with the powers of 0.75 and 0.89, respectively. The model accurately predicted the tAb concentrations using the observed acMMAE and unconjugated MMAE data.
Conclusions: The developed model described the observed data in patients with B-cell malignancies. The model predicted tAb PK based on conjugate (acMMAE) and unconjugated MMAE data. Thus, the model developed on tAb, acMMAE, and MMAE data in Phase I and II studies can be used in future studies to potentially eliminate the need to measure tAb in Phase III.

References:

1. Gibiansky L., Gibiansky E. Target-Mediated Drug Disposition Model and its Approximations for Antibody-Drug Conjugates, J Pharmacokinet Pharmacodyn. 2014 Feb; 41(1):35–47

T-012

Population PK/PD Modeling of Dietary Nitrate Effect on Blood Pressure in Healthy Subjects

Mariam Ahmed[1,*], Richard Brundage[1], John St. Peter[1,2]

[1] Experimental and Clinical Pharmacology, University of Minnesota, Minneapolis, MN, USA; [2] PepsiCo Global R&D, Purchase, NY, USA

Objectives: Dietary nitrate (NO_3) has been shown to increase plasma concentrations of nitrite (NO_2) which can further be reduced to nitric oxide and lower blood pressure [1]. While a recent study has demonstrated a dose-dependent effect of dietary NO_3 on blood pressure [2], a quantitative model characterizing the pharmacokinetic/pharmacodynamic (PK/PD) relationships among dietary nitrate dosing, nitrite plasma concentrations, and effect on blood pressure have not been reported.
Methods: Ten healthy subjects received four different acute doses (0, 4.2, 8.4, 16.8 mmol) of dietary nitrate (Beet It®) on four separate occasions separated by a 3-day washout period. For each occasion, NO_3 and NO_2 concentrations and systolic (SBP), diastolic (DBP) and mean arterial (MAP) blood pressures were obtained at seven time points over 24 h. Simultaneous population PK/PD modeling was performed with NONMEM 7.2 and the 95 % confidence intervals (CIs) were constructed from 1,000 bootstrap datasets.
Results: The PK of NO_3 and NO_2 were each adequately described by a 1-compartment model with the fraction of NO2 formation from NO_3 fixed at 5 %. The population PK parameters (95 % CIs) of NO_3 and NO_2, respectively, were: CL 2.92 (2.53, 3.34), 133 (110, 157) L/h; volume of distribution: 28.3 (22.2, 30.0), 58.0 (32.3, 87.0) L; and baseline concentration: 29.3 (26.1, 33.7) uM, 85.1 (76.5, 94.7) nM. For the pharmacodynamics, SBP, DBP and MAP were found to decrease linearly with increased NO2 plasma concentration. The population slopes (95 % CI) were −0.0152 (−0.02,−0.01), −0.007 (−0.01,−0.004), −0.0095 (−0.013,−0.007) mmHg/nM, respectively. The between-subject variability for SBP and MAP slopes were 49 and 26 %, respectively; it was not estimable for DBP.
Conclusions: Acute dietary nitrate consumption can reduce blood pressure short term in young adults. There is a linear PK/PD relationship of nitrite and blood pressure over the observed range. Between-subject variability was moderate for the effect of nitrate on SBP and low for MAP.

References:

1. Cardiovascular Research (2011) 89, 525–532.
2. J Appl Physiol (2013) 115, 325–336.

T-013

zscore - An R Package for Deriving Weight and Height for Age Z Scores and Exact Percentiles from Birth to 20 Years of Age

Chris Stockmann*, Catherine M. T. Sherwin, Michael G. Spigarelli

Division of Clinical Pharmacology, Department of Pediatrics, University of Utah School of Medicine, Salt Lake City, UT, USA

Objectives: Covariate model development for pediatric population pharmacokinetic studies is often limited to evaluations of weight, height, and age. Using these same variables, it is possible to derive standardized z-scores and growth chart percentiles, although such calculations must currently be performed manually or through the creation of user-defined functions.
Methods: zscore is an open-source R package that includes the United States Centers for Disease Control and Prevention's (CDC) most recent growth charts, including: weight-for-age, height-for-age, weight-for-height, and height-for-age values for children from birth to 20 years of age. To derive the z-scores and exact percentiles for each month of age, zscore includes the median (M), generalized coefficient of variation (S), and the power in the Box-Cox transformation (L) parameter values for both males and females at every month of age.
Results: Each subject's z-score may be expressed as a function of their age in months (X) and the LMS parameters corresponding to that age using the following equation: Z = (((X / M)**L)−1)/(LS), when L is not equal to 0. In the zscore package, a data frame containing the subject's unique identifier (id), gender (sex), age in months (age_mos), weight in kilograms (wt_kg), and height in centimeters (ht_cm) may be passed along to the zscore() function, which generates a new data frame that contains each subject's weight-for-age, height-for-age, weight-for-height, and height-for-age z-scores and exact percentiles.

Multiple observations per subject may be included, in which case z-scores and exact percentiles are calculated based upon the age, sex, weight, and height of the subject at each point in time.
Conclusions: zscore is an R package that is intended to be used as a covariate model building aid for the development of non-linear mixed effects (population) models. zscore will be made available for free from the Comprehensive R Archive Network (CRAN).

T-014

Population Pharmacokinetic Analysis to Recommend the Optimal Dose of Udenafil in Patients with Mild and Moderate Hepatic Impairment

AnHye Kim[1,a], Jongtae Lee[2,a], Kyung-Sang Yu[1], In-Jin Jang[1,*]

[1] Department of Clinical Pharmacology and Therapeutics, Seoul National University College of Medicine and Hospital, Seoul, Korea; [2] Department of Clinical Pharmacology and Therapeutics, St. Mary's Medical Center, The Catholic University School of Medicine, Seoul, Korea

Jongtae Lee and AnHye Kim contributed equally to this work

Objectives: This study was to develop a population pharmacokinetic (PK) model of udenafil and its active metabolite, DA-8164, in healthy subjects and patients with hepatic impairment (HI) and to recommend the optimal dose for HI patients using the modeling and simulation.
Methods: An open-label, 3-parallel group, age- and weight-matched control study was conducted in 18 subjects; healthy subjects (n = 6), patients with mild (Child–Pugh A, n = 6) and moderate (Child–Pugh B, n = 6) HI. Serial blood and urine samples were collected up to 72 h after a single administration of udenafil 100 mg. A population PK model was developed using a mixed effect method (NONMEM, ver. 7.2). Non-compartmental analysis and the comparison of PK parameters of the data simulated from the final PK model were performed to identify the optimal dose in HI patients.
Results: Two-compartments for both udenafil and DA-8164, linear PK model best described the data. A covariate included in the final model was prothrombin time on metabolic clearance of udenfil to DA-8164. Compared to AUClast after administration of udenafil 100 mg to healthy volunteers, the geometric mean ratio (90 % confidence interval) of those were 1.21 (1.12–1.30) and 1.02 (0.94–1.10) in mild (100 mg) and moderate (75 mg) HI patients, respectively.
Conclusions: The results of this study suggest that the recommended doses of udenafil are 100 and 75 mg in mild and moderate HI patients, respectively.

T-015

Development of Vancomycin Dosing Recommendations in Preterm and Term Neonates using Population Pharmacokinetic Modeling and Simulation

Jiraganya Bhongsatiern[1,*], Catherine M.T. Sherwin[2], Tian Yu[2], Chris Stockmann[2], Karel Allegaert[3], Catherijne A.J. Knibbe[4], David M. Reith[5], Pankaj B. Desai[1], Michael G. Spigarelli[2]

[1] Department of Pharmaceutical Sciences, College of Pharmacy, University of Cincinnati, Ohio, USA; [2] Department of Pediatrics, University of Utah School of Medicine, Salt Lake City, Utah, USA; [3] Neonatal Intensive Care Unit, University Hospitals Leuven, Leuven, Belgium; [4] Department of Clinical Pharmacy, St. Antonius Hospital, Nieuwegein, The Netherlands; [5] Department of Women's and Children's Health, School of Medicine, University of Otago, Dunedin, New Zealand

Objectives: Vancomycin is widely used to treat gram-positive infections in neonates. However, dosing recommendations have not been optimized. Consequently, this study aimed to develop an optimal vancomycin dosing regimens in neonates.
Methods: Data were collected from neonatal patients (≥44 weeks of postmenstrual age; PMA) who received vancomycin from 1/2006 to 9/2011. Population PK analysis was performed in NONMEM 7.2. The final model was evaluated using data obtained from three academic medical centers. Monte Carlo simulation was utilized to optimize dosing regimens in MATLAB R2013a. Target attainment was defined as predicted Cmin of 10–20 mg/L and AUC24/MIC of ≥400.
Results: A total of 1,458 vancomycin concentrations from 515 patients were included in the PK analysis. A one-compartment model with first-order elimination best described the data. Weight, serum creatinine (SCR), and PMA significantly influenced vancomycin clearance ($P < 0.001$). Clearance was estimated as 0.17 L/h/kg and volume of distribution was 1.36 L/kg. Simulated data (n = 11,519) without adjustment for patient covariates with a 15 mg/kg dose every 12 h achieved 52.3 and 63.4 % of target Cmin and AUC24/MIC, respectively. Dosing recommendations developed based on SCR breakpoints of 0.4 mg/dL achieved overall target attainment in ~70 % simulated patients.
Conclusions: A population PK model that incorporates weight, SCR, and PMA successfully predicted vancomycin clearance in preterm and term neonates. Monte Carlo simulations suggest that standard dosing regimens for patients with SCR breakpoints of 0.4 mg/dL provide a high probability of target attainment.

T-016

Modelling the Binding Kinetics of Antibody, Antigen and FcγRs

Linzhong Li*, Iain Gardner, Kate Gill, Masoud Jamei

Simcyp Limited (a Certara company), Sheffield, UK

Objectives: Fcγ receptors (FcγR) play a dominant role in the in vivo activity of anti-tumor antibodies. The in vivo activity of different IgG sub-classes correlates with the affinity ratio of their binding to activating and inhibitory FcγR [1], and clinical trials are being conducted with Fc-engineered antibodies with enhanced binding to activating FcγRs [2].
Cross-linking of FcγR and antibody-antigen complex is a prerequisite for FcγR-mediated cell-killing or immunomodulatory effect and thus the concentrations of antibody, antigen and FcγRs and the affinity with which these components bind to each other determine the strength and duration of the initial signal for downstream biological activity. The objective of this study is to mechanistically model this complex interaction.
Methods: IgG has two identical binding sites for antigen and one binding site for FcγRs. In this model competitive binding of two classes of FcγRs was considered (B and C in Fig. 1a). Binding is assumed to be at equilibrium and after thermodynamic considerations are accounted for the model is described by eight equilibrium constants, see Fig. 1a. A set of six nonlinear equations was derived, governing the fractional concentrations of free antibody, ternary and quaternary complexes relative to the total antibody concentration. For any given set of affinities and total concentrations of antibody, antigen, and FcγRs, the concentrations of all species can be numerically calculated by solving this set of equations.
Results: Figure 1b, c show simulations of competitive binding of activating and inhibitory FcγR for the Fc binding site. Increasing the affinity of activating FcγR can dramatically increase the cross-linking of FcγR with Ab–Ag complex, consistent with current in vitro and in vivo data.

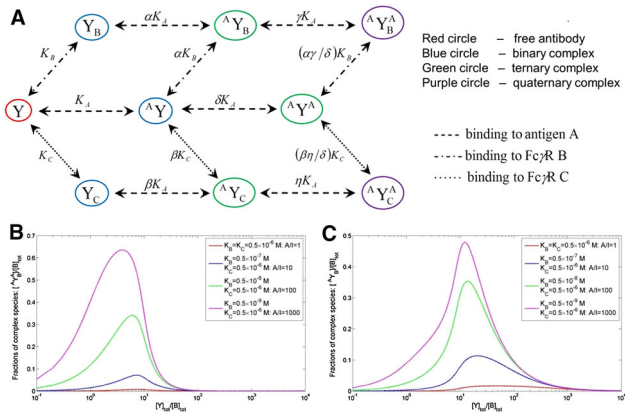

Fig. 1 **a** Equilibrium binding scheme for the interaction between antibody (Y), antigen A, and FcγRs B and C. The binding of FcγRs B and C to the Fe site is assumed to be competitive. *KA, K_B*, and *Kc* are equilibrium dissociation constants for bindings between Ab and Ag, Ab and FcγR B, and Ab and FcyR C, respectively. *a* is the affinity ratio between Y and A Y for FcγR B (which is equal to the ratio between Y and Y8 for antigen A due to equilibrium). **b**, **c** Simulation of competition between activating FcγR B and inhibitory FcγR C for varying affinity ratio A/I of binding to activating and inhibitory FcγRs by increasing the intrinsic affinity of FcγR B. Total antigen concentration $[A]_{tot} = 10^{-8}$ M, total FcγR concentrations: $[B]_{tot} = [C]_{tot} = 10^{-9}$ M. The intrinsic equilibrium dissociation constant for Ab–Ag binding, $K = 10^{-9}$ M, and $K_A = K$ /2, $\gamma = \delta = \eta = 4$, $\alpha = \beta = 1$. Figure **b** shows the fraction of cross-linked species through quaternary complex for Fcy R B and Figure **c** shows the fraction of cross-linked species through ternary complex for FcyR B

Conclusions: A mechanistic binding model has been developed to quantify the interplay of antibody, antigen, and FcγRs. Further work will incorporate the model into a PBPK framework to simulate in vivo conditions.

References:

1. Nimmerjahn F and Ravetch J. Cancer Immunity. 2012; 12: p 13
2. Lim SH et al. Haematologica 2010; 95: 135–143

T-017

Simultaneous Diarrhoea and Rash/Acne Exposure–Response Models of Afatinib

Ronald Niebecker[1,*], Matthias Freiwald[1], Mats O. Karlsson[2]

[1] Translation Medicine & Clinical Pharmacology, Boehringer Ingelheim Pharma GmbH & Co KG, Biberach, Germany;
[2] Department of Pharmaceutical Biosciences, Uppsala University, Uppsala, Sweden

Objectives: Afatinib is a potent irreversible ErbB family blocker with activity in a wide range of solid tumours. As expected from EGFR inhibition, the most common treatment-related adverse events (AEs) include diarrhoea and rash/acne. The objective of this analysis was the development of models characterising the exposure-safety relationship for both AEs of interest.
Methods: The analysis was based on pooled data from six phase II/III clinical studies [1]. AUC computed from individual PK estimates [1] served as predictor of the drug effect. Different models for ordered categorical data were compared for their ability to characterise AE data. Clinical trial simulation with adaptive dosing was used for model evaluation. Treatment discontinuation due to reasons other than both AEs of interest was assumed to occur completely at random and modelled separately using exponential hazard. The analysis was carried out in NONMEM 7.2 [2].
Results: Longitudinal mixed-effects ordered categorical data models with Markov elements for daily AE severity as well as time-to-first AE models were successfully implemented. Important factors in the drug effect models comprised delay in the drug effect, apparent tolerance development of the drug effect and interaction of the drug effects on diarrhoea and rash/acne. Clinical trial simulation allowed adequate prediction of maximum CTCAE grades and onset of first AE episodes.
Conclusions: This analysis showed that higher afatinib exposure was associated with increased occurrence of AEs. Model results and simulations will be used to investigate dosing regimens with regard to their impact on the AE pattern. Combined with further covariate analysis and modelling of the exposure–efficacy relationship, this model could support future integrated benefit-risk assessments.

References:

1. Freiwald et al., Cancer Chemother Pharmacol. 2004;73(4): 759–70
2. Beal et al., NONMEM user's guides. Icon Development Solutions, Ellicott City, MD, USA; 1989–2009

T-018

Physiologically Based Pharmacokinetic Modeling of Sorafenib Metabolism, Transport, and Enterohepatic Recycling in Mice

A. N. Edginton[1], E. I. Zimmerman[2], A. Vasilyeva[2], S. D. Baker[2], J. C. Panetta[2,*]

[1] University of Waterloo, Canada; [2] St. Jude Children's Research Hospital, Memphis, TN, USA

Objectives: Sorafenib, a tyrosine kinase inhibitor, has complex pharmacokinetics due to its hepatic metabolism [Sorafenib N-oxide by CYP3A4 and Sorafenib glucuronide (S-GLU) by UGT1A9] and liver transport. In addition, S-GLU is cleaved by intestinal β-glucuronidase leading to enterohepatic recycling (EHR) of Sorafenib. The aim of this study was to develop a physiologically based pharmacokinetic (PBPK) model to describe the disposition of Sorafenib and its metabolites in mice. Plasma and liver data from both wild-type and transporter knockout mice were used for model development. The model was then used to understand the kinetics of Sorafenib metabolism, transport, and EHR.
Methods: The PBPK model was developed and simulations were performed using PK-Sim® v5.3.2 and MoBi® v3.3.2 (Bayer Technology Services, Leverkusen, Germany). The physiochemical properties and enzyme kinetics of the drug metabolizing enzymes and transporters were obtained from literature. Serially sampled plasma and liver concentrations of Sorafenib and its metabolites were available in wild-type (WT) and transporter (Slco1b2, Slco1a/1b) knockout mice. EHR was quantified using pharmacokinetic samples from neomycin treated and control mice dosed with S-GLU. In addition, ex-vivo cecal material treated with S-GLU was available.
Results: The PBPK model was developed by adjusting the metabolism and transporter activities to describe the data from the WT mice and the in vivo neomycin study. β-Glucuronidase presence in caecum and large intestine and its absence in small intestine best described the

data. Influx transporter knockout mice showed a small change (<25 % in observed and predicted) in Sorafenib and Sorafenib N-oxide exposure but a 30-(observed) and 40-(predicted) fold increase in S-GLU exposure.
Conclusions: The PBPK model quantified the disposition of Sorafenib and its metabolites in WT, transporter knockout, and neomycin treated mice. This model helped us to better understand both the effects of transporters and EHR on Sorafenib. The model, scaled to humans, may be helpful in understanding factors that affect Sorafenib's highly variable disposition.

T-019

Model-Based Analysis of Pharmacokinetics of MK-3475, a Human Anti-PD-1 Monoclonal Antibody in Patients with Progressive Locally Advanced or Metastatic Carcinoma, Melanoma, and Non-Small Cell Lung Carcinoma[a]

Malidi Ahamadi[1,*], Marita Prohn[2], Stefaan Rossenu[2], Jung Hoon Lee[1], Rik de Greef[2], Dinesh de Alwis[1], and Jeroen Elassaiss-Schaap[2]

[1] Merck Research Laboratory, Merck and Co., USA; [2] Merck Research Laboratory, Merck and Co., Oss, Netherlands

[a] The results in this abstract have been previously presented in part at PAGE 2014 (Alicante, Spain, 10–13 June, 2014)

Objectives: MK-3475 is a potent antibody against the cellular immune 'switch' programmed death-1 (PD-1) with high activity in the treatment of metastatic melanoma. Using a model based approach; we characterized the pharmacokinetic (PK) properties of MK-4575 in patients and quantified the effect of intrinsic and extrinsic factors on exposure.
Methods: A total of 7034 serum concentrations from 337 patients were used to describe the PK of MK-3475. The relationships between PK parameters and various baseline covariates were examined. The posterior power of the analysis was performed to confirm negative covariate findings
Results: A two-compartment population PK model with linear clearance from the central compartment described MK-3475 concentration [1]. Albumin and IgG were identified as covariates for clearance, and gender for clearance and central volume of distribution. At 10th percentile of albumin (or IgG) distribution, clearance was increased by 25 % (decrease by 20 % for IgG) relative to a typical patient. Females had an estimated 13 % lower clearance and a 14 % reduction in central volume. Since MK-3475 has a wide therapeutic window, these effects on exposure were clinically insignificant. Other intrinsic or extrinsic factors, including hepatic and renal impairment, did not have an impact on MK-3475 exposure. The posterior power calculations demonstrated that the covariate search had sufficient power to detect clinically significant changes, which strengthens the negative findings.
Conclusions: PK profile of MK-3475 indicated a low clearance (~0.2 L/day), limited volume of distribution (~8 L) and low variability (15–30 %) consistent with other monoclonal antibodies [1]. The population PK analysis confirmed no clinically meaningful effect of intrinsic or extrinsic factor on MK-3475 exposure.

References:

1. Nathanael L. Dirks and Bernd Meibohm, Clin Pharmacokinet 2010; 49 (10): 633–659

T-020

Population Pharmacokinetic Modeling for Mirogabalin in Healthy Subjects and Patients with Diabetic Peripheral Neuropathic Pain

Ophelia Yin[*], Saeheum Song, Kenneth Truitt, Raymond Miller

Daiichi Sankyo Pharma Development, Edison, NJ, USA

Objectives: Mirogabalin (DS-5565) is the first preferentially selective α2δ-1 ligand with a unique binding profile providing high potency and long duration of action. This analysis was to characterize mirogabalin population pharmacokinetics in healthy subjects and patients with diabetic peripheral neuropathic pain (DPNP).
Methods: Data from 12 clinical studies including phase I in healthy volunteers (n = 239) and renal impairment patients (n = 24), and phase II in DPNP patients (n = 541) were included. For phase I, mirogabalin was given as a single oral dose of 3–75 mg, or for up to 14 days as once-daily or twice-daily dose of 5–25 mg. In phase II studies, DPNP patients with mild renal impairment were enrolled. Mirogabalin doses were 5, 10 and 15 mg once-daily, 10 and 15 mg twice-daily for 5 weeks; or 5, 10 and 15 mg twice-daily for 7 weeks. Full pharmacokinetic (PK) profiles were obtained from all phase I studies, while 4–5 samples per patient were collected in phase II studies. Population PK analysis was performed by nonlinear mixed effects modeling.
Results: Mirogabalin PK was described by a two-compartment model, with first-order absorption and elimination. Body weight was a significant covariate on all disposition parameters, while creatinine clearance affected both renal and non-renal clearance of mirogabalin. Other covariates identified were age ~V2, sex ~V3, and study phase ~Ka. Model estimated total clearance (CL) value were consistent with those observed (in parenthesis), being 17.4 (18.5), 12.4 (15.7), 7.71 (8.04), and 4.35 (4.39) L/h respectively, in subjects with normal, mild, moderate or severe renal impairment. Mirogabalin typical CL was similar between DPNP patients and healthy subjects. Inter-subject variability was moderate in all PK parameters (16.1–32.8 %), with the exception of Ka (79.8 %). Visual predictive check suggested the final model described the data well, and all parameter estimates had reasonable precision as per bootstrap analysis.
Conclusions: This analysis provided an appropriate description of the observed concentration data from phase I and II studies, and enabled an accurate prediction of PK profiles in subjects with varying degrees of renal impairment. The PK model will form the basis for optimizing future study designs and exposure–response analysis for mirogabalin.

T-021

Population Pharmacokinetic (PPK) Modeling and Simulation to Support Pediatric Dose Selection of Ceftaroline Fosamil (CPT-F) in Children Ages 28 Days to 12 Years

Tatiana Khariton[1,*], Todd Riccobene[1], William Knebel[2], Tanya O'Neal[1], Parviz Ghahramani[1]

[1] Forest Research Institute, Jersey City, NJ, USA; [2] Metrum RG, Tariffville, CT, USA

Objectives: Ceftaroline (CPT) is a novel cephalosporin with activity against gram-positive and common gram-negative organisms, including MRSA. The prodrug CPT-F is approved for adults with ABSSSI and CABP. No pediatric dosing is currently approved. This PK study in pediatric patients evaluated single-dose PK, safety/

tolerability in children 28 days to <12 years. PPK model was used to recommend dosing for pediatric safety/efficacy studies.
Methods: Children were enrolled in age-based cohorts sequentially and received single IV doses of CPT-F. Four PK samples were taken from each patient. Interim PK/safety evaluations were done for each cohort. Pediatric PK data were combined with adult data in PPK model. Maturation of renal function was accounted for in children <2 years. Dose recommendations were based on matching model predicted exposures (Cmax, AUC, time > MIC) in children to be comparable (but no lower than those seen in adults at US-approved dose of CPT-F 600 mg q12 h.
Results: Single doses of CPT-F were well tolerated in children 28 days to <12 years. The PPK model consisted of 2-compartment models for CPT-F and CPT. Creatinine clearance was the main predictor of CPT clearance. A dose of CPT-F 12 mg/kg (up to 400 mg) q8 h for children ≥6 months and 8 mg/kg q8 h for children <6 months is predicted to result in Time > MIC similar to or greater than in adults. Cmax and AUC in children 28 days to <18 years are predicted to be ≤12 and ≤38 % greater, respectively, than in adults. Lower dose in children <6 months was required due to immature renal function.
Conclusions: Based on PPK modeling/simulation, a dose of CPT-F 12 mg/kg (up to 400 mg) q8 h (1-h infusion) for children ≥6 months and 8 mg/kg q8 h for children <6 months is recommended for studies in ABSSSI and CABP in children 2 months to <18 years.
Note: Presented previously at ECCMID 2013

T-022

A Model-Based Approach to Dose Optimization of Neurotoxic Chemotherapy Drugs

Elizabeth Gray*, Shailly Mehrotra, Kehua Wu, Mark Ratain, Joga Gobburu, Manish R. Sharma

University of Chicago, University of Maryland, Adelphi, MD, USA

Objectives: CALGB 40502 randomized patients with metastatic breast cancer to paclitaxel, nab-paclitaxel and ixabepilone. Our objective was to develop a model of chemotherapy-induced peripheral neuropathy (CIPN) using a previously validated, patient-reported scale of neuropathy symptoms. We will use this model to propose a dosing adjustment algorithm to reduce CIPN in patients receiving these drugs.
Methods: FGSUM4 is the sum of scores from four questions rated 0–4 on a Likert scale (from "Not at all" to "Very much"): (1) "I have numbness or tingling in my hands"; (2) "I have numbness or tingling in my feet"; (3) "I feel discomfort in my hands"; (4) "I feel discomfort in my feet". Of 799 total patients, data from 655 with adequate early data and baseline FGSUM4 ≤4 were used for modeling. FGSUM4 data were used to fit a nonlinear mixed effects K/PD model in NONMEM [1] (see Fig. 1). The model was evaluated by standard diagnostic plots and bootstrapping was performed to evaluate the precision of parameter estimates. Posthoc simulations were done to evaluate the power of early CIPN data to predict later CIPN. Using individual posthoc estimates of the parameters, simulations are being performed to determine optimal dose adjustments to minimize later CIPN.
Results: Our model identified paclitaxel as the least neurotoxic drug in the study: for paclitaxel, the median average dose per day divided by SDK50 was 0.56, compared to 0.95 for nab-paclitaxel and 1.02 for ixabepilone. Using the first three cycles of data, our model predicts mean FGSUM4 at later time points with both 73 % specificity and sensitivity.

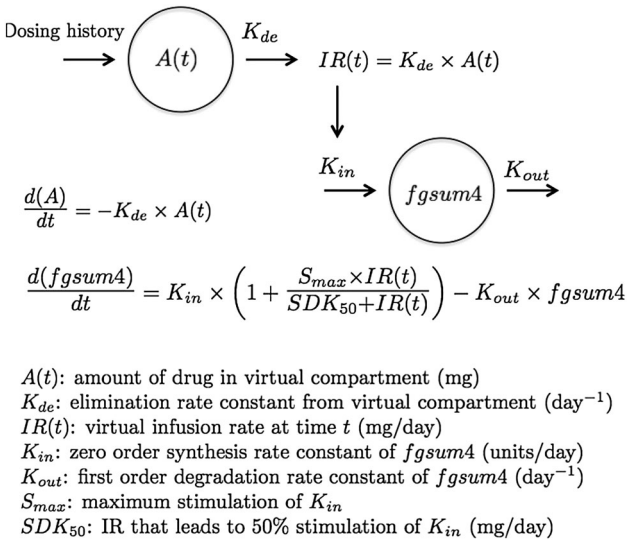

Fig. 1 Schematic representation of K-PD model for FGSUM4

Conclusions: Our K-PD model can use early assessments to predict later CIPN. In ongoing work, we are using the model to assess the impact of dose adjustments on the development of CIPN.

References:

1. Jacqmin P, et al. Modelling response time profiles in the absence of drug concentrations: definitions and performance evaluation of the K-PD model. J Pharmacokinet Pharmacodyn. 2007;34:57–85

T-023

Prognostic Factors for Efficacy of Axitinib from a Randomized Phase 2 Study in First Line Metastatic Renal Cell Carcinoma

John Craig Garrett[1], Yazdi K. Pithavala[2], Angel Bair[2], Ying Chen[2,*]

[1] Skaggs School of Pharmacy and Pharmaceutical Sciences, University of California at San Diego, San Diego, CA, USA; [2] Pfizer Oncology at San Diego, San Diego, CA, USA

Objectives: In a randomized, double-blind phase II trial in patients with first line metastatic renal cell carcinoma (mRCC), axitinib versus placebo titration yielded a significantly higher objective response rate. Potential prognostic factors for axitinib efficacy in first-line mRCC were explored using the data from the overall population.
Methods: Exploratory analyses were conducted to evaluate prognostic factors (eg, axitinib plasma exposure, age, gender, race, weight, smoking status, Eastern Cooperative Oncology Group [ECOG] performance status [PS], body surface area as well as baseline laboratory values) for progression free survival (PFS) using Cox proportional hazards model. This analysis was conducted for data from a randomized Phase 2 study (n = 167 patients) in first line mRCC to evaluate the effect of dose titration. Each covariate was tested in the univariate analysis and variables with $P < 0.05$ by log rank test were included in a multivariate model. The final multivariate model was identified by using Akaike's information criterion (AIC), Bayesian information criterion (BIC) and Deviance (−2 log-likelihood). Kaplan–Meier curves were generated for discrete covariates which demonstrated significance ($P < 0.05$) in univariate analysis based on the log-rank test.
Results: Among various baseline characteristics and axitinib plasma exposure assessed for prognostic potential for PFS in the univariate

Table 1 Univariate and multivariate analyses of prognostic factors for progression-free survival

Parameter	N	HR (95 % CI)	*P* value
Univariate analysis			
Cycle 1 AUC	167	1.00 (1.00–1.00)	0.16
Study AUC	167	1.00 (1.00–1.00)	0.67
Non-smoker	82	1.00	0.60
Smoker/ex-smoker	22/63	0.95 (0.77–1.16)	
Body surface area	167	0.89 (0.41–1.96)	0.78
Albumin	167	0.58 (0.41–0.82)	0.0022
Creatinine clearance	167	1.00 (1.00–1.01)	0.23
Serum creatinine	167	0.61(0.31–1.22)	0.16
Alanine transaminase (ALT)	167	1.00 (0.98–1.01)	0.47
Bilirubin	167	0.69 (0.29–1.64)	0.40
Body weight	167	1.00 (0.99–1.01)	0.58
Age	167	0.98 (0.96–1.00)	0.12
Gender			
Male	113	1.00	0.37
Female	54	1.20 (0.81, 1.79)	
ECOG performance status[a]			
0	111	1.00	0.042
1	55	1.51 (1.01–2.25)	
Race[b]			
Caucasian	124	1.00	0.028
Japanese	42	0.77 (0.61–0.98)	
Multivariate analysis			
Race[b]			
Caucasian	124	1.00	0.010
Japanese	42	0.73 (0.57–0.93)	
Albumin	167	0.52 (0.36–0.76)	0.00059

[a] Data not presented in table for one subject with baseline ECOG = 2

[b] Data not presented in table for one subject with race =''Other''

analysis, race, baseline albumin and baseline ECOG PS were identified as significant covariates (Table 1). Better prognosis was associated with Japanese (median PFS not reached) versus Caucasians (median PFS = 11.5 months), normal levels of albumin (median PFS: 2.7 vs 16.3 months for low and normal albumin level), and better performance status (median PFS: 15.7 vs 8.1 months for ECOG = 0 vs ECOG = 1).

The final multivariate model included race and albumin as potential prognostic factors for PFS (Table 1).

Conclusion: Exploratory analysis indicated that albumin and race are potential predictors of PFS in patients with first line mRCC.

T-024

Application of Pediatric Physiologically-based Pharmacokinetic (PBPK) Modeling to Predict Starting Dose of Tolvaptan in Children from 4 Weeks to 2 Years of Age

Cong (Claire) Xu*, Susan Shoaf

Department of Clinical Pharmacology and Pharmacometrics, Otsuka Pharmaceutical Development & Commercialization, Inc., Princeton, NJ, USA

Objectives: Tolvaptan, a selective oral arginine vasopressin V2 receptor antagonist, was approved for the treatment of specific forms of hyponatremia. It is primarily cleared via the CYP3A4-mediated metabolism. Initial interaction with the FDA agreed that bodyweight-based dose adjustment can be made for children >2 years of age and >10 kg. The gap remains for children <2 years of age and/or <10 kg. The objective of this study is to develop a pediatric physiologically-based pharmacokinetic (PBPK) model of tolvaptan to aid the selection of starting dose in children <2 years of age.

Methods: The drug dependent parameters of tolvaptan were derived from in silico, in vitro, and human PK data. The adult PBPK model was developed and qualified using Simcyp (V13.1). The pediatric PBPK model was developed using the pediatric module of the simulator and embedded CYP3A4 maturation profile. Additional sensitivity analysis was performed to explore the impact of CYP3A4 ontogeny on the prediction of tolvaptan PK in pediatric group.

Results: The full PBPK model provided a reasonably good prediction of PK profiles in healthy adult subjects and was successfully qualified. The pediatric PBPK model extrapolated from an adult model predicted that a single dose of 0.15 mg/kg oral suspension of tolvaptan in children from 4 weeks to 2 years of age would produce plasma concentrations comparable to that of adults receiving a standard 15 mg dose. The CYP3A4 ontogeny embedded in the Simcyp simulator produced similar predictions for the mean systemic exposures compared to those predicted using ontogeny profiles suggested in literature sources.

Conclusions: 0.15 mg/kg oral suspension dose of tolvaptan is recommended for children from 4 weeks to 2 years of age based on modeling and simulation for planned pediatric clinical trial. This study provides an example that prior data of in vitro and adult PK can be used for selecting starting dose of pediatric trial.

T-025

Development of a Physiologically-Based PK/PD Model of Exendin-(9-39) for Mode of Action Evaluation and Optimal Clinical Trial Design in Congenital Hyperinsulinism

S. Schaller[1,*], T. Eissing[1], S. Willmann[1], E. Dombrowsky[2], J. Barrett[2], D. De Leon[3]

Computational Systems Biology, Bayer Technology Services GmbH, Leverkusen, Germany; [2] Sanofi-Aventis Pharmaceuticals, Bridgewater, NJ, USA, United States; [3] Department of Pediatrics, Children's Hospital Philadelphia, Philadelphia, PA, USA

Objectives: Congenital hyperinsulinism (HI) is a rare genetic disorder of pancreatic beta-cell function characterized by dysregulated insulin secretion resulting in severe hypoglycemia. Currently, effective medical therapies are limited and many affected children require a near-total pancreatectomy with a high risk of complications. Exendin-(9-39) (ex-9), a GLP-1 receptor antagonist, has been shown to correct fasting hypoglycemia in a mouse model of HI and in affected children and adults.

Methods: To assess clinical benefit and the relationship between ex-9 exposure and fasting blood glucose, we developed a physiologically-based pharmacokinetic and pharmacodynamic (PK/PD) model of ex-9 by extending an existing model of glucose–insulin metabolism [1] by known PD effects of ex-9. The model was used for PK and mode-of-action (MoA) analysis for ex-9 using data from a randomized, crossover pilot clinical trial in nine subjects with HI. In the study,

subjects received either ex-9 (0.02–0.1 mg/kg/h) or vehicle on two different days over 6 h during fasting.
Results: The developed model helped in evaluating MoA of ex-9 and was able to describe clinical trial data with intravenous ex-9. Model results indicate a saturating effect of ex-9 on elevation of blood glucose but also additional, insulin secretion-independent, direct MoA, likely through modulation of the effects of glucagon or GLP-1 related pathways in hepatic glucose metabolism.
Conclusions: We developed a clinical trial simulation model of ex-9 which incorporates the observed PK/PD relationships to assess the effect, safety, tolerability, and PK/PD of intravenous ex-9 in individuals with HI. The developed model can be used to further guide dosing and scheduling questions to achieve relevant endpoints in upcoming trials of ex-9.

References:

1. Schaller S, Willmann S, Schaupp L, Pieber TR, Schuppert A, Lippert J, Eissing T: A generic integrated physiologically-based whole-body model of the glucose-insulin-glucagon regulatory system. CPT: PSP 2013.

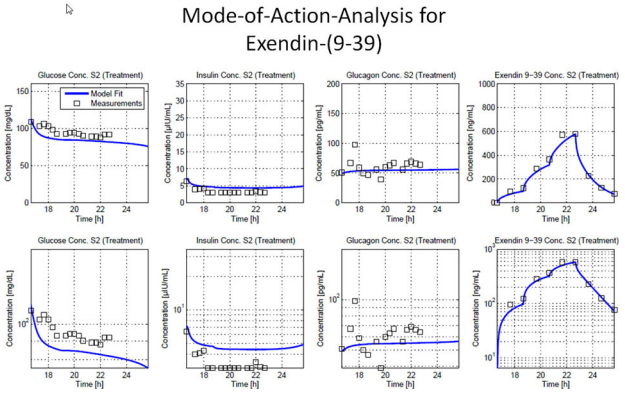

T-026

Population Exposure-Efficacy Response Analyses of Naloxegol in Patients with Opioid Induced Constipation (OIC)

N Al-Huniti[1,*], H Xu[1], KH Bui[1], J Lappalainen[1], M Sostek[1], JN Nielsen[2], MM Hutmacher[2]

[1] Quantitative Clinical Pharmacology, AstraZeneca, Wilmington, DE, USA; [2] Ann Arbor Pharmacometrics Group, Ann Arbor, MI, USA

Objectives: To develop exposure response models to describe the efficacy of naloxegol in phase III efficacy trials and to evaluate the influence of pre-specified covariates on the exposure response relationships.
Methods: Population exposure–response models were constructed based on data from two phase III trials comprising 1,331 adults with non-cancer pain and opioid-induced constipation. Number of spontaneous bowel movements (SBMs—bowel movements that occurred without the use of rescue laxatives or enema administered in the previous 24 h) was characterized by a longitudinal non-linear mixed-effects logistic regression dose-response model. Incidence of diary entry discontinuation (DED) was described by a time-to-event model.
Results: The mean number of SBMs per week increased with increasing naloxegol dose and/or exposure (average concentration). Response to naloxegol was predicted to be higher in patients with lower baseline SBM frequency and those taking a strong opioid. Posterior predictive checks demonstrated that the final SBM and DED models could predict percent responder rates consistent with observed data. Predicted placebo-adjusted responder rates (90 % confidence interval) were 10.4 % (4.6–13.4 %) and 11.1 % (4.8–14.4 %) for naloxegol 12.5 and 25 mg/day, respectively.
Conclusions: A nonlinear mixed effects logistic regression dose-response model adequately described the number of daily SBMs in patients with non-cancer-related pain and OIC.The SBM model in combination with the DED model can correctly predict responder rates in OIC phase III trials.

T-027

Glucagon-Like Peptide-1 (GLP-1) Receptor Agonists: Model-Based Meta-Analysis of HbA1c from Randomized Clinical Trials

Hongmei Xu*, Nidal Al-Huniti, Donald Stanski

Quantitative Clinical Pharmacology, AstraZeneca, Wilmington, DE, USA

Objectives: Gucagon-like peptide-1 (GLP-1) agonists are widely used for type 2 diabetes. The aim of this analysis to quantify the efficacy of the four FDA approved GLP-1 agonists (exenatide, exenatide LAR (long-acting release), albiglutide, liraglutide) by model-based meta-analysis.
Methods: A PubMed search for randomized (randomised) clinical trials (RCTs) investigating the effects of GLP-1 agonists on HbA1c was performed through May 2014. RCTs were included if they lasted at least 12 weeks, reported time course of HbA1c and/or change from baseline HbA1c over the study period. Summary-level longitudinal data on HbA1c were digitized and extracted. NONMEM 7.2 was used to perform meta-analysis modeling.
Results: A total of 24 RCTs met the selection criteria, which included 51 study arms and 9,667 patients. Most of trials were on exenatide or exenatide LAR, with only two trials on albiglutide. In the integrated

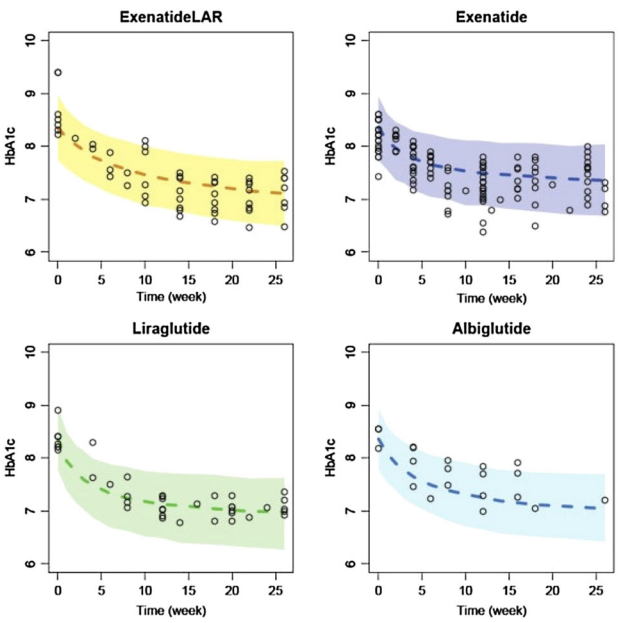

Fig. 1 Model-based predictions of the time course of HbA1c for GLP-1 agonists. *Solid circles* are mean data from each study arm of published clinical trials, *dashed lines* are model predicted median response, shaded area are 90 % prediction intervals

analysis, an Emax model on the duration of the treatment best described the data (Fig. 1). Exenatide LAR and liraglutide provided more reduction on HbA1c compared to other two GLP-1 agonists. Prior treatment before randomization included diet and exercise, metformin, insulin, sulfonylureas, thiazolidinedione, biguanides or a combination of a few of above. The baseline HbA1c level and the prior treatment were tested on the magnitude of HbA1c reduction. However, the reduction of HbA1c was significantly conditioned on the baseline HbA1c, not prior treatment, based on the likelihood ratio test.

Conclusions: The developed model with the impact of baseline HbA1c on Emax described the summary-level longitudinal data on HbA1c quite well. This model can be used to differentiate potential GLP-1 agonist candidate drug to evaluate the value of development.

T-028

Interspecies Allometric Meta-Analysis of the Comparative Pharmacokinetics of 85 Drugs Across Veterinary and Laboratory Animal Species

Qingbiao Huang[1], Ronette Gehring[1], Lisa A. Tell[2], Mengjie Li[1], Jim E. Riviere[1,*]

[1] Institute of Computational Comparative Medicine, Kansas State University, Manhattan, KS, 66502, USA; [2] Departments of Medicine and Epidemiology, School of Veterinary Medicine, College of Agricultural and Environmental Sciences, University of California-Davis, Davis, CA 95616, USA

Objectives: To apply the method of allometric analysis to a study of the comparative clearance (CL) and volume of distribution at steady state (Vss) of veterinary drugs to provide a fast and practical approach to extrapolate the first dose regime in different veterinary species.

Methods: Data of 85 drugs were first screened and collected from the FARAD (the Food Animal Residue Avoidance Databank) database. For each drug, linear regression was performed on the log-transformed data for CL and Vss according to the following equation: $\log(CL) = \log(a) + b*\log(W)$, $\log(Vss) = \log(a) + b*\log(W)$. Values for a and b were obtained from the intercept and the slope of the regression, along with the coefficient of determination (r^2).

Results: The results showed that 77 and 88 % of drugs displayed significant correlations between clearance (CL) and volume of distribution at steady status (Vss) versus body weight ($p < 0.05$) on a log-log scale, respectively. The distribution of the allometric exponent b for CL and Vss display approximate normal distribution, with means (0.87 and 0.99) and standard deviations (0.143 and 0.157) for CL and Vss, respectively. Twelve drugs were identified to have at least one outlier species for CL and ten drugs for Vss. The human CL and Vss were predicted for selected drugs by the obtained allometric equations. The predicted CL and Vss were within a threefold error compared to observed values, except the predicted CL values for warfarin and diazepam.

Conclusions: The results can be used to estimate cross-species pharmacokinetic profiles for predicting drug dosages in veterinary species, and to identify those species for which interpolation or extrapolation of pharmacokinetics properties may be problematic.

References:

1. Riviere, J.E., Martin-Jimenez, T., Sundlof, S.F. & Craigmill, A.L. (1997) Interspecies allometric analysis of the comparative pharmacokinetics of 44 drugs across veterinary and laboratory animal species. Journal of Veterinary Pharmacology and Therapeutics, 20, 453–463.

T-029

Population Exposure-Response Analysis of "On–Off" Time in Individuals with Parkinson's Disease following Preladenant Treatment

Malidi Ahamadi[1,*], Kevin Dykstra[2], Prajakti Kothare[1], Susan Huyck[1], Julie Stone[1], Kuenhi Tsai[1]

[1] Merck Research Laboratory, Merck and Co., USA; [2] qPharmetra LLC, Andover, MA, USA

Objectives: Preladenant is an Adenosine type 2A receptor antagonist that was in development for Parkinson's Disease (PD). Population exposure–response analysis was applied to: quantify efficacy and safety relationships for preladenant in a Phase 2B trial including individuals with PD and motor fluctuations on levodopa therapy; to assess interaction with concomitant anti-PD medications; to identify subpopulations demonstrating differential response; and to assist future Parkinson's disease clinical studies

Methods: A total of 199 individuals with moderate to severe idiopathic PD provided data for this analysis. Individuals on a stable antiparkinsonian treatment regimen were treated with placebo or oral preladenant, 1, 2, 5 or 10 mg BID. A hierarchical, longitudinal PK-PD model related predicted preladenant concentration to the probability of a patient being in the "off" state at each half-hourly assessment over the three days preceding a clinical visit.

Results: A two-compartment population PK model with transit compartment absorption model described preladenant concentration. The effect of concomitant anti-PD medication was modeled based on prior historical data in combination with the reported frequency of a given patient's treatment regimen. An Emax model of the synergistic effect of preladenant described the reduction in "off" probability as a function of time and concomitant anti-PD drug effect. To explore implications of the models for development decisions, statistically realistic predictions of how Preladenant affects key "off" time endpoints were generated. The final model was used to predict efficacy responses for subjects under possible treatment and population scenarios.

Conclusions: This work identified an exposure-relationship between preladenant and "off" probability. Concomitant treatment frequency was identified as a key covariate predicting this endpoint. Simulations based on this model provided a quantitative framework in support of PD dosing and development recommendations. More frequent levodopa users have less "off" time response. Future clinical studies need to consider this important factor.

T-030

Exposure-Response Model of Brodalumab in Psoriasis: Modeling of Continuous PASI Response Predicts Categorical PASI 75 and PASI 100 Endpoints

David H. Salinger[1,*], Christopher J. Endres[1], Megan A. Gibbs[2]

Amgen Inc., [1] Seattle, WA, USA; [2] Thousand Oaks, CA, USA

Objectives: Brodalumab is a monoclonal antibody that selectively targets human IL-17RA and has been shown to provide efficacious treatment for psoriasis. Objectives of the population PK/PD analysis were to:

- Characterize the time-course of brodalumab exposure–PASI response relationship in subjects with psoriasis.
- Assess the ability of the model to predict related categorical endpoints (PASI 75, PASI 100).

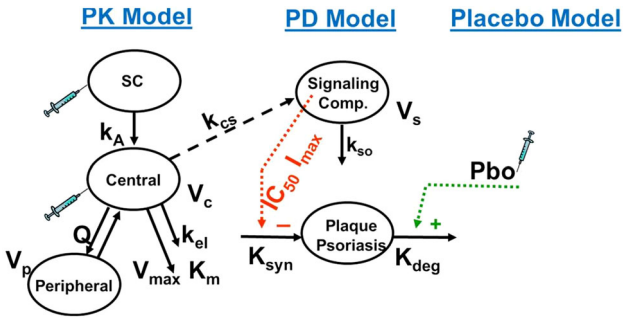

Fig. 1 PKIPD Model schematic

- Evaluate whether there is further body weight impact on PASI response after accounting for its impact on PK.

Methods: For the population PK/PD analysis, 25 subjects received single SC (140 or 350 mg) or IV (700 mg) dose of brodalumab or placebo and 195 subjects received 70, 140, or 210 mg SC Q2 W or 280 mg SC Q4 W or placebo. PASI scores were assessed bi-weekly for up to 112 days.
Population PK modeling (reported previously) featured linear and nonlinear elimination pathways (Fig. 1); body weight was a significant covariate. Small parameter shrinkages and no evidence of feedback of PD to PK justified using the sequential PK/PD modeling approach.

The time-course of PASI response was modeled by linking PK to a signaling compartment, which indirectly modulated psoriatic plaque (PASI score) turnover through inhibition of plaque formation rate (Fig. 1).
Results: Diagnostics indicated that the model fit the data well and also predicted the observed categorical response (PASI 75, PASI 100) time-course. The signaling compartment was necessary for linking the nonlinear PK to the relatively stable PASI response and improved model fit by decoupling individual rates of effect onset and offset.
The IC50 was 0.637 (31 %) μg/mL. Plaque formation rate was similar to that reported for other compounds, providing corroboration for the disease kinetics portion of the model.

There was no further body weight impact on PASI response after accounting for the impact on PK.
Conclusions: A population exposure–response model characterized the PK and PASI response (including PASI 75 and PASI 100) of brodalumab and supported Phase 3 dose selection.

T-031

Development of a CYP2C19 Genotype Guided Dosing Algorithm for Voriconazole

Naveen Mangal[1], Issam Hamadeh[2], Tanay Samant[1], Stephan Schmidt[1,*]

[1] Center for Pharmacometrics and Systems Pharmacology, College of Pharmacy, University of Florida, Orlando, FL, USA; [2] Department of Pharmacotherapy and Translational Research, College of Pharmacy, University of Florida, Gainesville, FL, USA

Objectives: Voriconazole is recommended as a first line agent for the treatment or prevention of invasive fungal infections in immunocompromised patients. The clinical utility of its "one size fits all" weight based dosing regimen is being questioned due to large inter-individual differences in its pharmacokinetics as a result of CYP2C19 polymorphisms [1, 2]. The objective of this project was to develop a CYP2C19 genotype-guided dosing algorithm for Voriconazole to optimize the dose-concentration-response relationship in patients with CYP2C19 polymorphisms, particularly in ultra-rapid metabolizers to ensure sufficient anti-fungal coverage.
Methods: A population pharmacokinetic (pop-PK) model was developed in NONMEM v.7.2 for different CYP2C19 genotypes based on literature data. Non-linearity in clearance was accounted for by respective Vmax and Km values, which were scaled up from in vitro enzyme assay data by accounting enzyme expression levels and liver size. The developed model was externally qualified via literature data not used for model building. Once developed and qualified, the model was used in clinical trial simulations to predict maintenance doses for patients with different CYP2C19 genotypes sufficient to exceed therapeutic trough concentrations of 1 μg/mL.
Results: A 2-compartment body model with non-linear clearance from the central compartment characterized all data reasonably well. Table 1 (attached) shows the proposed dosing recommendations for different CYP2C19 genotypes.
Conclusion: A model-guided dosing strategy was applied to optimize the use of voriconazole in patients with invasive fungal infections. The proposed dosing algorithm will now be prospectively tested in the clinic to determine if a CYP2C19 genotype-directed dosing strategy is superior to the current one size fits all dosing regimen.

Table 1 Proposed dosing recommendations for different CYP2C19 genotypes

Phenotype	Genotype	Maintenance dose (mg/kg)
Extensive metabolizers	*1/*1	4
Ultra metabolizers	*1/*17	7
Poor metabolizers	*2/*2, *3/*3	1.5
Intermediate metabolizers	*1/*2, *1/*3	3.25

References:

1. Weiss et al. J. Clin. Pharmacol. 2009; 49: 196–204
2. Obeng et al. (Pharmacotherapy 2014) doi:10.1002/phar.1400

T-032

A Population PKPD Model for Changes in Sexual Function Questionnaire (CSFQ) in Patients with Major Depressive Disorder (MDD) Treated with Vilazodone or Placebo

Tatiana Khariton[1,*], Martin Bergstrand[2], Elodie Plan[2], Parviz Ghahramani[1]

[1] Forest Research Institute, Jersey City, NJ, USA; [2] Pharmetheus, Uppsala, Sweden

Objectives: Characterize the relationship between vilazodone plasma exposures (AUC) and changes in sexual function.
Methods: A PKPD model using a nonlinear mixed-effect modeling approach was used to explore the relationship between plasma levels of vilazodone (described by AUC) and longitudinal Changes in Sexual Functioning Questionnaire (CSFQ scores). Data from a double-blind, placebo and active-controlled Phase 4 clinical study in patients with MDD were used for these analyses. The data included placebo and two vilazodone treatment arms (20 and 40 mg/day). A previously developed population PK model for vilazodone was used to predict AUC for each patient. Linear and Emax exposure–response relationships were investigated. In addition to drug effect, placebo

effect and covariate-parameter relationships were explored. Montgomery–Åsberg Depression Rating Scale total scores (MADRS), were included in the PK-CSFQ model as a covariate.
Results: Exploratory graphical analysis indicated that changes in CSFQ were correlated with changes in MADRS across placebo and active treatment arms. There was no evidence of relationship between CSFQ and vilazodone exposures. During model development, CSFQ scores were primarily thought to be influenced by two factors: (1) MADRS (improvement or worsening of depression might have an impact on patient's sexual function), and (2) vilazodone exposures. Final exposure–response model for CSFQ identified the time-varying MADRS score to be a statistically significant predictor of the placebo response (worse MADRS depression symptoms were associated with worse CSFQ). After controlling for MADRS, no additional statistically significant effect of vilazodone on CSFQ over time could be detected ($p > 0.05$).
Conclusions: After accounting for MADRS total score, no additional effect of vilazodone exposures on sexual function (as measured by CSFQ total score) over time could be detected. Thus, vilazodone can be expected to improve sexual function in MDD patients by reducing depressive symptoms, while, it does not have any additional direct effect on sexual function.

T-033

A Model-Based Assessment of the Impact of Intravenous Infusion Setup Configurations on Pharmacokinetics

Kevin Litwiler*, Lance Wollenberg, Caleb Wagner, and Micaela Reddy

Array BioPharma, Boulder, CO, USA

Objectives: Administration of oncology therapeutics by intravenous (IV) infusion is commonplace. However, the physical configuration for an infusion apparatus using piggy-back bags can alter pharmacokinetics (PK). Here we assess the variability and bias introduced into PK due to clinically relevant differences in IV infusion procedures.
Methods: A model describing infusion-based drug administration was developed that accounted for drug delivery from a piggy-back bag, via a mixed drip chamber and zero-order IV transfer lines, to a patient with multi-compartment PK. Deterministic and stochastic simulations were conducted across a range of configurations expected in clinical infusion centers using a combination of R and the Phoenix modeling language (PML) in Phoenix 6.3. Effects of bag volume, infusion rate, line lengths, infusion interruption and flush methods were assessed. Simulated profiles were evaluated post hoc using clinically relevant sampling times and standard noncompartmental methods.
Results: Observed PK can be significantly affected by infusion method. Example PK profiles are shown below versus piggy-back bag size. Because lines are typically primed with saline, there is a lag before drug reaches the patient. For a 50-mL bag infused over a 1-h period, ~40 % of the drug can remain in the lines at 60 min, with a flush resulting in a delayed time to maximum concentration, Cmax. Furthermore, if the infusion rate does not account for volume from the bag overfill or the drug added, the administered dose may be reduced. Low-volume bags (<100 mL), long lines and variable flushing procedures can change PK values by >twofold. Values for Cmax are most impacted, followed by area-under-the-curve, but half-life values are less affected. Additionally, undelivered drug due to incomplete flushing can result in significant under-dosing.
Conclusions: Differences in infusion setup can introduce significant bias. Using a ≥100-mL bag and providing clear instructions on flush

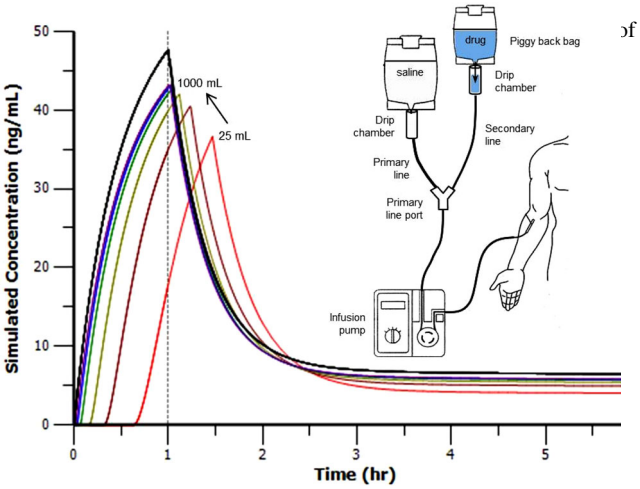

of

T-034

Population Pharmacokinetic Analysis of Tiotropium in Healthy Volunteers after Intravenous Administration and Inhalation

Z Parra-Guilln, B Weber, A Sharma, J Freijer, S Retlich, JM Borghardt, IF Trocniz*

Department of Pharmacy and Pharmaceutical Technology School of Pharmacy, University of Navarra, Navarra, Spain; Translational Medicine and Clinical Pharmacology, Boehringer Ingelheim Pharma GmbH&CoKG, Biberach, Germany

Objectives: Tiotropium (TIO) is an inhaled long-acting anticholinergic approved for the management of COPD. In the current evaluation, a population pharmacokinetic (POPPK) model for TIO in healthy volunteers (HV) was developed with the objective to characterize the pulmonary absorption properties.
Methods: Data were available from three phase I clinical trials. HV received TIO either as a single or two (on consecutive days) 15 min intravenous (IV) infusions (n = 24) or once daily via inhalation (Respimat®) for two weeks (n = 27). The IV and inhalation doses ranged from 2.4 to 14.4 and 5 to 10 mcg, respectively. TIO was measured in plasma and urine. Full TIO plasma concentration profiles and cumulative urines samples in intervals were obtained on the first and last administration days. Additional plasma trough concentrations and urine data (0–24 h) were obtained during the multiple dose inhalation study. Pharmacokinetic analysis was performed using the population approach and jointly modeling data after IV administration and inhalation (NONMEM 7.2).
Results: TIO exhibited a four compartment systemic disposition model with concentration dependent kinetics reflected as (i) a maximum binding capacity in one of the peripheral compartments, and (ii) a saturable non-renal elimination. Both processes had minor impact on the shape of the plasma concentration profiles. Pulmonary drug absorption was described by two parallel first order processes from two depot compartments. The lung dose was estimated as 56 % (population average) ranging between 21–82 % between individuals. Approximately 93 % of the lung dose was slowly absorbed (t1/2 = 54.5 h) while the other 7 % was absorbed faster (t1/2 = 5 min). Inter-individual variability was low (10–29 %) and moderate (55–72 %) with respect to the disposition and pulmonary parameters, respectively.
Conclusions Absorption and disposition characteristics of TIO in HV were simultaneously characterized with a POPPK approach. After inhalation of TIO via the Respimat®, a large fraction of the lung dose (93 %) has a prolonged lung residence time.

T-035

Longitudinal Safety Modeling and Simulation for Regimen Optimization of Vismodegib in Operable Basal Cell Carcinoma

Tong Lu[1,*], Russ Wada[2], Jeannie Hou[1], Mukta Tripathi[1], Ivor Caro[1], Mark Dresser[1], Richard A. Graham[1], Jin Y. Jin[1]

Genentech, Inc.; [2] Quantitative Solutions, Inc.

Objectives: To determine an optimal duration of treatment interruption of vismodegib to minimize adverse events (AE) in patients with operable basal cell carcinoma (oBCC) using longitudinal ordered categorical model.
Methods: AE data were obtained from a phase 2 trial evaluating the efficacy and safety of vismodegib treatment in oBCC patients. 74 patients were randomized to one of three cohorts receiving 150 mg QD treatment: 12 weeks (wk) dosing with 30 days (d) follow-up, 12 wk dosing with 24 wk observation and 30 d follow-up, or 8 wk dosing with 4 wk observation followed by 8 wk dosing and 30 d follow-up. The predicted unbound vismodegib profile based on population PK model incorporating individual covariates were used for PK/AE analyses in NONMEM7.2 (Laplacian). AE data for modeling included severity assessment (CTCAE v4.0) of dysgeusia, ageusia and muscle spasm, common AEs leading to treatment interruption/ discontinuation (I/D). Dysgeusia and ageusia were grouped representing taste disturbance.
Results: AE grades in patients experiencing at least one AE were best described by a mixed-effects longitudinal logistic regression model [1] with an effect compartment explaining lag time between PK and AE, and a linear drug effect. Simulations showed that after 12 wk QD treatment, 6 and 4 wk I/D could lead to complete resolution for all grades of muscle spasms in 80 % of patients, and for grade $\geq$2 muscle spasms in 95 % of patients. For dysgeusia/ageusia, 12-wk I/D could lead to complete resolution of all AE grades in 80 % of patients, and 6-wk I/D could lead to complete resolution of grade $\geq$2 AE in 95 % of patients.
Conclusions: Our work exemplified how longitudinal PK/PD modeling can help elucidate the onset and offset of AE events and the effect of treatment I/D, thereby enabling optimization of regimen duration.

References:

1. Kowalski KG, McFadyen L, Hutmacher MM, Frame B, Miller R. A Two-Part Mixture Model for Longitudinal Adverse Event Severity Data. J Pharmacokinet Pharmacodyn. 2003;30(5): 315–36

T-036

Human Pharmacokinetics Prediction of CKD-519 Using Non-clinical Data

Wan-Su Park[1], Sung Ho Park[2], Se-mi Kim[2], Jongtae Lee[1], Taegon Hong[1], Gab-Jin Park Sunil Youn[1], Seunghoon Han[1], Dong-Seok Yim[1,*]

[1] Pharmacometrics Institute for Practical Education & Training, the Catholic University of Korea, Seoul, Korea; [2] Chong Kun Dang Research Institute, Yongin, Korea

Objectives: CKD-519 (Chong Kun Dang, Seoul, Korea) is a newly developed anti-dyslipidemic agent of which the clinical studies are to be initiated. The prediction of human pharmacokinetic (PK) profile was performed to support the determination of the starting dose for a first-in-human clinical trial.
Methods: Single-dose data from hamster, rat and monkey were used. In each species, one intravenous dose level and three oral dose levels were taken into consideration (four individuals for each dose level). More than seven plasma concentration data were available which were obtained over 48 h after drug administration. The PK parameters by species were obtained through mixed-effect modeling using NONMEM (Ver. 7.2, ICON Development Solutions, Ellicott city, MD, USA). To obtain human PK parameter estimates, various interspecies scaling procedures was explored for clearance and volume parameters and the relationship which describes the estimates from three animal species best was selected.
Results: A 2-compartment model with Weibull-type absorption kinetics was chosen to be the final PK model for all species. In addition, relative bioavailability by dose level was also included. Clearance parameters were scaled using body weight and brain weight while volume parameters showed linear relationship with body weight. The estimates for absorption rate and bioavailability were assumed to be the mean values of three species. The predicted time–concentration profile of CKD-519 in human by dose is presented in the following figure.
Conclusions: The time–concentration profile in human was successfully predicted. It seemed reasonable when compared to the human concentration range achieved after the administration of a similar marketed drug.

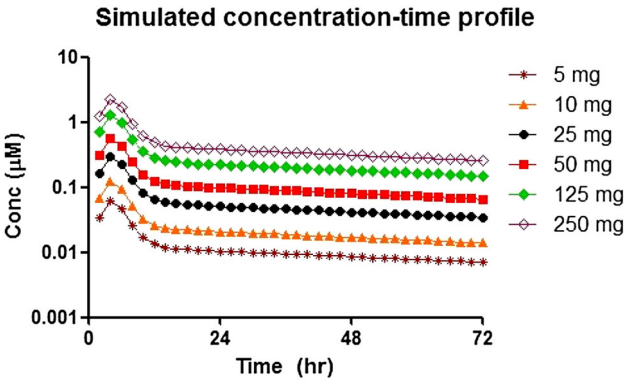

T-037

ABCC3 and OCT1 Genotypes Influence Pharmacokinetics of Morphine in Children

Raja Venkatasubramanian[1,2], Tsuyoshi Fukuda[2,3], Jing Niu[1,2], Tomoyuki Mizuno[2], Vidya Chidambaran[1,3], Alexander A. Vinks[2,3], Senthilkumar Sadhasivam[1,3,*]

**A manuscript documenting results in this abstract was accepted for publication to the journal "Pharmacogenomics"

[1] Department of Anesthesia, [2] Division of Clinical Pharmacology, Cincinnati Children's Hospital Medical Center, Cincinnati, OH, USA; [3] Department of Pediatrics, College of Medicine, University of Cincinnati, Cincinnati, OH, USA

Objectives: Large inter-individual variability in morphine pharmacokinetics could contribute to variability in morphine analgesia and adverse events. Our hypothesis was that common functionally defective genetic polymorphisms of key transporters and enzymes genes (including OCT1, ABCC3, ABCB1, ABCC2 and UGT2B7) can substantially alter the pharmacokinetics of morphine and its metabolites.
Methods: Serial blood samples up to 40 min post initial morphine dose were obtained from 220 children undergoing outpatient adenotonsillectomy to quantify morphine, morphine-3-glucuronide (M3G) and morphine-6-glucuronide (M6G) systemic concentration. Morphine,

M3G and M6G pharmacokinetics were described by a PK model with allometric scaling using NONMEM. The time profile for M3G and M6G was modeled using mass balance equations accounting for formation of each metabolite from morphine and its respective first order elimination clearance [1]. A hypothetical delay compartment was used to capture the delay observed in the formation of metabolites.
Results: Children with ABCC3 -211C > T polymorphism C/C genotype had significantly higher M6G and M3G formation ($\sim$40 %) than C/T + T/T genotypes ($p < 0.05$). In this extended cohort similar to our earlier report [2], OCT1 homozygous genotypes (n = 13) had lower morphine clearance (14 %; $p = 0.06$) and in addition complementing lower metabolite formation ($\sim$39 %) was observed. ABCB1 3435 C > T TT genotype children had higher M3G formation though no effect was observed on morphine and M6G PK.
Conclusions: Our data suggest that besides body weight, OCT1 and ABCC3 genotypes play a significant role in the pharmacokinetics of intravenous morphine and its metabolites in children.

References:

1. Bouwmeester, N.J., et al.,; Br J Anaesth, 2004. 92(2): p. 208–17
2. Fukuda T, et. al.,; OCT1 genetic variants influence the pharmacokinetics of morphine in children. Pharmacogenomics 14(10), 1141–1151 (2013).

T-038

Simultaneous Population Pharmacokinetic Analysis of Unbound Mycophenolic Acid (MPA), total MPA, and its MPAG and Acyl-MPAG Metabolites

Malek Okour*, Pamala Jacobson, Richard Brundage

Experimental and Clinical Pharmacology, University of Minnesota, Minneapolis, MN, USA

Objectives: MPA is an approved immunosuppressive agent used in most kidney transplant recipients to prevent acute rejection. Wide between-subject variability (BSV) in MPA exposure exists and our understanding of it is further complicated by its enterohepatic recirculation. The objectives of this study were to build a population pharmacokinetic model of unbound MPA, total MPA, MPAG, and acyl-MPAG; and evaluate clinical biomarkers and genotypes for their relationships with exposure.
Methods: Drug concentrations were measured in 92 adult transplant recipients receiving the prodrug mycophenolate mofetil. Blood samples were obtained at hours 0, 1, 2, 4, 6, 8, and 12 following the dose. Multiple covariates and genotypes were screened in the recipients and the donors. The pharmacokinetic model was built using nonlinear mixed-effects modeling (NONMEM), and covariates selected using LASSO, GAM, and SCM.
Results: A five-compartment model with first-order input into an unbound MPA compartment connected to the MPAG, acyl-MPAG, and gallbladder compartments. Estimates (%RSE) were for unbound MPA oral clearance (CL/F): 728 L/h (10 %); BSV of CL/F: 40.2 % (12 %); unbound MPA oral volume of distribution (V/F): 4,220 L (12 %); BSV of V/F: 70.2 % (12 %); fraction unbound (FU): 0.024 (6 % RSE); BSV of FU: 29.2 % (9 %); clearance of MPAG: 0.209 L/h (33 %); volume of MPAG: 3.78 L (9 %); clearance of acyl-MPAG: 15.6 L/h (8 %); volume of distribution of acyl-MPAG: 17.7 L (9 %); transfer rate constant of unbound MPA to gallbladder: 0.188 h^{-1} (26 %); and transfer rate constant of MPAG to gallbladder: 0.122 h^{-1} (18 %). Absorption rate constant, fraction metabolized (fm) to MPAG, and fm for acyl-MPAG were fixed to the literature values of 4 h^{-1}, 0.87, and 0.13, respectively. Covariate analysis showed that creatinine clearance and the donor carboxylesterase-2 enzyme polymorphism (rs2241409) have a statistically significant influence on the clearance of unbound MPA.
Conclusion: The proposed model adequately describes the data. Future directions include linking the current work with pharmacodynamics response.

T-039

Population Pharmacokinetic–Pharmacodynamic Model of Topiramate's Effect on Cognition in Healthy Volunteers

Chay Ngee Lim*, Susan E. Marino, Richard C. Brundage, Angela K. Birnbaum

Department of Experimental and Clinical Pharmacology, University of Minnesota, Minneapolis, MN, USA

Objectives: Cognitive impairment is a commonly reported side effect of topiramate (TPM). While a number of factors have been implicated in the wide variability in occurrence of TPM-induced cognitive impairment (TICI), they have not been well characterized. The objectives of this study were to describe TICI and identify covariates using a Pharmacokinetic–pharmacodynamic (PK–PD) modeling approach. Symbol Digit Modalities Test (SDMT), which requires elements of attention and psychomotor speed, is an accepted measure of cognitive impairment, and was the TICI outcome of interest.
Methods: Data were pooled from three randomized cross-over studies in healthy volunteers for the development of the PK–PD model (n = 32). A population PK model was developed using TPM plasma concentrations measured following a 100 mg oral or IV dose. To characterize the effect of TPM on SDMT score, a sequential modeling approach was used, and linear, log-linear and Emax models were explored. Effect of site, age and multiple testing (practice effect) on baseline SDMT score were tested using forward inclusion and backward elimination. Treatment of SDMT score as a discrete outcome was also explored using Poisson and Negative Binomial distribution models. All population analyses were conducted via nonlinear mixed-effects modeling with NONMEM® 7.
Results: A two-compartment PK model with first-order absorption for oral dosing described the data adequately. While all three PD models fitted the SDMT data reasonably, the Emax model was selected due to higher plausibility. Age and multiple testing were found to be significant covariates on SDMT baseline. With the assumption of relative Emax of 1, the TPM concentration that leads to half maximal drop in SDMT is 2.77 μg/mL. The continuous and discrete PK-PD models yielded similar results.
Conclusions: The relationship between SDMT score and TPM plasma concentration is adequately described by an inhibitory relative Emax model, and age, as well as the number of prior SDMT tests affects the baseline SDMT score.

T-040

Exposure–Safety Response Relationship for ABT 450/Ritonavir, Ombitasvir, Dasabuvir and Ribavirin in Hepatitis C Genotype 1 Virus-Infected Subjects: Analyses of Data from Phase 2 Studies

Chih-Wei Lin*, Rajeev Menon, Wei Liu, Sven Mensing, Thomas Podsadecki, Nancy Shulman, Barbara DaSilva-Tillmann, Walid Awni, Sandeep Dutta

AbbVie, North Chicago, IL, USA

Objectives: Characterize relationships between ABT-450 (HCV NS3/4A protease inhibitor identified by AbbVie and Enanta as a lead compound for clinical development) coadministered with ritonavir, ombitasvir (NS5A inhibitor), dasabuvir (NS5B polymerase inhibitor and ribavirin exposures) and clinical safety (adverse events [AE] and laboratory abnormalities [LA]), following administration in HCV genotype 1-infected subjects (N = 652) in 4 Phase 2 studies.
Methods: Exposure (steady-state AUC) was obtained using post-hoc estimations for individual subjects from population pharmacokinetic analyses for different doses and/or regimens. The response variables (ALT, total bilirubin, hemoglobin, rash) were adverse events of special interest. Relationships between AE/LA and drug exposures were evaluated graphically using ggplot2 and by multivariate logistic regression exposure–response analyses in R.

$$\begin{aligned}\text{Logit}\ (p(Y_i \geq \text{grade}_x)) &= \ln(\text{odds}(Y_i \geq \text{grade}_x)) \\ &= \alpha + \beta_1 x_i + \cdots + \beta_k x_i\end{aligned}$$

A full model approach that accounted for incidence rates at different severity/grades was used to explore all possible relationships between predictor variables (AUC of each drug) and covariates (demographics, comedication use, baseline values) with response variables while accounting for all correlations. Significant ($p < 0.05$) regression coefficients were used to identify meaningful association(s) between predictor variable(s)/covariates and the odds/probability of the outcome.
Results: Summary of predictor variables in multivariate logistic regression analyses are provided in the Table 1.
Conclusions: The regimens administered in these studies were generally well tolerated with low rates of serious AEs, or discontinuations due to AEs or LAs. No significant associations were found between dasabuvir and ritonavir exposures and safety variables. Higher exposures of ribavirin and ABT-450 (observed primarily at doses greater than those used in Phase 3) increased odds of ALT and total bilirubin elevations. Higher ribavirin exposure increased odds of Grade ≥ 2 hemoglobin decline. Rash was not associated with exposure to any of the drugs. In this dataset, comedications, age and bodyweight were not significant covariates, while baseline value, sex and race were significant covariates for some response variables.

Table 1 Summary of significant predictor variables in multivariate logistic regression analyses

Response variable[a]	Predictor variable[b]	Estimate (SE)	*p* value
Drug-induced rash (≥moderate)	Female vs. Male	1.25 (0.578)	0.0303
ALT elevation (≥Grade 2)	$\log_{10}$ AUC of Ribavirin	4.53 (2.09)	0.0304
	Baseline ≥ Grade 2	1.46 (0.73)	0.0444
ALT elevation (≥Grade 3)	BaseLine ≥ Grade 3	3.53 (1.43)	0.0136
	$\log_{10}$ AUCof ABT-450	2.41 (1.08)	0.0258
	Black vs. non-Black	2.14 (0.98)	0.0289
	$\log_{10}$ AUC of Ribavirin	6.24 (2.91)	0.0317
Total bilirubin elevation (≥Grade 2)	$\log_{10}$ AUG of ABT-450	1.40 (0.28)	6.91×10^{-1}
	$\log_{10}$ AUC of Ribavirin	1.37 (0.42)	0.0010
	Black vs. non-Black	−0.93 (0.40)	0.0208
	$\log_{10}$ AUC of Ombitasvir	−0.29 (0.13)	0.0272
	Female vs. Male	−0.56 (0.27)	0.0417
Total bilirubin elevation (≥Grade 3)	$\log_{10}$ AUC of ABT-450	1.41 (0.67)	0.0339
Low hemoglobin (≥Grade 2)	$\log_{10}$ AUC of Ribavirin	5.24 (1.63)	0.0013
	Female vs. Male	1.52 (0.50)	0.0025
	Black vs. non-Black	1.21 (0.46)	0.0093
	$\log_{10}$ AUC of Ombitasvir	1.00 (0.51)	0.0486

SE Standard error
[a] Adverse event or laboratory abnormality
[b] p value < 0.05

T-041

Where Top-Down Meets Bottom-Up: Combined Population PK (Poppk) and PBPK Approaches to Evaluate the Impact of Food and Gastric pH on the Pharmacokinetics of Pictilisib

Tong Lu[1,*], Grazyna Fraczkiewicz[2], Laurent Salphati[1], Nageshwar Budha[1], Gena Dalziel[1], Gillian S. Smelick[1], John D. Davis[1], Mark J. Dresser[1], Joseph A. Ware[1] and Jin Y. Jin[1]

[1] Genentech Research and Early Development, South San Francisco, CA, USA; [2] Simulations Plus, Inc., Lancaster, CA, USA

Objectives: Pictilisib (GDC-0941) is being investigated in clinical trials as an anti-cancer agent. Because of the steep pH-dependent solubility profile in vitro, a Phase I, randomized, open-label study was conducted in healthy volunteers to investigate the effect of food and proton pump inhibitor (PPI) on pictilisib PK. Both the top-down (PopPK) and bottom-up (PBPK) modeling approaches are used to quantitatively understand the factors that might influence pictilisib PK, such as food and PPI.
Methods: PopPK analysis was conducted for all Fed and Fasted subjects with or without PPI using NONMEM v.7.2. PBPK analysis was conducted for group mean and representative subjects using GastroPlus® v.8.0. System parameters in the PBPK model (stomach transit time, precipitation time, and stomach pH) were adjusted to mimic the effect of food and PPI on GI physiology.
Results: PopPK analysis suggested a decrease of absorption rate constant (Ka) with food or PPI. PPI also lead to decreased bioavailability regardless of food. The PK of fasted group was well-predicted using a PBPK model with default fasted physiology. Implementation of gastric physiology changes, reflecting transition from fed to fasted states, yielded good PK prediction in fed group. The PK of fed and fasted groups with PPI was well-predicted by considering the elevated gastric pH and delayed gastric emptying. Decreased solubility in vivo appears to explain the reduced bioavailability by PPI in the PBPK model.
Conclusions: The bottom-up PBPK approach provides mechanistic explanation of different pictilisib Ka and bioavailability in different groups, which was identified by the top-down PopPK approach. PBPK helped to quantify the determinants of Pictilisib absorption and was applied to explore hypochlorhydria mitigation strategies.

T-042

The Population Pharmacokinetics of Bayer's Sucrose-Formulated Recombinant Factor VIII: Lean Body Weight and von Willebrand Factor Affect Clearance

McLeay S[1,*], Garmann D[2], Shah A[3], Vis P[4], Ploeger B[5]

[1] Model Answers Pty Ltd, Brisbane, Australia; [2] Quantitative Pharmacology, Bayer Pharma AG, Wuppertal, Germany; [3] Bayer HealthCare Pharmaceuticals, Whippany, USA; [4] LAP&P Consultants BV, Leiden, The Netherlands; [5] Quantitative Pharmacology, Bayer Pharma AG, Berlin, Germany

Objectives: Subjects with hemophilia A are currently treated by intravenous administration of factor VIII (FVIII) on demand or as a prophylactic therapy administered 2–4 times a week. The aim of this study was to characterize the variability in the pharmacokinetics (PK) of rFVIII-FS and identify covariates that could explain the variability in the PK.
Methods: A total of 3,032 observations (measured using the one-stage assay) from 206 subjects were available for the population pharmacokinetic analysis. Covariate effects were evaluated using a forward inclusion/backward deletion procedure. Models were evaluated using visual predictive checks and the uncertainty in the parameter estimates were derived from a bootstrap analysis.
Results: Approximately 80 % of the subjects were white in the age range of 4–61 years. The best PK model was a 2-compartment model with zero-order input and first-order elimination defined by the clearance (CL), volume of distribution of the central (Vc) and peripheral (Vp) volumes of distribution and intercompartmental CL (CLp). In the covariate analysis, age, weight, body mass index, lean body weight (LBW), and von Willebrand factor (VWF) were evaluated for their effect on CL: The covariate analysis revealed that CL and Vc increased with LBW and CL decreased with increasing VWF. Although age was also found to have a significant effect on Vc during covariate analysis, it was highly correlated with LBW; therefore, only LBW was considered as a covariate. Model evaluation showed that the model could be used for simulations to determine the percentage of patients who maintain FVIII levels above a certain threshold for different dosing regimens.
Conclusion: The PK of FVIII after administration of rFVIII-FS was best described with a 2-compartment model with zero-order input. Both CL and Vc were found to increase with LBW, whereas increasing VWF decreased CL.

T-043

Experimental Verification of an Absorption–Disposition Kinetic Model

Helen H. Usansky[1,*] and Patrick J. Sinko[2]

[1] ClinPharm Pro, LLC, Hillsborough, NJ, USA; [2] Rutgers University, Ernest Mario School of Pharmacy, Township, NJ, USA

Objectives: To experimentally verify the predictive accuracy of our previously developed Absorption–Disposition Kinetic (ADK) model (JPET2005) and to compare the difference in permeability determined from perfusate (drug disappearing from intestine) and diffusate (drug entering into blood).
Methods: In an in situ single-pass perfusion study in rats, ^{14}C-saquinavir (SQV) at 100 μM in MES Ringer's buffer was perfused through a segment of jejunum (~10 cm) at 0.2 mL/min with or without transporter modulators, such as elacridar (20 μM), MK-571 (100 μM) and midazolam (100 μM). The effluent perfusate and blood from the collective mesenteric vein were collected for up to 1 h. Radioactivity in the perfusate and jejunum segment was measured using LSC, and SQV plasma concentrations were determined using LC-MS/MS. Effective permeability (Pe) and diffusive permeability (Pm) were determined from perfusate radioactivity and blood concentrations, respectively. Absorption-rate constant (ka) and fraction absorbed (Fa) were back-calculated from Pm using the ADK model and compared to observed ka and Fa in mesenteric blood.
Results: SQV Pm ranged from 0.258 (SQV alone) to 6.02×10^{-6} cm/sec (SQV + elacridar). SQV Pe ranged from 2.81 (SQV alone) to 11.9×10^{-5} cm/sec (SQV + elacridar + MK-571). Radioactivity recovered in the jejunum tissue was 4.47–14.2 % of total radioactivity perfused. Pm and Pe were poorly correlated ($r^2 = 0.18$, $n = 18$), and the difference averaged 10-fold (SQV + elacridar) to 100-fold (SQV alone). Predicted and observed values of ka and Fa were nearly identical and were highly corrected ($r^2 > 0.93$, $n = 18$). The Pm values were further used for in vitro-in vivo extrapolation which led to successful prediction of SQV kinetics, alone or with the transporter modulators.
Conclusions: Through the in-situ study we have experimentally proved that the ADK model accurately describes the kinetics of orally administered drugs and that the ka and Fa derived from the ADK model are indeed the analytical solutions. The differences in Pe and Pm values are partially attributed to the tissue binding of the drugs.

T-044

Serotonin and Dopamine Transporter Occupancy of SKL10406 in Humans: Comparison of Pharmacokinetic–Pharmacodynamic Modeling Methods for Estimation of Occupancy Parameters

Jongtae Lee[1], Jung-Shin Park[2], Seunghoon Han[1], Dong-Seok Yim[1,*]

[1] Pharmacometrics Institute for Practical Education & Training, the Catholic University of Korea, Seoul, Korea; [2] SK Biopharmaceuticals Co., Ltd., Seoul, Korea

Objectives: SKL10406, triple monoamine reuptake inhibitor, is a novel antidepressant candidate. A PET study was performed to investigate the occupancies of serotonin and dopamine transporters (SERT and DAT) in human brain, and the relationship between SKL10406 concentration and SERT occupancy was assessed using three different estimation methods.
Methods: Fifteen healthy volunteers were given SKL10406 100 mg/day for 6 days or 150 mg/day for 6 days after 100 mg/day for 4 days. Each subject underwent full pharmacokinetic sampling for SKL10406 and PET scans at pre-dose, 4 and 16 h after dosing at a steady state to investigate the occupancies of SERT and DAT using 11C-DASB and 11C-PE2I, respectively. Naive pooled method (NPM) and nonlinear mixed-effect methods (ME) including a direct ME (DME) and an effect compartmental ME (EME) were used (NONMEM Ver. 7.2).
Results: Six and five subjects completed the studies for SERT and DAT, respectively. The final estimates of Emax (53.4 %) and EC50 (11.8 ng/mL) from DME were relatively lower than those from NPM (Emax, 74.1 %; EC50, 36.8 ng/mL) and EME (Emax, 68.6 %; EC50, 40.2 ng/mL). DAT occupancy results were not modeled because of lower occupancies.
Conclusion: The results showed that the dosage regimens may be applied in patient studies. However, difference between estimation methods alerts that ME may not be a recommendable analysis tool for sparsely sampled PET scan data.

T-045

Physiologically-Based PK/PD Modeling for Oncology: Applications for Antibody Drug Conjugates

Michael Block[1,*], Rolf Burghaus[2], Kristin Dickschen[1], Thomas Gaub[1], Lars Küpfer[1], Jörg Lippert[2]

[1] Bayer Technology Services GmbH, Technology Development, Enabling Technologies, Computational Systems Biology, Leverkusen, Germany; [2] Bayer Pharma AG, Clinical Pharmacometrics, Wuppertal, Germany

A coupled full physiologically-based (PB) model including a representation of antibody drug conjugates (ADC) tumor pharmacokinetics (PK) and pharmacodynamics (PD) was developed by use of the systems biology platform for PBPK and PD modeling including PK-Sim and MoBi. The model includes mathematical description of full ADME properties for an ADC, an antibody (Ab) and the toxophore. It represents all relevant processes at a physiological level [1, 2]. In addition a PD model was integrated in order to represent the tumor growth [3]. The so-called two-pore concept for protein-like substances is the essential part for the ADME of the ADC/Ab.

The model is designed in a manner ready to address both; the full PK and PD for biologics as well as for small molecules within one model structure. Different applications of this model will be discussed in detail including the modeling for assessment of naked antibody pretreatment [4–5]. By example of a newly discussed concept of the therapeutic strategy of naked antibody predosing [4–5] the potential of this model will be shown. The comparison to the data (PK and PD) clearly demonstrates first: the ability for a very well mechanistic description of the related processes; and second: the potential to use the model to explain and predict the likelihood of successful application of naked antibody pretreatment scenarios. It can be used to support decision making in drug development processes.

References:

1. Sievers EL, Senter PD. Antibody-drug conjugates in cancer therapy. Annu Rev Med. 2013;64:15–29
2. Garg A, Balthasar JP. Physiologically-based pharmacokinetic (PBPK) model to predict IgG tissue kinetics in wild-type and FcRn-knockout mice. J Pharmacokinet Pharmacodyn. 2007 Oct;34(5):687–709
3. Simeoni M, Magni P, Cammia C, De Nicolao G, Croci V, Pesenti E, et al. Predictive Pharmacokinetic–pharmacodynamic modeling of tumor growth kinetics in xenograft models after administration of anticancer agents. Cancer Res. 2004 Feb 1;64(3):1094–101
4. Boswell CA, Mundo EE, Zhang C, Stainton SL, Yu SF, Lacap JA, et al. Differential effects of predosing on tumor and tissue uptake of an 111In-labeled anti-TENB2 antibody-drug conjugate. J Nucl Med. 2012 Sep;53(9):1454–61.
5. Boswell CA, Mundo EE, Firestein R, Zhang C, Mao W, Gill H, et al. An integrated approach to identify normal tissue expression of targets for antibody-drug conjugates: case study of TENB2. Br J Pharmacol. 2013 Jan;168(2):445–57

T-046

Robust Inference in Thorough QT Studies

Dosne AG[1,*], Bergstrand M[1], Karlsson MO[1], Renard D[2], Heimann G[2]

[1] Uppsala University, Sweden; [2] Novartis Pharma AG, Basel, Switzerland

Objectives: Thorough QT studies are pivotal safety studies which assess whether a drug prolongs the QT interval. Model-based analysis of these studies could increase efficiency over the currently used intersection–union test by making use of the full concentration–response relationship. However, robustness against model misspecification needs to be guaranteed in pivotal settings. The objective of this work was to develop an efficient, fully pre-specified model-based inference method for thorough QT studies where type I error is controlled.

Methods: We adopted an approach developed in a discrete dose–response setting with independent data [1] to a continuous concentration–response setting with dependent data. Estimation of the concentration–response relationship was performed using model averaging over a parametric (linear) and a nonparametric estimator. Different nonparametric estimators as well as different model weighting strategies were explored. The selected endpoint was drug-induced QT prolongation at the estimated mean maximum drug concentration. Type I error, bias in the selected endpoint and power of the developed method were investigated under different simulation scenarios with and without model misspecification.

Results: I-splines [2] were selected as the nonparametric estimator as they could handle dependent data and enable straightforward implementation of monotonicity constraints. I-splines settings were found that performed well for all investigated scenarios. Global model weights based on the mean integrated square error adapted from [1] performed well. The developed method was able to control type I error in all scenarios. Model averaged estimates of drug effect at the mean maximum concentration were unbiased and satisfactory power was achieved.

Conclusions: An efficient, fully pre-specified model-based inference method for thorough QT studies where type I error is controlled was developed. The gain in power of the model averaged method over nonparametric regression alone was however limited given the investigated simulation settings.

References:

1. Yuan Y, Yin G, Dose–Response Curve Estimation: A Semiparametric Mixture Approach. Biometrics, 2011. 67: p. 1543–1554
2. Ramsay JO, Monotone Regression Splines in Action. Statistical Science, 1988. 4(5):p. 421–465

T-047

Generalizable Sampling Strategy and Sample Size Calculation for Linear Monoclonal Antibodies in First-in-Pediatrics Studies

Ping Chen, Lubna Abuqayyas, Adimoolam Narayanan, Juan Jose Pérez-Ruixo, Murad Melhem*

Amgen Inc, One Amgen Center Drive, Thousand Oaks, CA 91320, USA

Objectives: Due to the logistical and ethical challenges in conducting clinical studies in pediatrics, optimal pharmacokinetic (PK) sampling schemes (OPKSS) and sample size are of particular importance in pediatric studies. In the current work, we propose a generalizable framework for OPKSS and sample size calculation for linear monoclonal antibodies (mAbs) in pediatrics, which ensure adequate accuracy and precision of PK parameter estimates.

Methods: For a typical linear intravenously administered single dose mAb, PK parameters in pediatrics were scaled from adult parameters [1], using standard allometric exponents for clearance and volume terms. OPKSS and sample size were determined using population Fisher Information Matrix (PFIM), followed by stochastic simulation re-estimation (SSE) to assess the bias and precision of parameter estimates. Optimization was performed in each pediatric age group (0–<2, 2–<6, 6–<12 and 12–<18 years) using the candidate sample sizes of 3, 5, 8, 10, 12, 15 and 20 subjects per age group. A minimal design (MD: 5 samples/subject), an optimal design for non-compartmental analysis (NCAD: 10 samples/subject) and a rich design (RD: 20 samples/subject) were compared.

Results: Slightly different OPKSSs for different age groups were suggested by PFIM. However, implementing the same OPKSS across age groups resulted negligible changes in PK parameter precision (<0.2 %). The OPKSS for the MD was on day 0, 2, 8, 10 and 168. Compared to NCAD and RD, MD provided very similar precision estimates (<0.1 %) and accuracy (<10 %). The precision of PK parameter estimates improved as sample size increased. Based on these results, 8 subjects per age group with MD provided imprecision ≤30 % and bias <20 % in all PK parameters.
Conclusions: For a typical mAb exhibiting linear PK, 8 subjects per age pediatric group with MD provides adequate accuracy and precision on PK parameter estimates.

Reference:

1. Davda et al. mAbs. 2014; 6(4).

T-048

Population Pharmacokinetics of Intravenous Zanamivir in Adult Healthy and Hospitalized Influenza Patients

Rajendra Singh[1,*], Steve Weller[2], Bela Patel[1], Mary Wire[2]

[1] CPMS GlaxoSmithKline, King of Prussia, PA, USA; [2] RTP, NC, USA

Objectives: Zanamivir, as a dry powder for oral inhalation, is approved for the treatment and prophylaxis of uncomplicated seasonal influenza in adults and children ≥5 years of age. An intravenous (IV) formulation of zanamivir is in clinical development for the treatment of influenza in hospitalized patients. The present work aims to characterize the pharmacokinetics (PK) of zanamivir in adults following IV administration.
Methods: Population PK analysis was performed using NONMEM version 7.1.2 (ICON, Ellicott City, MD) with data from a total of 260 adult subjects from 8 studies, including 7 Phase I studies in healthy subjects (doses 50–1,200 mg) and a Phase II study in hospitalized patients with influenza (standard dose of 600 mg twice daily for 5–10 days). A two-compartment structural model with linear first-order elimination was selected to describe zanamivir PK. Model development including covariate identification was performed using first-order conditional estimation (FOCE) with interaction. Final model selection was based on goodness-of-fit, biological plausibility, precision of parameter estimates, and reduction in objective function value. Nonparametric bootstrap and visual predictive checks were implemented for final model evaluation.
Results: A two-compartment model with weight, creatinine clearance and age as covariates on clearance (CL); weight and disease status on central volume of distribution (Vc); and disease status on peripheral volume of distribution adequately defined the PK in adults. Estimated CL and Vc were 5.4 L/h and 10.3 L, respectively. Inter-individual variability on CL and Vc was ~37 and 24 %, respectively.
Conclusions: A 2-compartment model developed using data from Phase I/II studies adequately characterized IV zanamivir PK in healthy adults as well as hospitalized patients with influenza, and identified covariates that affected PK variability. This model will further be used to design and characterize PK in future trials.

T-049

Multiple Model Experiment Design to Support Optimal Dosing

David S. Bayard[1], Alona Kryshchenko[1,*], Roger Jelliffe[1] and Michael N. Neely[1,2]

[1] Laboratory of Applied Pharmacokinetics and Bioinformatics, Children's Hospital Los Angeles, Los Angeles, CA, USA; [2] University of Southern California, Los Angeles, CA, USA

Objectives: To introduce weightings into our previously described Multiple Model Optimal Design (MMopt) strategy. The weightings induce MMopt to extract information specific to optimizing the patient's next doses to achieve a given target for the target type, e.g. AUC, trough concentration, etc. Multiple model applications arise when the Bayesian prior is discrete, for example, when generated by nonparametric population modeling programs such as NPML, NPEM and NPAG.
Methods: The multiple model estimation process is interpreted as a classification problem. Estimator performance is scored in terms of how well it minimizes the Bayes risk, i.e., the probability of misclassification. Numerical minimization of Bayes risk is facilitated using a recent theoretical upper bound (cf., Blackmore, Rajamanoharan and Williams 2008). Weightings introduced into the Bayes risk function are shown to preserve this upper bound and computational simplicity. An example is studied where the weightings are chosen to induce the designed experiment to extract information specific to dosing for a desired target AUC (see Fig. 1). Performance is compared to the ED optimal design from the literature.
Results: For a 1 compartment model with parameters V and Kel, and a 1-h infusion IV, the 2-sample strategy was best at times of 1 and 13 h, with a cost of 2.1102 (root-mean-square AUC units). The 3-sample strategy was best at 1, 10.5, and 10.5 h, with cost of 1.6967. Both sample design cases improve on the ED-optimal design to high statistical significance ($p < 0.00001$).
Conclusions: The weightings introduced in the MMopt strategy provide sampling designs which extract information useful for dosing patients. In the 1-compartment model simulated example, dosing is improved relative to using ED-optimal design. MMOpt has the advantage of discriminating models by using global differences in model response curves rather than relying on local sensitivity to small parameter variations.
Supported by NIH Grants GM068968 and HD070886.

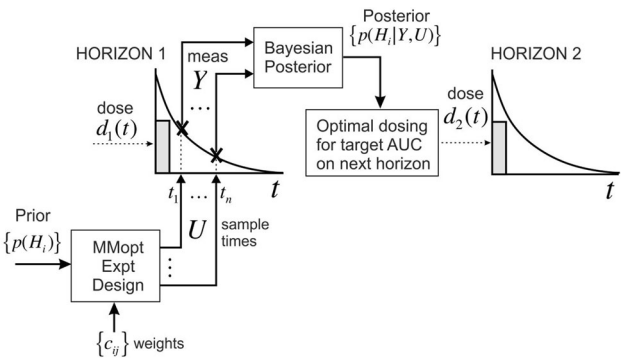

Fig. 1 Weights introduced into MMopt induce the designed experiment for Horizon 1 to extract information most relevant to supporting optimal dosing on Horizon 2

T-050

A Population Pharmacokinetic Model Characterizing the Multiphasic Disposition of Intramuscular VIVITROL

Devin Pastoor[1,*], Wen-I Li[2], Ryan Turncliff[2], Jogarao V.S. Gobburu[1]

[1] Center for Translational Medicine, University of Maryland School of Pharmacy, Baltimore, MD, USA; [2] Alkermes Inc, Waltham, MA, USA

Objectives: VIVITROL (naltrexone for extended-release injectable suspension; XR-NTX) is a long-lasting opioid receptor antagonist used as a treatment for opioid and alcohol dependence. The objective of this analysis was to characterize the population pharmacokinetics (PPK) of naltrexone (NTX) following monthly intramuscular (IM) administration of XR-NTX.
Methods: Data from 24 healthy volunteers administered single- or multiple-dose XR-NTX (380 mg) were analyzed using a nonlinear mixed effects modeling approach using NONMEM 7.2. A PPK model describing the multiphasic drug release profile was developed and a robust model qualification was performed using a quantitative predictive check.
Results: A two-compartment linear PK model was found to describe NTX concentrations following XR-NTX administration. The multiphasic (three peak) profile was described through three separate absorption processes: (1) an initial release, (2) a fast absorption phase with simultaneous dual zero- and first-order processes, and (3) a slow process with a transit-compartment disposition (Fig. 1). Estimated typical values were 2,720 L/h for apparent clearance (CL), 3,840 for intercompartmental clearance (Q), 2,640 L for central volume (Vc), and 7,950 L for peripheral volume (Vp). Between subject variability (BSV) was 9.79 % for CL and 19.5 % for Vc. BMI, weight, and gender were identified as covariates in the final model. A quantitative predictive check of the various clinically relevant PK measures found that the model adequately described the population mean and variability across all portions of the concentration–time profile.
Conclusions: The final model well describes intramuscular XR-NTX in the population studied and is suitable for future clinical trial simulations.

Disclosures: Mr. Pastoor and Dr. Gobburu were compensated by Alkermes Inc as consultants. Drs. Li and Turncliff are employees of Alkermes Inc.

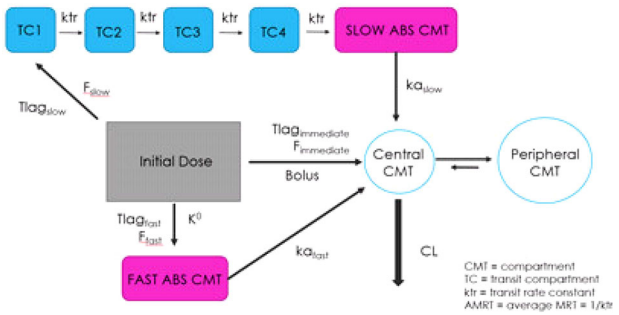

Fig. 1 .

T-051

Self-auditing Data Tables for R

Timothy Bergsma*, Scott Pivirotto

Metrum Research Group LLC, Tariffville, CT, USA

Objectives: Exclusions from pharmacometric analysis datasets should be well-documented for transparency. Literate programming techniques [1, 2] generally provide exclusion details only at an intermediate scale, while data flagging techniques are only applicable to format-compliant records.

To improve data exclusion documentation, we sought methods to visualize exclusion impact on subject and record count, and to capture the excluded records themselves, without significant increases in programming burden.
Methods: We implemented the R class audited [3] as a variant of data.frame. Class methods support typical operations while populating an internal transaction table and optionally preserving dropped records as an attribute. The transactions capture record counts, subject counts, and a descriptive label for each operation. Additional methods extract and report transactions; plot them using igraph [4]; and write the dropped records to an Excel workbook using xlsx [5]. We created a test assembly to illustrate use of self-auditing tables.
Results: Use of the audited class effectively summarized counts of dropped records and optionally captured the records themselves. Transaction tables were easily saved as files or visualized as directed graphs. Workflow required only minor modification; graph labels and worksheet names could be precisely controlled without secondary intervention. The visualization of the test assembly (Fig. 1) effectively accounted for dropped subjects and records.
Conclusions: With modest alteration of workflow, use of self-auditing data tables allowed generation of graphs and workbooks capturing the broad and fine detail of data exclusions during pharmacometric data assembly.

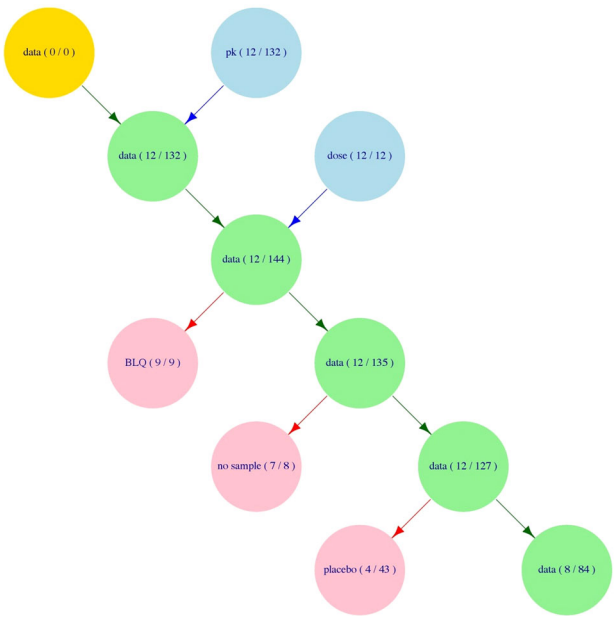

Fig. 1 Disposition of subjects and records during data assembly

References:

1. Knuth, DS. Literate Programming (1984). The Computer Journal 27(2): 97–111.
2. Leisch, F. Sweave: Dynamic generation of statistical reports using literate data analysis (2002). In Wolfgang Härdle and Bernd Rönz, editors, Compstat 2002—Proceedings in Computational Statistics: 575–580.
3. https://github.com/bergsmat/audited
4. Csardi G, Nepusz T. The igraph software package for complex network research (2006). InterJournal (Complex Systems): 1695. http://igraph.org
5. Dragulescu, AA. xlsx: Read, write, format Excel 2007 and Excel 97/2000/XP/2003 files (2013). R package version 0.5.5. http://CRAN.R-project.org/package=xlsx

T-052

Characterization of Dasatinib Exposure–Efficacy Relationship for Patients with Chronic Myeloid Leukemia (CML) Using Interval Censored Time-To-Event (TTE) Analysis

Xiaoning Wang[1,*], George Manos[2], Glenn Kroog[1], Amit Roy[1]

[1] Bristol-Myers Squibb Co., Princeton, NJ 08543; [2] Bristol-Myers Squibb Co., Wallingford, CT 06492

Objectives: Dasatinib (SPRYCEL) is indicated for the treatment of newly diagnosed chronic phase CML (CP-CML), and for CML and Ph + ALL with resistance or intolerance to prior therapy including imatinib. Exposure–efficacy in previously treated CP-CML was characterized with respect to major cytogenetic response (MCyR). An interval censored TTE analysis was employed as MCyR was only assessed at intervals of approximately 3-months.
Methods: The exposure–response (E–R) analysis was conducted with data from 567 CP-CML subjects enrolled in CA180034, a 4-arm Phase 3 study [100 or 140 mg daily, taken once (QD) or in divided doses twice (BID)]. The relationship between dasatinib exposure and time to achievement of MCyR with 1-year follow up was characterized using a parametric survival model. Time-varying exposure was examined as predictor for TTE, to account for dose modifications and interruptions. Baseline demographic and disease covariates were also examined. The impact of dose modification was assessed by model-based simulation.
Results: The TTE was adequately described by a Weibull survival distribution. The probability of achieving MCyR would increase with increasing Cavg (hazard increasing 1.18-fold (95 % CI 0.98–1.27) at the nominal dose of 140 mg compared with 100 mg total daily dose). The probability decreased with increasing age (hazard decreasing 18 % at 74 years compared with 55 years). Imatinib intolerant patients were more likely to respond compared with imatinib-resistant patients (hazard ratio 2.13). Model-based simulation showed that dose modification or interruption would decrease the MCyR rates. As actual dose modifications were more frequent and with greater increments for 140 mg daily, the recommended 100 mg QD regimen showed comparable efficacy with 70 mg BID
Conclusions: The analysis demonstrated the utility of interval censored TTE for analyzing E–R data when the response was assessed at fixed time interval. Results showed that dasatinib Cavg, patient age and response status to imatinib were associated with efficacy.

T-053

Longitudinal Assessment of OFFtime in Parkinson's Disease

Timothy Nicholas*, David Stiles, Yao Zhang, Marielle Delnomdedieu, Spyros Papapetropoulos

Pfizer, Inc.

Objectives: Chronic levodopa therapy in Parkinson's disease is characterized by optimizing a dosing regimen that maximizes the duration of beneficial effects while minimizing adverse events, such as dyskinesia. Duration of effect on motor function can be quantified as time "ON" (benefit) or "OFF" (lack of benefit) during the waking day. The objective of this research was to describe the longitudinal nature of OFFtime in Parkinson's disease patients receiving pharmacological treatment while on stable levodopa therapy.
Methods: Literature data were extracted from double blind, randomized, controlled trials. A total of 51 References containing 29 pharmacological treatments were utilized. Pharmacological treatments were grouped by drug class and included COMT inhibitors, adenosine A2A receptor antagonists, dopamine agonists, and MAO-b inhibitors. Treatment duration ranged from 3 to 56 weeks. The longitudinal model was developed using OpenBUGS v3.2.2 and R v3.0.2.

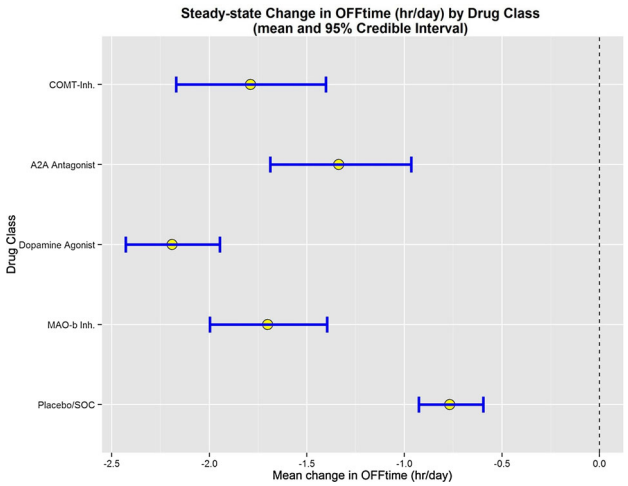

Fig. 1 Steady-state change in OFFtime (h/day) by drug class (mean and 95 % credible interval)

Results: The analysis population had a modified Hoehn–Yahr stage between 2 and 4, median disease duration of 8.6 years (minimum of 5.4 years) and mean OFFtime of 6.4 h/day. Mean awake time was 16.1 (SD: 0.54) h/day. Studies were excluded if levodopa regimen was allowed to be increased during the trial, though levodopa dose could be temporarily reduced if needed.
A placebo effect was estimated at −0.8 h/day at steady-state and attained 90 % of maximal effect within 5 weeks. The greatest pharmacological effect was observed in the dopamine agonist class, which had an additional −1.4 h/day change in OFFtime and reached maximal effect within 7 weeks. The steady-state effect estimated for each drug class is shown in Fig. 1. Concomitant medication, baseline OFFtime, or publication year did not show an effect on the magnitude of response.
Conclusions: To reduce the influence of a placebo effect, prospective clinical trials measuring OFFtime as an endpoint should be greater than 5 weeks in duration. Current dopamine agonist therapies show an additional reduction beyond placebo of 1.4 h/day providing a benchmark for novel therapeutic strategies.

T-054

Association Between Immune-Checkpoint Inhibitors Induced Tumor Shrinkage and Overall Survival in Advanced Melanoma and NSCLC

Yan Feng, Manish Gupta, Amit Roy*

Bristol-Myers Squibb Company, Princeton, NJ, USA

Background and Objective: Immune checkpoint inhibitors enhance immunologic antitumor activity and thereby have the potential to provide an overall survival (OS) benefit in many types of cancer. We describe the association between tumor shrinkage (TS) and OS in patients (pts) with advanced melanoma (MEL) or Non-small cell lung cancer (NSCLC) receiving ipilimumab (IPI) or nivolumab (NIVO), two immune checkpoint inhibitors that augment T-cell activity by blocking cytotoxic T-lymphocyte antigen-4 and programmed death-1 receptors, respectively.

Methods: The association between TS and OS for IPI in pts with MEL was assessed using data from 3 phase II studies. The corresponding associations for NIVO were assessed in pts with MEL or NSCLC with data from a phase I study. A nonlinear mixed-effects tumor growth dynamics (TGD) model was used to describe longitudinal tumor burden data. The association of TS with OS was determined using %TS at Week-8 (%TS-WK8), estimated from the TGD model. The relationship between %TS-WK8 and prognostic factors with OS was characterized by a multivariable Cox proportional-hazards model.
Results: For nivolumab in NSCLC and MEL, the risk of death decreases with decreasing drug clearance (CL), increasing %TS-WK8, increasing body weight, and in MEL additionally with Glasgow Performance Score (PS) < 1. For ipilimumab in MEL, the risk of death deceases with decreasing CL, increasing %TS-WK8, and decreasing LDH, and ECOG PS < 1. For both NIVO and IPI, drug exposure (Cavgss) was not a significant predictor of OS after accounting for the effect of %TS-WK8.
Conclusions: An association was found between the extent of TS at week 8 and OS across melanoma pts receiving ipilimumab or nivolumab and NSCLC pts receiving nivolumab. Measuring the extent and timing of TS may have use in predicting potential OS benefits of immune checkpoint inhibitors, however, this observation would need to be evaluated in a prospective well-controlled study.

T-055

Prediction of Human Efficacious Dose of IWP-051, a Novel, Orally Available Soluble Guanylate Cyclase (sGC) Stimulator with Once-Daily Dosing Potential for the Treatment of Cardiovascular Disease

Peter Germano[1,*], Renee Sarno[1], Jim Wakefield[1], Daniel Zimmer[1], Jou-Ku Chung[2], Erik Solberg[2], Nick Perl[1], Joel Moore[2], Maria Ribadeneira[1]

[1] Ironwood Pharmaceuticals, Cambridge, MA, USA; [2] Previously with Ironwood Pharmaceuticals

Objectives: To characterize the efficacy, safety and predicted clinical dose range of IWP-051, a novel sGC stimulator by applying PK/PD modeling
Methods: The pharmacokinetic (PK) profile of IWP-051 was characterized in several species and the PK/pharmacodynamic (PD) profile was evaluated in rats. The PK was described by a one-compartment model with first-order absorption and absorption lag time. A simple, direct effect response curve was used to assess potency of both IWP-051 and the marketed sGC stimulator riociguat (Adempas®). Empirical efficacy scaling and allometric scaling of IWP-051 PK/PD results were then used to predict a human dose response.
Results: In normotensive rats, IWP-051 decreased mean arterial pressure in a sustained and dose–responsive manner for oral doses of 1–30 mg/kg. The blood pressure response equated to an Emax of 34 mmHg and EC50 of 21 μM. For riociguat, an EC50 of 700 nM was estimated in rats using published data and an efficacious human plasma concentration range of 46–174 nM was modeled for the maximum recommended human dose. Adjusting for free fraction (Fu = 0.006), IWP-051 was equipotent to the comparator in rats. Simulation of PK/PD using empirical efficacy scaling and allometrically scaled human PK parameters (Table 1) suggested that 6 mg QD could be the maximum tolerated dose of IWP-051, assuming hypotension is the dose limiting effect.
Conclusions: IWP-051 is a novel sGC stimulator with a PK/PD profile that suggests a median clinical dose of 6 mg once daily would produce the same blood pressure reduction as the marketed maximum dose of the comparator riociguat.

Table 1 Multispecies PK values

Parameter	Mouse	Rat	Dog	Human (predicted)
CI (mL min/kg)	1.6	1	0.2	0.1
Vss (L/kg)	0.35	0.39	0.95	0.67
$T_{1/2}$ (h)	2.3	5.6	5.1	7.5
Oral $T_{1/2}$ (h)	2.8	4.6	6.7	8.1
F (%)	>100	96	45	35

IWP-051 exhibited dose-related oral exposure

References:

1. Chien et al, 2005; The AAPS Journal

T-056

A Model-Based Approach to Describe Olopatadine Itching in Ocular Allergy Patients for a CAC Study

Matthew Fidler[1,*], Abhijit Narvekar[2], Ramesh Sarangapani[1]

[1] Modeling and Simulation and [2] Clinical Development, Alcon Research, Fort Worth, TX, USA

Objectives: Olopatadine is an anti-histamine which reduces the inflammatory response associated with ocular allergies. A PK/PD model was developed to describe the Olopatadine itching response for high dose product (0.77 %), Pataday (0.2 %) and Patanol (0.1 %).
Methods: PK data from single dose Olopatadine 0.1 % (Patanol), 0.2 % (Pataday) and 0.77 % (High Dose) rabbit studies and 7-day Olopatadine 0.77 % QD clinical PK study was modeled by a naive pooled three-compartment model. The three compartments were the highly vascularized tissues (conjunctiva, retina, plasma and choroid), the lens, and the other middle ocular tissues (aqueous humor, cornea, and ICB). The vascularized and middle tissues had both constant elimination and either bolus or first order (aqueous humor) absorption. The lens was in equilibrium with the vascularized tissues and distributed to the middle tissues. Tissue and species differences were predicted based on tissue-specific bioavailabilites, physiological volumes of tissues, and lens/globe surface area scaled clearances.
Itching data (0–4 scale; 0 = no itching) from single dose Olopatadine 0.1, 0.2 and 0.77 % CAC trials was measured at onset of action, 16, and 24 h post-dose and described by a conjunctival concentration

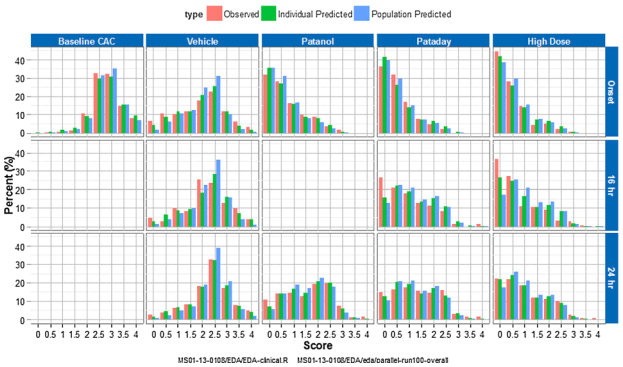

Fig. 1 Olopatadine predicted probabilities versus observed proportions

linked indirect-effect log-odds model of olopatadine's change in itching-score probability.

Results: The PK model was predictive of both human and rabbit concentrations. The subsequent PK/PD model had at most a 19 % under-prediction of itching score which was reduced to 10 % when correcting for individual changes (Fig. 1).

Conclusions: The Model is predictive of the Olopatadine itching response. This model may be used to project ocular itching scores based on different formulation PK properties.

T-057

Translational Modelling of Vemurafenib, Selumetinib and Docetaxel in Metastatic Melanoma with Virtual Tumour Clinical

Frances Brightman[1,*], Hitesh Mistry[1], David Orrell[1], Eric Fernandez[1], Deborah Guest[1], Linda Collins[2], Avinash Gupta[2], Mark Middleton[2], Christophe Chassagnole[1]

[1] Physiomics plc, Oxford, UK; [2] Department of Oncology, University of Oxford, Churchill Hospital, Oxford, UK

The translation of results from animal to man is a key phase in oncology drug development. Being able to determine efficacious doses and when to start taking key biopsy measurements are important for successful evaluation of a new drug within early clinical development. Furthermore, being able to accurately translate combination schedules from mouse to man would provide significant cost savings and accelerate clinical development.

We have developed a mathematical model of a tumour cell population called the Virtual Tumour, which has been used extensively to predict the efficacy of monotherapy or combination treatments in preclinical studies. We have now extended and adapted our preclinical model to predict efficacy in the clinic, thus creating the "Virtual Tumour Clinical". Here we present two sets of results highlighting the translational predictivity of Virtual Tumour Clinical.

We first demonstrate the back-translational capabilities of the model for vemurafenib: the Virtual Tumour was trained to clinical data and used to predict the outcome of xenograft studies. Subsequently we explored forward translation using the model: the Virtual Tumour was trained to preclinical monotherapy data only for docetaxel and selumetinib, and applied to the prediction of efficacy in both arms of a recent phase II trial evaluating the combination versus docetaxel monotherapy.

Virtual Tumour Clinical was able to accurately back-translate the effects of vemurafenib and also made accurate predictions of clinical efficacy in both arms of a phase II trial of docetaxel and selumetinib. Thus, this case study highlights the potential applicability of Virtual Tumour Clinical in translational science.

The results in this abstract have been previously presented in part at PAGE 2014, Alicante, Spain, and published in the conference proceedings as abstract I-32.

T-058

Incorporation of the Time-Dependent Postprandial Increase in Splanchnic Blood Flow into a PBPK Model to Predict the Effect of Food on Oral Propranolol Pharmacokinetics

Rachel H. Rose[1,*], David B. Turner[1], Sibylle Neuhoff[1], Amin Rostami-Hodjegan[1,2], Masoud Jamei[1]

[1] Simcyp Limited (a Certara Company), Sheffield, UK; [2] Manchester Pharmacy School, University of Manchester, UK

Table 1 Predicted and observed fed/fasted state ratio for the area under the plasma concentration curve (AUC) and peak plasma concentration (C_{max}) of propranolol

Study	n	Fed/fasted ratio (geometric mean [range])	
		AUC	C_{max}
Simulated	1	1.28	1.32
Liedholm [3]	11	1.24 (0.29–3.54)	1.40 (0.38–4.62)
McLean [4][a]	8	1.97 (1.30–3.90)	2.29 (1.06–6.54)
McLean [4][b]	8	1.68 (0.70–4.59)	1.48 (0.69–6.28)
Walle [5]	6	1.50 (1.02–1.92)	1.70 (NA)
Meleander [6]	7	1.47 (0.89–2.25)	1.55 (0.97–2.00)
Olanoff [7]	6	1.21 (0.73–1.85)	1.42 (0.48–3.09)

NA Not available

[a] Protein–lipid rich meal

[b] Carbohydrate-rich meal

Objectives: Following a meal, a transient increase in splanchnic blood flow occurs that may result in increased exposure to orally administered high extraction drugs (e.g. propranolol) [1]. We aimed to extend a PBPK model to incorporate this time-dependent change in splanchnic blood flow (TD-QSplanch) and to use the model to predict the food-effect on exposure to orally administered propranolol.

Methods: A PBPK model in Simulink (V2013a) that uses similar structure to the Simcyp minimal PBPK model was extended to incorporate a model describing the post-prandial TD-QSplanch. The model included changes in small intestine and liver blood flows and maintained mass balance in blood flow rates [2]. A PBPK model for propranolol was developed in Simcyp (V13.2) and used to generate the parameter inputs to the Simulink model. Simulations of the fasted and fed state were performed for a single, population representative healthy Caucasian volunteer.

Results: The simulated increase in propranolol AUC and Cmax in the fed state were in reasonable agreement with 6 clinical reports (Table 1).

Conclusions: Incorporation of the TD-QSplanch following a meal resulted in prediction of the food effect on propranolol pharmacokinetics consistent with clinical observation. Future work will integrate the TD-QSplanch model into the Simcyp Simulator to extend predictions to include interindividual variability in the food effect.

References:

1. McLean (1978) Clin Pharmacol Ther, 24:5–10
2. Rose et al., Development of a model of the time-dependent postprandial change in splanchnic blood flow. 9th World Meeting on Pharmaceutics, Biopharmaceutics and Pharmaceutical Technology, Lisbon, Portugal, March 31–4, 2014 (Poster presentation)
3. Liedholm (1990) Eur J Clin Pharmacol 38:469–475
4. McLean (1981) Clin Pharmacol Ther 30:31-–4
5. Walle (1981) Clin Pharmacol Ther 30:790–795
6. Meleander (1977) Clin Pharmacol Ther 22:108–112
7. Olanoff (1986) Clin Pharmacol Ther 40:408–414

T-059

Population PK/PD of Albiglutide

JA Wald[1,*], MA Young[1], R Reinhardt[1], B Budda[2], P Watanalumlerd[3], C Smith[3]

[1] GlaxoSmithKline, Research Triangle Park, NC, USA; [2] Vertex, Inc, Berwyn, PA , USA; [3] PPD, Wilmington, NC, USA

Objectives: Albiglutide, a novel analogue of glucagon-like peptide-1 (GLP-1), maintains the therapeutic actions of GLP-1 by prolonging its duration of action. Subcutaneous injections of 30–50 mg administered once weekly results in significant glycemic improvements in subjects with type 2 diabetes mellitus (T2DM). This population PK/PD analysis was performed using data from four Phase III clinical studies, including patients with a range of renal impairment. Albiglutide PK/PD in patients, the relevance of covariates, and PK/PD information to be factored into patient care were addressed.
Methods: 1,113 subjects receiving albiglutide were included in the PK model (most providing 4 samples). The PD model included 1,327 subjects (active and placebo) with 14–21 glycosylated hemoglobin (HbA1C) and fasting plasma glucose (FPG) samples according the study duration of 1–3 years.
Sequential PK/PD modeling demonstrated that PK was well described by a 1-compartment model with first-order absorption. HbA1C and FPG were described by Emax models with placebo responses. The delayed onset of HbA1C effect is characterized with an effect compartment.

Sparse PK sampling dictated estimation of inter-individual variability only for CL/F defined with an exponential model. Residual variability was characterized with additive and proportional terms. Clinically related covariates (e.g., demographics, eGFR, antibody formation, concomitant medications) and a term to account for changed assay procedures were tested in the model.
Results: The models adequately characterized the PK and PD profiles while providing parameter estimates with acceptable precision (PK prediction corrected VPC with median and 5–95 % CIs and percentiles shown). The population estimate of CL/F was 67 mL/h for typical patient.
No covariates for CL/F were clinically relevant. Whereas, no covariates were identified for albiglutide's effect on HbA1C and FPG, age and sex (FPG only) improved characterization of baseline and glycemic rescue medication use improved characterization of placebo response.
Discussion: Pop-PK/PD modeling provided insight into the use of albiglutide in T2DM patients including those with renal impairment. The parameter estimates were consistent with previous experience and demonstrated no clinically relevant factors which would require dose individualization.

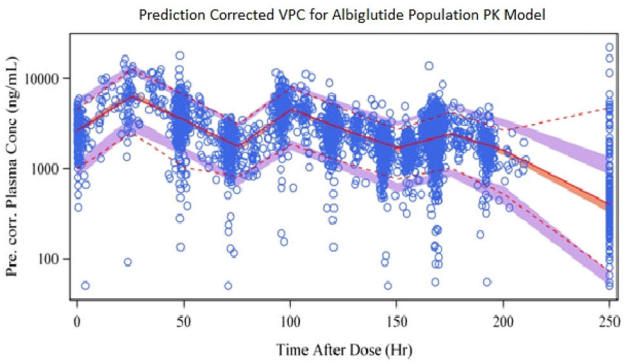

T-060

Population Pharmacokinetic Analysis of Apixaban in Venous Thromboembolism Treatment Patients

Wonkyung Byon[1,*], Kevin Sweeney[1], Charles Frost[2], Rebecca Boyd[1]

[1] Clinical Pharmacology, Pfizer, CT, USA; [2] Clinical Pharmacology, Bristol-Myers Squibb Company, NJ, USA

Objectives: A population pharmacokinetic (PPK) analysis was performed to describe the pharmacokinetics (PK) of apixaban and to characterize the apixaban plasma concentration and anti-Xa activity (AXA) relationship in VTE treatment (VTEtx) patients.
Methods: Based on prior knowledge, a two-compartment PK model was fitted to the observed data with empirical separation of total apparent CL/F into renal (CLR/F) and nonrenal (CLNR/F) components. Covariate identification used a full model estimation approach. The PK-AXA model was developed using the final PPK model in a sequential PK/PD analysis. Analyses were performed using NONMEM 7.2.
Results: The PPK analysis used 8,323 PK observations from 970 healthy (270) and VTEtx (700) subjects, including 459 subjects from AMPLIFY (apixaban 10 mg BID for 7 days followed by 5 mg BID for 6 months) and AMPLIFY-EXT trials (2.5 or 5 mg BID for 12 months). The PK-AXA analysis used 3,139 AXA observations from 795 subjects. Apixaban exposure was adequately characterized by a 2-compartment PPK model with first-order absorption and elimination. The CLR/F and CLNR/F were estimated to be 1.83 and 2.52 L/h, respectively, for a reference VTEtx patient: a 60 year-old, non-Asian, 85 kg male with creatinine-clearance of 100 mL/min. VTEtx patients with mild, moderate, and severe renal impairment had approximately 17, 34, and 56 % higher daily AUC values, respectively, than the reference subject. Age, sex, and Asian race had less than 25 % impact on AUC. The PK-AXA relationship was described by a direct linear model (slope of 0.0159 IU/ng). The table below provides a summary of predicted daily steady-state exposure and AXA values for VTEtx patients by dose.
Conclusions: The PPK and PK-AXA models were successfully developed in VTE treatment. Individual intrinsic and extrinsic factors had a modest effect on apixaban exposure and the direct linear PK-AXA relationship was consistent with a mechanism of action of direct reversible inhibition of FXa.

Table 1 Predicated apixaban steady-state exposure and AXA in VTE Treatment population

Steady state parameters[a] (Units)	2.5 mg BID			5 mg BID			10 mg BID		
	Median (90 % CI)	5th percentile (90 % CI)	95th percentile (90 % CI)	Median (90 % CI)	5th percentile (90 % CI)	95th percentile (90 % CI)	Median (90 % CI)	5th percentile (90 % CI)	95th percentile (90 % CI)
Daily AUC (ng h/mL)	1240 (1185, 1301)	655 (606, 707)	2437 (2240, 2649)	2446 (2346, 2554)	1293 (1197, 1398)	48.7 (4433, 5174)	4649 (4439, 4875)	2456 (2271, 2664)	9136 (8445, 9836)
C_{max} (ng/mL)	67.0 (63.7, 70.7)	29.7 (26.7, 33.1)	153.2 (138.9, 168.4)	132.3 (125.2, 139.3)	58.6 (52.9, 64.7)	302.2 (273.3, 331.9)	251.2 (237.5, 265.2)	111.4 (100.2, 123.2)	572.4 (516.0, 630.1)
C_{min} (ng/mL)	32.0 (29.9, 34.2)	11.0 (9.4, 12.6)	89.5 (79.6, 100.0)	63.2 (59.0, 67.9)	21.78 (18.8, 25.3)	176.5 (156.5, 196.2)	120.2 (112.1, 129.2)	41.1 (35.0, 47.6)	334.5 (295.8, 378.8)
AXa at C_{max} (IU/mL)	1.07 (1.01, 1.12)	0.47 (0.43, 0.53)	2.44 (2.21, 2.68)	2.10 (1.99, 2.21)	0.93 (0.84, 1.03)	4.80 (4.35, 5.28)	3.99 (3.78, 4.22)	1.77 (1.59, 1.96)	9.10 (8.20, 10.02)
AXa at C_{min} (IU/mL)	0.51 (0.48, 0.54)	0.17 (0.15, 0.20)	1.42 (1.27, 1.59)	1.00 (0.94, 1.08)	0.35 (0.30, 0.40)	2.81 (2.49, 3.12)	1.91 (1.78, 2.05)	0.65 (0.56, 0.76)	5.32 (4.70, 6.02)

[a] Represents daily steady state parameters

[b] Patients; received apixaban 2.5 mg BID if they met at least 2 of the following criteria: weight ≤ 60 kg, age ≥ 80 years or serum creatinine ≥1.5 mg/dL

T-061

Evaluation of in Silico Models for Clinical Proarrhythmia Predictions Using Preclinical Knowledge

I.G. Girgis*, J. Rohrbacher, B.P. Damiano, M.K. Pugsley, D.J. Gallacher, P. Nandy

Janssen Research & Development, LLC, South Raritan, NJ, USA

Objectives: The main goal of this work is to evaluate the potential utility of in silico models and assess their performance towards defining the new paradigm in detecting proarrhythmic risk of drugs1.
Methods: In this work, moxifloxacin was used as a test compound since it is usually utilized as a positive control in TQT studies and has known effects on QT interval. Simcyp2 was employed to predict moxifloxacin pharmacokinetics and the Cardiac Safety Simulator2 (CSS) was used to simulate the cardiac effects. Both O'Hara–Rudy and Ten Tuscher models in CSS were used to generate QT profiles, using multiple ionic currents data from in vitro experiments. Using physico-chemical properties and in vitro study settings for moxifloxacin, QSAR models were also evaluated to predict drug mediated ionic current inhibition.
Results: CSS simulations were conducted for a full human left ventricle (HLV) cardiomyocyte string as well as three single HLV cardiomyocyte tissues (epicardium, midmyocardium, and endocardium). Predictions of changes in QT interval using in silico pseudo-ECG of a virtual population and action potential profiles were compared with available clinical and preclinical data for moxifloxacin. The Ten Tusscher model is very stable and does not show any early afterdepolarizations even at very high exposures; however, the O'Hara model did (Fig. 1).
Conclusions: The results show some agreement between in silico and clinical effects of moxifloxacin on QT prolongation. The intra- and inter-variation of the reported IC50 values, the availability of Hill coefficients, and cycle length have varying impacts on the model predictions.

References:

1. CSRC-HESI-FDA Meeting, Rechanneling the Current Cardiac Risk Paradigm: Arrhythmia Risk Assessment During Drug Development Without the Thorough QT Study White Oak Facility, FDA Headquarters, Silver Spring, MD, July 23, 2013
2. Simcyp® (v12) and Cardiac Safety Simulator® (v1.1), Simcyp Limited (a Certara Company

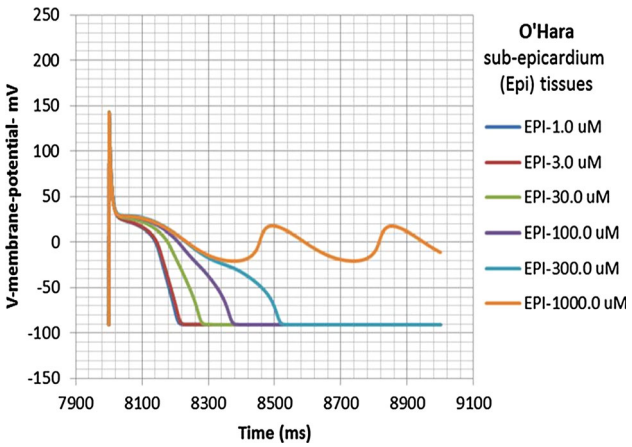

Fig. 1 Subepicardial action potential profiles at different concentrations of moxifloxacin using O'Hara–Rudy model

T-062

Isavuconazole (ISA) Population Pharmacokinetic Modeling from Phase I and Phase III Clinical Trial and Target Attainment Analysis

Amit Desai*, Laura Kovanda, Donna Kowalski, Qaioyang Lu, Robert Townsend

Astellas Pharma Global Development, Inc., Northbrook, IL, USA

Objective: The objective of this analysis was to develop a population pharmacokinetic (PPK) model for ISA, to identify covariates that affect ISA pharmacokinetics (PK) and to determine the probability of target attainment (PTA) over a range of Minimum Inhibitory Concentration (MIC) values.
Methods: Data from 9 phase I studies and one phase III study were pooled from subjects administered single and multiple, oral and intravenous (IV) doses of ISA ranging from 40 to 400 mg. PPK models were developed with NONMEM version 7.2 (GloboMax LLC, Hanover, MD). The covariates examined included various continuous covariates (age, weight, height, lean body mass, body mass index, creatinine clearance, liver function tests), and categorical covariates (race, sex, differences between patients and healthy subjects, CYP3A conmed's). Stepwise covariate modeling (SCM) was performed in PSN by using the forward selection ($\alpha = 0.01$) and backward elimination ($\alpha = 0.001$) method. Area under the curve (AUC) to steady state was calculated for 5,000 simulated patients based on parameter estimates. PTA using the total AUC/MIC ratio estimated from in vivo pharmacodynamics (PD) studies of invasive aspergillosis over a range of MIC values was calculated using Monte Carlo simulations.
Results: A total of 6,363 concentrations records (5,828 from Phase I studies and 535 from Phase III study) from 189 healthy subjects and 232 patients were used. A 2-compartment model with Weibull absorption function and first order elimination process adequately described plasma ISA concentrations. The population mean estimates for clearance (CL) was 2.39 L/h. Asian population had ~40 % decreased total clearance compared to Caucasian population. Peripheral volume of distribution increased with body mass index (BMI). PTA was calculated over a range of MIC values.
Conclusion: A 2-compartment model adequately described the data. No pharmacokinetic differences were noted between patients and healthy volunteers. PTA confirmed the appropriateness 200 mg dose used in Phase III clinical trials.

T-063

Population Pharmacokinetic Modeling of Quetiapine after Administration of SEROQUEL and SEROQUEL XR Formulations to Western and Chinese Patients with Schizophrenia, Schizoaffective Disorder, or Bipolar Disorder

Diansong Zhou*, Khanh Bui, Jianguo Li, Nidal Al-Huniti

Quantitative Clinical Pharmacology, AstraZeneca, Wilmington, DE, USA

Objectives: The objectives of current analysis were to develop a population model describing the quetiapine pharmacokinetics (PK) in Western and Chinese patients following oral administration of immediate release (SEROQUEL) and extended release (SEROQUEL XR) formulations, and to predict quetiapine exposure in Chinese patients after administration of SEROQUEL and SEROQUEL XR.
Methods: The quetiapine population PK analysis dataset contained 4,359 quetiapine plasma concentrations in 127 patients from 5 Phase I

studies with SEROQUEL and/or SEROQUEL XR in Western patients and one Phase I study in Chinese patients with SEROQUEL XR. NONMEM (Version 7.2) was used for the population PK modeling

Results: A one-compartmental model with first-order absorption and first-order elimination adequately described the quetiapine PK. The typical apparent volume of distribution was 574 L, which is within reported values ranging from 513 to 710 L [1, 2]. The typical elimination rate was 0.12 h^{-1}, and the typical apparent oral clearance was 69 L/h, which is also in close agreement with reported values 55–87 L/h [1, 2]. The typical absorption rate constants were 1.46 and 0.10 h^{-1} for SEROQUEL and SEROQUEL XR formulations, respectively. The effect of age on elimination rate of quetiapine was the only covariate identified in the covariate search. The simulation conducted with final quetiapine population PK model predicted that 200 mg twice daily dose of SEROQUEL in Chinese patients would achieve steady-state AUC (AUCss) (±standard deviation) of 3,087 ± 1,480 ng/mL h, which is in close agreement with the reported value (3,538 ± 1,728 ng/mL h) [1].

Conclusions: The quetiapine population PK model adequately described the clinical data observed in Western and Chinese patients. The model predicted that the once-daily administration of 300 mg SEROQUEL or SEROQUEL XR would achieve similar exposure in terms of AUCss in Chinese patients.

References:

1. Li et al. Acta Pharmacol Sin 2004;25(3):390–4Li et al. Acta Pharmacol Sin 2004;25(3):390–4
2. Mauri et al. Clin Pharmacokinet 2007;46(5):359–88

T-064

Model Based Meta-analysis of Montgomery-Åsberg Depression Rating Scale (MADRS) in Major Depressive Disorder (MDD) Patients

Diansong Zhou, Khanh Bui, Nidal Al-Huniti, Donald Stanski

Quantitative Clinical Pharmacology, AstraZeneca, Wilmington, DE, USA

Objectives: Many approved antidepressants failed to demonstrate superiority in clinical trials due to the significant placebo response [1]. The purpose of current analysis was to evaluate the time course of antidepressants in treatment of MDD through longitudinal modeling [2], to characterize the placebo response and drug effect and to guide internal decision making.

Methods: A PubMed search was conducted to obtain clinical trials for antidepressive agents published after 2010. Only randomized, placebo-controlled studies in MDD patients with reporting MADRS above 30 at baseline were included. A total 21 published clinical trials with 58 arms for 12 antidepressants representing 10,231 patients and 2 internal clinical studies with 6 arms and 450 patients were included in the final analysis. An empirical exponential model that varied in time was applied to describe depression effect and was implemented in NONMEM 7.2.

$$Response_i = (BASL + \eta 1) + (PE + \eta 2 + \eta 3/\sqrt{n}) * \left(1 - e^{-k*\exp(\eta 4)*t}\right) + \varepsilon/\sqrt{n}$$

where BASL is the baseline score and PE is a parameter describing the magnitude of placebo/drug effect; η1, η2 and η4 accounts for between study variability, η3 accounts for between arm variability and ε is the residual error.

Results: The baseline MADRS score was estimated to be 31.9 (1.2 % RSE) for MDD clinical trials. The estimated magnitude of placebo response was −13.7 (4.5 % RSE) while the magnitudes of drug effect were in the range of −14.5 and −21.2. The trial simulations indicated certain established drugs (such as duloxetine, venlafaxine) demonstrated superior drug effect over placebo, while the other drugs (such as bupropion and AZ internal compound) failed to show efficacy over the placebo response (figure below).

Conclusions: The meta-analysis of a longitudinal model permitted a good fit to the antidepressive effect in MDD patients. The analysis has been used to guide a more informed decision making.

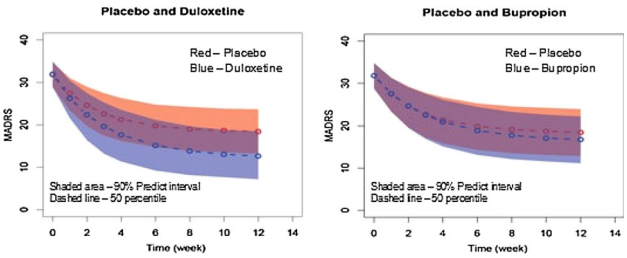

References:

1. Turner et al. N. Engl. J. Med. 2008, 358, 252–260
2. Ahn and French J Pharmacokinet Pharmacodyn. 2010, 37, 179–201

T-065

SMARTR (Shiny Meta-analysis Research Tool Using R): A Browser Based Meta-analysis Visualization Tool Using R Shiny

Jinzhong Liu[1,*], Timothy Nicholas[2], Jing Liu[2], Kaori Ito[2], Tina Checchio[2], Sima Ahadieh[2], David Flockhart[1] and Brian Corrigan[2]

[1] Division of Clinical Pharmacology, Indiana University School of Medicine, Indianapolis, IN, USA; [2] Pfizer Inc., Groton, CT, USA

Objectives: "Shiny" is an R package developed by the Rstudio team that allows development of interactive web applications to visualize and summarize data. The result is an application that can utilize all the power of R programming and packages, but does not require the end users to have or use R. A web application was created for data visualization and summarization of standard types of literature based datasets used in model based meta-analyses.

Methods: Literature summary datasets were collected from various therapeutic areas. Two R scripts (ui.R and server.R) were prepared that allowed reactivë relations between inputs and outputs in the shiny package. Useful R packages such as "ggplot2" and "metafor" were also incorporated. The scripts were placed on an R server to allow a user link to be developed that could be shared with non-R users.

Results: Using only R code contained in two scripts, data from any user-uploaded file can be summarized and visualized (Fig. 1 shows the user interface of the web application, https://jzliu.shinyapps.io/SMARTR/). Once the user selects the variables, including time, treatment, dose and endpoint, the plots of endpoint versus time or dose by treatment or by dose are available to view or download. Commonly used visualizations such as dynamic plots, by study plots and linear regression analysis, can also be obtained. In addition, forest plots utilizing the "metafor" package can be automatically obtained.

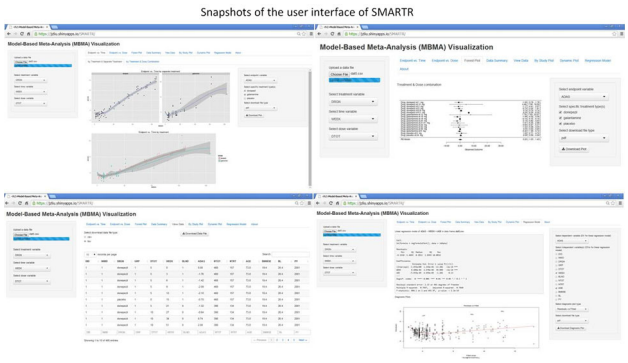

Fig. 1 Subepicardial action potential profiles at different concentrations of moxifloxacin using O'Hara–Rudy model

The application can be used with different datasets without the user ever needing to refresh the web page.
Conclusions: SMARTR is a shiny-based interactive web application that makes data visualization, summarization and basic data plotting easy for non-R users. The R code used and made available at the link above may also be useful for use in developing other types of modeling dataset web applications.

T-066

Exposure–Response Modeling and Power Analysis of ACR Core Components in Rheumatoid Arthritis

Yi Zhang, Lian Ma*, Ping Ji, Sarah Yim, Suresh Doddapaneni, Jiang Liu, Rekic Dinko, Satjit Brar, Yaning Wang, Chandrahas Sahajwalla

Food and Drug Administration, Silver Spring, MD, USA

Objectives: Rheumatoid Arthritis (RA) is a chronic inflammatory disease with autoimmune disorders and predominantly joint manifestations. Efficacy endpoints commonly used in RA clinical trials, such as American College of Rheumatology (ACR) score (ACR20, ACR50, ACR70) and Disease Activity Score using 28 joints (DAS28), are composite scores and are often criticized as not being sensitive measures to detect differences between doses and products. In this study, subcomponents of ACR, including tender-joint count (TJC), swollen-joint count (SJC), and improvement in three of the five (3/5) remaining ACR core measures (patient/physician global assessments, pain, disability and acute-phase reactant), were evaluated with Exposure–response modeling and sensitivity analysis.
Methods: The data sets were extracted from 8 clinical trials for four approved RA drugs (N = 3,013). All trials were randomized, double-blind, placebo-controlled studies in RA patients with methotrexate (MTX) background therapy. For each drug, an exposure–response modeling on the subcomponents of ACR scores was conducted with the pooled dataset using sequential PK/PD approach in NONMEM VII. Relative sensitivity of these endpoints was assessed using power analysis based on trial simulation.
Results: Empirical Bayesian estimates for individual PK parameters were obtained from population PK modeling and then fixed for PD estimation. The probabilities of three subcomponents in ACR20, ACR50 or ACR70 were modeled with logistic regression combining the mechanism-based indirect-response drug model with empirically exponential-decaying placebo/MTX effect. None of the covariates evaluated significantly contributed to between-subject variability. The trial simulation and subsequent power analysis showed that ACR20 subcomponents (TJC/ACR20, SJC/ACR20, 3/5/ACR20) had the highest power in distinguishing active treatment versus placebo in 8/12 comparisons at evaluated dosing regimens, and among these 8 comparisons, relative sensitivity of 3/5/ACR20 was higher than the other two ACR20 subcomponents.
Conclusions: The developed exposure–response models adequately described the relationship between drug concentrations and ACR subcomponents. ACR20 subcomponents, especially 3/5 response, appeared to be more sensitive in evaluating treatment effect in RA.
Disclaimer: The views expressed in this abstract are those of the authors and do not necessarily reflect the official views of the FDA.

T-067

An Integrated Disease-Progression Model of Cognitive and Biomarker Endpoints in Alzheimer's Disease

AL Quartino[1,*], DG Polhamus[2], J Rogers2, JY Jin[1]

[1] Genentech, South San Francisco, CA, USA; [2] Metrum Research Group, Tariffville, CT, USA

Objectives: Progression in Alzheimer's Disease (AD) manifests as changes in biomarker and cognitive endpoints. The aim is to establish a disease-model integrating multiple endpoints for AD.
Methods: The analysis included 298 mild AD patients (baseline MMSE 20–26) from the Alzheimer' s Disease Neuroimaging Initiative database [1]. Longitudinal changes up to 3 years in CDR, ADAS-cog12 and volumetric MRI were modeled. The model was based on a previous disease model [2] and estimated using OpenBUGS v.3.2.2.
Results: The model for mild AD patients linked the nine endpoints via a latent "disease status" variable that evolves linearly over time according to patient-specific rates, controlled by APOE4 status and baseline MMSE. The model correctly identifies healthier patients with slower progression rates with an increase of baseline MMSE, and more rapid disease progression in APoE4 positive patients. Residual likelihoods were best described by multinomial for CDR, lognormal for volumetric MRI, and beta distributed for ADAS-cog [3].
Model simulated 2-year disease progression (90 % credible intervals) are: ADAS-cog12, 42.3 (35.9–49.9) %; CDR-SOB, 93.3 (81.0–107.8) %; hippocampal volume, −7.6 (−8.8–6.6) %; and ventricular volume as 24.0 (21.4–26.9) %. These are consistent with observed two-year rates; 38.5 % ADAS-cog12, 85.2 % CDR-SOB, −7.8 % hippocampal volume, and 23.0 % ventricular volume, confirming the adequacy of the model.
Conclusion: We developed an integrated disease-progression model, quantifying the interaction between nine endpoints and covariates relevant to AD. Such models, compared to single endpoint disease models, may provide greater insight of the drug and covariate effects on disease; the sensitivity of the different endpoints in subpopulations; and permits trial simulation of multiple endpoints with an appropriate joint distribution, useful for multi-endpoint decision criteria.

References:

1. www.loni.ucla.edu/ADNI
2. Polhamus et al. Clinical Dementia Rating Modeling and Simulation: Joint progression of CDR and biomarkers in the ADNI cohort. AAIC 2013
3. Rogers et al. Combining patient-level and summary-level data for Alzheimer's disease modeling and simulation: a beta regression meta-analysis. JPKPD 2012

T-068

Impact of Sampling Time Deviations on the Prediction of AUC Using Limited Sampling Strategies

S Sarem[1,2], F Nekka[1,3,4], I.S. Ahmed[5], C Litalien[2,6,7], J Li[1,3,4,*]

[1] Faculty of Pharmacy, Univ. Montreal, Montreal, QC, Canada; [2] Clinical Pharmacology Unit, CHU Ste-Justine, Montreal, QC, Canada; [3] Centre de Recherches Mathematiques, Univ. Montreal, Montreal, QC, Canada; [4] Centre for Applied Mathematics in Biosciences and Medicine, McGill Univ., Montreal, QC, Canada; [5] College of Pharmacy, Univ. Sharjah, Sharjah, United Arab Emirates; [6] Dept. of Pediatrics CHU Ste-Justine, Montreal, QC, Canada; [7] Dept. of Pharmacology, Univ. Montreal, Montreal, QC, Canada

Objectives: Accumulating evidence supports the usefulness of the area under the concentration–time curve (AUC) in performing therapeutic drug monitoring of cyclosporine (CsA). Regression limited sampling strategy approach (R-LSS) can allow estimating AUC with precision and accuracy. However, irregularity in collecting blood samples may have an important impact on R-LSS prediction. We aim here to study this impact for different scenarios of sampling time deviations (STD).

Methods: To have a complete and rational investigation, simulated concentration–time PK profiles are used to mimic diverse STD scenarios. Three types of sampling scenarios were discussed, namely fixed, random, and mixed STD. In addition, the sensitivity of AUC estimation by R-LSS to occasional errors in each single sampling time point separately was evaluated.

Results: Our investigation clearly proved an important impact of STD on the performance of R-LSS. This impact depends on the number of LSS sampling points and more importantly on the whole duration of the sampling process. In addition, errors at sampling time points where the concentration changes rapidly were relatively more critical for the prediction of AUC. Moreover, by considering the additional criterion of their tolerance to STD, we were able to differentiate R-LSS that share similar performance at nominal times. Nomograms, determining ranges of fixed and random STD, were proposed to illustrate different degrees of R-LSS tolerance to STD.

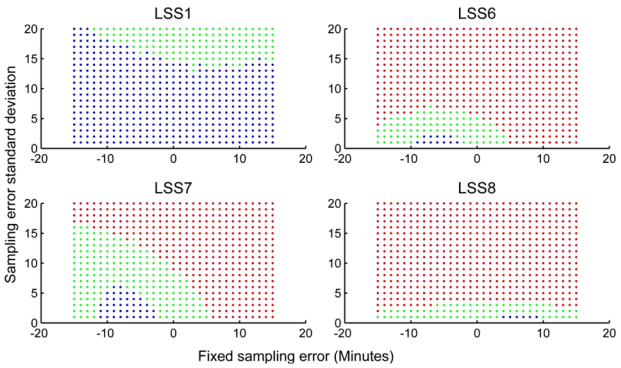

Fig. 1 Nomograms for various combinations of random and fixed STD for selected four R-LSS (LSSl: $C_{0.5}$, C_2, C_4, C_8, LSS6: C_0, $C_{1.5}$, C_4, LSS7: C_0,C_2, C_4, and LSS8: C_0,C_1 C_4) used for PO CsA AUC prediction in pediatric hematopoietic stem cell transplantation (HSCT). LSS1 had the best tolerability to STD. LSS7 had a better tolerability than LSS6 and LSS8 even though these three LSS share similar performance at nominal times. Red dot for 95th PAE% more than 20 %, green dot equal or less than 20 %, and blue dot equal or less than 15 %, 95th PAE% is 95th percentile of a absolute values of prediction errors

Conclusions: To be more reliable, the use of R-LSS can benefit from the knowledge of the impact of STD on their performance to predict AUC. STD nomograms can be used as informative tools for the selection and use of R-LSS Fig. 1.

T-069

Population Pharmacokinetic Modeling of Idelalisib, a Novel PI3Kdelta Inhibitor, in Healthy Subjects and Patients with Hematologic Malignancies

Feng Jin*, Yuying Gao, Huafeng Zhou, Lorna Fang, Xiaoming Li, Srini Ramanathan

Gilead Sciences, Foster City, CA 94404, USA

Background: Idelalisib is a potent PI3Kdelta inhibitor that demonstrated efficacy in monotherapy and combination-therapy clinical studies in hematologic malignancies. The objective of this analysis was to develop a population pharmacokinetic model for Idelalisib and its inactive metabolite GS-563117, and to evaluate the impact of covariate on Idelalisib/GS-563117 PK.

Methods: Data from phase I studies in healthy volunteers (n = 137) and phase I/II studies in patients with hematologic malignancies (n = 599) were included in this analysis. Data were analyzed using NONMEM 7.1.2 with first order conditional estimation allowing for interaction (FOCE-I). Stepwise forward addition followed by backward elimination was implemented in the covariate (age, gender, race, body weight, baseline CLcr, AST, ALT, disease status, and type of cancer) model building process to develop final PopPK model. Various model assessment methods were used to evaluate the model performance.

Results: Idelalisib plasma PK was best described by a two-compartment model with first-order absorption, first-order elimination from the central compartment and a lag time. A nonlinear relationship between dose and relative bioavailability (F1) was included in the final model. Two covariates were identified in the model building process and were incorporated into the final model: health status (healthy vs. patient) on CL/F and Q/F, and body weight on CL/F. Typical Idelalisib PK parameters are summarized in Table 1. The typical half-life of Idelalisib was 8.2 h. Although a statistically significant relationship was observed between body weight and Idelalisib PK parameters, the effect of body weight was weak, as evidenced by minor changes of steady-state exposure (Ctrough:16 %; AUC and Cmax:10 %) for a patient with extreme body weight (5th and 95th

Table 1 Idelalisib population PK parameters

PK parameters	Estimate	Inter-individual variability (%)
CL/F (L/h)		
Patient	14.88	38.21
Healthy volunteer	19.69	
Q/F (L/h)		
Patient	11.82	38.86
Healthy volunteer	7.846	
V_c/F (L)	22.65	85.15
V_p/F (L)	72.97	73.35
k_a (h^{-1})	0.482	38.34
Residual variability as coefficient of variation (%)	53.48	–

percentile) relative to the typical patient, and not considered to be clinically relevant.
Conclusions: A two-compartment model with first-order absorption, first-order elimination from the central compartment and a lag time adequately described the population pharmacokinetics of Idelalisib. There were no covariates that had a clinical meaningful impact on Idelalisib exposure.

T-070

A Population Pharmacokinetic (PPK) Model of Memantine in Pediatric Patients with Autistic Spectrum Disorder (ASD)

Timothy J Carrothers*, Antonia Periclou, Tatiana Khariton, Parviz Ghahramani

Forest Research Institute, Jersey City, NJ, USA

Objectives: (1) Characterize the pharmacokinetics of memantine; (2) simulate exposures in pediatric patients with ASD; (3) ensure that the weight-based dosing used in ASD efficacy/safety trials resulted in AUCs with at least a 10-fold safety margin over the animal toxicology.
Methods: Data from 12 clinical studies (9 conducted in healthy adult subjects, 18–45 years and 3 in ASD patients, 5–16 years) were pooled for the analysis. ASD patients were stratified by weight group (A: ≥60 kg; B: 40–59 kg; C: 20–39 kg; and D: <20 kg). Previous PPK analyses [1, 2] informed model development.
Daily AUCss were calculated and compared to the value of 2,100 ng h/mL, which represents a 10-fold safety margin. Population simulations of AUCss were conducted to determine the percentage of subjects expected to exceed the 10-fold safety margin using the weight based dosing described in Methods.
Results: A two-compartment open model with first-order absorption and elimination and lag time in absorption adequately described the observed data. Formulation impacted absorption rate, lag time, and relative bioavailability. Weight, the only demographic covariate in the model, was prespecified based on earlier PPK analyses 1, 2 (Table 1).

Table 1 Parameter estimates for population pharmacokinetic model

Parameter	Estimate (95 % CI)	IIV (%CV)
CL/F, typ (L/h)	6.96 (6.66–7.26)	20.9
V2/F, typ (L)	501 (482–520)	16.4
Q/F (L/h)	0.83 (0.17–1.49)	n.e.
V3/F (L)	37 (27–47)	n.e.
Ka-IR, typ (h^{-1})	1.17 (0.82–1.52)	61.5
Ka-ER, typ (h^{-1})	0.0819 (0.067–0.097)	
ALAG-IR (h)	0.792 (0.75–0.83)	n.e.
ALAG-ER (h)	1.69 (1,62–176)	n.e.
F-IR (−)	1 (Fixed)	n.e.
F-ER (−)	0.927 (0.86–0.99)	n.e.

ALAG absorption lag time, *CI* confidence interval, *CL/F* oral plasma clearance, *CV* coefficient of variation, *ER* extended release, *F* oral bioavailability, *IR* immediate release, *IIV* interindividual variability, *Ka* absorption rate constant, *n.e.* not estimated, *Q* inter-compartmental clearance, *V2/F* apparent volume of distribution of central compartment, *V3/F* apparent volume of distribution of peripheral compartment

Based on the recommended doses in ASD patients, ie 15, 9, 6, and 3 mg/day of an extended-release capsule for Groups A, B, C, and D, respectively, only one patient in Group A and one in Group B had an estimated safety margin slightly less than 10 9-fold).
Simulation of AUCss at various weight ranges demonstrated that less than 1 % of patients for Groups B, C, and D and 5 % for Group A were predicted to exceed the AUC of 2,100 ng h/mL based on the proposed doses.
Conclusions: The PPK analysis and simulations confirmed the appropriateness of the weight-based dosing in pediatric patients with ASD.

References:

1. Periclou A and Ghahramani P. ACoP 2011
2. Findling RL et al. J Child Adolesc Psychopharmacol 2007;17 (1): 19–33

T-071

Population Pharmacokinetic Modeling of Combination Treatment of Intravenous Ceftazidime and Avibactam

Carrothers, T.J.[1,*], Green, Michelle[2], Chiu, Joannellyn[2], Riccobene, Todd[1], Lovern, Mark[2]

[1] Forest Research Institute, Jersey City, NJ, USA; [2] Quantitative Solutions, Menlo Park, CA, USA

Objectives: Establish population pharmacokinetic (PopPK) models for avibactam (AVI) and ceftazidime (CAZ) in complicated urinary tract infection (cUTI) and complicated intra-abdominal infection (cIAI) patient populations, including a quantitative description of the impact of renal impairment and other intrinsic/extrinsic factors.
Methods: Data from ten Phase 1 and two Phase 2 studies were used to establish the PopPK models. For AVI, this included subjects with a range of renal function down to end-stage renal disease, as well as septic subjects with augmented renal function. For CAZ, literature data on subjects with impaired renal function was used to supplement the CAZ PopPK modeling, as the CAZ-AVI development program did not include appreciable data on CAZ in subjects with moderate (or worse) renal impairment. The first-order conditional estimation with interaction (FOCE-I) method in NONMEM was used for implementation of all PopPK models.
Results: CAZ PK following IV dose administration was well described by a two-compartment model with first-order elimination from the central compartment. The primary predictors of variability in CAZ PK were identified to be subject status (cIAI or cUTI patients vs. healthy subjects), creatinine clearance (CrCL), and body weight. AVI PK following IV dose administration was well described by a two-compartment model with first-order elimination from the central compartment. The primary predictors of variability in AVI PK were identified to be subject status (cIAI or cUTI patients vs. healthy subjects), renal function category (i.e., end-stage renal disease [ESRD] and augmented renal clearance [ARC]), CrCL (for non-ESRD and non-ARC subjects), and body weight. There was no pharmacokinetic interaction between CAZ and AVI.
Conclusions: Population pharmacokinetic models for CAZ and AVI were established with a quantitative description of the impact of renal impairment, subject status, and body weight, enabling future support of exposure–response explorations for the Phase 2 studies as well as establishing a basis for future target attainment simulations in the cIAI and cUTI subject populations.

T-072

Relationship of Levomilnacipran Exposure to Anti-depressant Effect

Carrothers, T.J.[1,*], Green, Michelle[2], Kastrissios, Helen[2], Bax, Leon[2], Chen, Laishun[1], Khariton, Tatiana[1], Ghahramani, Parviz[1]

[1] Forest Research Institute, Jersey City, NJ, USA; [2] Pharsight Corporation, Sunnyvale, CA, USA

Objectives: To determine whether the level of levomilnacipran exposure relates to effect, as assessed by reduction in Montgomery-Åsberg Depression Rating Scale, Clinician Rated (MADRS-CR) score in the treatment of patients with major depressive disorder (MDD).
Methods: Data for the exposure–response modeling consisted of pooled data from three placebo-controlled parallel arm Phase 3 studies (one fixed-dose, two flexible-dose), with 1,528 patients with MDD. A population exposure–response approach explored both linear and nonlinear relationships in the longitudinal dataset, utilizing estimates of exposures derived from individual predictions obtained in a pooled Phase 1/Phase 3 population pharmacokinetic analysis [1].
Results: The final model for MADRS-CR consisted of terms representing baseline MADRS-CR, a time-varying placebo effect, a time-invariant drug effect, and residual variability. The typical baseline estimate was 35.9 points for MADRS-CR score with inter-subject variability of 3.0 %. The magnitude of the placebo effect increased over time to a typical maximum of −12.6 points, reaching 50 and 90 % of the maximum at 1.4 and 4.6 weeks, respectively. Changes in MADRS-CR showed a statistically significant linear relationship with exposure, specifically, two-week lagged MADRS-CR relative to steady-state area-under-the-curve (AUCss). This was superior to a model utilizing concurrent AUCss, a finding that agrees with the clinical understanding of the delayed onset of drug effect in the treatment of depression. The model-predicted placebo-adjusted change in MADRS-CR for typical exposures was −3.25 points following maintenance treatment with the maximum therapeutic dose of 120 mg levomilnacipran once-daily.
Conclusions: This analysis demonstrated a statistically significant relationship between levomilnacipran exposures and placebo-adjusted change from baseline MADRS-CR (the main measure of anti-depressant effect), supporting up-titration to 120 mg

References:

1. Carrothers, TJ, et al. Population Pharmacokinetic Model for Levomilnacipran in Healthy Subjects and Patients with Major Depressive Disorder. Poster presented at ACoP 2013

W-001

Improved Dose Selection Rationale Using PKPD Relationships Derived from Discrete Clinical Data

Helen H. Usansky*

ClinPharm Pro, LLC, New York, NY, USA

Objectives: Biological response to exogenous stimulation can be bistable, which manifests as either low or high activity stages or all-or-none reactions. In such cases, using a graded response to describe the process can be inadequate even when the response is somewhat "continuous". In the following two case studies, hepatic toxicity and treatment success data were converted to binominal data and their PKPD relationships were evaluated.
Methods and Results: *Case 1* In a first-in-man study, 40 cancer subjects received Drug A once-daily (5–600 mg) for 2–3 cycles. A few subjects developed mild to moderate elevation of liver transaminases. The relationship between Drug A exposure and ALT elevation data were evaluated using both Emax model (ECmax, EAUC) and logistic regression (Grade 1 or 2 elevation). No significant trends were detected with the Emax model. In contrast, logistic regression showed that Drug A exposure was related to a higher probability of ALT elevation when Cmax ≥500 ng/ml and AUC ≥4,000 ng h/ml. This finding was in agreement with clinical outcomes in a later clinical trial.
Case 2 In an early phase clinical trial, 18 subjects with severe anemia received Drug B (2–10 mg) once daily for 14 days. Within the 2-week treatment period, 4 subjects showed clinical treatment success (hemoglobin (Hb) ≥11 g/dl or ΔHb ≥1 g/dl). PKPD analyses were performed using both continuous and discretized Hb data. With continuous PD data, no significant relationships were detected between PK exposure and the Hb or other PD biomarker data. The outcomes from logistic regression, however, indicated that Cmax <500 ng/ml and AUC <4,000 ng h/ml were sub-clinical while Cmax >1,000 ng/ml or AUC >8,000 ng h/ml could lead to treatment success in the majority of subjects.
Conclusions: Clinical data sometimes are better described qualitatively rather than quantitatively. This is probably attributed to the bistable nature of biological reactions. Discretized PD data can be valuable in establishing clinically meaningful PKPD relationships and in guiding clinical dose selection.

W-002

Dose Finding Based on the Model Averaging Approach

Dinko Rekić[1,*], Jeffry Florian[1], Lars Johannesen[1,2], Liang Zhao[1], Satjit Brar[1]

[1] US Food and Drug Administration, Silver Spring, MD, USA; [2] Karolinska Institutet, Stockholm, Sweden

Objectives: To compare the estimated dose-effect based on the model averaging approach (MA), linear (LFE) and nonlinear (NFE) fixed effects modeling.
Methods: Data from 6 phase II and phase III trials of drug X was pooled. The dataset, denoted as the true dataset, consisted of seven doses and 7,505 total observations (min–max: 145–3,793 observations per dose). The true dataset was sampled with replacement creating 1,000 datasets with 100 subjects per dose. The lowest dose above a predefined threshold was defined as the "right dose". MA, LFE and NFE modeling was applied to each dataset. Using the estimated variance-covariance matrix 1,000 trials were simulated for method. Estimates of the effect (mean and 90 % CI) for each dose, bias and precision, as well as the probability of finding the "right dose" were computed for each method.
Results: The "right dose" was identified correctly in 49 % of the cases using LFE modeling (LS means obtained from ANOVA), compared to 62 and 71 % for NFE modeling and MA, respectively.
Conclusions: Given the current monotonic shape of the dose–response curve used for these analyses, model identification heuristics and MA approach applied, NFE and MA resulted in an increased probability to identify the "right dose", as defined in this investigation. Choice of method for analyzing dose-finding studies may greatly influence probability of identifying the "right dose".
Disclaimer: The views expressed in this here are those of the authors and do not necessarily reflect the official views of the FDA.

W-003

Population Pharmacokinetics of Tenofovir in HIV-1 Uninfected Members of Sero-discordant Couples and Effect of Dose Reporting Methods: An Analysis from the Partners PrEP Study

Y. Lu[1], V. Goti[2], A. Chaturvedula[2,*], J. E. Haberer[3], M. J. Fossler[4], M. E. Sale[5], D. Bangsberg[3], J. Baeten[6], C. Celum[6], C. W. Hendrix[1]

[1] The Johns Hopkins University School of Medicine, Baltimore, MD, USA; [2] Mercer University, Macon, GA, USA; [3] The Massachusetts General Hospital/Harvard Medical School, Boston, MA, USA; [4] GlaxoSmithKline, King of Prussia, PA, USA; [5] Next Level Solutions Inc., Fresno, CA, USA; [6] University of Washington, Seattle, WA, USA

Objectives: To develop population pharmacokinetic models of tenofovir to evaluate the effect of different dose reporting methods.
Methods: Data from the Partners PrEP Study (a phase III, randomized, double blind, placebo-controlled, three-arm clinical trial of daily oral tenofovir and emtricitabine/tenofovir) and ancillary adherence substudy was used. Patient-reported dosing information (PRDI) was collected in the main trial (404 subjects associated with 1,278 concentration records), and medication event monitoring system (MEMS®)-based adherence was also collected in the adherence substudy (211 subjects associated with 327 concentration records). Population pharmacokinetic analysis was conducted using NONMEM (7.2, FOCEI) with PRDI with steady-state assumption or PRDI substituted with MEMS® records where available.
Results: A 2-compartment model with first-order absorption was the best model from both modeling approaches with a need of lag time when including MEMS® based dosing records in analysis. Model diagnostics were acceptable. Age, body weight and creatinine clearance were significant covariates on clearance but only creatinine clearance was retained in the final model. Final model parameters along with bootstrap results are provided in Table 1. Although the point estimates parameters differed with varying degrees (8–35 %), bootstrap confidence intervals were widely overlapping.

Table 1 Final model parameters with bootstrap results

Parameter	PRDI only dataset			PRDI + MEMS® dataset		
	Base model Mean (%RSE)	Final model Mean (%RSE)	Bootstrap Median (95 % CI)	Base model Mean (%RSE)	Final model Mean (%RSE)	Bootstrap Median (95 % CI)
OFV	9,965.62	9,912.71	NA	9,915.52	9,852.25	NA
CL (L/h)	55	57 (2)	58 (52–61)	58 (2)	62 (2)	62 (57–66)
Vc (L)	478	393 (14)	393 (109–653)	518 (14)	345 (10)	345 (211–692)
Ka (/h)	2.21	4.7 (77)	4.7 (1.46–128.15)	1.5 FIX	1.5 FIX	1.5 FIX
a (L/h)	167	178 (18)	178 (90– 227)	187 (17)	231(9)	231 (125–335)
Vp (L)	667	614 (10)	614 (523–869)	735 (18)	830 (10)	830 (612–1,102)
ALAGl (h)	NA	NA	NA	0.37 (22)	0.41 (18)	0.41 (0.30–0.67)
CrCI on CL	NA	0.38 (12)	0.38 (0.29–0.44)	NA	0.38 (13)	0.38 (0.27–0.49)
IIV on CL (ω^2)	0.0379	0.02 (9)	0.02 (0.02–0.03)	0.04 (3)	0.03 (14)	0.03 (0.02–0.04)
IIV on Vc (ω^2)	NA	NA	NA	0.19 (51)	0.06 (119)	0.06 (0.05–0.38)
IIV on Ka (ω^2)	NA	NA	NA	0.48 (71)	0.37 (29)	0.37 (0.20–0.67)
IIV on ADD (ω^2)	1.73	2.03 (12)	2.03 (1.18-2.68)	0.86 (14)	1.85 (11)	1.86 (1.07–2.39)
Residual variability						
Additive (SD) (ng/ml)	30	28 (9)	28 (22–40)	41 (7)	30 (8)	30 (23–41)
Proportional (%CV)	21	21 (7)	21 (11–25)	14 (22)	20 (5)	20 (12–25)

Conclusions: Tenofovir population pharmacokinetic parameter estimates were comparable (CI, %RSE, residual variability) between two modelling approaches. These findings indicate that the PRDI was sufficient for population pharmacokinetic model development in this study. Partners PrEP study had very high levels of adherence (99.1 % by unannounced pill counts and 97.2 by MEMS®) and may not have had sufficient non-adherence to test the effect of MEMS® based dosing records on improving model estimates.

References:

1. Haberer, J.E., et al., PLoS Med, 2013. 10(9): p. e1001511

W-004

Reproducible and Automated Pharmacokinetic Study Report Using R and LaTeX

Hye Min Wang, Yong-Jin Im, Eun-Young Kim, Ji-Young Jeon, Changyun Jin, Min-Gul Kim*

Clinical Trial Center and Biomedical Research Institute, Chonbuk National University Hospital, Jeonju, Republic of Korea

Objectives: Trustworthy pharmacokinetic study reports have to be reproducible. The objective of our study was to develop the reproducible pharmacokinetic study reporting application. We also aimed for users who do not know R language to use the application by simplify instruction.
Methods: The main tools we developed are the R language using the lmer4, Hmisc, ggplot2, and knitr packages. For document formats, we mainly used LaTeX. Subject data listings and pharmacokinetic tables were made by Hmisc, lmer4 package. The application computes non-compartmental analysis, analysis of variance and 90 % CI. The plots for visualizing data are made by ggplot2 package. The application generated the LaTeX and PDF formatted report. This also provided outputs (.xlsx, .png) for users to modify their report. All of the works are performed at a time and automatically generate the pharmacokinetic study report.
Results: The application takes advantage of reducing the time and errors to complete pharmacokinetic study report for regulatory submissions by FDA and ICH. We also have tested that all results to be the same as those generated by commercial software.
Conclusions: Our reproducible pharmacokinetic study reporting application will significantly shorten the time and improve quality of pharmacokinetic reports leading to reduced effort of pharmacokinetic scientists.

References:

1. Din Chen and Karl E. Peace (2010). Clinical Trial Data Analysis Using R, Analysis of Bioequivalence Clinical Trials (p. 257–298), CRC Press
2. Yihui Xie (2013), Dynamic Documents with R and knitr, CRC Press
3. Winston Chang (2012), R Graphics Cookbook Practical Recipes for Visualizing Data, O'Reilly Media
4. ICH Topic E9, Statistical principles for clinical trials, 1998
5. ICH Topic E3, Structure content of clinical study reports, 1995
6. FDA, Guidance for Industry: Bioavailability and Bioequivalence Studies for Orally Administered Drug Products, 2006
7. FDA, Guidance for Industry: Statistical approaches to establishing bioequivalence, 2001

W-005

Effect of Body Temperature on QT Interval: Decoupling of Indirect and Direct Effect of Sylatron

Azher Hussain*, Matt S. Anderson, David Cutler, Ilias Triantafyllou, Harold Bernstein, Pravin Jadhav

Merck and Co., Inc., White House Station, NJ, USA

Objectives: Traditional E14 and concentration-QT (CQT) modeling indicated a potential for QT interval shortening after PEG-interferon (Sylatron) administration. With exploratory analysis and mechanistic reasoning, it was hypothesized that the direct effect of PEG-interferon on QT was confounded by a drug related effect on temperature. The objective of this work was to investigate the effect of potential confounding variables, and investigate an appropriate correction approach that addresses the collinearity among key variables of interest i.e., RR interval, temperature and concentration.
Methods: Two linear mixed effect models (Fig. 1) were applied to sequentially correct for heart rate and temperature to derive the corrected QT interval for an updated CQT analysis. Final model selection was based on various GOF plots, OFV, and precision of parameter estimates. Two additional modeling approaches proposed in the literature (QT60 and Binning) were applied.
Results: The modeling results indicated that (i) due to differences in HR on and off drug, the use of correction coefficients from the RR versus QT relationship from the placebo group leads to significant bias if applied to the treatment group, (ii) heart rate correction was insufficient to address temperature related changes due to the direct effect of temperature on QT interval. The sequential correction approach was proposed to account for the proven mechanism of temperature effect on QT while ignoring collinearity between concentration and temperature. The proposed approach led to a slope that was not significantly different than zero across concentrations of interest. The data from two other orthogonal methods, QT60 and binning, also showed a non-significant difference of QT interval between placebo and treatment group.
Conclusions: An unprecedented use of two sequential corrections with heart rate and temperature for CQT modeling as well as analyses using two supportive methods suggests that the QT shortening seen in this study is not directly related to PEG-interferon concentration, but as an indirect result of elevated body temperature with no drug related clinical implications.

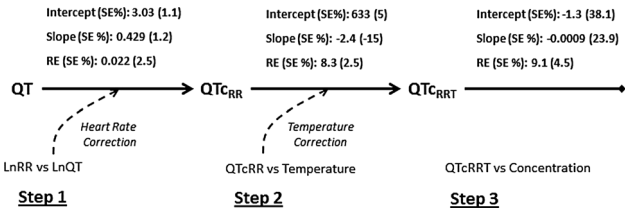

Fig. 1 Stepwise correction of QT interval and the parameter estimates from final mixed effect models

W-006

Modeling and Simulations of Equine Botulinum Antitoxin to Support Study Design in Pediatrics

Nastya Kassir[1,*], Martin Beliveau[1], JF Marier[1], Jason Richardson[2]

[1] Pharsight, Montreal, QC, Canada; [2] Cangene (doing business as Emergent BioSolutions), Winnipeg, MB, Canada

Objectives: BAT™[Botulinum Antitoxin Heptavalent (A,B,C,D,E, F,G)–(Equine)] (NP-018) is an antitoxin consisting primarily of F(ab')2, and Fab' plus F(ab')2 related immune globulin fragments derived from horses immunized with Clostridium botulinum toxoids and toxins. BAT is intended for treatment of symptoms following documented or suspected exposure to seven botulinum neurotoxin serotypes. Objectives presented here were to develop a POPPK model of BAT in adults and use this model to perform simulations to support PK study design for confirming pediatric dosing.
Methods: A POPPK model was developed for each serotype following IV dosing of BAT in adults. Optimal sample size and PK sampling scheme were determined using a simulation-refitting approach. The smallest number of subjects and PK samples across age groups that provided RSE and CI <20 % was defined as the optimal pediatric trial. Pediatric dose was adjusted based on body weight according to the "Salisbury Rule".
Results: Serum concentrations of BAT in adults were modeled using a 2-compartment model with allometric function. Mean CL for serotypes A,B,C,D,F, and G were predicted in patients ≤23 months (35.1–74.6 mL/h), 2–11 years (78.0–161.5 mL/h) and 12–17 years (146.7–291.4 mL/h). For serotype E, mean CL in patients ≤23 months, 2–11 years and 12–17 years were 205.0, 452.6, and 858.7 mL/h, respectively. A sample size of 10 patients and a sampling strategy involving one trough at 22 h for serotypes A,B,C,E,F, and G; and at 11 h for serotype D resulted in RSE and CI < 20 % for CL.
Conclusion: Population PK model was leveraged to predict CL post-IV dosing of BAT in pediatrics. Based on the simulation-refitting approach, a study design involving 10 patients and one trough sample is expected to result in a robust estimation of CL for all serotypes.
This work was funded by the Biomedical Advanced Research and Development Authority (BARDA), Department of Health and Human Services (DHHS) under contract HHSO100200600017C.

W-007

Simulations to Support Dose Selection in an Adaptive Phase IIb Trial

Pavan Vaddady[1,*], Xiujiang Li[1,3], George Philip[1], Davis Gates[1], Karim Azer[1], Malidi Ahamadi[1], Ferdous Gheyas[1], Thomas Kerbusch[2], Pravin Jadhav[1]

[1] Merck Research Laboratories, Merck and Co., Whitehouse Station, NJ, USA; [2] Merck Research Laboratories, Merck Sharp & Dohme B.V., Oss, The Netherlands; [3] Current Affiliation: Boehringer Ingelheim Pharmaceuticals, Inc., Ridgefield, CT, USA

Objectives: MK-1029 is being evaluated in an adaptive Phase-IIb trial with doses ranging from 10 to 150 mg. If there is insufficient characterization of dose–response for the primary endpoint (FEV1) at the interim analysis, the design was provisioned to add a lower dose. The objective of this simulation experiment was to derive the decision criteria with reasonable operating characteristics such that the probability of correct decision (adding a dose when truly needed, for example) was maximized. Further, operating characteristics were derived for range of plausible scenarios because there was no a priori PK/PD knowledge.
Methods: Simulation and re-estimation method was employed using the FEV1 disease model from literature, PK model for MK-1029 Phase I data, and assumed range of plausible drug effect parameters (Emax and ED50). For each scenario, 500 clinical trials were simulated under the Phase IIb design. The decision criterion was derived based on the relationship between ED50 and the lowest dose, i.e. if true ED50 <10 mg, then a dose would be needed to better characterize the dose response. For each trial, posterior probability of achieving the proposed effect size threshold to evaluated dose–

response, i.e. Probability (Eff150-10 < 0.5*Eff150|Data) > X % was derived. Different probability thresholds (30–80 %) were evaluated for assessing the probability of making a correct decision.
Results: We found that the proposed threshold to add a lower dose (Effect at 10 mg is greater than half of effect at 150 mg) was reasonable and clinically interpretable. The posterior probability threshold of 60 % was selected based on the operating characteristics under various plausible scenarios. It was recognized that if the true ED50–10 mg, the probability threshold needs to balance the desire to declare the dose response versus adding a lower dose.
Conclusions: The simulations were used to recommend a decision criterion to maximize the probability of correct decision-making.

W-008

Implementing Reproducible Research with R and Git

Devin Pastoor*

Center for Translational Medicine, University of Maryland School of Pharmacy, Baltimore, MD, USA

Objectives: A minimal standard for data analysis and other scientific research is they are reproducible. Code and data should be maintained so that other groups can re-create all results (figures, tables, etc). The importance of such reproducibility is now widely recognized, but it is still not so widely practiced as it should be, in large part because many scientists have not adopted the tools and techniques for reproducible research. Science is based on building on, reusing, and critiquing published research. Without the underlying methods, codes, data scientific publications more so represent advertising of the research. Thus, final report should strive to not only include the final report, but details on the full software development environment, including all codes and data used.
Methods: Literate programming offers one solution to these issues. At its core, literate programming offers the ability to combine written text with the underlying code and data to generate a final report containing the output of the code, such as figures and tables, woven directly into the document. While sharing of this final report with all underlying data may not always be feasible due to data confidentiality issues, this process can be applied to at least maintain internal reproducibility and can greatly facilitate the dissemination of as much of the underlying workflow as possible. For methodological or simulation-based research, the opportunity for fully reproducibility and replicability is possible. A basic and extensible reproducible research toolkit is composed of R, knitr, and git. These tools allow for automated scripting and traceability from file creation, data manipulation, subsequent analyses, and creation of publication-quality figures and tables in reports and slide-decks. It is demonstrated that applying these techniques is not difficult.
Results: An example workflow is shown, including how each tool is used, as well as how data and results can be managed at each stage of the project.

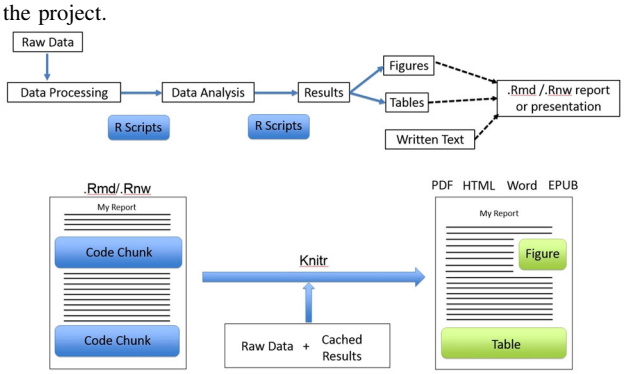

W-009

A Population-Based Approach to Systems Pharmacology (SP) Modeling of the Effect of Blinatumomab in Adult B-Precursor Acute Lymphoblastic Leukemia Patients

Theresa Yuraszeck*, Min Zhu, Indrajeet Singh

Pharmacokinetics & Drug Metabolism, Amgen Inc., Thousand Oaks, CA, USA

Objectives: Unlike PKPD models, SP models typically capture dynamics in a single virtual patient (VP) due to the models' complexity. Although such models are able to describe pharmacology processes, one VP may not be representative of the average response in the patient population and variability in pharmacology and clinical responses cannot be adequately predicted. We developed a population SP approach to advance a previously established SP model for describing the mechanism of action of Blinatumomab, an investigational bispecific T cell-engager (BiTE®) molecule that binds to CD19 on B-lineage cells and to CD3 on T cells [1].
Methods: A population of 1,000 VPs was created by selecting random combinations of 16 key parameters from the previous SP model based on ALL biology and sensitivity analysis. We assumed parameters were uniformly distributed in a range defined by clinical and literature data. The population was stratified by responder status and sensitivity was assessed.
Results: The proposed approach successfully captured the variability in the clinical data. Simulations indicate the majority of responders achieve fast reduction in malignant B-cells. Adequate T cell levels, affinity of Blinatumomab to its target, and Blinatumomab exposure appear to be key drivers of this response. The rate at which malignant B-cells decline during the first week of treatment was identified as a potential early predictor of response.
Conclusions: Characterization of variability in pharmacology and clinical responses is critical for the development of models with clinical utility. Our population SP approach captured the clinical data even in the absence of detailed information on parameter distributions. Our model was subsequently applied to identify key factors influencing response and to explore alternative dosing regimens in the intended patient population. This approach can be generally applied to any systems pharmacology model.

Reference:

1. Singh et al. "Pharmacology Model to Characterize the Effect of Blinatumomab in Patients with Adult B-Precursor Acute Lymphoblastic Leukemia." Poster presented at ACoP, Atlanta, GA (2014)

W-010

Modeling and Simulation of Caffeine Pharmacokinetic Changes during Pregnancy

Tian Yu[1], Sarah Campbell[1], Chris Stockmann[1], Erin A. S. Clark[2,3], Michael W. Varner[2,3], Michael G. Spigarelli[1,4], Catherine M. T. Sherwin[1,4,*]

[1] Division of Clinical Pharmacology and [4] Clinical Trials Office, Department of Pediatrics, [2] Maternal-Fetal Medicine, Department of Obstetrics and Gynecology, School of Medicine, University of Utah; [3] Intermountain Healthcare, Women and Newborns Clinical Programs, Salt Lake City, Utah, UT, USA

Table 1 PK estimates of caffeine across 3 trimesters in pregnant women

	First trimester	Second trimester	Third trimester
PK parameters			
<CL/F (L/h)	13.8	7.79	4.39
V/F (L)	14.5	14.6	11.0
K_a (h^{-1})	5.0	2.5	1.9
Between subject variability			
CL	27.1 %	20.0 %[a]	20.0 %[a]
V	17.0 %	55.4 %	52.3 %
Residual unexplained variability			
Additive (SD)	0.315	0.316	0.316

[a] Fixed

Objectives: Caffeine is frequently consumed by pregnant women. It is metabolized by hepatic CYP1A2, which is markedly inhibited during pregnancy. This study evaluated caffeine pharmacokinetic (PK) changes throughout pregnancy.
Methods: A prospective, multi-center PK study was conducted among pregnant women (≥18 years) who were recruited once per trimester. One beverage with 34–75 mg caffeine was consumed and a blood sample was collected 30–45 min later. Caffeine concentrations were measured by LC–MS/MS. Nonlinear mixed effects modeling (NONMEM 7.2) was used to develop the PK models across each of the trimesters. Monte Carlo simulation was used to assess the model fit.
Results: 69 study visits were completed among 57 unique women (93 % White). The mean age (±SD) was 30.0 ± 5.0 years, weight 75.4 ± 15.3 kg, height 162.7 ± 6.5 cm. Nine, 25, and 35 encounters took place in the 1st, 2nd, and 3rd trimesters, respectively. A one compartment model with first order absorption was used to describe the data with an additive error model (Table 1). There was a significant decrease in apparent clearance between the 1st and 3rd trimester ($p < 0.001$). Simulation results showed that the prediction errors for the 1st, 2nd, and 3rd trimester were 18, 23, and 21, respectively.
Conclusions: Trimester specific models and simulations demonstrated marked caffeine PK changes, revealing evidence of the large role that pregnancy plays in influencing CYP1A2-mediated drug metabolism. Future studies are underway to develop a caffeine metabolite model for pregnant women.

W-011

Modelling the Kinetics of Human Respiratory Syncytial Virus and Clinical Disease Symptoms

Kashyap Patel[1,*], Carl M. Kirkpatrick[1], Craig R. Rayner[2] and Patrick F. Smith[2,3]

[1] Centre for Medicine Use and Safety, Monash University, Clayton, VIC, Australia; [2] d3 Medicine, Parsippany, NJ, USA; [3] School of Pharmacy, University at Buffalo, Buffalo, NY, USA

Background: Respiratory Syncytial Virus (RSV) is the primary cause of lower respiratory infection in infants [1], and is associated with significant morbidity and mortality [2]. However, the clinical development of anti-RSV therapies is constrained by the understandable reluctance to conduct trials in pediatric patients. One solution is the development of mechanistic models in human adults, which can then allow for dose extrapolation to infants.
Objectives: To develop a viral kinetic (VK) model for RSV in human adults and investigate the link between viral load and clinical disease measures.
Methods: Viral load and clinical symptom score data from untreated human adults infected with RSV were obtained from published reports [3]. Mechanism-based models were then developed using the Monte Carlo Expectation Maximization (MCPEM) algorithm in S-ADAPT.
Results: The time course of RSV virus and clinical symptoms was adequately described using previously established structural VK models for influenza virus [4]. Inter-individual variability (IIV) was significant for parameters describing viral infection and production rates. A turnover model characterized the development of clinical symptom scores with an estimated EC50 of 4.92 log10 PFU/mL (IIV 40.4 %).
Conclusions: The relationship between RSV exposure and clinical disease measures in human adults was described using a population VK model. This model can be used to predict anti-RSV pharmacodynamics with potential extrapolation to infant populations.

References:

1. Glezen WP et al. (1986). Risk of primary infection and reinfection with respiratory syncytial virus. Am J Dis Child 140:543–546
2. Thompson WW et al. (2003). Mortality associated with influenza and respiratory syncytial virus in the United States. JAMA 289:179–186
3. DeVincenzo JP et al. (2010). Viral load drives disease in humans experimentally infected with respiratory syncytial virus. Am J Resp Crit Care Med 182:1305–14
4. Canini L et al. (2011). Population Modeling of Influenza A/H1N1 Virus Kinetics and Symptom Dynamics. J Virol 85:2764–2770

W-012

Why PKPD Approaches Are Critical to Success in Oncology: Drug Development Cases & Optimal Dosing for Targeted Therapies

Jeffrey R. Sachs[1,*], Kapil Mayawala[1], Satvik Gadamsetty[2], Dinesh de Alwis[1]

[1] Merck/MSD/MRL/PPDM, Quantitative Pharmacology and Pharmacometrics, Whitehouse Station, NJ, USA; [2] M&S Informatics Department

Objectives: Elucidate historical ratio of MTD to approved dosing and identify cases of clinical impact of PKPD analysis in oncology development.
The primary goal of most phase 1 trials in oncology was, historically, to establish MTD: as the RP2D. For many targeted therapies, dose limiting toxicities (DLTs) may not be seen even at supra-therapeutic doses, and there is frequently a limited ability to objectively quantify adverse events (AEs) [1]. More subjective AEs create additional ambiguity in DLT determination, confusing decisions on dose. Higher than optimal dosing can increase toxicity in later trials (and use), which can negatively impact efficacy via lower adherence or direct sequelae of toxicities.

While MTD-based dose determination is often justified for cytotoxics, targeted therapeutics need alternative strategies. One alternative strategy is to develop target engagement (TE) and pharmacodynamic (PD) markers for identifying a biologically efficacious dose, e.g., antagonist mAb dose needed for >90 % TE. Biologically

Table 1 Review of doses for approved drugs, showing that most drugs are efficacious at doses below MTD

Percent of drugs with…	MTD same as approved dose	1 < MTD/approved dose ≤ 2	MTD > 2x approved dose
Percent of marketed drugs	42 %	34 %	24 %

There were many drugs (not included below) for which no MTD could be found, due either to high tolerability, or to drug development without establishing an MTD of record. When different doses are approved across indications, the maximum approved dose was used. Multiple indications and formulations for a single monotherapy were thus combined resulting to create a list of 70 drugs. (Preliminary results)

efficacious dose has been discussed previously without listing specific examples of clinical impact.
Methods: We reviewed MTD and approved doses for oncolytics [2], and surveyed literature (2000–2013) for specific examples of the clinical impact of PKPD approaches.
Results: More than half of oncolytics are dosed below MTD, roughly a quarter are below ½ MTD (Table 1). For some drugs, there is no DLT even at the highest tested dose.
Several cases of clinical impact of PKPD have been documented. Decitabine, for example, was only successfully developed with a biologically efficacious dosing strategy, and was approved at a dose of roughly 1/20 MTD—20 years after its initial clinical trials.
Conclusions: Utility of PD/TE markers can go beyond dose selection to patient selection (e.g., Crizotinib efficacy for NSCLC with ALK-mutations) and combination therapies. Broader adoption of biologically efficacious dose mindset in modern clinical trials can enable faster access to effective drugs and save R&D costs.

References:

1. Invest. New Drugs 29:1414–1419, 2011
2. www.cancer.gov

W-013

A Multiscale Systems Pharmacology Model for Pharmacokinetic Disposition of Ketone Monoester and its Metabolism Products in Human

Vittal Shivva*, Ian G Tucker, Stephen B Duffull

School of Pharmacy, University of Otago, Dunedin, New Zealand

Objectives: There is increasing evidence of the therapeutic benefits of induced mild ketosis in various neurological disorders. A novel means of achieving ketosis is by nutritional consumption of a ketone monoester ((*R*)-3-hydroxybutyl (*R*)-3-hydroxybutyrate). The aim of this study was to develop a systems pharmacology model with an intention to (1) collate information from the literature and identify what mechanisms describing ketone disposition are known and (2) to design future studies. This work builds on a previous empirical population PK model for D-β-hydroxybutyrate (BHB) [1].
Methods: A literature search was conducted to identify and collate information on processes such as production, transport and regulation of endogenous ketones and factors governing these processes. Model components were: (i) gut with different luminal sites and variability in expression of transporters, (ii) portal and systemic circulation, (iii) the liver as the site of production of endogenous ketones, (iv) all other lumped organs/tissues that metabolise and excrete ketones. The model was developed as differential equations in MATLAB®.
Results: A systems pharmacology model was developed by integrating information from the literature specifying metabolic pathways, transporters involved in the flux and the knowledge gained from the empirical model. There was limited information regarding transporter affinity and maximum velocity of transport for each of the ketone species at the different transporters (MCT1, MCT2, MCT4 and SMCT1) as well as limited information available describing transcellular and paracellular passive diffusion processes. In contrast, there was considerably more information describing metabolic fate and energy production. Preliminary simulations have produced blood BHB profiles comparable to the empirical data.
Conclusions: The current work has highlighted that while there is detailed information on metabolic fate of ketones, there is significant missing information on their production and transport. Further PK studies are needed to characterise the uptake and disposition of ketones when used therapeutically.

Reference:

[1] Shivva et al. PAGANZ conference; University of Otago, Dunedin, NZ. 2014

W-014

Mechanism-Based Modelling of Artemisinin Combination Therapy in Murine Malaria

Kashyap Patel[1,*], Kevin T. Batty[2, 3], Brioni R. Moore[4], Peter L. Gibbons[2, 5], Carl M. Kirkpatrick[1]

[1] Centre for Medicine Use and Safety, Monash University, Clayton, VIC, Australia; [2] School of Pharmacy, Faculty of Health Sciences, Curtin University, Bentley, WA, Australia; [3] West Coast Institute, Joondalup, WA, Australia; [4] School of Medicine and Pharmacology, University of Western Australia, Crawley, WA, Australia; [5] Department of Medical Technology & Physics, Sir Charles Gairdner Hospital, Nedlands, WA, Australia

Objectives: To develop a mechanistic model that describes the growth, antimalarial killing and recrudescence of parasite following dihydroartemisinin and piperaquine combination therapy to infected mice.
Methods: Antimalarial drug concentration and parasite density data were obtained from Swiss mice inoculated with Plasmodium berghei. The mice were administered a single intraperitoneal dose of 30 mg/kg dihydroartemisinin, 10 mg/kg piperaquine phosphate or a combination of both antimalarials at 64 h post-inoculation. A mechanism-based population model was developed using the Monte Carlo Expectation Maximization (MCPEM) algorithm in S-ADAPT. Parasite recrudescence was defined using a previously published structural model that incorporated each erythrocytic stage of the P. berghei life-cycle [1].
Results: One- and two-compartment models described the disposition of dihydroartemisinin and piperaquine, respectively. The estimated mean clearance was 1.95 L/h for dihydroartemisinin and 0.109 L/h for piperaquine. A turnover model described the parasite killing curve after single agent dosing, with an IC50 of 0.747 μg/L for dihydroartemisinin and 16.8 μg/L for piperaquine. In addition, the rate of parasite killing by dihydroartemisinin was almost 50-fold faster than that for piperaquine. Parameters from the monotherapy models adequately described the parasite density-time curve following combination therapy of dihydroartemisinin with piperaquine.

Conclusions: This study has developed mechanistic models that describe the parasite-time curve after single, multiple or combination dosing of antimalarial drugs to mice. These structural models have potential application to design and refine dosage regimens for artemisinin-based combination therapy.

References:

1. Patel K, Batty K et al. (2013). Mechanism-based model of parasite growth and dihydroartemisinin pharmacodynamics in murine malaria. Antimicrob Agents Chemother 57:508–16

W-015

A PK/PD-Based Simulation of Dopamine Agonist Self-Administration Behavior in Rats

Alexander C. Ross, Vladimir L. Tsibulsky, Andrew B. Norman*

Department of Pharmacology, University of Cincinnati College of Medicine, Cincinnati, OH, USA

Objectives: In rats trained to self-administer dopaminergic agonists IV, the time between self-administration events, T, is predicted by $T = Ln(1 + DU/DST)*t_{1/2}/Ln(2)$, where DU is the agonist unit dose, $t_{1/2}$ is the agonist elimination half-life, and DST is the minimum level of agonist maintained in the body, which is assumed to correspond to an amount of agonist-receptor complexes in the brain [1]. Self-administration behavior was simulated with this assumption incorporated in a PK/PD modeling framework.
Methods: Simulations were executed using a PK/PD model containing an agonist (A), a competitive antagonist (B), and a receptor (R) in the brain compartment. This model (shown below) was generated in MATLAB Simbiology (Fig. 1).
Self-administration events were programmed around the amount of agonist-receptor complexes, AR(t): if AR(t) is less than the amount corresponding to satiety, this induces further agonist administration. If AR(t) becomes greater than the amount corresponding to satiety, the system ceases agonist administration events. Agonist self-administration simulations with a single competitive antagonist administration event were also performed. Irreversible antagonism was simulated through a reduction of the receptor population while preserving the amount of agonist-receptor complexes corresponding to satiety.

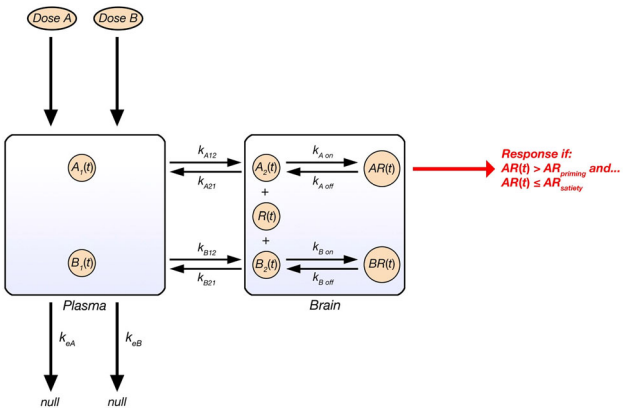

Fig. 1 A two-compartment PK/PD model proposed to underlie self-administration behavior where the value of AR(t) determines whether further agonist administration occurs

Results: Simulations show that increasing the agonist unit dose, DU, during a simulated session yields a proportional increase in T. Simulation of a competitive antagonist intervention event results in a decrease in T and an increase in DST, both of which gradually return to baseline values as the competitive antagonist is pharmacokinetically eliminated. Simulation of irreversible antagonism leads to a sustained decrease in T and a sustained increase in DST.
Conclusions: Simulations are in line with what has been observed in rats [1,2], suggesting that this model is a valid explanation for dopamine agonist self-administration behavior and the effects of antagonists.

References:

1. Tsibulsky, V. L. & Norman, A. B. Brain research 839, 85–93 (1999)
2. Norman, A. B., Tabet, M. R., Norman, M. K. & Tsibulsky, V. L. Journal of neuroscience methods 194, 252–258, (2011)

W-016

Evaluation of a Mechanism-Based PBPKPD Model for the Prospective Prediction of Human Receptor Occupancy of Anti-schizophrenic Agents

Theresa Yuraszeck*, Carl Davis, Yihong Zhou, Ramesh Palaparthy

Pharmacokinetics and Drug Metabolism, Amgen, Thousand Oaks, CA, USA

Objectives: A mechanistic physiology-based pharmacokinetic pharmacodynamic (PBPKPD) model was published that predicts the dopamine (D2) receptor occupancy (RO) of olanzapine in the absence of in vivo preclinical data, a potentially powerful method for discovery and development (1). Nonetheless, the broad applicability of the model must be assessed before this method can be recommended. To this end, we have expanded the published PBPKPD model to clozapine, quetiapine, haloperidol, and ziprasidone, and retrospectively evaluated predictions of the RO observed in humans.
Methods: Pharmacokinetic models, physiological and drug-specific parameters used to inform the PBPKPD model, and observed D2 RO from clinical studies for clozapine, quetiapine, haloperidol, and ziprasidone were extracted from the literature. With these data in hand, the RO of the four compounds was simulated and compared to the observed human RO.

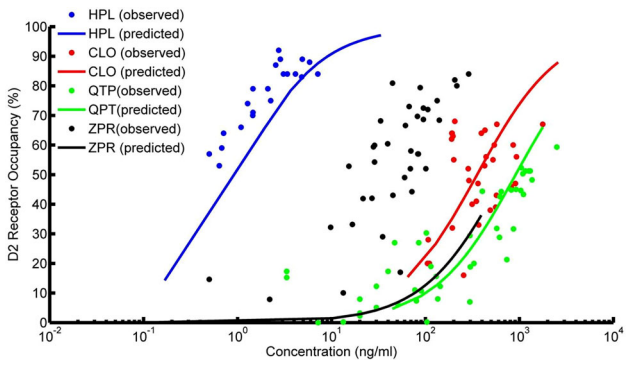

Fig. 1 Comparison of observed RO data extracted from the literature with the predictions from the PBPKPD model. *HPL* haloperidol, *CLO* clozapine, *QTP* quetiapine, *ZPR* ziprasidone

Results: The published PBPKPD model predictions were consistent with the RO data for haloperidol, clozapine, and quetiapine, but the D2 RO of ziprasidone was significantly under-predicted (Fig. 1). Global sensitivity analysis indicated that plasma and brain unbound fraction and the D2 receptor equilibrium dissociation constant are key parameters that need to be accurately determined experimentally.
Conclusions: The proposed method of predicting RO in the absence of preclinical in vivo data can enable compound selection, help optimize preclinical experimental design, inform Phase I dose selection, and facilitate second generation drug design. The method can also be applied to the development of compounds that interact with other targets across the blood brain barrier. However, given the model's performance for the four drugs studied here, further characterization of its predictive capabilities must be undertaken before the method is used as a prospective development tool for any target. Thus, we have initiated a more expansive comparison of antipsychotic drugs and sensitivity analysis with internally generated data to assess the general utility of the model and the conditions that favor its use.

Reference:

1. Johnson, M., et al. (2011). Pharm Res 28(10): 2490–2504

W-017

Potential Surrogate Endpoints for Progression-Free Survival (PFS) and Overall Survival (OS) in Non-Hodgkin Lymphoma: A Literature-Based Meta-analysis of Phase II and Phase III Studies

Rui Zhu[1*], Dan Lu[1], Wayne Chu[1], Akiko Chai[1], Michelle Green[2], Nancy Zhang[2], Jin Yan Jin[1]

[1] Genentech, Inc., South San Francisco, CA, USA; [2] Quantitative Solutions, Menlo Park, CA, USA

Objectives: Survival-based endpoints such as progression-free survival (PFS) and overall survival (OS) are considered the gold standard in clinical trials of non-Hodgkin lymphoma (NHL) but demonstration of clinically meaningful differences in treatment regimens necessitates large and lengthy trials. The correlation between efficacy endpoints in NHL clinical trials was investigated to identify potential surrogate endpoints for PFS and OS in major histologic subtypes of NHL.
Methods: Phase II and Phase III studies in patients with diffuse large B cell lymphoma (DLBCL), follicular lymphoma (FL), or mantle cell lymphoma (MCL) published from 1993 to 2013 were identified. Correlations between efficacy endpoints were analyzed using weighted linear regression.
Results: Data used in the analysis were from 127 trials (148 trial arms), representing over 13,000 patients. In trials of newly diagnosed DLBCL, 6-month PFS was moderately correlated with 2-year OS ($R^2 = 0.81$ with 95 % confidence interval [CI] 0.51–0.96) and 3-year OS ($R^2 = 0.74$ with 95 % CI 0.45–0.95). Linear regression determined that a 10 % increase in 6-month PFS would predict for a 13 ± 1.2 % increase in 2-year OS or a 14 ± 1.4 % increase in 3-year OS. For trials of FL (newly diagnosed and relapsed/refractory combined), 6-month PFS was highly correlated with 3-year PFS ($R^2 = 0.89$ with 95 % CI 0.62–0.96). No clear correlation was observed between complete response (CR) rate (%) and median PFS or OS or landmark PFS or OS in DLBCL, FL, and MCL patients.
Conclusions: Six-month PFS was moderately correlated with 2- and 3-year OS in newly diagnosed DLBCL and highly correlated with 3-year PFS in FL patients, indicating 6-month PFS may be an appropriate surrogate endpoint. Further exploration of these correlations may facilitate future trial design and interpretation of interim data analyses.

W-018

Mixed-Effect Modeling of Ethanol Pharmacokinetics in Korean Healthy Male Subjects

Seunghoon Han[1], Taegon Hong[1], Gab-Jin Park[1], Sunil Youn[1], Wan-Su Park[2], Daejin Kim[2], Dong-Seok Yim[1,*]

[1] Pharmacometrics Institute for Practical Education & Training, the Catholic University of Korea, Seoul, Korea; [2] Department of Psychiarty, the Catholic University of Korea Seoul St. Mary's Hospital, Seoul, Korea

Objectives: Ethanol is known to follow non-linear elimination kinetics with substantial inter- and intra-subject variability. The aim of this study was to develop a mixed-effect pharmacokinetic model from Korean healthy males and to identify the influential factors.
Methods: A total of 13 subjects received oral dose of 1 g/kg ethanol twice with 7-day interval. Blood sampling for full pharmacokinetic study was done just before and 0.33, 0.67, 1, 1.33, 1.67, 2, 3, 4, 5, 6, 8 h after dosing. Gas chromatography-mass spectrometry was used for plasma concentration measurement of ethanol. Non-linear mixed effect modeling was performed using NONMEM (ver.7.2). Subjects' age, body weight, and hepatic enzyme levels were investigated as potential covariates.
Results: A one-compartment model with Michaelis–Menten elimination gave the best description for time-concentration profile of ethanol. Mixture of zero-order and first-order absorption was recruited to explain the double peak and a lag-time for first-order absorption was included in the model. Approximately 42.7 % of dose was absorbed by the zero-order absorption. The parameter estimates were 10.6 g/h for maximum elimination rate, 68.2 mg/L for Michaelis–Menten constant (km), 42.8 l for apparent volume of distribution (Vd/F), 0.4 h for duration of zero-order absorption, 0.57 h^{-1} for the absorption rate constant and 0.78 h for the lag time. Use of inter-occasional variability (period effect) for km and fraction of zero-order absorption significantly improved the model. Body weight was the only covariate influencing Vd/F in our model.
Conclusion: This ethanol model may be utilized for further population pharmacokinetic-pharmacodynamic investigation in Koreans.

W-019

Simulating Pharmacokinetics and Pharmacodynamics of Colistin and Doripenem Combination Therapy in Patients

Neang S. Ly[1,*], Jürgen B. Bulitta[1,2], Alan Forrest[1], Brian T. Tsuji[1]

[1] University at Buffalo, Buffalo, NY, USA; [2] Monash University, Clayton, VIC, Australia

Background: Combination therapy has been widely used in the clinic against multidrug-resistant *P. aeruginosa*. However, the design of combinations is largely empirical. Our objective is to project the time-course of bacterial killing and resistance for colistin-based combinations in critically ill patients using patient specific pharmacokinetics [1,2] and our in vitro pharmacodynamic model [3].
Methods: Free plasma concentrations of both antibiotics were used to drive the in vitro PD in three different P. aeruginosa strains: colistin hetero-resistant (ATCC 27853 and FADDI PA033) and colistin resistant (FADDI PA070) at an inoculum of 109 CFU/mL. A standard colistin dose (i.e. the inactive prodrug colistin methanesulfonate

[CMS] given as 400 mg every 12 h), 'front-loaded' dose (800 or 1,200 mg CMS every 12 h for 1 day follow by 400 mg every 8 h), or 'short-term burst' dose (1,200 mg of CMS at 0 and 12 h only) and/or doripenem (250 or 500 mg every 8 h) dose were simulated based on the package insert. Three different groups of patients with differing renal function were simulated for 10 days using Berkeley Madonna (v.8.3.18).

Results: Simulations suggested that colistin alone was unable to elicit any killing, and selection of resistance was predicted for colistin steady-state concentrations above 1.41 mg/L. Doripenem monotherapy displayed rapid killing for hetero-resistant strains and minimal killing for resistant strain followed by regrowth against all strains. The combination regimens were beneficial against hetero-resistant strains when the free colistin concentration was >1.41 mg/L, and these were achieved primarily in patients with low renal function. 'Front-loaded' regimens of CMS or a "short term burst" regimen of CMS suppressed the total bacterial count to 4 log10 CFU/mL for strain ATCC 27853 in patients with moderate renal function.

Conclusions: Our simulations suggest that combination therapy employing high concentrations of colistin were highly beneficial to combat difficult to treat infections by *P. aeruginosa*.

References:

1. Garonzik et al. Antimicrob Agents Chemother 55:3284–3294
2. Nandy et al. Antimicrob Agents Chemother 54:2354–2359
3. Ly et al. Abstract #W-019 G3 ACoP 2013

W-020

Population Pharmacokinetics of Acetaminophen in YJAT-SR Tablet in Healthy Korean Subjects

Changyun Jin, Ji-young Jeon, Yong-Jin Im, Eun-Young Kim, Hye Min Wang, Min-Gul Kim*

Clinical Trial Center and Biomedical Research Institute, Chonbuk National University Hospital, Jeonju, 561-712, Republic of Korea

Objectives: Fixed dose combination of acetaminophen and tramadol, UltracetTM, is the most widely used analgesic for treating moderate to severe pain in the world. Its incrementally modified drug YJAT-SR of Yungjin Pharm (Seoul, Korea) contains sustained-release tramadol, and sustained- and immediate- release acetaminophen that work fast and long-lasting, simultaneously. This study aimed to describe the population pharmacokinetics of acetaminophen in Korean subjects.

Methods: Plasma concentration data of 24 healthy Korean subjects received a single dose of YJAT-SR in fasting condition was collected from a phase 1 clinical study. Plasma concentrations of acetaminophen were measured using a validated liquid chromatography-mass spectrometric method. The population pharmacokinetics parameters of acetaminophen were estimated by nonlinear mixed-effect modeling with first-order conditional estimation with interaction method. One- and two-compartment with one- or two-depot modeling were used for fitting the index data set.

Results: The time course of acetaminophen concentrations is best described by a two-compartment, two-depot model with lag time. The final estimate of parameters were as follow: total body clearance, CL was 7.05 L/h, the volume distribution of the central compartment, V_3 was 47.1 L. Rate constants for immediate- and sustained-release, K_{IR} and K_{SR}, were 10.2 h^{-1} and 1 h^{-1}, respectively. K_{34}, K_{43}, and lag time for immediate-release were 0.0759 h^{-1}, 0.152 h^{-1}, 0.161 h, in respective.

Conclusions: A nonlinear mixed effect model for acetaminophen of YJAT-SR was developed in healthy Korean subjects. Two-compartment with two-depot model was adopted as a final population model. For progressed modeling of acetaminophen, it is needed to assess the influence of covariates such as age, weight, height, or other laboratory test results including serum creatinine, creatinine clearance, and to evaluate the predictive performance of the model.

References:

1. Guidance for Industry Population Pharmacokinetics, February 1999, U.S. Department of Health and Human Services Food and Drug Administration Center for Drug Evaluation and Research (CDER)

W-021

Is 400 mg Moxifloxacin Acceptable for TQT Studies in Korean Subjects? Pharmacokinetic–Pharmacodynamic Model Based Approach

Taegon Hong[1], Seunghoon Han[1], Jongtae Lee[1], Gab-Jin Park[1], Wan-Su Park[1], Kyoung Soo Lim[2], Jae-Yong Chung[3], Kyung-Sang Yu[2], Dong-Seok Yim[1,*]

[1] Pharmacometrics Institute for Practical Education & Training, The Catholic University of Korea, Seoul, South Korea; [2] Department of Clinical Pharmacology and Therapeutics, Seoul National University College of Medicine and Hospital, Seoul, South Korea; [3] Department of Clinical Pharmacology and Therapeutics, Seoul National University College of Medicine and Bundang Hospital, Seoul, South Korea

Objectives: A single 400 mg dose of moxifloxacin has been the standard positive control for thorough QT (TQT) studies. However, it is not clearly known whether a 400 mg dose is also applicable to TQT studies in Asian subjects including Koreans. Thus, we aimed to develop a pharmacokinetic (PK)–pharmacodynamic (PD) model for moxifloxacin to evaluate its time course of QT intervals in Koreans.

Methods : Data from three TQT studies of 33 healthy male Korean subjects who received 400 and 800 mg of moxifloxacin and placebo (water) were used. Twelve lead electrocardiograms were taken for two consecutive days: one day to record diurnal changes and the next day to record moxifloxacin or placebo effects. Peripheral blood samples were also obtained for PK analysis. The PK-PD data obtained were analyzed using a non-linear mixed effects method(NONMEM ver. 7.2).

Results: A two-compartment linear model with first-order absorption provided the best description of moxifloxacin PK. Individualized QT interval correction by heart rate was performed by a power model and the circadian variation of QT intervals was described by two mixed-effect cosine functions. The effect of moxifloxacin on QT interval prolongation was well explained by the Emax model, and the effect by 800 mg was only slightly greater than that of 400 mg.

Conclusions: Although Koreans appeared to be more sensitive to moxifloxacin-induced QT prolongation than Caucasians, the PK–PD model developed suggests that a 400 mg dose of moxifloxacin is also applicable to QT studies in Korean subjects.

References:

1. Piotrovsky V. Pharmacokinetic–pharmacodynamic modeling in the data analysis and interpretation of drug-induced QT/QTc prolongation. AAPS J. 2005;7:E609–24

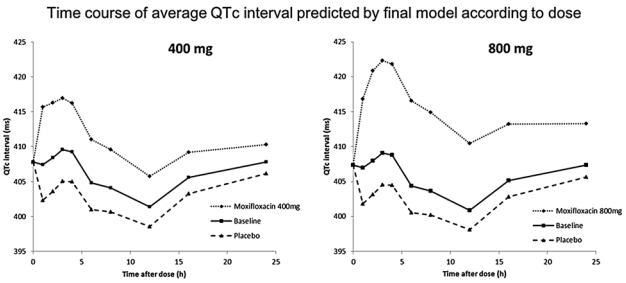

Conclusion: The novel PBPK model for elderly individuals adequately describes the plasma concentrations of acetaminophen and its main metabolites in elderly individuals of different age and, thus, demonstrates the general feasibility of the knowledge-driven PBPK ageing model. Further disease implementations in these age groups conceding a diversification of age- or disease-related (patho-) physiological alterations are possible Fig. 1.

References:

1. Liukas, A. et al. Pharmacokinetics of intravenous paracetamol in elderly patients. Clin Pharmacokinet. 2011; 50(2):121–9

W-022

A Physiologically-Based Pharmacokinetic (PBPK) Approach to Assess the Impact of Age on the Pharmacokinetics of Acetaminophen in Elderly Individuals

Jan-Frederik Schlender[1,2,*], Kirstin Thelen[2], Michaela Meyer[2], Stefan Willmann[2], Ulrich Jaehde[1]

[1] Institute of Pharmacy, Clinical Pharmacy, University of Bonn, Bonn, Germany; [2] Bayer Technology Services GmbH, Computational Systems Biology, 51368 Leverkusen, Germany

Objectives: The objective of this study was to analyze the effects of increasing age on the pharmacokinetics (PK) of acetaminophen using a newly developed physiologically-based pharmacokinetics (PBPK) ageing model. In particular, alterations on kidney function, the metabolization via cytochrome P450 (CYP) 2E1, the reaction via sulfotransferase (SULT) 1A1 and metabolism via UDP-glucuronosyltransferase 1A6 on the total body clearance of acetaminophen were investigated.
Methods: Age-related anatomical and physiological changes from early adulthood up to the age of 100 years were derived from various literature sources and introduced into a novel ageing whole-body PBPK model. Plasma concentration-time profiles following short-term infusions of 1,000 mg acetaminophen were simulated in three virtual elderly populations in the age range between 60 and 90 years and in healthy adults for comparison. Simulation results were compared to clinical data observed in age- and gender-matched patients [1].
Results: The incorporated ageing function for glomerular filtration rate and the altered enzyme kinetics were verified in different age groups. Increases of the AUC0-24 h values between the adult and the oldest elderly group were 1.7 fold for acetaminophen, 2.3 and 2.7 fold for the glucuronide and sulphate conjugates, respectively.

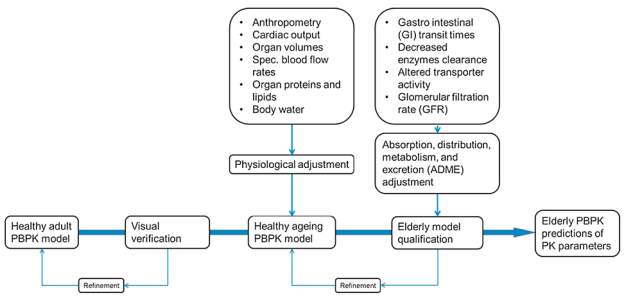

Fig. 1 Workflow for the development of a knowledge-driven PBPK ageing model

W-023

A Population Pharmacokinetic analysis of Zabofloxacin in Patients with Mild to Moderate Community Acquired Bacterial Pneumonia

Ji-young Jeon, Yong-Jin Im, Eun-Young Kim, Changyun Jin, Hye Min Wang, Min-Gul Kim*

Clinical Trial Center and Biomedical Research Institute, Chonbuk National University Hospital, Jeonju, Republic of Korea

Objectives: Zabofloxacin, a new fluoroquinolone, showed a broad-spectrum antibacterial activity. This study aimed to describe the population pharmacokinetics of zabofloxacin and to identify the covariates related to zabofloxacin disposition in patients infected with community acquired bacterial pneumonia (CABP).
Methods: A population pharmacokinetic analysis was conducted on zabofloxacin in patients infected with CABP who were enrolled in a phase II clinical trial. The data consisted of 396 plasma concentrations from 66 patients who received zabofloxacin hydrochloride capsule at a dose of 300 or 400 mg once daily for 3 days. The analysis was performed using nonlinear mixed-effect modeling as implemented in NONMEM (version 7.2). Different covariates, such as age, sex, weight, height, serum creatinine, estimated glomerular filtration rate (eGFR), stage of renal function, AST and ALT, were identified by the various methods.
Results: A two-compartment model with first-order absorption best described the data. There were no obvious relationships between covariates of renal function (e.g., serum creatinine, eGFR, and stage of renal function) and the pharmacokinetic parameters. Clearance and central volume showed a negative relationship with age.
Conclusions: We developed a population pharmacokinetic model which identified covariate that account for zabofloxacin disposition in CABP patients. Further studies are needed to clarify the effects of age on zabofloxacin pharmacokinetics and to optimize dosing regimen of zabofloxacin in elderly population.

References:

1. Guidance for Industry Population Pharmacokinetics, February 1999, U.S. Department of Health and Human Services Food and Drug Administration Center for Drug Evaluation and Research (CDER)
2. Guidance for Industry Pharmacokinetics in Patients with Impaired Renal Function: Study Design, Data Analysis, and Impact on Dosing and Labeling, 2010, U.S. Department of Health and Human Services Food and Drug Administration Center for Drug Evaluation and Research (CDER)

W-024

Simultaneously Model Multiple Endpoints in a Single Model Fit: Application in a Phase I Study

Farkad Ezzet*

Aycer Pharma Consulting, Chatham, NJ, USA

Objectives: To simultaneously characterize and compare multiple responses in a single model.
Methods: We address modeling multiple endpoints (MME) simultaneously as opposed to the traditional approach of modeling single endpoints (MSE) one at a time. Multiple endpoints can be several biomarkers from phase I, or different efficacy and safety endpoints in phase II/III. The different measurement scales, and corresponding error models of different endpoints, pose technical modeling challenges, rendering MME less commonly used. We implemented a bivariate version of MME in a phase I dose finding study, investigation drug effects on a pair of efficacy and safety biomarkers measured on the continuous scale, as a function of either dose or drug concentration following multiple dosing. We also conducted a simulation study [1] to explore properties of MME under various design scenarios. MME is a general modeling framework requiring software capable of handling heteroscedasticity.
Results: The Phase I study modeling results adequately characterized the biomarker dose–response profiles. Predictions provided guidance regarding safety margin of the compound, and allowed calculation of the probability a dose or concentration producing the desired biomarker levels. The simulations revealed adequacy of MME in accurately estimating true model parameters. MME offers the advantage of directly testing magnitude or differences of disease or drug effect on multiple endpoints, e.g. testing if ET_{50} is different between biomarkers. When endpoints share similar characteristics, but one endpoint is sparsely sampled (due to cost or practical constraints), then inference on that endpoint produces considerably less bias with MME as compared with MSE.
Conclusion: Modeling multiple endpoints in a single model fit offers a means of estimating and comparing drug effects on multiple endpoints. Using MME approach in phase I and early phase II studies should help optimize, streamline and potentially reduce data collection costs.

References:

1. Ezzet, F, Raddad, E, Dose Response Models for Multiple Endpoints: A Simulation Study, PAGE, Alicante, June 2014. http://www.page-meeting.org/default.asp?abstract=3084

W-025

Population Modelling of QT-Interval Prolongation: Estimation Approaches and Translational Opportunities

Eleonora Marostica[1,*], Karel Van Ammel[2], An Vermeulen[3], Jan Van Bocxlaer[1], Koen Boussery[1], David J. Gallacher[2]

[1] Laboratory of Medical Biochemistry and Clinical Analysis, Ghent University, Ghent, Belgium; [2] Global Safety Pharmacology, Beerse, Belgium; [3] Model Based Drug Development, Janssen R&D, Beerse, Belgium

Objectives: The QT-interval prolonging effects of drugs are a risk factor for Torsades de Pointes and sudden death. In the context of drug development, drug-induced QT-interval prolongation represents a major issue that needs investigation. The objectives of this work were: (i) to develop a pharmacokinetic/pharmacodynamic (PK/PD) model to describe QT data in dogs receiving moxifloxacin (the clinical reference standard); (ii) to compare different parameter estimation procedures; (iii) to assess the potential translational opportunities of the approach.
Methods: A population PK model was developed using data from a crossover study in awake dogs receiving placebo and moxifloxacin (10, 30, and 100 mg/kg). Data from a satellite group were also included for model development. The QT-interval was then modelled incorporating three components (see [1]): an individual heart-rate correction, the circadian rhythm, and the drug effect. Different model structures were compared in terms of the objective function using NONMEM 7.1. The final PK/PD model was then compared to a fully Bayesian implementation using WinBUGS 1.4.3.
Results: The PK of moxifloxacin was adequately described using a one-compartment model with first-order absorption and elimination. The final PK/PD model was able to capture the QT profiles satisfactorily. Comparable performances in terms of parameter estimates and profiles were obtained with both estimation approaches. The probability of QT-interval prolongation greater than 10 ms was also assessed. Consistent results to the ones reported in [1] were obtained.
Conclusions: Although both estimation methods describe the data satisfactorily, the fully Bayesian method yields a more thorough assessment of parameter uncertainty. Moreover, the Bayesian paradigm may provide a framework for translational approaches by leveraging historical knowledge. This will be the subject of further investigation.

Reference:

1. Anne S.Y. Chain, Vincent F.S. Dubois et al, Identifying the translational gap in the evaluation of drug-induced QTc interval prolongation, Br J Clin Pharmacol 76, pp. 708–724, 2013

W-026

Population Pharmacokinetics (PK) of Tocilizumab Following Intravenous (IV) and Subcutaneous (SC) Administration to Patients with Rheumatoid Arthritis (RA)

Leonid Gibiansky[1,*], Nicolas Frey[2], Joy C. Hsu[3]

[1] QuantPharm LLC, North Potomac, MD, USA; [2] F. Hoffmann-La Roche Ltd., Pharma Research and Early Development, Roche Innovation Center, Basel, Switzerland; [3] Roche TCRC, Inc. Pharma Research and Early Development, Roche Innovation Center, New York, NY, USA

Objectives: Tocilizumab is a recombinant humanized anti-IL-6R monoclonal antibody. The analysis aimed to establish a predictive population PK model of tocilizumab following administration of 8 mg/kg IV Q4 W (IV1), and 162 mg SC QW (SC1) and Q2 W (SC2), including identification of covariate factors influencing tocilizumab exposure.
Methods: Serum concentrations (13,642) of 1,759 RA patients from two 24-week Phase III studies were analyzed.
Results: A two-compartment model with parallel linear and Michaelis-Menten elimination and first-order SC absorption accurately described tocilizumab concentrations. Parameter estimates (Table 1) were consistent with earlier results [1]. Tocilizumab clearance increases with weight (BW). For IV1, steady-state Ctrough (ssCtrough) was 30 % lower for BW $<$ 60 kg and 65 % higher for BW $>$ 100 kg compared with BW $=$ 60–100 kg. For SC1 (SC2), ssCtrough was 48 % (122 %) higher for BW $<$ 60 kg and 46 % (78 %) lower for BW $>$ 100 kg compared with BW $=$ 60-100 kg. Nonlinear clearance was more prevalent at low concentrations which led to stronger weight-dependence

Table 1 Parameter estimates for the final PK model

Parameter	Estimate	%RSE
CL (L/day)	0.216	1.18
V_2 (L)	4.51	1.61
Q (L/day)	0.274	2.2
V_3 (L)	2.77	1.7
V_M (mg/L/day)	1.85	1.04
K_M (mcg/mL)	0.343	2.49
ka (l/day)	0.233	2.68
Fsc	0.795	1.05
CL_{WT}, Q_{WT}	0.512	4.36
$V_{2,WT}$, $V_{3,WT}$	0.683	3.86
CL_{HDL}	−0.256	10.9
$V_{albumin}$	−0.672	9.38
$V_{protein}$	0.728	12.2
$V_{M,CRCLN}$	0.229	7.43
$K_{a,age}$	−0.442	17.2
$K_{a,study}$	0.61	3.54
$F_{SC,thigh}$	1.11	0.712
σ_{study}	1.94	3.1
ω^2_{CL}	CV = 27.6	4.49[a]
ω^2_{V2}	CV = 22.5	5.04[a]
$R\omega_{V2}\omega_{V3}$	R = 0.661	8.26[a]
ω^2_{V3}	CV = 30.3	7.22[a]
ω^2_{ka}	CV = 46.5	6.3[a]
ω^2_{EPS}	CV = 53.8	3.72[a]
σ^2	CV = 20.7	3.99[a]

[a] % RSE for the estimate of variance

of exposure for SC2 compared to SC1. Apart from WT effect on linear clearance and volume parameters, no other covariates had clinically relevant effects on tocilizumab PK. ssCmean was similar for SC1 (49.1 μg/mL) and IV1 (58.7 μg/mL), while trough concentrations were 2.4-fold higher (45.3 vs. 18.8 μg/mL) and peak concentrations 3-fold lower (51.3 vs. 152.7 μg/mL) following SC1. Nonlinear clearance led to more than dose-proportional increase in exposure for SC1 and SC2, with ssCtrough (ssCmean) of 45.3 μg/mL (49.1 μg/mL) and 5.9 μg/mL (10.3 μg/mL), respectively.

Conclusions: The model indicated that nearly complete target saturation was achieved at steady-state during the entire dosing interval for 162 mg QW SC and 8 mg/kg Q4 W IV regimens. For 162 mg Q2 W SC regimen, the target-mediated elimination pathway was not completely saturated at steady-state, which led to high total clearance and high fluctuation of clearance over the entire dosing interval.

References:

[1] Frey N, Grange S, Woodworth T. J.Clin.Pharmacol. 2010;50(7):754–66

W-027

Tutorial: Advanced Phoenix Nlme Capabilities

Samer Mouksassi*, Serge Guzy

Pharsight, Montreal, QC, Canada

Objectives: User-friendly software with a modern graphical user interface is an important component into training junior scientists in the science of pharmacometrics. Since launch of Phoenix NLME® 1.0 under the Phoenix® platform the modelling capabilities has been improving with each release and the current objective is to highlight some new and advanced features in Phoenix NLME® 1.4 (currently in beta testing) which is scheduled to be released later in 2014.

Methods: Several sources were used to select case studies. The first source was users' feedback and questions through a public extranet website. The second source was real life projects where the 1.4 beta capabilities were required. The third source was from academic PhD students.

Results: The following case studies were selected and successfully implemented: (1) Specifying complex dosing regimens including asymmetric steady state dosing where different doses are given in the morning and in the evening. (2) Absolute Neutrophil Count model of myelosuppression after Paclitaxel administration. (3) Tumor growth inhibition based on animal data and using the Simeoni et al. model. (4) Joint Modeling of a longitudinal biomarker and a time to event endpoint with the possibility to incorporate interval censoring. The tested parametric survival sub-models were the Weibull and the exponential distributions. The graphical model editor helped to generate 90 % of the code in all cases. Not only does it support differential equations but it also had several built in statements that considerably reduced the writing of required code. For example the event statement generates the hazard and cumulative hazard differential equations behind the scenes. A very helpful feature is the initial estimates tab where the users can see the model predictions "live" with the ability to interactively move parameters estimates and visualize the corresponding model predictions. The final code with comments for each Case Study will be detailed in the poster.

Conclusion: Phoenix NLME® 1.4 under the Phoenix® interface provides powerful modelling and simulation tools. This tutorial is to guide users into implementing more advanced models into their daily workflow.

W-028

Population Pharmacokinetic and Pharmacodynamic Analysis of Tesamorelin in HIV-Infected Patients and Healthy Volunteers

Mario González-Sales[1,2,*], Olivier Barrière[2], Pierre Olivier Tremblay[2], Fahima Nekka[1] Fethi Trabelsi[3], Marie-Helene Valle[3], Jean-Claude Mamputu[4], Diane Potvin[4], Sylvie Boudreault[2], Mario Tanguay[2]

[1] Université de Montreal, Montreal, QC, Canada; [2] Inventiv Health Clinical, Montreal, QC, Canada; [3] PharmaNet Canada Inc., Montreal, QC, Canada; [4] Theratechnologies Inc, Montreal, QC, Canada

Objectives: To characterize the time course of the selected pharmacodynamics markers of tesamorelin: growth hormone (GH) and insulin-like growth factor (IGF-1) concentrations, after subcutaneous administration of tesamorelin in HIV-infected patients and healthy volunteers.

Methods: A total of 41 patients receiving doses of 1 or 2 mg of tesamorelin daily during 14 consecutive days were included in this analysis. A previously developed population pharmacokinetic model of tesamorelin [1] was used as input function for the population pharmacokinetic and pharmacodynamics (PK/PD) models of GH and IGF-1. Indirect response models were used to describe the data. Model parameters were estimated using NONMEM® VII. The effect of the selected covariates on the model parameters was also evaluated. The models were qualified using predictive checks.

Results: For GH the typical values (between-subject variability; %) of the k_{in}, Base, E_{max}, EC_{50} and Hill were estimated to be 339 ng/L/h, 256 ng/L (22.9 %), 84.2 (42.5 %), 338 ng/L and 2.43, respectively. BMI was associated with E_{max} and explained a 20.7 % of its between subject variability. For IGF-1 the typical values (between-subject variability; %) of the k_{in}, Base, and α were estimated to be 1,170 ng/L/h, 168 µg/L (27.7 %) and 0.0193 L/ng (23.9 %), respectively. Within the range of values evaluated none covariates were associated with IGF-1 models parameters. Models evaluation procedures indicated accurate prediction of the pharmacodynamics-selected markers.
Conclusions: The time course of GH and IGF-1 concentrations following multiple doses of tesamorelin were well predicted by the PK/PD models developed using phase I data. Dose adjustment of tesamorelin based on BMI might be advisable.

References:

1. González-Sales M, Barrière O, Tremblay PO, et al. Population pharmacokinetic analysis of tesamorelin in HIV-infected patients and healthy volunteers [Submitted]

W-029

Baseline Modeling of Circadian Testosterone in Hypogonadal Men with a Stretched Cosine Function

Olivier Barrière[1,*], Mario González-Sales[1,2], Julie Desrochers[1], Pierre Olivier Tremblay[1], Fahima Nekka[2], Mario Tanguay[1]

[1] Inventiv Health Clinical, Montreal, QC, Canada; [2] Université de Montreal, Montreal, QC, Canada

Objectives: To characterize the circadian rhythm of the testosterone levels in hypogonadal men.
Methods: A total of 937 profiles from 259 hypogonadal men were included in this analysis. The circadian rhythm is usually described by a standard cosine function [1], which implies that the increasing and the decreasing behaviors are symmetric. A stretched cosine function parameterized by Tpeak, Tnadir, Amp and Base, within a 24 h cycle, was defined. It allows the time between Tpeak and Tnadir to be different from 12 h in order to model the slow increase and fast decrease observed in the dataset. Model parameters were estimated using NONMEM® 7.3. The effect of age, height, weight, BMI, race, ethnicity, smoking status and season on the model parameters was evaluated. The model was qualified using predictive checks.
Results: The typical values (between-subject variability; %) of the Tpeak, Tnadir, Amp and Base were estimated to be 9:17 clock time (13.9 %), 14:36 clock time (19.7 %), 32.5 ng/dL (48.9 %) and 239 ng/dL (24.9 %). The stretched cosine function undoubtedly improved the data goodness of fit compared to the standard trigonometric function ($p < 0.001$; DOFV $= -499$). The age and the season defined as winter and spring versus summer and fall were significantly associated with the testosterone baseline levels ($p < 0.001$; DOFV $= -39.0$) and ($p < 0.001$; DOFV $= -34.2$), respectively. Models evaluation procedures indicated accurate prediction of the circadian testosterone rhythm.
Conclusions: Circadian testosterone rhythm was well predicted by the stretched cosine function developed. Testosterone levels are 7.31 % higher during winter and spring compared to summer and fall, and decrease by 3 % every 10 years.

References:

1. Han S, Lee J, Jean S, et al. Mixed-effect circadian rhythm model for human erythrocyte acetylcholinesterase activity-application to the proof of concept of cholinesterase inhibition by acorn extract in healthy subjects with galantamine as positive control. Eur J Clin Pharmacol. 2012; 68: 599–605

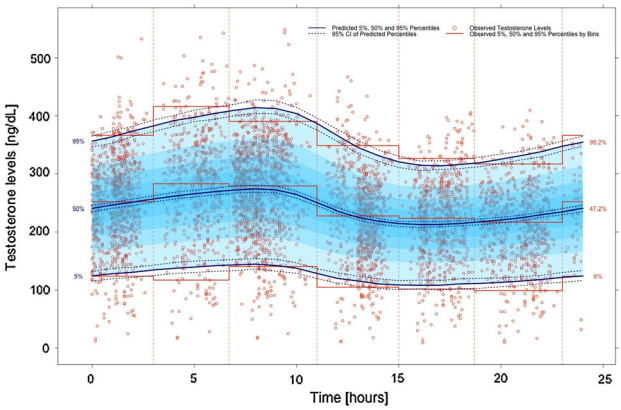

W-030

Validation and Control of R as a Key Tool for Modelling & Simulation

Andy Nicholls, Kate Hanley, Richard Chandler-Mant, Chris Campbell, Aimee Gott, Andrew Dyer, Michael Creed, Richard Pugh*

Mango Solutions, Chippenham, UK

Objectives:The R language is fast becoming a key tool to support M&S work. R is used primarily as a graphical tool, but is increasing used for a wider range of modellers' activities (from data preparation, to modelling, to simulation and reporting).
Within the heavily regulated life sciences arena, the onus is on the pharmaceutical companies to provide documented evidence to show that the software used consistently produces expected results. The flexible "package" structure of R, together with its open source nature, can present significant challenges when it comes to validating this key tool.

The aim of this work is to design an approach (and technologies) to support the validation and management of R for M&S teams.
Methods: Mango worked with modellers at a number of companies to understand the required capabilities (packages) and flexibility in terms of workflow and extensibility. Simultaneously, Mango engaged with the corresponding IT and QA teams to understand the validation and management requirements for a technology such as R.
Based on this, Mango designed a process to:

- Assess the quality of a package
- Identify any additional tests required
- Validate an "individual" package

In addition, Mango designed an approach to combine required packages (and dependencies) into a validated R "build", together with sufficient documentation to support the QA process. Working with IT teams, Mango also designed and created technologies to allow for the installation, management and deployment of validated (platform specific) R builds onto desktop, server, grid or cloud infrastructure via a simple installer.
Results: The approach (and associated technologies) created have been proven to provide an effective basis for the validation of R for an M&S team. This has enabled a number of IT teams to deliver qualified builds of R (containing functionality desired) to modellers in order to support regulatory work.
Conclusions: The approach design by Mango allows for the deployment of "validated" builds of R.

W-031

Development of a Plasma/Lung Population Pharmacokinetic Model for GSK1322322

John Zhu[1,*], Keith Rodvold[2], Etienne Dumont[3], David Tenero[1]

[1] GlaxoSmithKline, King of Prussia, PA, USA; [2] University of Illinois at Chicago, Chicago, IL, USA; [3] GlaxoSmithKline, Collegeville, PA, USA

Objectives: Develop a plasma/lung population pharmacokinetic (PK) model using Phase I data.
Methods: A plasma three-compartment model was initially developed using NONMEM based on healthy volunteer data from six Phase I studies in which subjects received single or multiple bid doses of 500–1,500 mg GSK1322322 orally (as powder-in-bottle or tablet formulations) or 500–3,000 mg GSK1322322 intravenously (IV). Covariates (body weight, CLcr, age, race, gender) were added to the base model using step-wise forward addition, and a final plasma model was obtained. Seventeen epithelial-lining-fluid (ELF) data points from a single bronchoalveolar lavage (BAL) sample at 2, 6, or 12 h post-dose in 17 subjects after multiple bid IV doses of 1500 mg from one of the studies were added to the plasma dataset and simultaneously analyzed. ELF concentration data were described by being placed into one of the two peripheral compartments with a distribution factor to account for differences between total plasma and ELF concentrations. Both the final plasma model and plasma/lung model were evaluated with bootstrap analysis and visual predictive check.
Results: Plasma data were best described by a three-compartment model (ADVAN12 subroutine) with CLcr as a covariate on clearance (CL). The distribution factor to account for differences between plasma and ELF concentrations was 1.4. Parameter and variability estimates were similar when plasma data were modeled alone compared to in combination with ELF data. Pharmacokinetic parameters were precisely estimated (RSE 0.6–27.6 %). Inter-individual variability (IIV) estimates ranged 18.1–96.2 % for CL, V2, Q3, V3, F, and Ka. No IIV on Q4, V4, and ALAG was needed. Separate residual error estimates were determined for plasma (CV 38.3 %) and ELF (CV 41.5 %) data.
Conclusions: A three-compartment plasma/lung population PK model was developed to describe plasma and ELF concentration-time data for GSK1322322. The distribution factor of 1.4 shows good penetration of GSK1322322 into ELF. The model can be used to support dose selection for clinical studies in patients with pneumonia.
Funded by GSK.

W-032

Model-Based Meta-analysis of Longitudinal Clinician Administered PTSD Scale (CAPS) for Post Traumatic Stress Disorder (PTSD)

Francois Gaudreault[1,*], Tim Nicholas[2], Danny Chen[1]

[1] PTx Neuroscience Clinical Pharmacology, Pfizer, Cambridge, MA, USA; [2] Pharmacometrics, Pfizer, Groton, CT, USA

Objectives: The objective of this analysis was to assess the longitudinal responses to traumatic events, as measured by CAPS, in patients with primary diagnosis of PTSD. The CAPS is the gold standard in PTSD assessment and the quantitative understanding of the progression of PTSD symptoms is as of yet incomplete.
Methods: A database was developed by a systemic search for all publicly and internally available efficacy information of SSRIs drugs evaluated for the treatment of PTSD. The time-course of change from baseline for the 17 core symptoms was analyzed based on summary-level data for ~4,418 patients in 17 placebo controlled trials using an exponential model as follow:

$$Yij = \alpha \cdot \theta \cdot (1 - e^{-k \cdot time}) + \epsilon_{ij}$$

where Y represent the observation from the ith study at the jth time, α is the drug effect on the asymptote (θ), k is the rate constant for the disease progression and ε_{ij} represents the residual unexplained subjects-weighted (N_{ij}) random effect. Between subjects variability was included on the asymptote. Model parameters were estimated using NONMEM 7.2. Stochastic simulations were performed to assess the predictive power of the model.
Results: The placebo effect was estimated to be a reduction of 25.3 [−28.8, −21.9] points in CAPS after 12 weeks. SSRIs effect was separable from placebo effect with an estimated mean placebo adjusted drugs effect of −6.68 [−8.92, −4.41] after 12 weeks of treatment. The minimum time to reach a clinically meaningful effect was estimated to be 1 week, with a 1.68 [−2.34, −1.03] points reduction.
Conclusions: Overall, placebo response for PTSD is consistently significant and needed to be accounted for in designing PTSD trials. These results suggest that trial duration of at least 1 week would be required to observe clinically meaningful separation of SSRIs response from placebo.

W-033

Effects of Tocilizumab on DAS28 in Patients with Rheumatoid Arthritis (RA)

Leonid Gibiansky[1], Nicolas Frey[2], Joy C. Hsu[3,*]

[1] QuantPharm LLC, North Potomac, MD, USA; [2] F. Hoffmann-La Roche Ltd., Pharma Research and Early Development, Roche Innovation Center, Basel, Switzerland; [3] Roche TCRC, Inc. Pharma Research and Early Development, Roche Innovation Center, New York, NY, USA

Objectives: Tocilizumab is a recombinant humanized anti-IL-6R monoclonal antibody. The analysis aimed to establish a predictive population PK-PD model that describes DAS28 time-course following administration of 8 mg/kg IV Q4 W (IV1), 162 mg SC QW (SC1) and Q2 W (SC2) tocilizumab, or placebo, including identification of covariate factors influencing PK-DAS28 relationships.
Methods: DAS28 observations (13,998) of 1890 RA patients from two Phase III studies were analyzed. Tocilizumab concentrations were predicted using the population PK model developed earlier. Impact of identified covariates was investigated by simulations.
Results: The indirect-response model with an inhibitory Emax effect on DAS28 "production" rate by tocilizumab concentrations adequately described the time-course of DAS28. Model parameters were estimated precisely (Table 1). The population mean of the maximum effect of tocilizumab corresponded to 56.5 % reduction of DAS28 from baseline (ΔDAS28). The relationship between tocilizumab concentrations and DAS28 was independent of route of administration. The efficacy of tocilizumab was similar for IV1 and SC1 regimens (50 % ΔDAS28), and was higher compared to SC2 (41 % ΔDAS28). Following 24 weeks of treatment, ΔDAS28 was predicted to be 50 % for IV1 and SC1 regimens, and 41 % for SC2 regimen. No covariates, including presence of neutralizing anti-tocilizumab antibodies had a clinical impact on the effect of tocilizumab on DAS28.
Conclusions: The indirect-response model with an inhibitory effect on DAS28 "production" rate by tocilizumab serum concentrations adequately described the magnitude and the time-course of DAS28

Table 1 Parameter estimates for the final model

Parameter	Estimate	%RSE	Parameter	Estimate	%RSE
EC_{50} (μg/mL)	1.86	12.8	$L_{Emax,IL6}$	−0.457	19.9
LE_{max}	0.77	3.46	ω^2_{EC50}	CV = 135 %	12.1[a]
k_{out} (1/day)	0.0402	2.33	$R\omega_{EC50}\omega_{BASE}$	R = 0.317	25.6[a]
BASE (DAS28)	6.67	0.289	ω^2_{BASE}	CV = 44.7 %	9.18[a]
C_{DMAHD}	0.581	16.7	$R\omega_{EC50}\omega_{kout}$	R = 0.455	19.3[a]
$BASE_{CRP}$	0.02	11.3	$R\omega_{kout}\omega_{BASE}$	R = −0.622	9.37[a]
$BASE_{HAQ}$	0.0962	8.18	ω^2_{kout}	CV = 62.9 %	7.56[a]
$BASE_{PAIN}$	0.103	7.95	$R\omega_{LEmax}\omega_{BASE}$	R = 0.176	34.5[a]
$BASE_{VASP}$	0.134	7.45	$R\omega_{LEmax}\omega_{kout}$	R = 0.144	34.7[a]
$LE_{max,SEX}$	0.641	6.08	ω^2_{LEmax}	CV = 81.4 %	5.58[a]
$LE_{max,AGE}$	0.594	15.2	σ^2	SD = 0.676	1.09[a]
Derived parameter: Emax = 1 (1 + LEmax)					
$E_{max,females}$	0.565				
$E_{max,males}$	0.670				

"System-related" parameters: BASE = DAS28 score, k_{out} = rate constant of elimination of DAS28

"Drug-related"parameters: E_{max} = maximal inhibition of K_{in}, EC_{50} = tocilizumab serum concentration at half of the effect, C_{DMARD} = parameter describing the effect of DMARD medications

HAQ baseline health assessment questionnaire, *VASP* physicians global score of disease activity at baseline, *PAIN* patient's assessment of pain at baseline, CRP = C-reactive protein concentration at baseline, *IL6: IL6* concentration at baseline

[a] %RSE for the estimate of (co)variance

score reduction following both IV and SC administrations. There were no differences in the exposure-response relationships between the IV and SC administrations. Similar to the PK-safety relationship (shown on another poster at this conference), the PK-efficacy relationship of tocilizumab are similar for 8 mg/kg IV Q4 W and 162 mg SC QW dosing regimens, and the efficacy for the 162 mg SC QW was higher than that of the 162 mg Q2 W SC regimen.

W-034

Rationale for PML Design

Michael R. Dunlavey*, Robert H. Leary

Certara/Pharsight Corp, St. Louis, MO, USA

Objectives: Explain the rationale behind the design of the Pharsight Modeling Language, how and why it is similar to and differs from other modeling languages used in pharmacometrics.
Results: PML uses the same semantics as other nonlinear mixed-effect modeling languages, where there are fixed effects, random effects, and observational error. It differs in that it follows the principle that the language should describe the problem, not the solution. To this end, (1) It simplifies the writing of unusual models, such as enterohepatic reflux, time-to-event, count, ordinal, bql, etc. (2) It is not necessary to rewrite the model if a different ODE solver is used, or a different model fitting engine. It makes heavy use of symbolic differentiation to accomplish this. (3) It is embeddable in an existing statistics-oriented language (R), facilitating orchestration of model development from within scripts. (4) It facilitates the inclusion of fitted models, without transcription errors, into trial simulation models.

References:

1. Certara Corp. "Phoenix 1.4 Modeling Language Reference Guide.pdf"

W-035

Effects of Tocilizumab on Neutrophil Counts in Patients with Rheumatoid Arthritis (RA)

Leonid Gibiansky[1], Nicolas Frey[2], Joy C. Hsu[3]

[1] QuantPharm LLC, North Potomac, MD, USA; [2] F. Hoffmann-La Roche Ltd., Pharma Research and Early Development, Roche Innovation Center, Basel, Switzerland; [3] Roche TCRC, Inc. Pharma Research and Early Development, Roche Innovation Center, New York, NY, USA

Objectives: Tocilizumab is a recombinant humanized anti-IL-6R monoclonal antibody. The analysis aimed to establish a predictive population PK-PD model that describes the time-course of peripheral neutrophil counts (NTC) following tocilizumab administration of 8 mg/kg IV Q4 W (IV1), 162 mg SC QW (SC1) and Q2 W (SC2) regimens, or placebo, including identification of covariate factors influencing PK-NTC relationships.
Methods: NTC observations (15,870) of 1887 RA patients from two Phase III studies were analyzed. Tocilizumab concentrations were predicted using the population PK model developed earlier. Impact of identified covariates was investigated by simulations.

Table 1 Parameter estimates for the final model

Parameter	Estimate	%RSE
BASE (10^9/L)	4.70	1.22
k_{out}(1/day)	0.206	7.69
EC_{50} (μg/mL)	6.67	4.76
Emax	0.832	2.21
γ	1.85	4.98
$BASE_{CRP}$	0.102	5.84
$BASE_{PCOR}$	1.23	1.47
$BASE_{SMK}$	1.18	1.87
$k_{out,AGE}$	0.676	16.4
$EC_{50,SEX}$	0.78	11.3
$E_{max,CRP}$	0.0635	25.4
$E_{max,IL6}$	0.665	9.3
ω^2_{BASE}	CV = 28.4 %	3.66[a]
ω^2_{kout}	CV = 152 %	12.1[a]
ω^2_{EC50}	CV = 88.8 %	12.1[a]
ω^2_{EMAX}	CV = 52.8 %	6.47[a]
σ^2	CV = 23.0 %	1.01[a]

BASE baseline NTC, k_{out} rate constant of NTC elimination, *Emax* maximal stimulation of k_{out}, *EC50* tocilizumab concentration at half of the effect, γ sigmoidicity parameter, *PCOR* previous treatment with corticosteroids

a %RSE for the estimate of variance

Results: The indirect-response model with stimulatory Hill effect on NTC elimination by tocilizumab provided an excellent fit of the observed NTC data. The relationship between neutrophil counts and tocilizumab concentration is independent of the route of administration. The parameter estimates (Table 1) translate into 3.36 days half-life of the effect, 45 % maximal decrease of NTC from baseline, and the lowest possible NTC level of 2.56×10^9/L. The effect of tocilizumab on NTC was smaller and fluctuations were larger for SC2 compared to SC1 and IV1 regimens. The effects were similar for SC1 and IV1 regimens.
Six covariates remained in the final PK/PD model: C-reactive protein (CRP) and IL-6 levels at baseline, previous administration of corticosteroids, smoking, age, and gender. No covariate, including presence of neutralizing anti-tocilizumab antibodies, was found to have a clinical impact on the effect of tocilizumab on circulating neutrophil counts.
Conclusions: The NTC time-course following IV and SC administration of tocilizumab was well described by the indirect-response model with stimulation of elimination. Analyses results have confirmed that there were no differences in exposure-response relationships between the IV and SC administrations. Similar to the PK-efficacy relationship (shown on another poster at this conference), the PK-safety relationship of tocilizumab are similar for 8 mg/kg IV Q4 W and 162 mg SC QW regimens.

W-036

Oncology Phase I Trial: Increasing the Chance to Detect Treatment Effects using a Model Based Approach

Sylvie Retout[1], Gwen Nichols[2], Olga Rutman[2], Joy C. Hsu[2,*], Alex Phipps[3]

[1] Pharma Research and Early Development, Roche Innovation Center Basel, Basel, Switzerland; [2] Innovation Center, New York, NY, USA; [3] Roche Innovation Center Welwyn, UK

Objectives: We recently demonstrated [1], on a large simulated dataset, that assessing the change in tumor growth rate (TGR) using tumor burden assessments prior to treatment [2] provides higher sensitivity (Se) to true treatment effect (TTE) of antitumor agent than RECIST criterion. Here, the objectives are to further challenge the ability of the Growth Rate Based Method (GRBM) to detect a TTE as well as a dose response relationship when considering a real Phase I setting.
Methods: 500 phase I trials of 30 of patients divided into 6 dose groups were simulated. Individual observations of the sum of the longest diameters (SLD) were generated, assuming CT scans at two points before treatment initiation (TI) (between [8–4] weeks and between 2 weeks and one day before TI) and at 8 and 16 weeks after TI. A Gompertz growth model with a high variable TGR distribution, as encountered in phase I was assumed. Population analyses of the simulated trials were performed using NONMEM. TTE was defined as the difference between the simulated SLDs at 16 weeks with and without treatment. GRBM response was defined as the model-predicted difference between the SLD's with and without treatment. Probability of correctly classifying a patient as responder or non-responder and ability to detect graphically a dose response were assessed for both RECIST and GRBM.
Results: The performance of GRBM was consistently good over the 500 trial replicates to 1—detect a TTE (median Se $\sim$ 83% vs. only $\sim$23% for RECIST) 2—provide relevant dose response signal (much noisier with RECIST).
Conclusions: Assessing TGR before and during treatment provides a higher chance to detect TTE in a heterogeneous TGR phase 1 setting.

References:

1. Retout et al, ACOP 2013
2. Gomez-Roca et al, Eur J Cancer 2011

W-037

The Task Execution Language (TEL) for DDMoRe: Providing the "Glue" for Modellers

Jonathan Chard[1,*], Mike K. Smith[2], Kate Hanley[1], Henrik B. Nyberg[1]

[1] Mango Solutions; [2] Pfizer

The Drug Disease Model Resources (DDMoRe) consortium builds a public drug and disease model library and an open source interoperability framework containing standards and tools to cover the identified gaps in the Modelling & Simulation software ecosystem. Users of the DDMoRe framework will interact with models via the Modelling Description Language (MDL) comprising the Model Coding Language (MCL) and Task Execution Language (TEL). If the MCL defines "nouns" in the modelling language, then TEL defines the "verbs". Thus TEL says "DO ≪THIS≫ using ≪THESE MCL OBJECTS≫". Through the TEL, the user can bring together the elements of the MCL necessary to perform given modelling and simulation tasks and combine these to create workflow steps. The modularity of MCL allows the user to change data or design, parameters and task properties easily to perform several different tasks using the same model. TEL allows the user to define tasks, execute these tasks, work with the MCL objects and access outputs from the modelling tasks for inference and post-processing. TEL is written in R in order to leverage existing tools and functionality within that language. TEL needs to be able to read in and work with MCL elements defined with a brand new language, read "raw" ASCII output from the different modeling tools, and interface with tools hosted in a variety of environments, from local to grid. Using a dedicated Integrated Development Environment (IDE), we will demonstrate how R can leverage this new language, integrate remote services, and use a common output standard to exchange this information between packages such as xpose4, RNMImport and PFIM, and new functionality such as the clinical trial simulation engine Simulx. We will also show how TEL provides users access to low level functions to enable them to write their own, more complex workflows that will be repeatable across models.

Keywords: TEL, DDMoRe, Modelling, Simulation, DSL

This work is part of the DDMoRe project (www.ddmore.eu).

W-038

Evaluation of Methods to Predict Joint Probability of PK/PD Target Attainment in the Development of β-Lactam (BL) and β-Lactamase Inhibitor (BLI) Combination Antibiotics

Jianguo Li*, Diansong Zhou, Nidal Al-Huniti

Quantitative Clinical Pharmacology, AstraZeneca, Waltham, MA, USA

Objectives: To evaluate methods to estimate joint probability of PK/PD target attainment (JPTA) in dose determination for Phase 2b/3 studies in the development of BL and BLI combination.
Methods: JPTAs for piperacillin (PIP) and tazobactam (TAZ), 30 % free PIP concentration above minimum inhibition concentration (% fT > MIC) and the same time of free TAZ concentration above a threshold concentration (% fT > CT), were evaluated using 5 methods (M1–M5) and compared to a "true" JPTA for PIP-TAZ dose

Table 1 Predicted median (5th and 95th percentile) of JPTAs for the 3 cases of BSVs for PIP and TAZ PK

Method	Description	25 % BSV	50 % BSV	75 % BSV
M0	Simulation of the true "PTA" with the literature reported Pop PK models of PIP and TAZ and correlation of PK parameters [2, 3] for a large population	99.9	94.2	83.1
M1	PopPK modeling and PTA calculation for PIP and TAZ are independently implemented, and the JPTA was calculated as the product of individual PTA of PIP and TAZ, respectively	99.9 (99.7, 100)	93.8 (92.6, 94.7)	79.9 (78.6, 81.1)
M2	The same as M1 except that PTA calculations for PIP and TAZ were based on the same c.ovariates and meeting the PK/PD targets of PIP and TAZ simultaneously for each individual subject	99.9 (99.7, 100)	96.0 (95.2, 96.9)	87.4 (86.4, 88.2)
M3	M3: the same as M2, but correlations of between subject variability (BSV) between PIP and TAZ were estimated post hoc and used for the PTA calculation	99.9 (99.7, 100)	96.1 (95.2, 96.9)	85.8 (84.8, 86.7)
M4	PIP and TAZ were modelled simultaneously with the correlation between BSVs of PIP and TAZ being estimated, and the joint PopPK models of PIP and TAZ was used for the JPTA simulation	99.9 (99.6, 100)	95.9 (95.1, 96.7)	85.5 (84.4, 86.4)
M5	The same as M4, but uncertainty of parameter estimates were included to the PTA calculation	99.9 (99.6, 100)	95.4 (94.5, 96.2)	84.5 (83.4, 85.5)

regimen of 3.75 mg, 0.5 h infusion every 6 h. The detailed descriptions for the calculation of "true" JPTA (M0) and each method of M1-M5 are shown in the Table 1. The MIC used in the JPTA calculation was the PIP-TAZ non-species specific PK-PD breakpoint (8 mg/L), while the stringent CT of 2 mg/L was used for TAZ [1]. Three cases of between subject variability (BSV) for clearance and volume of distribution of PIP and TAZ, small (25 %), medium (50 %) and large (75 %), were examined for the impact of the magnitude of BSVs on JPTA prediction. 100 data sets each with 100 subjects were simulated, and each data set was re-fit for PIP and TAZ separately or simultaneously according to M1-M5 methods.

Results: The calculated "true" JPTA by M0, and predicted median, 5th and 95th percentiles of JPTAs from the 100 simulated data sets for the joint PK/PD targets are shown in the Table 1.

Conclusions: While M5 produced the least biased prediction of JPTAs among 5 methods, M3 is a resource-saving method and produced similar JPTA predictions to M5. M2 could be used reasonably to predict JPTAs for small and medium BSVs of PK for the BL and BLI. The larger the BSV, the lower the JPTA.

References:

1. Nicasio et al. Poster A-298, 2013 ICAAC Denver
2. Li et al. J Antimicrob Chemother, 2005,56:388–395
3. Shoji et al, Br J Clin Pharmacol, 2013,77:509–521

W-039

Model-Based-Meta-Analysis of Longitudinal MATRICS Consensus Cognitive Battery (MCCB) for Cognitive Impairment Associated with Schizophrenia (CIAS)[a]

Francois Gaudreault*, Beesan Tan, Jing Liu, Danny Chen

Pfizer Worldwide Research and Development, Cambridge, MA, USA

Objectives: The objective of this analysis was to assess the longitudinal cognitive performance, as measured by MCCB, in chronic stable schizophrenic patients using literature data. MCCB is the standard battery in measuring the cognition outcome and given its novelty, there is a lack of quantitative understanding of the progression of cognitive function in CIAS.

Methods: A systematic literature search was conducted using public databases for randomized clinical trials with reported MCCB scores. The time-course of change from baseline for composite score and each domain score were analyzed separately based on summary-level data for 686 patients in 8 placebo controlled trials using an Emax model in NONMEM. The general model building strategy involved modeling the placebo effect first and then adding the treatment effect as a covariate on Emax.

Results: Time-dependent placebo effect was observed in MCCB Composite Score and sub-domain scores except for Social Cognition. The average time to reach 50 % of maximum placebo effect (ET50) was estimated to be 8.46 $\pm$ 4.31 weeks for the Composite score, with a shorter ET50 for the Working memory (WM) domain (4.37 $\pm$ 2.23 weeks). Treatment effect was separable from placebo effect for Composite and WM scores, suggesting that WM might be a more sensitive endpoint compared to Composite Score and other domain scores for early signal of detection.

Conclusions: Despite the limited data, results of this analysis have provided some important consideration in designing future clinical trials in CIAS. Overall, placebo response for MCCB is consistently significant and highly variable for these trials. In order to fully capture cognitive performance in CIAS trials, longer study duration is needed.

To this end, WM might be more suitable for early signal of detection if this is the relevant cognition domain in a CIAS trial.

[a] The results in this abstract have been previously presented in part at ASCPT 2012, National Harbor, Maryland and published in the conference proceedings as abstract PI-57.

W-040

Pharmacokinetic/Viral Kinetic Modeling of Early Viral Kinetics in Different Hepatitis C Virus Ggenotypes During Alisporivir Monotherapy or in Combination with Peg-IFN

Thi Huyen Tram Nguyen[1,2], France Mentré[1,2], Jing Yu[3], Micha Levi[4], Jérémie Guedj[1,2,*]

[1] IAME, INSERM UMR 1137, University Paris Diderot, 75018 Paris, France; [2] University Paris Diderot, Sorbonne Paris Cité, Paris, France; [3] Novartis Institutes for BioMedical Research, Inc, Cambridge, MA 02139, USA; [4] Novartis Pharmaceutical Corp., East Hanover, NJ 07936, USA

Alisporivir (ALV) is a first in class cyclophilin inhibitor in clinical development with potent activity against hepatitis C virus (HCV) [1]. Here we aimed to estimate the antiviral effectiveness of combination treatment with ALV and pegylated Inteferon (Peg-IFN) in patients infected with different HCV genotypes (GT 1, 2, 3, 4). For that purpose we analyzed the pharmacokinetics (PK) of both drugs and the viral kinetics (VK) observed in 88 patients treated for four weeks with different doses of ALV (200, 600 or 1000 mg) +/− weekly injections of Peg-IFN (Study DEBIO-025-A2203) [2]. The PK of ALV was best described by a two compartment model with Michaelis-Menten elimination and time-dependent bioavailability. Further we found a significant effect of Peg-IFN on the clearance of ALV. PK model predictions of ALV and Peg-IFN were used as a driving function for the viral kinetic model [3]. A model assuming multiplicative effect of both agents (ALV and Peg-IFN) in blocking viral production could describe well the viral load data and allow teasing out the effects of ALV and Peg-IFN. GT was found to significantly affect Peg-IFN effectiveness, ε^{IFN} (median $\varepsilon = 86.3$ and 99.1 % in HCV GT-1/4 and GT-2/3, respectively, $p = 10^{-7}$) and the infected cells' half-life, $t_{1/2}$ (mean $t_{1/2} = 0.22$ vs 0.39 day^{-1} in GT-1/4 and GT-2/3, respectively, $p = 10^{-6}$). ALV's effectiveness, ε^{ALV} was not significantly different across GT and was higher at doses 600 mg QD (median $\varepsilon^{ALV} = 50.5$, 89.4, 97.1 and 93.6 % in 200, 600 and 1,000 mg dual therapy and 1,000 mg monotherapy, respectively). The model was used to simulate various ALV dosing regimens without IFN in HCV GT-2/3 patients and could well predict the virological responses observed, suggesting this model may be a useful predictive tool for ALV use with and without IFN and optimal duration of ALV treatment.

References:

1. Gallay P, Lin. Profile of alisporivir and its potential in the treatment of hepatitis C. Drug Des Devel Ther; 2013 Feb;105
2. Neumann AU, Lam NP, Dahari H, Gretch DR, Wiley TE, Layden TJ, et al. Hepatitis C viral dynamics in vivo and the antiviral efficacy of interferon-alpha therapy. Science; 1998; 282(5386):103–7

W-041

A Population PK/PD Analysis of Nebivolol and Valsartan Combination Therapy

Chun Lin Chen[1,*], Mats O. Magnusson[2], Timothy Carrothers[1], E. Niclas Jonsson[2], Parviz Ghahramani[1]

[1] Forest Research Institute, Jersey City, NJ, USA; [2] Pharmetheus AB, Uppsala, Sweden

Objectives: To develop population PK/PD models that describe the effects of placebo, nebivolol and valsartan as single drugs and as a fixed-dose combination (FDC) on both sitting cuff-measured blood pressure (BP) and 24-h ambulatory measured BP.
Methods: Population PK/PD models were developed in NONMEM V7.2.0 based on data from a recent pivotal efficacy trial (NAC-MD-01study [1]), utilizing estimates of exposure for each individual derived from population PK models. The exposure–response population included 761 patients for sitting cuff-measured BP and 746 patients for ambulatory measured BP. The BP lowering drug effects were described by Emax models with a parameter (α) to account for the interaction between compounds. The diurnal rhythm in ambulatory BP data was described by the sum of cosine functions.
Results: For sitting cuff-measured BP model, total effect was comprised of drug and placebo effect. There was no detectable placebo response in ambulatory BP data. The estimated maximum drug effects were 13 mmHg for sitting cuff-measured BP, and 14 and 19 mmHg for diastolic and systolic ambulatory measured BP, respectively. The exposure-response relationships were statistically significant in valsartan and nebivolol monotherapy as well as in all FDC arms. The α parameter was estimated to be positive in all models. The PK/PD model was further used to simulate possible dosages in mono-, and combination therapy, including dosage strengths not studied in NAC-MD-01 study. The model-predicted changes from baseline in diastolic and systolic BPs demonstrated that all FDC doses had greater BP reductions compared to their monotherapy.
Conclusion: Modeling and simulation of nebivolol and valsartan combination therapy demonstrated a partially additive effect on both sitting cuff-measured BP and 24-h ambulatory measured BP.

References:

1. Thomas Giles, et al. Efficacy and safety of nebivolol and valsartan as fixed-dose combination in hypertension, Lancet 2014

The results in this abstract have been previously presented in part at PAGE, Alicante, Spain, 2014

W-042

A Simplification of Population Pharmacokinetic Model from Physiologically Based Red Blood Cell Model and Its Application to Drug CPRC-1 in Human

Kairui Feng[2,*], Xin Zheng[1], Robert H. Leary[2], Michael R. Dunlavey[2], Wenyuan Qi[1], Hongzhong Liu[1], Pei Hu[1], Ji Jiang[1]

[1] Peking Union Medical College Hospital (PUMCH), Beijing, 100032, China; [2] Pharsight, Cary, NC 27518, USA

Drug CPRC-1 was approved into phase I evaluation of ischemic stroke in China. A nonlinear red blood cell (RBC) binding/partition was observed in clinical trial within PUMCH. The clinical observation including 7 escalation dose studies of CPRC-1 shows that both partitioning and kinetic of binding happens at the same time and it possibly has active transporters involved. However, an In Vitro B/P experiment was conducted to determine the concentration and time dependent B/P relationship. It didn't show any evidence of RBC concentration or time dependent B/P. The RBC binding model described by Hinderling [1, 2] and Jusko [3] was used for the pop-PK development but cannot fully represent the clinical data for both drug plasma and whole blood concentration.

A physiologically based red blood cell model (Fig. 1) is simplified to a semi-mechanism population pharmacokinetic model (Fig. 2) with

time-dependent kinetics of RBC binding and partitioning. The model incorporated individual measured haematocrit level as a covariate and included the kinetics of CPRC-1 in blood, erythrocytes and plasma. This simplified RBC model from a physiologically based model gets best fit comparing to the previous models [1, 2, 3] by looking at the goodness of fit such as DV versus IPRED plot and DV versus PRED, the visual predicted check (VPC) etc. In Vitro B/P experiment is not possible to provide RBC kinetic binding mechanism due to its rapid ON rate versus slow OFF rate. The developed simplification population PK model best described plasma and whole blood profiles of CPRC-1 in Chinese subjects. This model has been used for the dose selection on multiple dose clinical trial.

References:

1. P Hinderling, Kinetics of Partitioning and Binding of Digoxin and Its Analogues in the Subcompartments of Blood, J Pharma, Vol. 73, No. 8, 1984
2. P Hinderling, Red Blood Cells: A Neglected Compartment in PKPD, Pharm Reviews, 2000 Vol. 49, No. 3: 473
3. W Jusko, et al., Pharmacokinetics of tacrolimus in liver transplant patients, Clin Pharmacol Ther. 1995, 57(3):281–90

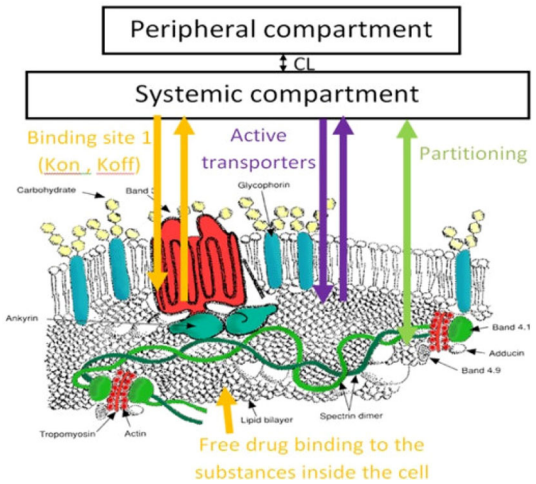

Fig. 1 .

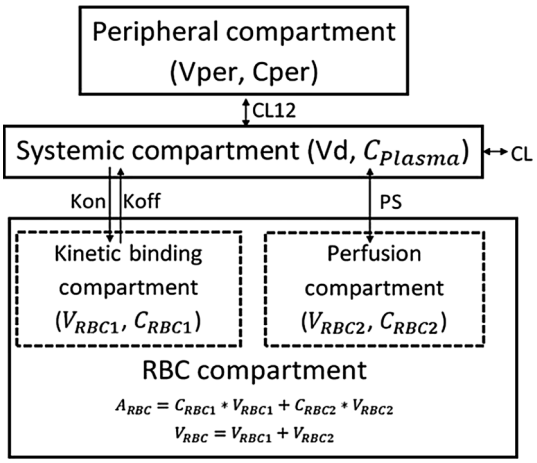

Fig. 2 .

W-043

Pharmacometric Workflow for Standardization and Automation of Population Pharmacokinetic Modeling

Nidal Al-Huniti*, Diansong Zhou, Hongmei Xu, Robert Fox, Sergey Aksenov, James Li, Craig Lambert, Donald Stanski

Quantitative Clinical Pharmacology, AstraZeneca, Waltham, MA, USA

Objectives: Population pharmacokinetic modeling (PopPK) has become a routine analysis to support internal decision making and regulatory submission. The workflow requires standardization for data analysis plan, data assembling, graphic visualization of data, modeling, simulation, and reporting. Appropriate workflow and automation will significantly streamline the analysis processes to maximize the productivity of pharmacometrician.

Methods: The developed workflow is expected to enable fast and reliable data preparation, exploratory analysis, model development and reporting that could be efficiently applied to different drugs with minimal modification. A schematic representation of the developed workflow is represented in the figure below. This is one of the approaches we are currently evaluating.

Results: The workflow is currently under evaluation for the ease of use, reliability and reproducibility. The R-scripts, model library and templates in eg. NONMEM can be stored in the secured version-controlled database and be retrieved for re-application to different projects. The standard data specification will enable the programmers to standardize SAS code for data preparation. Development and integration of specific R scripts into the workflow is a key requirement to link the whole process. The R-scripts will enable pharmacometrician to generate the same format of exploratory and diagnostic plots across different projects, to standardize model development steps, to accelerate reporting and publishing for regulatory submission. In addition the standard report template will also aid peer review efficiently.

Conclusions: PopPK modeling plays important role in the use of model-based drug development for correct decision making. AstraZeneca has planned to implement this workflow and is currently undergoing further evaluation including

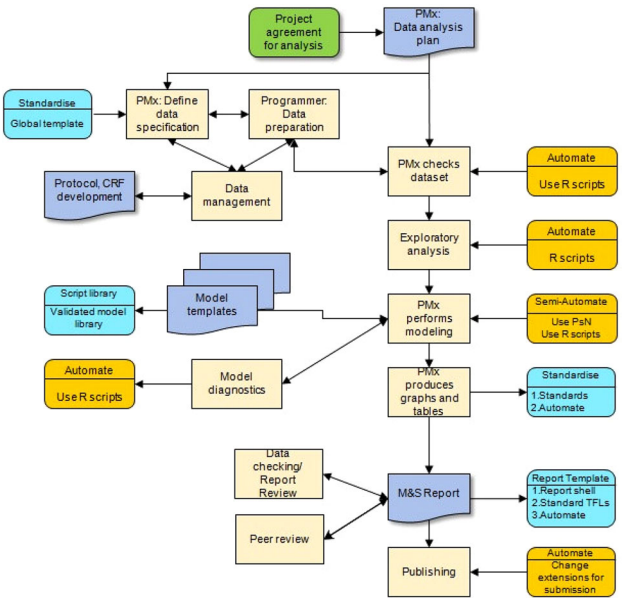

W-044

Clinical Simulations Facilitated Benralizumab Development in Adolescents with Asthma

Li Yan[1,*], Christine K. Ward[2], Lorin Roskos[2], Bing Wang[1]

[1] MedImmune, Hayward, CA, USA; [2] MedImmune, Gaithersburg, MD, USA

Objectives: Asthma in adolescents is a chronic disease with major unmet medical need. Benralizumab, a humanized afucosylated monoclonal antibody that specifically binds to interleukin-5 receptor, is currently in Phase 3 development for the treatment of asthma. Clinical simulations were conducted to determine whether adolescent can receive benralizumab adult dose (30 mg Q8W) in Phase 3 studies.
Methods: Pharmacokinetic (PK) data from two Japanese healthy volunteer studies and four early-stage studies in adult subjects with asthma simultaneously modeled using a population approach. Typical value and distribution of body weight of adolescents by gender and age were obtained from the CDC children growth charts. Such information was subsequently utilized to generate virtual adolescent asthmatic population. Stochastic simulations were performed to project and compare steady-state PK exposure in adult and adolescents with asthma at the Phase 3 dose level.
Results: Despite targeting a cell memberane-associated receptor, PK of benralizumab was dose-proportional and influenced only by body weight. Stochastic simulations demonstrated that with a 40-kg lower body weight limit, upon multiple 30 mg Q8W subcutaneous administrations, benralizumab PK in adolescents mostly overlaps with that in adults. The steady-state PK exposure difference between adolescent and adult populations is expected to be within normal range of interindividual variability in adults.
Conclusions: Stochastic simulations supported inclusion of adolescents ($\geq$40 kg) in Phase 3 studies and for them to receive the adult dosage.

W-045

Closed Form Solutions of Pharmacokinetic Models with Parallel First-Order and Michaelis–Menten Eliminations

X. Wu[1,2], J. Li[1,3,4], F. Nekka[1,3,4,*]

[1] Faculty de Pharmacie, University de Montreal, Montreal, QC, Canada; [2] Centre for Disease Modelling, York Institute for Health Research, Toronto, ON, Canada; [3] Centre de Recherches Mathmatiques, University de Montreal (CRM), Montreal, QC, Canada; [4] Centre for Applied Mathematics in Bioscience and Medicine-McGill University, Montreal, Montreal, QC, Canada

Objectives: Hormone drugs, such as granulocyte colony-stimulating factor (G-CSF), erythropoietin (EPO) and thrombopoietin (TPO), are widely used to stimulate the production of neutrophils, erythrocytes or platelets in oncology or other related diseases. Clearance of these drugs generally exhibit mixed eliminations, combining a linear renal elimination and a nonlinear internalization, with the latter being modeled as a saturable Michaelis-Menten process. Since these two routes may interact and greatly influence the performance of drug kinetics, analytic solutions of such models can offer an efficient way to demystify these drugs kinetics.
Methods: Motivated by the Lambert W function, we introduce a new W function to develop the closed forms of such models, using one compartment models with single and multiple administrations.
Results: Using W function, closed forms for single and multiple intravenous bolus administrations were obtained. The expression of elimination half-life ($t_{1/2}$) exhibits a dose-dependency and is upper limited by that of the classical first-order elimination. Moreover, we established the contribution of each elimination route and delineated dominant kinetics in terms of different model parameters. Moreover, we mathematically proved the convergence of multi-dose kinetics towards a stable kinetic status.
Conclusions: The closed forms we found can be used to facilitate the model fitting process and provide clear physiological meanings. The introduced W-function is well defined and can be easily implemented into PK/PD software packages for modeling of such combined elimination processes.

W-046

A Mechanistic Pk/Pd Model for Ropivacaine Complex Absorption During Femoral Nerve Block in Anesthetized and Unanesthetized Rabbits

Fady Thomas[1], Veronique Martin-Boyer[1], Pierre Drolet[2], France Varin[1,*]

[1] Université de Montreal, Montreal, QC, Canada; [2] Hospital Maisonneuve Rosemont, Montreal, QC, Canada

Objectives: The major challenge in developing pharmacokinetic/pharmacodynamic (PK/PD) model for local anesthetics (LAs) is their complex systemic absorption from their depot (effect site). In absence of perineural concentrations, a one-compartment model with parallel rapid inverse Gaussian (mean absorption time: 25 min) and slow time-dependent inputs (t½ of 3.9 h) best described ropivacaine plasma concentration–time curves in patients [1]. The assumption that two input functions were necessary to predict the systemic and effect site concentrations was tested in animals by measuring LAs concentrations nearby the femoral nerve by microdialysis .
Methods: A femoral nerve block (FNB) was performed with ropivacaine-HCL 0.5 % in seven anesthetized (1.8 mg/kg) and five unanesthetized rabbits (3 mg/kg). Degree of sensitive block was measured using transcutaneous electrical neurostimulation in preconditioned unanesthetized rabbits. Perineural and plasma samples were analyzed using HPLC-UV. Unbound concentration-time profiles were simultaneously fitted using NONMEM® (version VII) and subsequently linked with effect.
Results: In anesthetized rabbits, plasma and perineural profiles obtained over a 12 h-period were best described by two local (depot and tissue) and two systemic compartments (central and peripheral) with one first-order absorption rate constant (mean t½: 25.7 min) and a slower rate of release from tissue to perineural deposit compartment (mean t½: 1.5 h). In unanesthetized rabbits (Fig.1), blood sampling up to 22 h revealed a faster decline after a 10–15 h pseudoplateau, in agreement with patients data. Preliminary PK/PD analysis suggests that the slow release from the surrounding nerve tissues is the rate-limiting step for systemic absorption and determines onset of recovery, a finding also reported in patients.
Conclusions: This close agreement between animal and human data supports the assumptions previously made during modeling of ropivacaine analgesic effect in patients receiving a FNB and provides solid grounds for the development of a mechanistic PK/PD model.

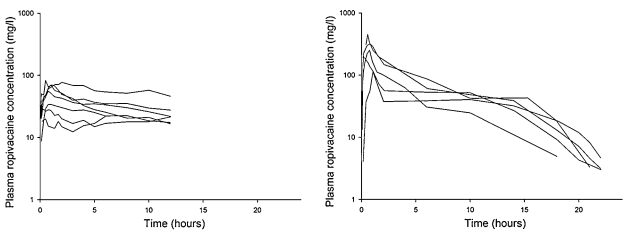

Fig. 1 Observed plasma concentration–time profiles of ropivacaine in anesthetized (*left panel*) and unanesthetized (*right panel*) rabbits

References:

1. Gaudreault, F., et al., J Pharmacokinet Pharmacodyn, 2012. 39(6): p. 635–42

W-047

Physiologically Based Pharmacokinetic Modeling of Bspirone and the Effect of Liver Cirrhosis on Its Disposition

J. S. Macwan*, G. Fraczkiewicz, V. Lukacova, M. B. Bolger, W. S. Woltosz

Simulations Plus, Inc. Lancaster, CA, USA

Objective: The aim of this work was to develop a physiologically based pharmacokinetic (PBPK) model of buspirone following oral administrations in healthy volunteers, and to extend this model to predict the effects of physiological changes associated with liver cirrhosis in compensated and decompensated hepatic impairment patients.
Methods: The GastroPlus™ 8.5 (Simulations Plus, Inc.) Advanced Compartmental Absorption and Transit™ (ACAT™) model and PBPKPlus™ module were used to build the buspirone model to mechanistically explain absorption, distribution, and clearance mechanisms. The model was validated by comparing simulated and observed plasma concentration-time profiles for parent drug and its two major metabolites (1-pyrimidinylpiperazine and 6-hydroxybuspirone) obtained after multiple oral administrations of buspirone across several different dose levels in healthy volunteers [1]. Physiological changes including cardiac output, cytochrome P450 enzyme expressions, liver size, hepatic blood flow, renal function, and plasma protein binding, all associated with different degrees of severity of liver cirrhosis [2], were incorporated into the program's built-in human physiologies created using the Population Estimates for Age-Related Physiology (PEAR Physiology™) module. The final validated model was used to predict concentration-time profiles of buspirone and 1-pyrimidinylpiperazine metabolite in both compensated and decompensated hepatic impairment patients [3].
Results: Simulated plasma concentration-time profiles of buspirone and two major metabolites were in close agreement with observed data from healthy subjects. The validated final model, which was extended to predict the effects of liver impairment, agreed reasonably well with observed data from patients with compensated and decompensated hepatic impairment.
Conclusions: The absorption and pharmacokinetics of buspirone and its metabolites in healthy subjects were accurately predicted using in silico and in vitro data describing the drug's physicochemical and biopharmaceutical characteristics, along with in vitro enzymatic kinetics. The model was also successfully extended to predict systemic exposure in patients with liver cirrhosis.

References:

1. Dockens, et al., JCP, 46: 1308–1312, 2006
2. Johansen, et al., AOS, 74: 253–258, 1996
3. Barbhaiya, et al., EJCP, 46: 41–47, 1994

W-048

Use of Physiologically-Based Pharmacokinetic (PBPK) Modeling to Assess Drug Interaction Potential of Antibody–Drug Conjugates (ADCs)

Divya Samineni*, Yuan Chen, Sophie Mukadam, Harvey Wong, Ben-Quan Shen, Dan Lu, Cornelis Hop, Sandhya Girish, Chunze Li, Jin Yan Jin

Genentech, Inc., South San Francisco, CA, USA

Objectives: The unconjugated cytotoxic agent, monomethyl auristatin E (MMAE) of an ADC is expected to undergo clearance mechanisms consistent with small molecules. Hence evaluation of the risk of drug–drug interaction associated with unconjugated cytotoxic agent is important in support of clinical development of ADCs.
Methods: A PBPK model linking antibody conjugated MMAE (acMMAE) as a parent drug to one of its metabolites, MMAE, was developed and implemented in the Simcyp simulator using a mixed bottom-up and top-down approach in 11 patients dosed with the anti-CD22-vc-MMAE ADC at 2.4 mg/kg. The model performance was verified by comparing predicted MMAE PK profiles with observed data obtained from dosing another vc-MMAE ADC i.e. Brentuximab vedotin in 28 patients at three clinical dose levels of 1.2, 1.8 and 2.7 mg/kg. Finally, the validated model was used to simulate the DDI between brentuximab vedotin and midazolam, ketoconazole, and rifampicin in a trial size of 10×15, 10×14 and 10×29 subjects, respectively. The simulated DDI (AUC and Cmax ratio) were compared with the published data [1].
Results: Model validation showed that the simulated values for the MMAE analyte at 1.2, 1.8 and 2.7 mg/kg were (Cmax: 2.7, 5.0 and 7.0 ng/mL; AUC: 20.3, 37 and 53.2 ng day/mL) in good agreement with the observed brentuximab vedotin pharmacokinetic data for the MMAE analyte (Cmax:3.4, 5.2 and 8.0 ng/mL; AUC: 23.4, 37 and 56 ng day/mL)), respectively. The magnitude of DDI predicted by the PBPK model were within a 2-fold range of the observed brentuximab vedotin values.
Conclusion: This work demonstrates the utility of the first PBPK model developed to predict the DDI potential of vc-MMAE ADCs. It is conceivable that this model can be extended to other vc-MMAE ADCs to inform their DDI strategy during the clinical development.

References:

1. Han, et al: J Clin Pharmacol 2013; 53(8) 866–877

W-049

Development of a Disease Model of Bruton's Tyrosine Kinase (BTK) Inhibition by PRN473 in Rat Collagen-Induced Arthritis (rCIA)

Patrick F. Smith*, Dane Karr, Angelina Bisconte, Ron Hill, David Goldstein, Phil Nunn, J. O. Funk

d3 Medicine, Parsippany, NJ, USA; University at Buffalo, Buffalo, NY, USA; Principia Biopharma, South San Francisco, CA, USA

Objectives: PRN473 is a novel covalent-reversible BTK inhibitor with potent activity, selectivity, and prolonged on-target residence time. The BTK enzyme is required for B-cell activation and inhibitors may have applications in oncology and inflammatory conditions. Our aim was to develop a PK/PD model linking PK, target occupancy, and efficacy of PRN473 in a model of rCIA.
Methods: PRN473 dosed PO for 10 day to female Lewis rats with CIA at 0 (vehicle) 1, 3, 10, and 30 mg/kg QD ($n = 8$/group). BTK occupancy in splenocytes was measured at 0, 1, 6, and 12 h post dosing on Day 10. PK ($n = 5$/group) were measured at 0, 1, 6, and 12 h post dose. The primary measure of drug effect was the timecourse in rat ankle diameter (AD) changes. Candidate models were fit to the data to link PRN473 exposure with BTK occupancy, and BTK occupancy to AD.
Results: PRN473 demonstrates potent dose-dependent activity in the rat CIA model, with a short PK half-life and a long PD half-life. PRN473 PK was well characterized by a 2-compartment PK model (MLEM, ADAPT V) with CL = 14.2 L/h/kg; BTK occupancy was modeled using an effect site compartment with drug binding BTK with a Hill-function; The PRN473 IC50 for BTK occupancy was

estimated to be 37.7 ng/mL. AD was modeled as an indirect response model with transit compartments on kout, and BTK-occupancy inhibiting kin via a Hill-function (EC_{50} 72.5 %). Simulations confirm a minimum BTK occupancy level of ~70 % is required in this model to maintain maximal efficacy.

Conclusions: PRN473 is a novel reversible-covalent BTK inhibitor with potent activity in the rCIA model with a unique PK/PD profile. A disease model was successfully developed which may be a valuable translational tool to estimate human therapeutic doses, and to efficiently identify PD-targeted doses for proof-of-concept studies.

W-050

Population PK/PD Modeling of Dietary Nitrate Effect on Blood Pressure in Healthy Subjects

Mariam Ahmed[1,*], Richard Brundage[1], John St. Peter[1,2]

[1] Experimental and Clinical Pharmacology, University of Minnesota, Minneapolis, MN, USA; [2] PepsiCo Global R&D, Purchase, NY, USA

Objectives: Dietary nitrate (NO_3) has been shown to increase plasma concentrations of nitrite (NO_2) which can further be reduced to nitric oxide and lower blood pressure [1]. While a recent study has demonstrated a dose-dependent effect of dietary NO_3 on blood pressure [2], a quantitative model characterizing the pharmacokinetic/pharmacodynamic (PK/PD) relationships among dietary nitrate dosing, nitrite plasma concentrations, and effect on blood pressure have not been reported.

Methods: Ten healthy subjects received four different acute doses (0,4.2,8.4,16.8 mmol) of dietary nitrate (Beet It®) on four separate occasions separated by a 3-day washout period. For each occasion, NO_3 and NO_2 concentrations and systolic (SBP), diastolic (DBP) and mean arterial (MAP) blood pressures were obtained at seven time points over 24 h. Simultaneous population PK/PD modeling was performed with NONMEM 7.2 and the 95 % confidence intervals (CIs) were constructed from 1000 bootstrap datasets.

Results: The PK of NO_3 and NO_2 were each adequately described by a 1-compartment model with the fraction of NO_2 formation from NO_3 fixed at 5 %. The population PK parameters (95 % CIs) of NO_3 and NO_2, respectively, were: CL: 2.92 (2.53,3.34), 133 (110,157) L/h; volume of distribution: 28.3 (22.2,30.0), 58.0 (32.3,87.0) L; and baseline concentration: 29.3 (26.1,33.7) μM, 85.1 (76.5,94.7) nM. For the pharmacodynamics, SBP, DBP and MAP were found to decrease linearly with increased NO2 plasma concentration. The population slopes (95 % CI) were −0.0152 (−0.02, −0.01), −0.007 (−0.01, −0.004), −0.0095 (−0.013, −0.007) mmHg/nM, respectively. The between-subject variability for SBP and MAP slopes were 49 and 26 %, respectively; it was not estimable for DBP.

Conclusions: Acute dietary nitrate consumption can reduce blood pressure short term in young adults. There is a linear PK/PD relationship of nitrite and blood pressure over the observed range. Between-subject variability was moderate for the effect of nitrate on SBP and low for MAP.

References:

1. Cardiovascular Research (2011) 89, 525–532
2. J Appl Physiol (2013) 115, 325–336

W-051

Application of the Integrated Glucose–Insulin Model to the Graded Glucose Infusion and Glucose Clamp Studies

Craig Fancourt*, Wei Gao, Rolien Bosch, Chandni Valiathan, Ryan Vargo, Prajakti Kothare, Teun Post

Merck & Co., Inc., Whitehouse Station, NJ, USA

Objectives: The Integrated Glucose-Insulin (IGI) model [1] semi-mechanistically describes glucose-insulin homeostasis and has been used to characterize pharmacodynamic responses following experimental provocations. We examine the performance and parameter sensitivity of the model when applied to the graded glucose infusion (GGI) and glucose clamp provocations. The present work assesses whether predicted beta-cell sensitivity (BCS) in GGI and glucose disposal rate (GDR) in the clamp exhibit physiologically plausible glucose and insulin trends.

Methods: The steady-state IGI model state-variables were calculated for a range of exogenous insulin and glucose infusions, using non-diabetic (ND) or T2DM human population parameter sets from [1], assuming negligible first-pass insulin secretion. BCS was calculated as the slope of insulin secretion rate (Isec) versus glucose (Gc). GDR was calculated as glucose infusion rate (GIR) + endogenous glucose production (Gprod).

Results: For the GGI (Fig. 1), the model predicts a linear relationship between insulin secretion and glucose, with a larger slope (BCS) for ND compared to T2DM, in agreement with literature. The model can represent the physiological range of BCS. The most sensitive parameters are CLi and IPRG. CLgi has no effect on BCS.

For the clamp (not shown), the model predicts a larger GDR for ND compared to T2DM, in agreement with literature. However, for GDR vs. glucose, the model slope increases with respect to glucose, in contrast to literature, which exhibits saturation. Also, model GDR vs. insulin is linear, in contrast to literature, which exhibits a sharp Emax behavior.

Conclusions: The IGI model sufficiently characterizes beta-cell sensitivity in a GGI experiment, but not glucose disposal rate in the glucose clamp. The results suggest an opportunity to refine the IGI model to better match provocation experiments.

References:

1. Silber et al., An integrated model for glucose and insulin regulation in healthy volunteers and type 2 diabetic patients following intravenous glucose provocations. J Clinical Pharmacol. 2007;47(9):1159–71

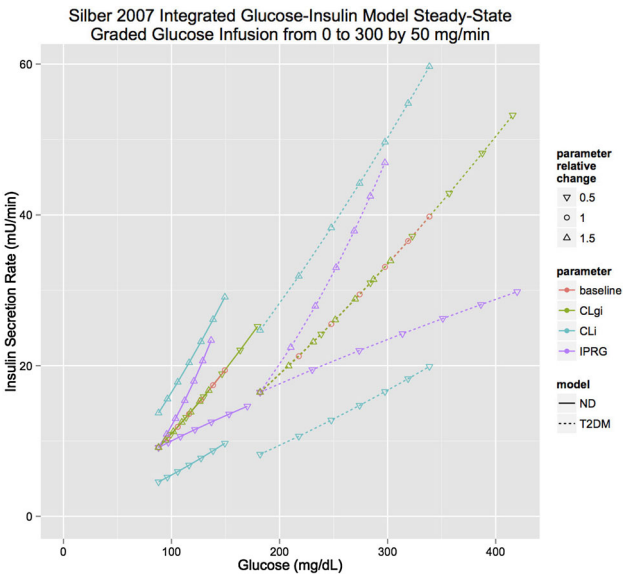

Fig. 1 Silber 2007 integrated glucose–insulin model study-state graded glucose infusion from 0 to 300 by 50 mg/min

W-052

Multi-compartment Population PK Model of Tenofovir (TFV) and Emtricitabine (FTC) for HIV Prevention

Kuo-Hsiung Yang*, Mackenzie Cottrell, Craig Sykes, Heather A. Prince, Kristine B. Patterson, Angela D. M. Kashuba

Eshelman School of Pharmacy, UNC, Chapel Hill, NC, USA

Objectives: The majority of HIV prevention studies in women using daily oral TFV+FTC dosing have demonstrated futility, primarily due to poor adherence. Rather an intermittent dosing strategy will be required for successful prevention in this population. Using data from a Phase I single-center open-label two-arm single-dose PK study with sequential assignment, we developed a predictive pharmacokinetic model for two antiretrovirals in three mucosal tissues that will allow for concentration predictions given a specific dose and dosing frequency that can inform future clinical trial design.
Methods: 48 premenopausal healthy women were sequentially assigned to a single oral dose of one of the following drug combinations for a total of 2 drug combinations with 6 arms: (a) Maraviroc/TFV 150/150 mg, 300/300, or 600/600; (b) FTC/Raltegravir 100/200, 200/400, or 400/800. Over 48 h, 13 blood samples and 4 vaginal, cervical and rectal tissue samples were collected. TFV, FTC, intracellular TFV-diphosphate, FTC-triphosphate concentrations were determined by validated LC-MS/MS methods. Simultaneous nonlinear mixed effect modeling was done using NONMEM 7.3 (FOCE-I) on a linux cluster. 1,000 subject Monte Carlo Simulation was performed for visual predictive checks. R was used for pre/post-processing/plotting, Berkeley Madonna for model exploration/initial estimates.
Results: A 16 compartment, bolus input, linear kinetic model best described the data. (Fig. 1) A second peak in the rectal tissue (gut transit time) was described with 7 transit compartments. Tissue volumes were fixed to physiologically relevant values. Inter-individual variability was described with an exponential model, residual variability with proportional error model. Using goodness of fit plots, the model well predicted concentrations in all seven compartments.
Conclusions: This model is useful for predicting mucosal tissue concentrations of TFV+FTC and their active metabolites. It also allows for simultaneous prediction of plasma concentrations, important for estimating systemic toxicity. With target mucosal tissue concentration defined for efficacy, this model can be used to optimize the dose and dosing frequency by maximizing efficacy and minimizing toxicity through Monte Carlo simulations.

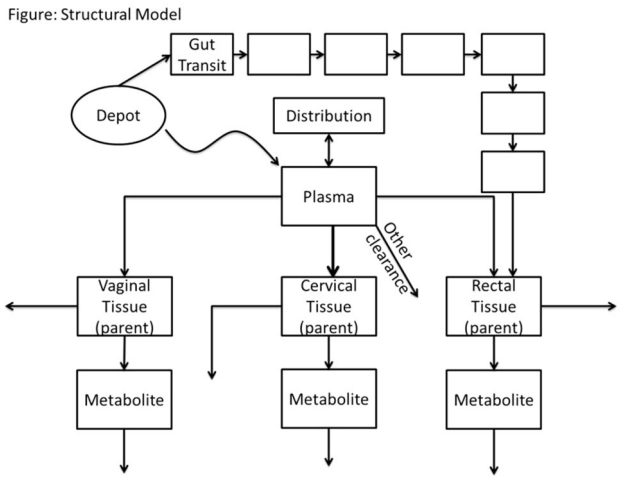

Fig. 1 Structural Model

W-053

Enzyme Focused PBPK Modelling in Adults for Candidate Drugs Using GastroPlus

Tanay Samant[1], Naveen Mangal[1], Viera Lukacova[2], Larry Lesko[1], Stephan Schmidt[1,*]

[1] Center for Pharmacometrics and Systems Pharmacology, University of Florida, Orlando, FL, USA; [2] Simulations Plus, Inc., Lancaster, CA, USA

Objective: Physiologically-Based Pharmacokinetic (PBPK) Modelling has gained ground for dose selection, clinical trial design and regulatory submissions [1]. Our main objective is to use an enzyme focused approach to individually characterize the metabolism pathways of specific drugs and mechanistically corroborate this knowledge to predict pharmacokinetics of a probe compound having multiple metabolism pathways (acetaminophen).
Methods: Specific substrates for five phase I metabolic pathways (caffeine and theophylline for CYP1A2, midazolam for CYP3A4, warfarin for CYP2C9, omeprazole for CYP2C19 and desipramine for CYP2D6) were chosen. In vitro Km Vmax values were used for individual enzymes and scaled to adult human in vivo values. Overall clearance was evaluated for each substrate–enzyme combination following intravenous (IV) and oral administration at different dose levels. Model qualification was performed by an external data set. The qualified metabolism information was merged for model building and qualification of IV and oral acetaminophen.
Results: The model building and qualification was successful for all the studied enzyme-substrate combinations and acetaminophen. The developed PBPK models provide consistent representation of the drug exposures of different intravenous and oral doses. The model predicted AUCs lie within the 0.8–1.2 range of the observed AUCs for enzyme–drug combinations. In addition, visual predictive checks (VPC) showed that observations were contained in the 95 % prediction interval.
Conclusions: Individual enzymatic metabolism pathways with specific substrates are well characterized and qualified for adult PBPK models using GastroPlus. The proposed enzyme focused approach towards PBPK modelling in adults would enhance the knowledge-base in predicting pharmacokinetics of drugs having multiple metabolism pathways. Our future research will focus on the utilization of this knowledge for studying the underlying ontogeny of the enzyme interplay in the pharmacokinetics and dose estimation in pediatrics.

References:

1. Rowland M, Peck C, Tucker G. Physiologically-based pharmacokinetics in drug development and regulatory science. Annual review of pharmacology and toxicology. 2011;51:45–73

W-054

Clinical Pharmacokinetics (PK) of the Angiopoietin 1/2 Neutralizing Peptibody, Trebananib, in Acute Myeloid Leukemia

L. B. Pitzonka[1], E. S. Wang[1], J. Greene[2], C. E. Vigil[1,3], J. H. Mendler[4], M. W. Becker[4], K. O'Dwyer[4], M. Wetzler[1], J. Liesveld[4], G. J. Fetterly[1,*]

[1] DOM, RPCI, Buffalo, NY, USA; [2] CRS, RPCI, Buffalo, NY, USA; [3] DOM, Instituto Nacional De Enfermedades Neoplasicas, Lima, Peru; [4] J.P. Wilmot CC, U of R., Rochester, NY, USA

Background: Angiopoietins (Ang-1/2) are pro-angiogenic factors implicated in acute myeloid leukemia (AML) development. Trebananib is a first-in-class Ang-1/2 neutralizing peptibody that sequesters Ang-1/2, leading to tumor inhibition. Trebananib PK data is limited in hematological malignancies. A population PK model was developed to characterize trebananib drug exposure and investigate the effect of patient covariates on inter-subject variability in AML patients.
Methods: Trebananib was administered alone or with cytarabine at 15 and 30 mg/kg via a weekly 1 h IV infusion in 24 AML patients. PK samples were collected on days 1 and 22 at EOI, 1–3, 4–6, 72, and 168 h post EOI. Population PK modeling was performed using NONMEM to investigate the effect of patient covariates: [BW (53–118 kg), BSA (1.52–2.48 m^2), age (29–85 years), CrCL (41–168 mL/min), ALT (6–372 U/L), AST (19–193 U/L), ALP (61–1118 U/L), and TBIL (0.1–4.7 mg/dL), sex, and race] on trebananib PK.
Results: A 3-comp. PK model adequately characterizes trebananib PK, with a mean (IIV) CL and Vp of 0.09 L/h (29.7 %) and 2.74 L/kg (75.9 %), respectively. A significant correlation exists between CrCL and CL ($P < 0.05$), consistent with Lu et al., 2012. These data suggest CrCL in part explains the inter-subject variability of CL, however, step-wise covariate analysis with forward selection ($P < 0.005$)/ backward elimination ($P < 0.001$) demonstrate that no covariates significantly influence CL and V. Residual variability was 30.6 %.
Conclusions: This population PK analysis shows that trebananib possesses a good PK profile in AML patients that is dose proportional, a mean terminal half-life of 122 h suitable for weekly administration, and, and is consistent with solid tumor PK data in the literature.

W-055

Is It Markov Versus Latent Variable or Should It be State Space Versus Marginal Probability?

Matthew M. Hutmacher*

Objectives: The pharmacometric literature suggests that the Markov and Latent Variable (LV) approaches for modeling binary or ordered categorical data are competing. The relationship between these approaches is clarified here and a different terminology is proposed—i.e., state space (SS) or marginal probability (MP). Additionally, a simulation study was conducted to assess the effects of misspecification of transition probabilities on predictions of and inferences on marginal probabilities.
Methods: The connection between the Markov and LV approach was derived analytically. Handling of the transition probabilities highlights the different focuses of the SS and MP models. The simulation study was conducted using a Phase 2-type longitudinal trial design with an Emax model for binary responses. Data were simulated using various autoregressive correlations with random effects on baseline and the maximum placebo effect. "True" and reduced (fewer variance components) models were evaluated using 1,000 replicates per scenario. Biases in the predicted marginal probabilities and their confidence interval coverage rates were evaluated primarily. Biases in the parameters estimates and transition probabilities were evaluated secondarily.
Results: The general likelihood for the Markov and LV approaches is identical. The SS approach models directly and structurally the conditional probabilities of transitioning from state-to-state. Marginal probabilities are derived from the transition probabilities. In contrast, the MP approach focuses on the marginal probabilities, and derives the transition probabilities from stochastic components. For these reasons, the new reference terminology is proposed. No notable biases in the marginal probabilities were observed in the simulation study for the MP model. Confidence interval coverage rates were reasonable except for the model without autoregressive/variance components, which demonstrated less than nominal coverage rates.
Conclusions: SS models are tailored to focus on transitions from state-to-state. If the primary focus is on the marginal probabilities of response, then the MP approach is more appropriate. Correct specification of transition probabilities is not necessary for unbiased MP prediction, yet some modeling of correlation is necessary for acceptable inference.

W-056

Comparison Between Two Methods for the Assessment of Equivalence in Clinical Efficacy of Inhaled Formoterol

Bhargava Kandala[1,*], Leslie Hendeles[1], Brian Maas[1], Roy Joseph[1], Lawrence Winner[2], Guenther Hochhaus[1]

[1] Department of Pharmaceutics, College of Pharmacy, University of Florida, Gainesville, FL, USA; [2] Department of Statistics, University of Florida, Gainesville, FL, USA

Objectives: To establish bioequivalence (BE) of generic β2 agonists at the site of action, pharmacodynamic (PD) approaches such as bronchoprovocation (methacholine challenge) studies using PC20 as the primary end-point have been employed both by the FDA and European Medical Agency (EMA).

Objectives: To analyze a PD crossover study conducted to demonstrate BE between two dry powder inhalers—formoterol Aerolizer 12 mcg (reference (FA)) and formoterol Novolizer 12 mcg (test (FN)) and to evaluate the agreement between the Finney bioassay and the the Dose-scale approach1 in the assessment of BE.
Methods: Forty four patients inhaled methacholine until their FEV1 reduced by 20 % (PC20) of control following inhalation of placebo, 12 mcg, or 24 mcg of formoterol via the FA or FN in a crossover fashion. BE of formoterol administered by the Aerolizer and the Novolizer was assessed by calculating the (a) Relative bioavailability (FDS) of FN relative to FA and its 90 % CI (non-parametric bootstrap approach) using a dose-scale approach (FDA). (b) Relative potency of FN relative to FA (Fieller 90 % CI) using the Finney 2-by-2 bioassay (EMA). The outcome was evaluated based on (0.67–1.5) BE limits.
Results: The FDS of the 12 mcg dose of FN relative to FA was calculated to be 1.18 (90 % CI (0.94–1.45)). For the Finney bioassay the assumptions of parallel line assay were met. The point estimate and the 90 % Fieller CI for relative potency of FN relative to FA was 1.131 (0.97–1.34).
Conclusions: FN was shown to be bioequivalent to FA using the dose-scale approach and the Finney bioassay, as the 90 % CI interval of FDS for the 12 mcg dose and 90 % CI of relative potency were within the BE limits of 0.67–1.5. Results show that PC20 is a sensitive biomarker and hence methacholine challenge is a viable assay for β2 agonists.

References:

1. FDA. Draft Guidance on Orlistat

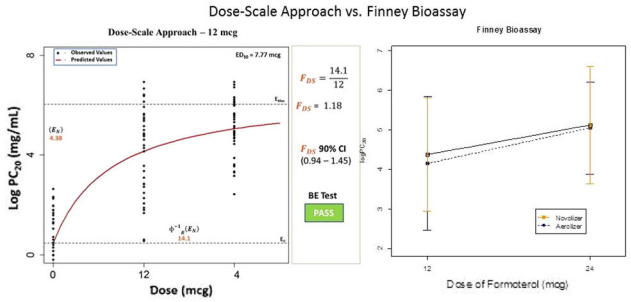

W-058

Population-Based Meta-analysis of Roxithromycin Pharmacokinetics

Michael J. Dolton*, David Z. D'Argenio

Biomedical Simulations Resource, University of Southern California, Los Angeles, CA, USA

Objectives: The macrolide antibiotic roxithromycin is used in the treatment of respiratory tract infections, community acquired pneumonia and skin infections. Despite widespread clinical use for several decades, no population pharmacokinetic analysis has been published and few studies have investigated pharmacodynamic target attainment. Early studies of roxithromycin indicated that drug exposure increases by a less than dose proportional extent at doses within the approved range, which may have important implications for target attainment since dosing regimens of 150 mg twice daily and 300 mg once daily are used interchangeably in clinical practice. The objectives of this analysis were to develop a population-based meta-analysis of roxithromycin pharmacokinetics, and utilize this model to simulate pharmacodynamic target attainment and inform optimal dose selection.
Methods: Following an extensive literature search, roxithromycin pharmacokinetic data was collected or digitized from literature publications using DigitizeIt (V1.5.8). Population modeling was undertaken with ADAPT (version 5.0, MLEM program) [1].
Results: Thirty-three aggregate roxithromycin concentration-time profiles and 12 individual profiles across a 6-fold dose range were available for analysis. A two-compartment model with dose-dependent absorption and first-order elimination adequately described the dataset (Table 1). Saturable absorption was characterised by the equation F = 1 − (FImax/(F50 + dose))*dose. Dose simulations indicated that a 300 mg once daily regimen is associated with a 24 % lower median free AUC (fAUC) (15.4 mg.h/L) compared to 150 mg twice daily (20.2 mg.h/L). Both regimens led to acceptable pharmacodynamic target attainment (fAUC/minimum inhibitory concentration (MIC) ratio > 20) in > 90 % of simulated patients up to an MIC of 0.5 mg/L; at an MIC of 1 mg/L, 19.6 % of patients receiving 300 mg once daily achieved an adequate fAUC/MIC compared to 51 % of patients receiving 150 mg twice daily.
Conclusions: Roxithromycin displays dose-dependent, saturable absorption leading to reduced bioavailability. Pharmacodynamic target attainment is similar between commonly used roxithromycin dose regimens but is lower with less susceptible isolates when once daily dosing is used.

Table 1 Population parameter estimates for roxithromycin

Parameter	Mean (% RSE)	IIV as CV % (% RSE)
CL (L/h)	2.07 (7.64)	26.4 (18.0)
V_c (L)	21.6 (6.88)	9.20 (56.4)
Ka (h^{-1})	1.50 (9.59)	31.3 (21.8)
F50 (mg)	433 (50.7)	88.0 (74.0)
FImax	0.5 FIX	NE
V_p (L)	10.2 (34.6)	26.4 (137)
CL_D (L/h)	1.30 (37.4)	18.2 (354)
SD_{inter}	0.379 (5.57)	–
SD_{slope}	0.125 (3.35)	–

References:

1. D'Argenio DZ, Schumitzky A, Wang X. ADAPT 5 Users Guide: Pharmacokinetic/Pharmacodynamic Systems Analysis Software. Biomedical Simulations Resource, Los Angeles, 2009

W-059

Dose Selection for Subcutaneous (SC) Abatacept in Pediatric Subjects with Juvenile Idiopathic Arthritis (JIA)

Zexun Zhou, Bindu Murthy, Amit Roy*

Bristol-Myers Squibb

Objectives: To determine a target abatacept exposure range for SC abatacept in JIA patients, and select pediatric SC abatacept dose(s) for a pediatric Phase 3 study that achieve exposures within the target range, by utilizing available pharmacokinetics (PK) and efficacy data of intravenous (IV) abatacept in adult rheumatoid arthritis (RA) and JIA patients, and SC abatacept in RA patients.
Methods: The lower bound of target abatacept exposure for JIA patients was determined based on a an exposure-response (E-R) analysis of efficacy that characterized the probability of achieving American College of Rheumatology Pediatric (ACRp; ACRp30, ACRp50, ACRp70) responses at Month 4 as a function of abatacept steady-state trough concentration (Cminss). The upper bound of target abatacept exposures was determined from approved SC abatacept doses in RA patients. SC abatacept doses that achieved the target Cminss in pediatric patients 4–18 years were selected for the Phase 3 study by developing a population pharmacokinetic (PPK) model of SC abatacept in JIA patients, and applying the model to determine the dose(s). The SC JIA PPK model was developed by combining the absorption and bioavailability from the adult SC PPK model with systemic PPK parameters from the unified JIA and adult RA model.
Results: The E–R of ACRp was described by an ordered categorical proportional-odds model with log-transformed Cminss as a significant predictor variable of ACRp response. The probability of ACRp response increased with increasing Cminss, and concomitant methotrexate use. A weight tiered approach was used to ensure that the exposure (Cminss) in JIA patients were bound between 10 μg/mL (efficacy) to 50 μg/mL (safety).
Conclusions: The probability of achieving an ACRp response in JIA patients increases with increasing abatacept Cminss, but approaches a plateau for Cminss >10 μg/mL. Body weight-tiered weekly SC doses

of 50, 87.5, and 125 mg for JIA patients weighing <25, 25 to <50, and ≥50 kg, respectively, are predicted to achieve Cminss values that are within the target range of 10–50 μg/mL.

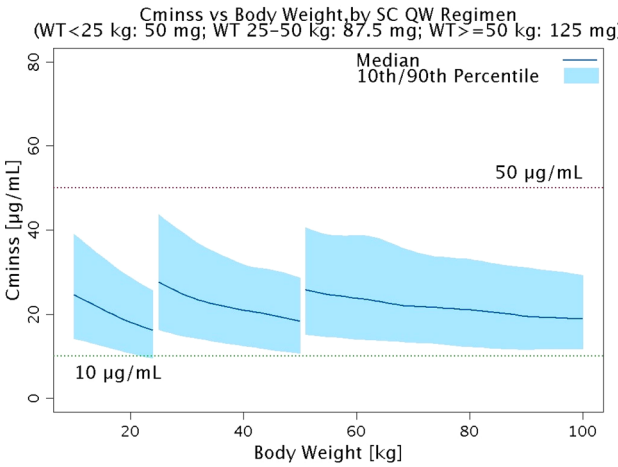

W-060

A Web-Based Application for Limited Sampling Strategy

Guillaume Bonnefois[1], Olivier Barrière[1], Sarem Sarem[1], Jun Li[1,2,3], Fahima Nekka[1,2,3]

[1] Faculté de pharmacie University de Montreal, Montreal, QC, Canada; [2] Centre de Recherches Mathmatiques Université de Montreal (CRM), Montreal, QC, Canada; [3] Centre for Applied Mathematics in Bioscience and Medicine McGill University, Montreal, QC, Canada

Objectives: Limited sampling strategies (LSS) are widely used to estimate surrogates of drug exposure, such as the area under the concentration-time curve (AUC), which generally correlates with drug effect. The aim of these LSS techniques is to reduce the inconvenient and frequent blood samplings, while keeping the precision of the derived estimates. A regression procedure is usually proposed for the prediction of AUC involving only a small number of blood samples collected at specific times as dependent variables. Considering the trade-off between the accuracy of the estimation and the clinical convenience, the challenge of LSS is to identify a suitable set of sample concentrations that can achieve this twofold goal.
Methods: We developed a set of performance criteria with confidence intervals computations and cross-validation methods to appropriately assist the judgement of multiple linear regression. As direct fallout, we have implemented a user friendly tool, with a graphical user interface, that can help clinicians to set up LSS for their practical needs.
Results: Exemplified by the case of cyclosporine in pediatric hematopoietic stem cell transplantation, our proposed algorithms proved to be able to efficiently identify the best LSS and the associated statistics, as well as to evaluate the performance of different LSSs based on various criteria.
Conclusions: With the progress in computerized tools, this web-based approach is a good example of the translational aspect that should be a primary consideration for developers in pharmacometrics in order to outreach to clinical end users.

Reference:

1. O. Barrière, A user friendly tool to assist clinicians in the development of Limited Sampling Strategies, CAIMS 2013

W-061

Modeling the Spread of Pandemic Influenza in the United States: Impact of Antiviral Interventions, Pharmacology, and Resistance

Mary Fidler, Michael Murillo, Craig Rayner, Mohamed Kamal, Patrick F. Smith*

New Mexico Consortium, Los Alamos, NM, USA; d3 Medicine, Parsippany, NJ, USA; Roche, NY, USA

Objectives: Antivirals such as oseltamivir are a crucial part of the armamentarium to reduce morbidity and mortality of pandemic influenza, having demonstrated benefits in treating active infection and in disease containment. Our objective was to evaluate the impact of various oseltamivir intervention strategies on spread of pandemic influenza, including dosing regimens, stockpiling, and resistance.
Methods: A stochastic, agent-based, metapopulation model was utilized to examine the temporal and geographical spread of influenza in the U.S. The model included census data for each of the 3,143 U.S. counties, daily commuter traffic, and U.S. airline traffic network (RITA). Individuals were represented by agents, which could be susceptible, infected, or recovered from influenza; agents interacted and moved amongst commuter and airline networks. Agent characteristics included oseltamivir PK/PD parameters derived from population distributions linking exposure to duration of viral shedding (Rayner, AAC 2013). The model was qualified by comparing simulated influenza seasons to historical CDC statistics. Antiviral intervention strategies examined included oseltamivir dose, time to initiate therapy, proportion of the infected population treated, prophylaxis and stockpiling strategies, and antiviral resistance. Each scenario was informed by published data, and were simulated for viral strains with varying levels of infectivity (R0).
Results: Oseltamivir had significant impact on reducing spread of pandemic influenza, as both prophylaxis and treatment. To maximize containment, an optimal target treatment goal of ~60 % of infected individuals was predicted, which can inform stockpiling decisions. Increasing the standard oseltamivir treatment dose from 75 to 150 mg bid had modest impact on influenza spread, and was greater as Ro increased (3 M fewer infections at $R0 = 2.5$). Time to treatment initiation and targeted prophylaxis strategies were also important mitigation strategies.
Conclusions: The proposed model is useful to examine influenza intervention strategies, including deployment of antivirals. The model may have additional utility to evaluate the potential impact of novel antivirals from a public health perspective.

W-062

Impact of System Variablity on the Prediction of Numerical Convolution and Deconvolution

J. Li[1,2], F. Nekka[1,2]

[1] Faculty de Pharmacie, Université de Montreal, C.P. 6128, Succ. Centre-ville, Montreal, QC, H3C 3J7 Canada; [2] Centre de recherches mathmatiques, Université de Montreal, C.P. 6128, Succ. Centre-ville, Montreal, QC, H3C 3J7 Canada

Objectives: Numerical convolution and deconvolution methods are widely used in drug design and bioequivalence studies. However, point estimation of the output always occupies the central position in the development of current numerical algorithms as it is rooted in the concept of traditional data fitting. The fact is, even for a deterministic mechanism, the randomness emanating from the system variability or

measurement errors, can be predominant in in vivo or in vitro data, asking thus for more sophisticated but formal statistical description of these processes. In this work, we aim to give a mathematical evaluation of the system variability (input and disposition) through numerical convolution and deconvolution processes and discuss the resampling approach for the control of variability in the predicted in vivo response or in vitro drug dissolution (drug absorption).
Methods: We mathematically characterized the variability inherited by the output of the numerical convolution or deconvolution process from the variability carried out by the inputs. Inspired by the Monte Carlo resampling approach, we propose an algorithm that can be used to calculate the confidence (prediction) interval of the results of convolution or deconvolution, solely based on observations. Well known algorithms, such as point area method for deconvolution and simple trapezoidal numerical convolution were used to guide our investigation.
Results: The precision of output signal of a convolution or deconvolution process depends on the type of system variability, which can be annihilated or carried out. A correct factor should be added for lognormal variability. In terms of accuracy, a closed form of the inherited variability in numerical convolution is given. The inherited variability in numerical deconvolution was characterized.
Conclusions: Several traditional assumptions about the output variability are not correct in terms of accuracy and precision. This study is a starting point towards the understanding of the impact of system variability in convolution and deconvolution.

W-063

Development of a Non-human Primate, Semi-mechanistic Pharmacokinetic Model for Pediatric Dose Prediction for the Treatment of Spinal Muscular Atrophy

Puneet Gaitonde[1], Dan Norris[2], Ivan Nestorov[3], Stephan Schmidt[1], Mark Rogge[3], Lawrence J. Lesko[1], Mirjam N. Trame[1]

[1]Center for Pharmacometrics and Systems Pharmacology, University of Florida, Orlando, FL, USA; [2] ISIS Pharmaceuticals, San Diego, CA, USA; [3] Biogen Idec, Cambridge, MA, USA

Objectives: Spinal Muscular Atrophy (SMA) is a genetic, motor neuron disorder resulting in loss of voluntary muscle function. Patients have a defective Survival Motor Neuron (SMN)-1 gene that leads to lack of SMN protein for motor function. The aim of this analysis was to (1) develop a semi-mechanistic, Pharmacokinetic (PK) model using non-human primate data and (2) predict pediatric Phase I PK profiles in various tissues for a therapeutic biologic using interspecies scaling.
Methods: Dose-ranging PK data from various non-human primate tissues were used for model development. Interspecies scaling was used to predict the PK profiles for various tissues in pediatrics based on the non-human primate semi-mechanistic compartment model. During scaling and predictions the analysts were blinded to the pediatric Phase I PK concentrations up until predictions of the PK concentrations had been performed. After simulating the median, 5th and 95th percentiles and the 95 % confidence intervals of the percentiles were computed from the simulated data and after unblinding, the observed pediatric Phase I PK concentrations were overlaid.
Results: The developed multi-tissue compartment model characterized the drug-concentration profiles adequately well across all non-human primate tissues for different doses and dosing regimens. After unblinding of the pediatric Phase I PK concentration data, it revealed that the simulations agreed well with the typical trends and variability of the observed clinical data.
Conclusion: A novel, mechanism-based PK model was successfully developed from data of non-human primates. Interspecies scaling was utilized to scale non-human PK concentrations from various tissues to pediatric PK profiles which allowed for accurate predictions of pediatric Phase I PK concentration profiles in multiple tissues. The model will later be used to predict the possible PK concentration profiles in various tissues for pediatric Phase III trials for different doses and dosing regimens.

W-064

Applying Quantile Regression Approach for Modeling the Correlation Between Two Platelet Aggregation Biomarkers

Nidal Al-Huniti*, Jianguo Li, Diansong Zhou, Renli Teng, Donald Stanski

Quantitative Clinical Pharmacology, AstraZeneca, Waltham, MA, USA

Objectives: Quantile regression approach assesses how conditional quantiles of the dependent variable vary with respect to measured covariates. It also allows examination of the entire distribution of the variable of interest rather than a single measure of the central tendency of its distribution. The objective of current analysis was to analyze the correlation (linkages) between two biomarkers namely, ADP-induced platelet aggregation (PA, final extent) measured by the light transmission aggregometry (20 mM adenosine diphosphate) and platelet P2Y12 reaction units (PRU) measured by VerifyNow P2Y12 Assay using quantile regression approach.
Methods: Platelet aggregation results from a study of 50 patients with stable coronary artery disease have been used in the analysis. The correlation between PA and PRU was analyzed using quantile regression package (quantreg) in R. Linear and nonlinear regression (OLS) analysis was also conducted for comparison.
Results: Scatterplot associated with the OLS model of PA as function of PRU revealed a large unexplained variability ($R^2 = 0.59$) and a relatively poor correlation due to biomarkers heteroscedasticity. Conditional quantile regression assessed the strengthening of the two biomarkers linkages and showed a nonlinear interdependence. The estimated parameters versus quantile are shown in Figure below. The slope and intercept estimated from linear regression are presented as horizontal dash lines in the plots.
Conclusions: Quantile regression showed that the analysis of the conditional densities can provide an additional insight into possibly complex relationships between PRU and the PA concentrations. It also allowed for a better correlation between the two biomarkers by allowing the PRU to have different impacts at different points of the PA distribution and the robustness to departures from normality and skewed tails.

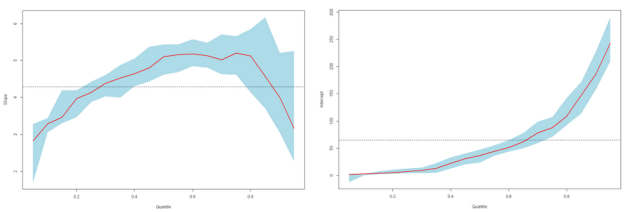

W-065

Application of Web-Based Interactive R-Based Models Using Shiny

Jinzhong Liu[1,*], Timothy Nicholas[2], Brian Corrigan[2]

[1] Division of Clinical Pharmacology, Indiana University School of Medicine, Indianapolis, IN, USA; [2] Pfizer Inc., Groton, CT, USA

Introduction: Shiny is a free R package that allows development of interactive web applications using only two reactive R scripts. Figure 1 shows an example of linear regression model using shiny. It was postulated that this package may be useful for developing interactive model-based pharmacometric analyses.
Methods: Combinations of "uiLayout" functions including "sidebarPanel", "wellPanel", "sidebarLayout" and "tabsetPanel" were conducted to obtain a multi-level interface. Elements of user interface were created using "fileInput", "checkboxGroupInput" and "sliderInput" that allow users to upload a data file, select variables or input values. By using the "uiOutput" function, interactive variables selection can be achieved once a valid data file was uploaded. Using these functions, examples of various types of model-based activities (PK/PD, literature-based meta-analyses, etc.) that had been implemented in R were coded to two interactive R scripts (server.R and ui.R) by various R users, to determine whether typical pharmacometric type models could be readily turned into reusable, interactive web-based applications suitable for use by non-technical users.
Results: Various project specific and generic web applications were developed that allowed non-R users to interact with R-based models. Code development, implementation, testing and debugging could be readily completed in common R tools such as RStudio. The applications could be run off servers located internally or externally, thereby not requiring end users to have R installed at all.
Conclusions: Development of web-based modeling applications using the R package shiny were easily completed using their existing R scripts. Development of the web-based applications builds on the skill sets and expertise of modelers proficient in R. It can be built into workflows and practices currently being used and supported (NONMEM to R, BUGS to R, or analyses using R only). Data summaries, visualizations, literature-based meta-analyses, and patient level analyses can easily be altered to make them interactive web based applications. Shiny applications may provide a rapid, cost-neutral, reusable method for sharing modeling and simulation results with non-R users.

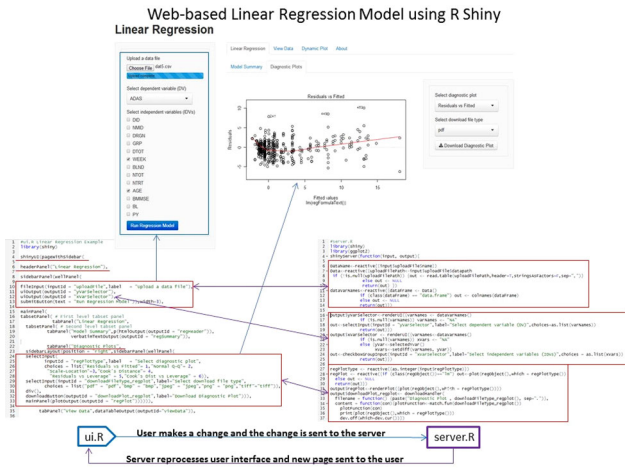

Fig. 1 Web-based linear regression model using R shiny

W-066

Population Pharmacodynamic Modeling of Lorenzo's Oil in Patients with X-Linked Adrenoleukodystrophy

Mariam Ahmed[1,*], Reena Kartha[1,2], Richard Brundage[1,2], Gerald Raymond[3], James Cloyd[1,2,3]

[1] Experimental and Clinical Pharmacology; [2] Center for Orphan Drug Research; [3] Department of Neurology, University of Minnesota, Minneapolis, MN, USA

Objectives: Accumulation of saturated very long chain fatty acids (SVLCFAs) in plasma and tissue is the main cause of mortality and morbidity in X-linked adrenoleukodystrophy (X-ALD) patients. Lorenzo's Oil (LO), a currently used therapy for X-ALD is a 4:1 mixture of oleic and erucic acid. While several studies demonstrated that LO can normalize plasma concentrations of SVLCFAs, exposure-response relationships have not been characterized.
Methods: LO was administered once daily at 2–3 mg/kg for 105 boys with X-ALD and patients were followed for 4.5 ± 3.1 years. Single paired plasma concentrations of erucic acid, the active component of LO was taken as the exposure, and hexacosanoic acid (C26:0), one of the SVLCFAs was taken as the response to LO. 2413 observations were obtained at pretreatment and multiple times during follow-up. A pharmacodynamic model was developed to link the effect of erucic acid on C26:0 plasma levels using NONMEM 7.2 and the 95 % confidence intervals (CI) were constructed from 1,000 bootstrap datasets.
Results: An inhibitory Imax model fit the data reasonably well. The population estimates (95 % CIs) for the maximum effect of erucic acid on C26:0 (Imax), the plasma concentration of erucic acid at which half of the maximum effect was achieved (IC50), and the pretreatment C26:0 plasma concentration (E0) were 0.855 (0.77–1.01) mg/L, 1.11 (0.78–1.52) mg/L, and 1.22 (1.13–1.37) mg/L, respectively. Between-subject variabilities were 13.3 and 85.2 % for Imax and IC50, respectively; it was not estimable for E0. Residual unexplained variability (RUV) was estimated to be 25.1 % with between-subject variability in RUV of 28.6 %.
Conclusions: The population pharmacodynamic analysis confirmed that erucic acid significantly reduced C26:0 plasma concentrations. The between-subject variabilities were low for Imax but high for IC50. This suggests that some patients may benefit from dose escalation if adequate drops in C26:0 are not observed. Further analysis characterizing the effect of erucic acid on time-to-positive brain scan is planned.

W-067

A Physiologically-Based Pharmacokinetic (PBPK) Model to Explore ALX-0171 PK in Infants Following Inhalation

Massimiliano Germani[1,*], Christoph Niederalt[2], Tobias Kanacher[2], Thomas Stohr[1], Laurent Detalle[1], Thomas Wendl[2], Laura Sargentini[1]

[1] Ablynx nv, Technologiepark 21, B-9052 Zwijnaarde, Belgium; [2] Bayer Technology Services GmbH, Leverkusen, Germany

Objectives: ALX-0171, a Nanobody® (therapeutic protein based on the smallest functional fragments of naturally occurring heavy-chain antibodies) targeting the F-protein of the Respiratory Syncytial Virus (RSV), is being developed for treatment of RSV infection. RSV is a recurrent cause of human lower respiratory tract infection during the winter months and can lead to severe respiratory infections such as pneumonia and bronchiolitis, especially in infants.

The primary goal was to estimate a dose resulting in a target concentration, derived from in vitro assays and supported by preclinical studies, that potently inhibits viral replication in the alveolar space of RSV infected infants.
Methods: A multistep learn and confirm process, incorporating observed data from several studies (in vitro and in vivo) and from several species, has been established for supporting the pediatric development of ALX-0171 with PBPK simulations. An inhalation PBPK model was developed starting from animal data (rats and dogs). The model was further scaled and refined for describing the PK in human adults (plasma, lungs and urinary excretion). Finally the model was scaled to RSV infected infants by adjusting anatomical and physiological parameters, clearance and absorption processes. The fraction of the dose deposited in the lungs after inhalation was estimated with the Multiple-path Particle Dosimetry Model (MPPD) V2.11.
Results: PBPK population simulations for the pre-defined pediatric age groups were performed in order to estimate a dose that would reach the predefined alveolar target concentration for 95 % of the individuals.
Conclusions: A PBPK model of ALX-0171 in adult humans for pulmonary administration was established based on preclinical as well as clinical data. This model was scaled to infants with RSV infection to simulate the systemic and local PK of ALX-0171 in patients aged 0–2 years.

W-068

Mechanistic-Based Translational Model for the Optimisation of the Concurrent

Morgan Craig, Antony R. Humphries, Jun Li, Jacques Blair, Michael C. Mackey, Fahima Nekka*

Université de Montréal, Montreal, QC, Canada; McGill University, Montreal, QC, Canada

Objectives: Chemotherapy regimens are constrained by the patients' tolerance and must be adapted in function of this dose-limiting factor. To prevent therapy interruptions, granulocyte colony-stimulating factor (GCSF) is administered during chemotherapy to increase neutrophil counts and hopefully avoid neutropenia. Its use is, however, largely dictated by trial and error processes. Here, we aim to establish optimal regimens for the concurrent administration of zalypsis, a chemotherapeutic drug and filgrastim (rhG-CSF), a supportive adjuvant.
Methods: Adopting a hypothesis-based modelling approach, we extended our previous work by progressively building upon physiological models of granulopoeisis through the addition of neutrophil reservoir pools in the bone marrow and other tissues, and then subsequently incorporating comprehensive PKPD models for zalypsis, and filgrastim (rhG-CSF), to determine optimal dosing schemes. Through the use of delay differential equations and ordinary differential equations, our work incorporates an up to-date understanding of the physiological aspects of myelopoiesis along with well accepted PK models. Keeping our investigation within a clinical scope, we considered different scenarios of first post-zalypsis administration days, variable doses, and time intervals of rhG-CSF administrations to find optimal clinical dosing schedules.
Results: Our results indicate that the number of administrations of G-CSF post-chemotherapy plays a dominant role on therapeutic outcomes and that the timing of the first administration of G-CSF post chemotherapy becomes less important when the number of administrations are increased. Moreover, administering the first dose of filgrastim seven days post-chemotherapy improves the neutropenic status of the average patient.
Conclusion: This physiological-driven approach ensures a broad clinical applicability of our model, particularly for processes involving activation and proliferation of stem cells.

W-069

InsightRX: Mobile Platform for Model-Based Dose Individualization

R. J. Keizer*, S. Goswami, R. M. Savic

University of California, San Francisco, San Francisco, CA, USA

Objectives: To provide a cloud-based platform for model-based treatment individualization, accessible from mobile devices and electronic medical systems, allowing (a) easier dissemination of PK/PD model-based dosing algorithms into the clinic, and (b) clinicians to use such algorithms at the point of care.
Methods: A mobile platform was developed using state-of-the-art open source technologies and libraries on client-side (HTML5, Javascript) and server-side (AWS, NodeJS, MongoDB, R). An application programming interface (API) was implemented to allow access from within electronic medical record (EMR) systems. As proof-of-concept, dosing algorithms for two compelling clinical dosing problems were developed in our platform:

(a) the dosing of busulfan in neonates pretreated for leukemia, and (b) the dosing of vancomycin in neonates treated for MRSA infection. For both applications, population PK models had been developed and validated previously [1, 2]. Key results parameters studied were: feasibility, security (performed stress-tests for common security flaws), ease-of-use (performed end-user interviews) and dose precision (comparison with manual calculation).

Results: We successfully developed a stable and secure on-line platform. Due to its (scripted) implementation on AWS, the platform is easily scalable. On-line delivery of laboratory results into the platform is currently in development, as is HIPAA compliant data storage. Several iterations of the user interface have led to a very easy-to-use interface. For both examples, initial and individualized (Empirical Bayes Estimate) recommended doses using our R-based algorithms were in all cases the same as when calculated using Excel / NONMEM. Investigations into the gain in workflow efficiency, increased patient outcome / safety are currently pending.
Conclusions: A dose individualization platform was developed that facilitates the transfer of PK-PD models from pharmacometric science to the clinic. The availability of both a mobile web application and an API ensures easy access to dosing algorithms from the point of care, and greatly enhances the clinicians workflow compared to manual model-based dose individualization. A busulfan model of the platform will further be evaluated in the multicenter national clinical trial evaluating busulfan efficacy. The platform is under further development to support dosing algorithms for other NTW drugs and beyond, and will be available commercially soon.

References:

1. Savic RM et al., BMT 2013
2. Frymoyer A et al., PAS 2014

W-070

Surface Area-Based Dosing Versus Fixed Dosing of Omacetaxine in Chronic Myeloid Leukemia

Jee Eun Lee*, Kevin Krudys

Office of Clinical Pharmacology, Center for Drug Evaluation and Research, US Food and Drug Administration, Silver Spring, MD, USA

Objectives: Omacetaxine mepesuccinate (Synribo®) was approved for treatment of chronic phase (CP) or accelerated phase (AP) chronic myeloid leukemia (CML) with resistance and/or intolerance to two or more tyrosine kinase inhibitors. An apparent gender effect on efficacy was observed: Major Cytogenetic Response (MCyR) and Major Hematology Response (MaHR) CML-CP was 22 and 71 % in men and 16 and 66 % in women, respectively. MAHR rate for CML-AP was 32 % in men and 19 % in women. Significant difference in omacetaxine exposure (AUC) by gender was also observed (Fig 1). Thus, the reviewers evaluated if this apparent gender effect was caused by body size-based dosing.
Methods: Blood samples obtained from a Phase 1 study in 21 patients with hematologic tumors were utilized. Omacetaxine was administered based on body surface area (BSA, 1.25 mg/m^2) and intensive PK sampling occurred on Days 1 and 11. Population PK analysis was performed to characterize omacetaxine PK and the effects of covariates on it.
Results: Median age was 58 [40–76] years and median BSA was 1.83 [1.4–2.4] m^2. Apparent clearance (CL/F) was not different by gender. No correlation with BSA was observed. The higher efficacy rates with higher BSA suggest BSA-based dose might have caused the apparent gender effect. Moreover, a relationship between age and efficacy was observed: MCyR in CML-CP 26 % (<65 yoa) versus 9 % (≥65yoa) and MHaR in CML-AP 42 % (<65 yoa) versus 14 % (≥65 yoa). The potential causal effect of dose on efficacy was supported by the effect of age on exposure and efficacy. The apparent gender effect disappeared with simulation following a fixed dosing regimen (Fig. 2). The logistic regression shows increasing efficacy as BSA increases.
Conclusions: The apparent effect of gender on exposure might be rather attributable to lower dosing in female patients due to BSA-based dosing. A fixed-dosing regimen might be adequate for omacetaxine.

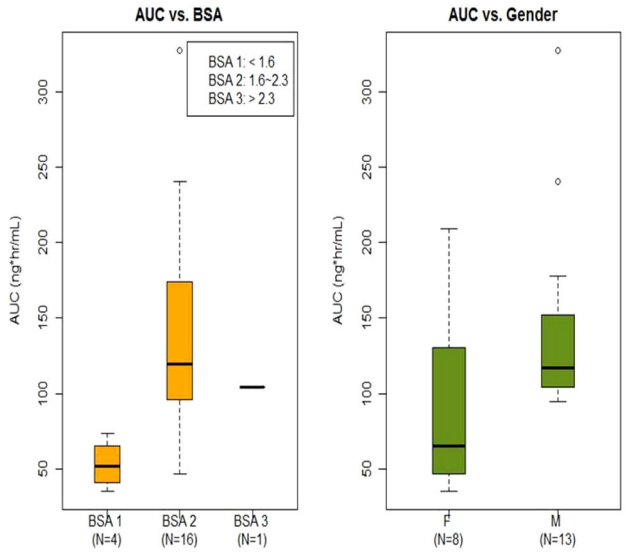

Fig. 1 .

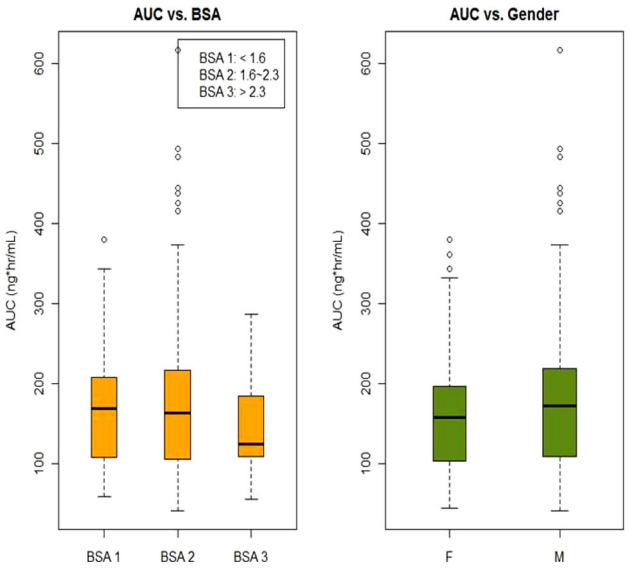

Fig. 2 .

W-071

Effect of Random Non-compliance on Plasma Concentration Targets: A Proof-of-Concept Analysis

J. Korell[1,*], S. McLeay[1], B. Green[1], A. Vermeulen[2]

[1] Model Answers Pty Ltd; [2] Janssen Research & Development, Janssen Pharmaceutica NV, Beerse, Belgium

Objectives: Population reference ranges for plasma concentration target values such as the trough, average, and maximum concentration (C_{trough}, C_{ave}, C_{max}) over a dosing interval are frequently used in therapeutic drug monitoring. These reference ranges are commonly determined via simulations assuming perfect adherence. The objective of this proof-of-concept simulation analysis was to assess the effect of random non-compliance on these target values using a theoretical example.
Methods: A one-compartment population pharmacokinetic model for a hypothetical drug with first-order absorption and elimination was used for the simulations. The simulation dataset included 100 subjects receiving daily doses of 10 units over 60 days. All subjects were assumed to be at steady-state at the beginning of the study. The 80 % prediction intervals for the absolute C_{trough}, C_{ave} and C_{max} over the 60-day study period were calculated from a simulation assuming perfect adherence and used as population reference ranges. Ten adherence simulations were conducted in which 40 % of subjects were assumed to miss 10, 20, 30, 40, 50, 60, 70, 80, 90 and 100 % of their doses, respectively. An additional adherence simulation was also performed where 40 % of subjects randomly missed 10 to 100 % of their doses. The fraction of observed absolute C_{trough}, C_{ave} and C_{max} outside of the population reference ranges were calculated for each adherence simulation.
Results: Random non-compliance increased the number of observed target values falling below and decreased the number of observations falling above the population reference ranges depending on the level of non-compliance. The effect was most pronounced for C_{trough}, followed by C_{ave}, and lastly C_{max}.
Conclusions: Random non-compliance results in deviations from the reference ranges for plasma concentration target values determined

under the assumption of perfect adherence. Further simulations are required to assess the impact of changes in the pharmacokinetic parameters and the underlying structural model on expected distributions of exposures in non-compliant populations.

W-072

A Quantitative Model for Prediction of Hepatic Diclofenac Concentration following a Single Oral Dose

Derek E. Murrell, Sam Harirforoosh*

Gatton College of Pharmacy, East Tennessee State University, Johnson City, TN, USA

Objectives: Diclofenac (DICLO), a nonsteroidal anti-inflammatory drug (NSAID), is utilized to reduce pain and inflammation [1]; while rebamipide (REB), a gastroprotectant, lessens NSAID-related gastric damage [2]. This study sought to develop a model to predict hepatic DICLO concentration 24 h post dose in the absence and presence of REB.

Methods: Hepatic DICLO concentration was predicted using Eq. 1 based on Eqs. 2–4 presented by Rodgers and Rowland [3] for tissue:plasma water partition coefficient (K_{pu}) estimation at steady state. The octanol:water partition coefficient and pKa of DICLO, the albumin liver:plasma ratio, and the fractional volume of neutral lipids, neutral phospholipids, and water in rat liver were gathered from literature [3–5]. Plasma DICLO concentration, unbound drug fraction, and livers were from a previous study [1], in which rats were dosed twice-a-day with either vehicle (VEH) or REB (30 mg/kg) for two days then administered DICLO (10 mg/kg) on day three following a respective dose of VEH or REB. Homogenized livers were assayed for hepatic DICLO concentration using HPLC. The relationship between predicted and observed DICLO liver concentrations were examined using regression analysis.

Results: The respective predicted vs experimental hepatic DICLO concentration were found to be 3.10 ± 0.33 versus 2.33 ± 0.90 μg/g for VEH + DICLO and 4.66 ± 1.45 versus 4.02 ± 1.24 μg/g for REB + DICLO. Predicted and in vivo values were closely correlated, VEH + DICLO ($r^2 = 0.997$; $p = 0.032$; n = 3) and REB + DICLO ($r^2 = 0.997$; $p = 0.001$; n = 4). Prediction sets gave an average-fold error of <2. The HPLC assay showed a CV of 3.5 %

Conclusions: These results indicate that hepatic DICLO concentration at 24 h following a single oral dose may be predicted using the K_{pu} and 24 h plasma DICLO concentration.

References:

1. Cooper, DL et al. Eur J. Pharm Sci 2014; 53, 28–34
2. Ishihara, T et al. Bio Pharm 2010; 79, 1622–1633
3. Rodgers, R and Malcolm Rowland. J Pharm Sci 2006; 95, 1238–1257
4. Rodgers, R and Malcolm Rowland. J Pharm Sci 2005; 94, 1259–1276
5. Toxnet. 2014. Available from: http://toxnet.nlm.nih.gov/cgi-bin/sis/search/a?dbs+hsdb:@term+@DOCNO+7234

$$C_{l,24} = C_{p,24} \cdot K_{pu} \quad (1)$$

$$K_{pu} = \frac{X \cdot f_{IW}}{Y} + F_{EW} + \left(\frac{P \cdot f_{NL} + (0.3P + 0.7) \cdot f_{NP}}{Y}\right) + \left[\left(\frac{1}{f_u} - 1 - \left(\frac{P \cdot f_{NL,p} + (0.3P + 0.7) \cdot f_{NP,p}}{Y}\right)\right) \cdot AR_{lp}\right] \quad (2)$$

$$X = 1 + 10^{pH_{IW} - pKa} \quad (3)$$

$$Y = 1 + 10^{pHp - pKa} \quad (4)$$

$C_{1,24}$, liver concentration at 24 h post dose; Cp, 24, plasma concentration at 24 h post dose; K_{pu}, tissue: plasma water partition coefficient; f_{IW}, fractional liver volume of intracellular water; f_{Ew},fractional liver volume of extracellular water; P, octanol-water partition coefficient; f_{NL}, fractional liver volume of neutral lipids; f_{NP}, fractional liver volume of neutral phospholipids; fu, unbound drug fraction in plasma; $f_{NJ,p}$, fractional plasma volume of neutral lipids; $f_{NP,p}$, fractional plasma volume of neutral phospholipids; AR_{lp}, albumin liver:plasma concentration ratio; p_{HIW}, pH of intracellular water; pHp, pH of plasma.